THE UNIVERSITY OF HULL

Compliant Polymeric Actuators as Robot Drive Units

being a Thesis submitted for the Degree of

Doctor of Philosophy

in the University of Hull

by

Darwin Gordon Caldwell

B.Sc; Dipl. Eng.

September 1989

Summary of Thesis submitted for PhD degree

by Darwin G. Caldwell

on

Compliant Polymeric Actuators as Robotic Drive Units

A co-polymer made from Polyvinyl Alcohol and Polyacrylic Acid (PVA-PAA) has been synthesized to form new robotic actuation systems which use the contractile and variable compliance properties of this material. The stimulation of these fibres is studied (particularly chemical activation using acetone and water), as are the factors which influence the response, especially those relating to its performance as an artificial muscle.

Mathematical models and simulations of the dynamics of the polymeric strips have been developed, permitting a thorough analysis of the performance determining parameters. Using these models a control strategy has been designed and implemented, with experimental results being obtained for a gripper powered by a flexor/extensor pair formed using these polymeric actuators.

An investigation of a second property of the polymer, its variable compliance is also included. Use of this feature has lead to the design, construction and testing of a multi degree-of-freedom dextrous hand, which despite having only a single actuator, can exercise independent control over each joint.

To

Two—10 and 6—Eight

xxx

Abstract

A co-polymer made from Polyvinyl Alcohol and Polyacrylic Acid (PVA-PAA) has been synthesized to form new robotic actuation systems which use the contractile and variable compliance properties of this material. The stimulation of these fibres is studied (particularly chemical activation using acetone and water), as are the factors which influence the response, especially those relating to its performance as an artificial muscle.

Mathematical models and simulations of the dynamics of the polymeric strips have been developed, permitting a thorough analysis of the performance determining parameters. Using these models a control strategy has been designed and implemented, with experimental results being obtained for a gripper powered by a flexor/extensor pair formed using these polymeric actuators.

An investigation of a second property of the polymer, its variable compliance is also included. Use of this feature has lead to the design, construction and testing of a multi degree-of-freedom dextrous hand, which despite having only a single actuator, can excerise independent control over each joint.

Acknowledgements

I would like to thank the Department of Electronic Eng. and the Department of Education (N.I.) for giving me the opportunity and finances to undertake this research.

Thanks are also due to all the postgraduates and staff (academic, technical and non-technical) in the department. Particularly I would wish to acknowledge the assistance given by the various members of the Robotics Research Unit, both by way of discussion and through their ungrudging willingness to donate equipment.

Finally I would like to thank my supervisor Paul Taylor for his guidence and advice throughout this work.

Contents

List of Figures

List of Tables

Chapter 1
Introduction

1.1 Research Motivation

At the commencement of this research project the primary objective was the development of a dextrous manipulator, (a manipulating device usually possessing three or more articulated fingers, which are capable of not only grasping, but also manipulating a range of awkward shaped and sized objects), and aspects of related technology.

Manipulators in one form or another have been in existence for many hundreds of years. The initial demand was stimulated by the need for limb replacements and devices were usually in the form of a hook. Aesthetic considerations did, however, produce some very clever designs, such as the metal hand made for the German knight Goetz von Berlichingen in 1509 [Simons, 1986]. This combined functionality with aesthetic appeal.

Many limbs were developed during and subsequent to this period, often with fingers powered by springs, ratchets or leavers. This spring/lever concept has been developed more recently by institutions such as the Army Prosthetic Research Laboratory to form a "voluntary closing hand" [Alexander, 1975].

Although quite advanced devices are now available, cost and a lack of real versatility means that the majority of manipulators are of the Dorrance split hook type, which combines a scissor motion with the holding action of the hook [Alexander, 1975].

The second area of research from which dextrous hands developed was the teleoperators used in space, nuclear and undersea environments to permit remote handling. This is obviously a very new area of research, but it is the

area in which advances in gripper technology are likely to be first applied.

When combined, these two areas of interest formed a platform for the development of dextrous manipulators for use in robotics.

The demands of automation make flexible manipulative machines much more attractive than fixed automation, since they can be adapted to different assembly tasks without requiring extensive hardware changes. In the past 15 years the need for industrial efficiency has further stimulated robotic research and led to the introduction of a number of dextrous manipulator designs. The early Belgrade Hand [Tomovic, 1962], used a motor to power springs, levers and balances which combined to move all four fingers simultaneously, and was able to grasp spherical and cylindrical objects. Since then sophistication and complexity have increased [Okada, 1977; Okada, 1979; Skinner, 1975; Hanafusa, 1977], while the apparently mammoth number of finger orientations has been evaluated [Crossley, 1977] and the basic manipulative requirements narrowed down to a relatively small subset. This handling knowledge combined with advances in computer and sensor technology have led the development of hands with very high performance levels such as Utah/MIT, Stanford/JPL and Karlsruhe hands [Jacobsen, 1986; Mason, 1986; Doll, 1988].

1.2 Background

Although no thorough analysis or optimisation of the gripper configuration has been conducted, it was felt that the best way to proceed was to base the design on the human hand. This does not, however, mean that an anthropomorphic design is the optimum in all circumstances.

Several factors influenced this decision. First the human hand shows that an anthropomorphic gripper when properly controlled can perform a tremendous range of handling movements. Second, research into dextrous hands has a wide range of applications in areas such as, remote handling (teleoperator), and as prosthetic devices. Third, manipulation movement can be easily tested on a readily available simulator, the operator's hand. Finally the development of a

flexible gripper means that a single manipulation unit can perform a multitude of tasks, many of which were not considered when the original design was made, and this versatility has obvious economic advantages.

The development of an advanced dextrous hand capable of performing a wide range of tasks requires the blending of a number of important features;

1. The mechanical layout, which establishes the dexterity of the gripper.

2. The type of drive, which governs the strength, compliance, compactness, and speed of the finger motions.

3. The number and size of the actuators, which effects the arm compactness and power available to perform tasks.

4. Sensors and control, which determine the sensitivity with which objects can be handled.

Following the identification of the major areas open to research in this field, the next stage was to study and appraise the state of the technologies, and hence determine if any aspect was being neglected. It was felt that the mechanical design has been relatively well covered and proven in recent years [Jacobsen, 1986; Mason, 1986; Doll, 1988]. Hence with the actual design of end-effectors having reached a fairly advanced stage, the next important step seemed to be the provision of a superior power source.

Actuators which govern the maximum objects load which can be manipulated, the speed at which grasping and manipulation tasks occur and the compactness of the arm/hand design have generally been ignored. This neglect has meant that the prime mover designs have been subject to many constraints, especially when applied to flexible, high precision, and high throughput robotic assembly tasks.

A final, but very important point which must be emphasized when characterizing the requirements of an actuator, is that actuators are needed to drive not only the arm, the hand and the wrist, but also in most instances a drive mechanism is required to perform the gripper functions of holding and releasing. This use of multi-axis machines, where in general a prime mover

will be part of the dynamic load of another prime mover means the force to weight ratio becomes extremely important in the machine system design. These very stringent conditions mean that even in the human hand the actuators (muscle) are positioned in the lower and upper arm because of extreme power/volume problems.

In view of the overall importance of actuator technology to the provision of a truly flexible manipulation device, the primary objective of this research became the development of new compact drive units which can meet the very stringent precision, force/weight ratio, force/volume ratio and response rate specifications.

This thesis reports on the development of new systems using polymer gels which may provide a viable future alternative to electrical, pneumatic, and hydraulic power systems. Two systems have been developed;

1). The first uses the contractile properties of certain polymers to produce a pseudo-muscular actuator.

2). While in the second system the variable compliance properties of these polymers are used in a new power distribution mechanism which provides independent control and motion in many joints using a single conventional actuator.

1.3 Thesis Plan

This work has been divided into a 9 chapters designed to show the processes involved in the development of a pseudo-muscular actuator - variable compliance tendon, and their application in a dextrous manipulator.

Chapter 1. In this chapter a basic introduction to dextrous manipulators is developed with particular reference to the areas which are most in need of research: power systems. From this evaluation a series of research objectives are produced. Clearly there is at present no shortage of power systems for use in robotics, most of which are based on hydraulic, pneumatic, or electric principles, but it is suggested that contractile polymer may provide a potentially superior range of devices.

Chapter 2. In the second chapter the advantages and disadvantages of conventional (electric, hydraulic, and pneumatic) units are evaluated based on a number of criteria, such as, power/weight ratio, response rate, ease of control and other factors which are specific to the actuator being studied. In a summary of this chapter the actuation systems used in a number of modern robots are compared, showing how different manufacturers have approached this power generation and distribution problem. This chapter, while being mainly concerned with the properties of the three main drive systems, also considers a number of new systems which may in future find their way into robots.

Chapter 3. The power systems which have been considered to date have largely ignored one method of energy generation which is actually the basis of the power systems used by most animals and plants. The direct conversion of chemical energy into mechanical energy (mechano–chemical conversion), is common in organic devices providing the efficient, flexible and very powerful drive units seen in animals such as horses, cheetahs and even in man. In Chapter 3 the development of artificial muscle based units is considered. A number of systems using these mechano–chemical cycles have been produced using different methods of stimulation. These methods are reviewed with particular reference to there potential use as an actuation system in a dextrous robotic gripper. This chapter also includes an appraisal of the mechanisms governing dilation and contraction, and how the various stimuli affect the internal energy balance. Through this work an understanding of the internal processes is sought, which aids in the development of new and improved systems.

Chapter 4. Having determined the mechanism which governs the dilation/contraction (muscle replicating cycle), chapter 4 catalogues the development and testing of a suitable material. This analysis also includes a study of the thermodynamics of the swelling and deswelling which again helps to further understand the internal mechanism. Tests on a range of polymers shows that the required motion can be produced using a number of materials,

but one material seems more suited than the others. This is a polyvinyl alcohol (PVA) - Polyacrylic acid (PAA) co-polymer which gives rapid, high force contractions, and possesses a high intrinsic strength. Details of the production of strips of this material are given together with an investigation of the factors (temperature of annealing, period of annealing, PVA-PAA ratio and stress) which affect production. Tests are also conducted to gain a fuller understanding of the physical and chemical properties of the crosslinked polymer (infra-red and x-ray tests). Finally the material's response to stimuli (pH, electrical, and thermal) is investigated and it is during a series of tests to improve the thermal response of the 'muscle' fibres that it is discovered that very impressive response characteristics can achieved through chemical activation using water to produce dilation and acetone to produce contraction. This mechanism is used in all subsequent tests.

Chapter 5. Now that a polymer has been prepared and its static properties have been characterised, the next step is to study the dynamic and force generation effects (the macroscopic muscle mimicking action) of chemical stimulation. As before, a number of parameters such as the degree of crosslinking, the polymer thickness, the solvent temperature, and the nature of the solvent affect the response, and these are thoroughly investigated, in chapter 5. The muscle is then tested for force generation and dynamic rate (using both single and multi-fibred devices), and force/velocity profiles are obtained which permit comparison with natural muscle. This comparison with natural muscle is developed throughout chapter 5, giving a good indication of the potential of this system. Also included in this chapter is work on the development of a work cycle for the polymer actuator based on the Carnot cycle principles. Using this study the theoretical potential and efficiency of the muscle can be compared with the experimentally determined values.

Chapter 6. In chapter 6 a mathematical model and simulation of the polymer responses to stimuli are developed using the knowledge derived in the experiments in the previous chapters. This shows that the mechanism of

dilation/contraction is basically governed by Fick's Law, but there are a number of anomalies and non-linearities which must be considered if an accurate model is to be obtained. For this model it is of paramount importance that an accurate estimate of the initial diffusion coefficient and the effects of concentration are obtained. This is accomplished in this chapter. Using this model, a simulation is written which models the response to chemical stimuli of a single strip and this is subsequently developed (following verification of the model accuracy by comparison with experimental results) to form a simulation of a muscle actuator pair which could be used in powering a robot gripper. The control requirements are outlined in this chapter with the reasoning being given in more detail in the next chapter. Three control strategies are developed and tested on a full pseudo-muscular actuator simulator, and from these results a force/position control mechanism is chosen as giving the 'optimum' response. Further control tests are conducted on this simulator before implementation on an experimental device in Chapter 7.

Chapter 7. Based on the work in the previous chapters, a muscle actuator pair consisting of a flexor to close the gripper, and an extensor to open the gripper, was built and is detailed in chapter 7. The development and reasoning involved in the design of this actuator is outlined in this chapter, together with details of the mode of operation and the control algorithm regulating the flow of chemicals in to and out of the polymer muscle cells. Results showing the performance of this actuator are also included, as are details on possible improvements which could significantly enhance the system performance. This chapter is effectively the culmination of the work on the development of a new pseudo-muscular actuator and attempts to demonstrate the full potential of such a mechanism.

Chapter 8. In chapter 8 an application of another of the properties of the polymer (variable compliance) is put to use in the design and development of a dextrous manipulator, powered by a single stepper motor. Through the use of strips of polymer in the inter-connecting tendons linkages, the compliance of

the tendons can be selectively varied permitting regulation of the transmission of power to any particular joint. Included in this chapter is an analysis of the motions and abilities of a human hand, which shows that using this single actuator configuration all common/working 'grasps' can be achieved. Initial results using this system are included in this section of the thesis, together with suggestions for improvements which could be incorporated into a later series of demonstrators.

Chapter 9. The final chapter summarises the properties and the abilities of the pseudo-muscular actuator, mechano-chemical materials, and PVA-PAA co-polymers in particular, outlining possible benefits, conclusions drawn from the research, and suggesting future lines of development which might be worth pursuing.

A short section is also included outlining a few applications which would be possible using properties of the material other than its mechano-chemical response and its variable compliance.

Chapter 2
Power Systems

2.1 Introduction

Industrial motivation to increase efficiency has led to a need for robots using compact drive units which must meet very stringent precision, power/weight ratio, and response rate specifications. Virtually all modern robots use either hydraulic, pneumatic, or electrical drive systems to meet these requirements. This chapter describes the most common types of actuator which use these power systems, permitting a comparison of their relative abilities. This is then developed to include a section on new actuator technologies which may be incorporated into robotic systems in the future.

2.2 Hydraulic Drives

Traditionally, hydraulics has been the most common of the primary systems, but it is now being superseded by electric motors, both AC and DC [Automation, 1987]. Hydraulic actuators extract energy from a fluid (hydraulic oil) and convert it into a mechanical output which is used to perform useful work. The power is transmitted to the load as either linear or rotary motions using linear actuators (hydraulic cylinders) and rotary actuators (hydraulic motors) respectively. Drives of this type have excellent power and force/weight ratios, while at the same time being very compact. The high pressures used (up to 200 bar is common) [Elonka, 1967], mean that the fluid compressibility is low giving good velocity and positional control, which combined with high stiffness means that heavy loads and high torques can be withstood without degrading the accuracy. Fluid systems are also found to be easy to implement,

durable and resistant to harsh environments, but they do have a number of drawbacks.

Currently they are the most expensive of the common drive units [Maus, 1986], filtering to remove impurities and contaminants is also costly, with leakages at best being inconvenient and at worst preventing the use of hydraulic systems in clean environments such as the food and drink industry. The piping also creates problems, being bulky and awkward to install, and finally, fire is a potential hazard with the more common petroleum based fluids having to be replaced by water-glycol or phosphate ester mixtures.

The most simple, reliable, and least expensive hydraulic systems are the piston type linear actuators. These units consist of an external cylinder with a central sliding piston attached to a rod. Pressure on the piston, (either pushing or pulling) generates forces which are transmitted through mechanical connections to the load. These cylinders may be either single-acting, figure 2.1a, or double-acting, figure 2.1b.

With the single-acting cylinder, forces can be applied in one direction only, motion being produced when fluid enters the chamber and impinges on the piston head. The force generated is dependent on the piston area and the fluid pressure. The return stroke which is passive, is powered either by gravity or by the release of energy stored in a spring compressed during the initial stroke. In the double acting design, forces can be applied in both directions, with fluid on both sides of the piston. At the end of each stroke the 'spent' fluid is returned to a central reservoir to be reused.

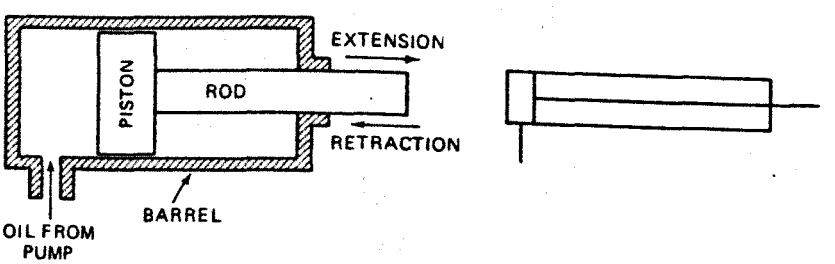

Fig. 2.1a

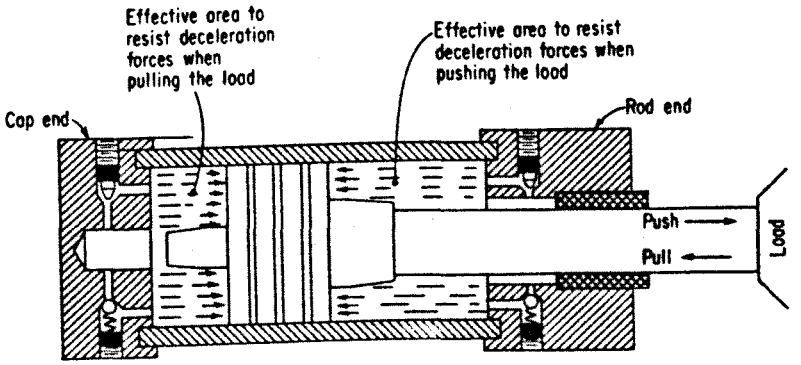

Fig.2.1b

Fig. 2.1a. Single Acting Hydraulic Cylinder. Fig. 2.1b Double Acting Hydraulic Cylinder with cushions at both ends [Elonka, 1967].

To prevent damage during operation the double-acting cylinders often have cylinder cushions at their ends to dissipate the energy developed during motion. This cushioning is achieved either by trapping fluid between the piston and the mechanical end of travel, or else an external deceleration valve may be used.

The actuators considered so far all have stroke lengths which are limited by the overall length of the cylinder, and this can cause difficulties where space is restricted. Such problems can, however, be overcome by using telescopic or multi-stage cylinders, figure 2.2, which produce relatively long strokes in a short unit by using pistons and cylinders which move into each other.

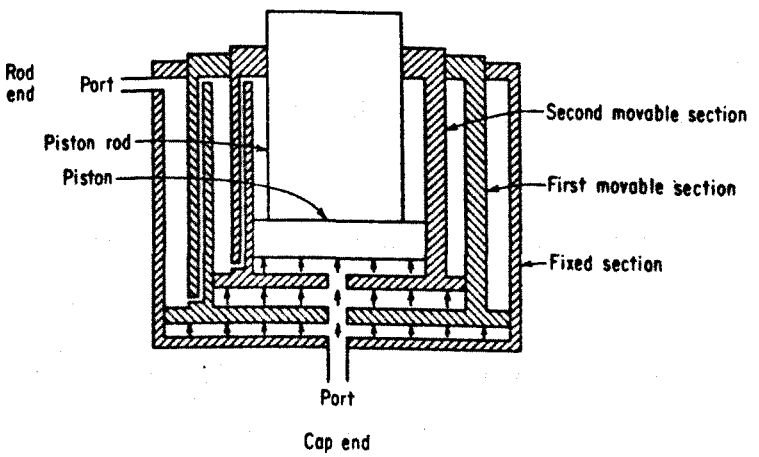

Figure 2.2. Multi-stage Hydraulic Cylinder [Elonka, 1967].

Rotary hydraulic motions are classified as either limited or continuous. In the limited motion system, the rotation is less than one revolution with the same basic operating principle as is used in the linear actuator. These rotary actuators are used when high instantaneous torques (up to 110,000Nm) are needed [Esposito, 1980], but the space available is small. Actuators based on this design, figure 2.3, are formed into chambers containing the fluid and a movable surface against which the fluid acts. This movable surface is then connected to a shaft which distributes the power as required. By introducing the fluid at different ports the direction of rotation can be controlled, while combined inputs hold the unit steady under loading. As with the linear actuator, cushioning can be used to prevent damage.

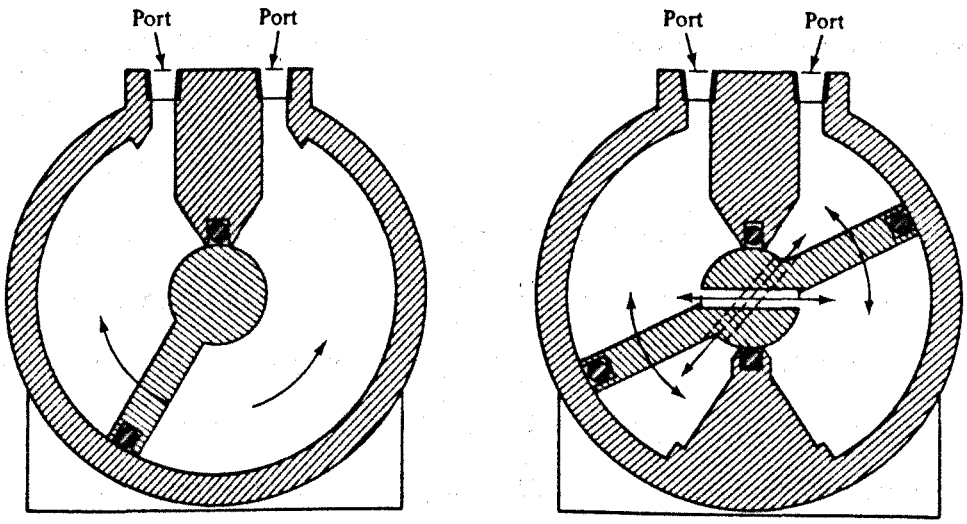

Figure 2.3. Single and Double Vane Rotary Actuators [Esposito, 1980].

Rotary hydraulic motors are actuators which can rotate continuously. Unlike linear actuators which are widely available, rotary motors are very specialised and this tends to make them very expensive [Banks, 1988]. Three type of motor are in common use; gear, vane and piston, the choice being determined by the application, the performance required and the cost.

With the gear motor, figure 2.4, pressurized fluid is pumped in at the inlet. The tight fit of the gear mesh means that to reach the outlet the fluid must move the gears; one of which is coupled to the drive shaft, providing the actuation force. The direction of motor rotation is determined by which of the

ports is used as the inlet and which is used as the outlet. The relatively high internal leakages and the unsymmetrical input pressures make this design unsuitable for high torque operations, and it is most commonly used as a constant speed drive where rotation speeds >500rpm are necessary [Banks, 1988]. The main advantages with gear motors are that they are fairly simple and cheap relative to other hydraulic motors.

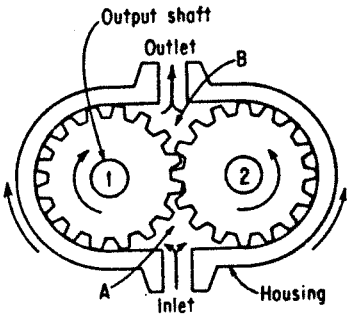

Figure 2.4. Hydraulic Gear Motor. [Elonka, 1967].

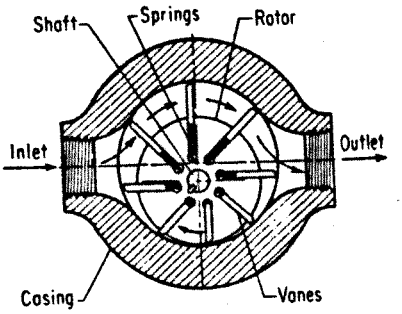

Figure 2.5. Hydraulic Vane Motor

Vane motors, figure 2.5, use the pressure differences on vane surfaces to produce torque. These vanes which are connected to the shaft, are sprung or pressure loaded forcing them to form a seal with the motor body. At higher speeds the vanes are held out by centripetal forces. The high pressure fluid is fed in at a series of opposing ports. This reduces pressure distortion and gives a balanced system. The outflow is through a second series of ports which are 180° offset, with each vane forming a chamber for the transfer between the inlet and the outlet port. These motors are more suitable for low speed operation than gear motors and are capable of starting from stall under load. Internal leakages are, nevertheless, still a problem preventing maximum torque from being generated at low speeds.

Piston motors, can be either radial or axial in form [Elonka, 1967]. In the radial motor, torque is produced when fluid flow through the port forces the pistons, which are within the cylinder block, out of the cylinder head. These pistons can only move out of the cylinder block when the whole assembly rotates, and hence by coupling this to a drive shaft power transmission is

obtained.

In the axial motor the operation is similar, with the fluid driving the pistons against an angled swash plate. The reciprocating action causes the drive shaft, swash plate and piston body to rotate. The torque produced is proportional to the area of the piston heads, and is a function of the swash plate angle, with increased angles giving increased torque capacity but decreased shaft speed. Often the swash plate is adjustable within set limits to allow variations as required.

Piston drives are the most efficient of the hydraulic motors, capable of operating at low speeds, and high torques, but they are not used extensively in robotics due to their complexity and expense.

In general a hydraulic drive system consists of a hydraulic pump, motor, and the appropriate valves and piping. Such a system is known as a hydrostatic transmission. In the first instance, energy is provided from a prime mover such as an electric motor or a combustion engine. These hydraulic drives are most often used to power very large robots, but the excellent power/weight ratio means that they can be used anywhere large forces must be generated in a confined space, or where there are limitations on the joint loading.

Recent research into smaller hydraulic motors has lead to the development of a range of compact systems (6.5mm x 6.5mm x 57mm) which when operating at 240 bar can provide up to 185W at rotation speeds up to 5000rpm [Findlay, 1988]. These new products may perhaps lead to renewed competition against electric motors.

2.3 Pneumatic Drives

Pneumatic systems use pressurized gases rather than liquids to transmit and control power. As the name implies these units usually use air as the fluid medium (although inert gases have been utilized), because it is relatively cheap, safe, and readily available. This makes pneumatics of particular benefit in high temperature environments or where an electrical spark may cause an explosion

or fire.

Although pneumatic actuators operate on the same basic principle as hydraulic systems, there are several reasons for using the pneumatic drives rather than the more common hydraulic devices. Since the fluid medium is gaseous rather than an oil, lower pressures (<250psi) can be used, giving actuators of lighter construction. The use of a gas in pneumatic drives also gives advantages in terms of inertia, with the greater mass of the oil in hydraulic systems making very rapid acceleration and deceleration of links or objects more difficult, while the lower viscosity of air can help to reduce friction and power losses. Using air as the fluid medium also means that pneumatic units are clean and can expel spent gas directly into the atmosphere. This does, however, make pneumatics quite noisy. As with most industrial projects a major consideration in choosing pneumatics actuators is the economic cost. In general pneumatic devices are cheaper than their electric or hydraulic equivalents, they are readily available 'off the shelf', have relatively low maintenance costs and are very reliable. This combined with the availability of compressed air in many industrial sites makes pneumatics quite an attractive proposition for certain robotic applications.

The main difficulties associated with pneumatic designs generally result from the compressibility of the air. Precise control of actuator velocity and position is difficult or impossible to obtain, with smooth and steady motion under variable loading requiring metering of the exhaust flow rate. It is also found that, unlike hydraulic systems, pneumatics require a lubricant to be injected into the airstream.

Air lubricators ensure correct lubrication of internal parts by inserting drops of oil directly into the air flow. These drops are transformed into an oil mist prior to being transported downstream. This oil mist is composed of coarse particles which may travel 6m or more, and fine particles which may remain in the air for up to 90m [Esposito, 1980]. Good lubrication means that friction between moving components is reduced, reducing wear and prolonging the

actuators working life.

Pneumatic systems have been used for many years, most often as low load systems where mechanical end stops can be fitted to limit the ranges of motion. This means that the poor controllability of pneumatics is not so critical. Nevertheless, as with hydraulics, pneumatic drives are now often being replaced by electric motors.

The pneumatic linear actuator has the same basic design and operation as its hydraulic counterpart, with cylinders available in single and double acting form, using air rather than hydraulic fluid as the actuating medium. The only significant difference is that it is no longer necessary to recirculate the fluid. When limited rotations are required, it is possible to use a rotary actuator which operates on the same principles as the linear model. This again gives a device which can be easily mounted in a confined area, while having high instantaneous torques in either direction.

Rotary pneumatic motors can be used as smooth sources of power. They, like their hydraulic equivalents, are not susceptible to overload damage and can be stalled for extended periods without 'burnout'. Low inertia means they can be started and stopped rapidly and by regulating the pressure and monitoring the flow, infinitely variable torques and speeds are possible. This has led to them replacing electric motors in many industrial handtools.

2.4 Electric Drives

Electrical drives, which now form the design most commonly used by robot manufacturers, are most often in the form of rotational motors, although linear drives are available for special applications. As with hydraulic motors, gearing, belts, chains or ball-screws are generally used in the transmission of power from the actuator to the load. The torque is generated when an electric current flows through a magnetic field, the direction of motion of the motor being dependent on the flow direction. The electric drives used in robotics fall into three classifications; DC motors, AC motors and stepper motors. Electric

motors of all three types are popular because of their ease of use, their speed variability, and accurate positional and velocity responses. They are also clean, acoustically quiet (although they may produce considerable electrical noise), relatively cheap and readily available.

As with the previous drive units, use of electric drives does have drawbacks, which include low power and torque/weight ratios, and the dangers of electric shock and sparking in a flammable environment. These advantages and disadvantages apply to different extents in each of the motors classified above and will be dealt with in more detail when studying the specific motor.

DC motors as the name implies all use electrical direct current as their power source and have most of their major components in common, although minor changes are usual in attempting to improve specific parameters.

There is a stator which along with other non-moving assemblies forms the frame. A rotating armature and windings form the rotor, while the flow of current into and out of the rotor is by way of the brush or commutator. Direct current motors are classified as series, shunt, compound, or permanent magnet, the type being determined by the method of connecting the armature and the field.

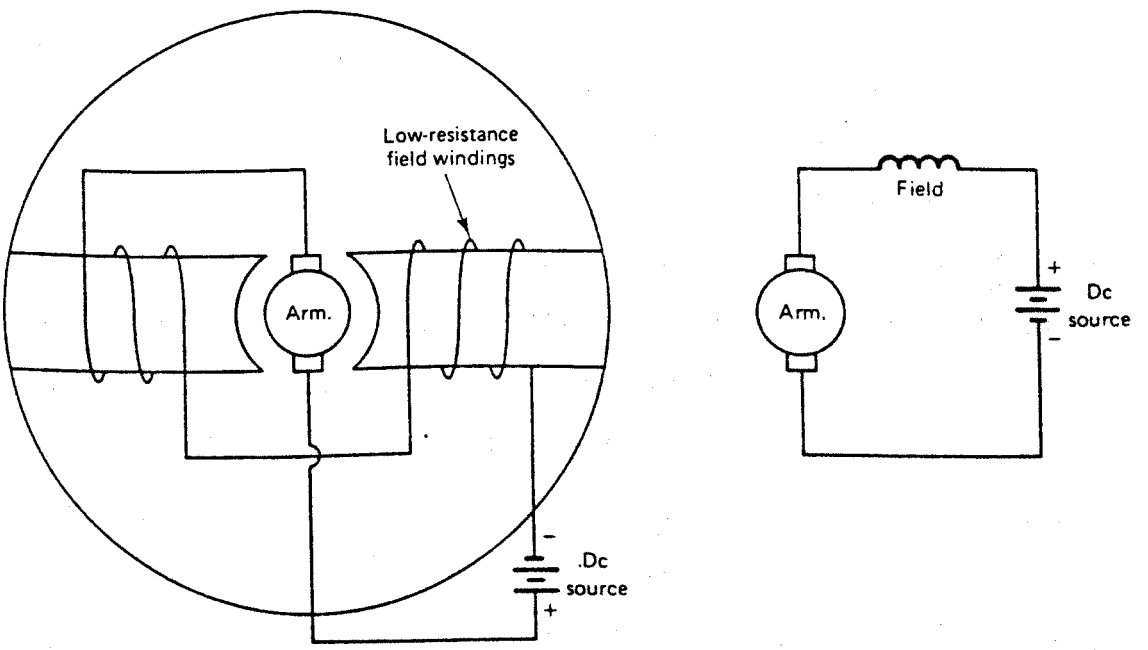

Figure 2.6. Series Wound DC Motor [Patrick, 1984].

In the series wound motor, figure 2.6, the armature and field circuits are connected in series. As all the armature current then flows through the field windings only a few turns of large diameter, low resistance wire are required. The large current flow at start-up induces a strong magnetic field and consequently a high torque. Series wound motors are, however, found to have poor speed stability, ie to have speeds which are very high under no load but drop rapidly as loading is increased [Patrick, 1984].

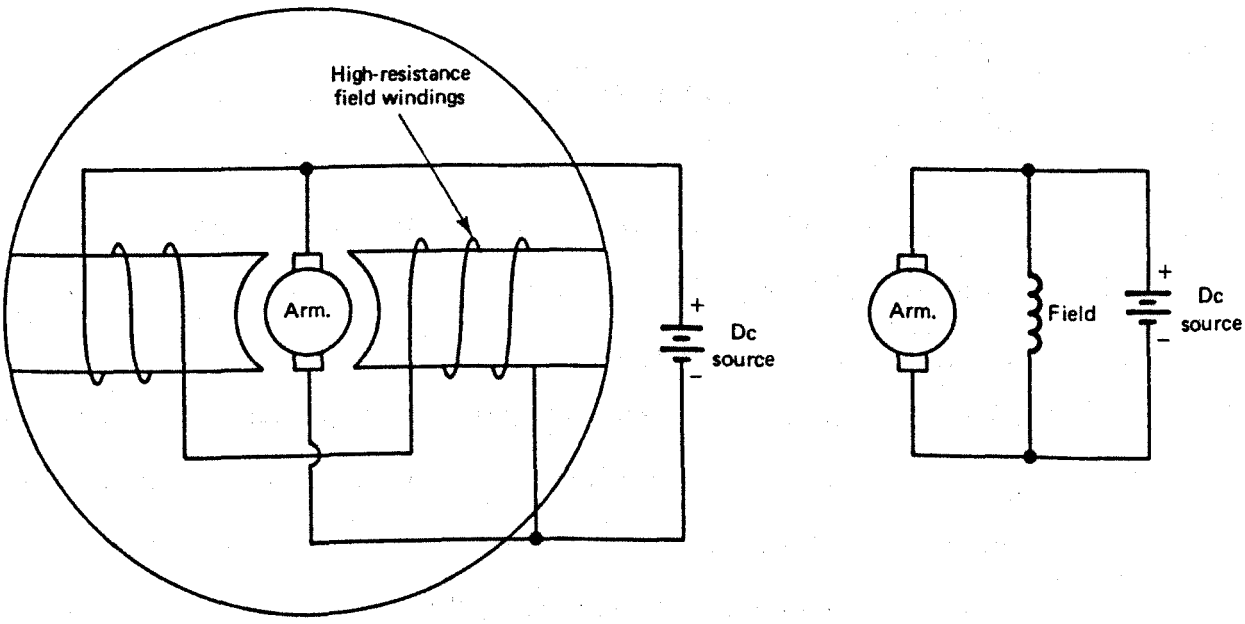

Figure 2.7. Shunt Wound DC Motor [Patrick, 1984].

In shunt wound motors, figure 2.7, the field coils which are wound a great many times using thin-diameter wire are connected in parallel with the armature. This high resistance path lets only a small current flow, although a high electromagnetic field is generated due to the number of turns; this gives a low to medium starting torque. Any variation in loading causes only small changes in the field strength and helps to improve the speed stability.

Combined shunt and series motors use both the techniques outlined above, which allows considerable latitude in design, and combines the desirable aspects of both series and shunt motors. This gives high starting torques and good speed stability under loading, the only real drawback is the increased expense of two sets of windings.

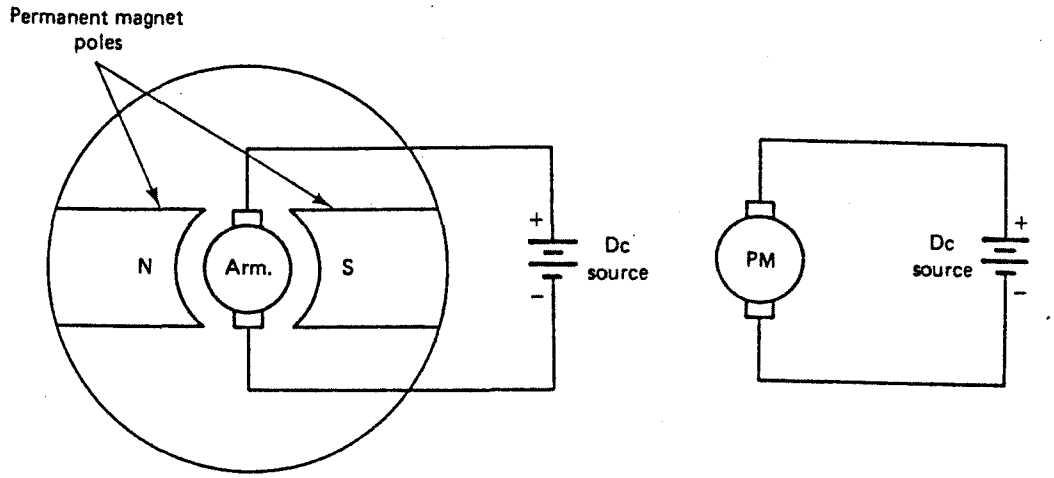

Figure 2.8. Permanent Magnet DC Motor [Patrick, 1984].

The fourth design, the permanent magnet motor, has no field windings, and the power source is connected directly to the armature, figure 2.8. The advent of low cost, rare-earth magnets has meant that relatively high torque, low weight motors are becoming commercially available. These devices now form the most common drive units in small robots because they are self-starting (able to start rotation when electrical power is made available), they can easily change direction by changing the voltage polarity, they are simple, and speed regulation is voltage controlled.

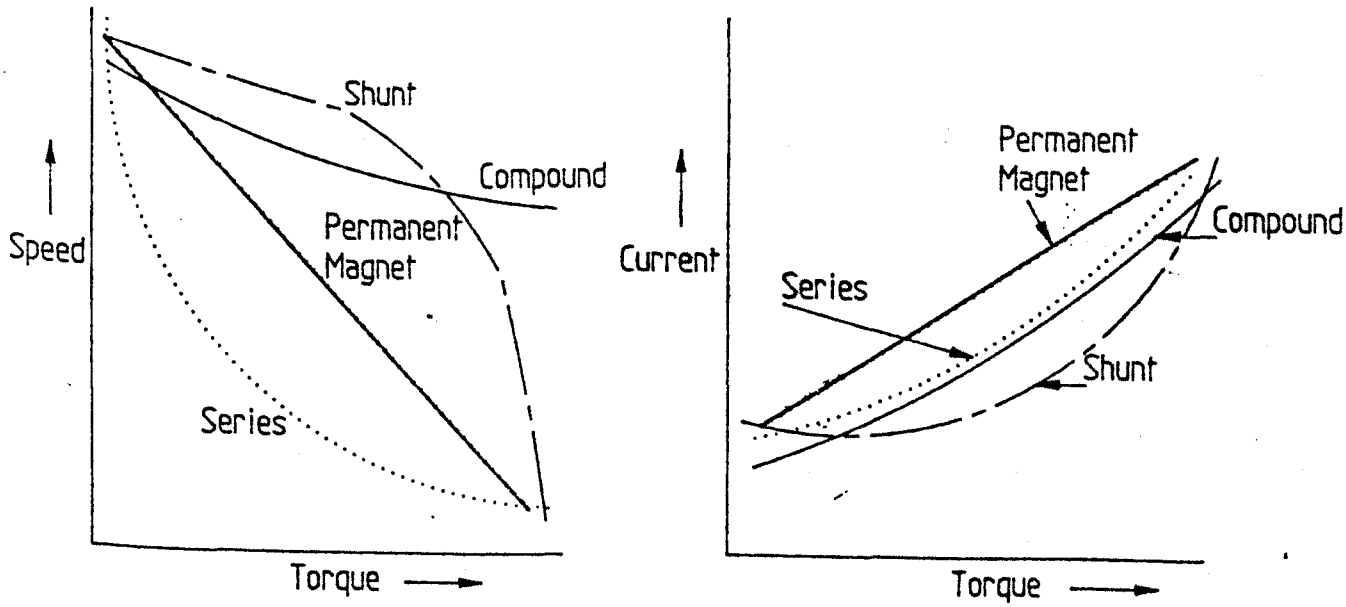

Figure 2.9a and b. Speed/Torque and Current/Torque DC Motor Profiles [Electro-craft, 1980].

A comparison of the relative merits of each of these designs in terms of the speed/torque and the current/torque characteristics is given in figures 2.9a and b.

Of similiar design to the standard DC motors are the brushless DC motors, which have electronic commutation to reduce noise (acoustic and electrical), and wear, although with the penalty of increased expense.

Brushless DC motors have the torque–speed characteristics of a conventional permanent magnet DC motor, but use control circuits which resemble those of stepper motors or frequency controlled AC motors. The stator in a brushless DC motor is most commonly formed in a outer ring with slotted windings, the rotor consisting of a shaft/hub assembly made from permanent magnet materials.

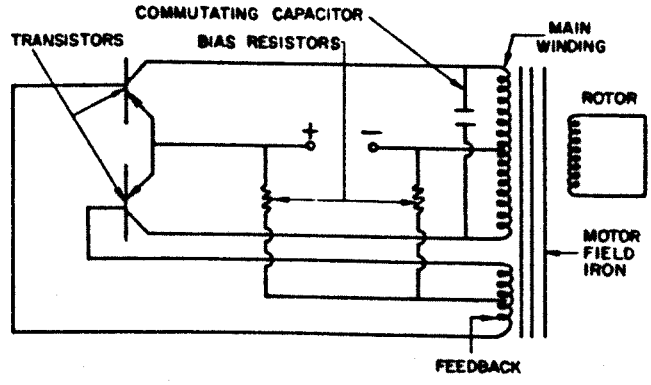

Figure 2.10. Typical Brushless DC Motor Drive Circuit [Greenwood, 1965]

Operation is by way of semiconductor switching circuitry, with two and three phase motors being preferred. By monitoring the motor position using feedback from the output and varying the power supplied between positive and negative V_S, forward and reverse torques can be produced. While by careful sequencing, the motor can be energised as required to give the rotary performance demanded, figure 2.10.

Open loop position and velocity feedback make computer control of DC

stepper motors simple and they have thus become very popular as robotic actuators. Operation depends on the conversion of electrical pulses into rotary or linear motion, with each step producing a constant known movement. This motion is repeatable, which gives accurate positional response, while the pulse rate can be varied giving accurate velocity control. Construction is much as for convectional motors, with stator coils (poles) and a permanent magnet rotor, figure 2.11.

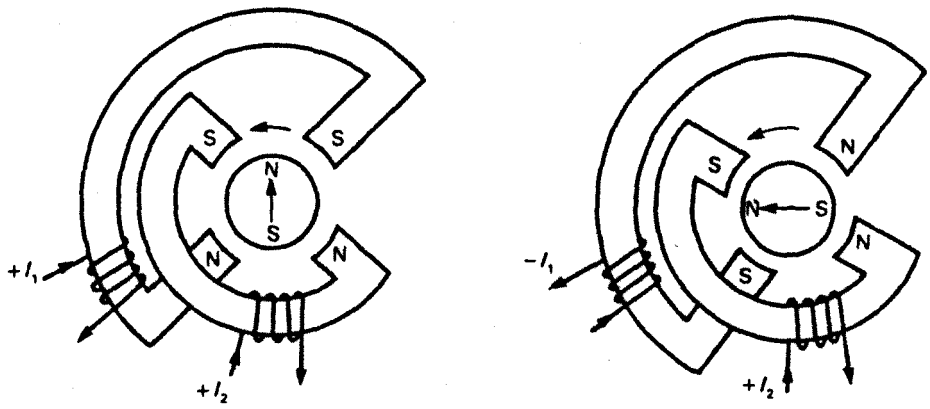

Figure 2.11. Stepper Motor Design [Bannister, 1986].

The positioning and step size can be made more accurate by increasing the number of poles, while the phasing arrangement determines the direction of rotation. The increased complexity of stepper motors makes them slightly more expensive than convectional DC motors while being slightly less powerful, but this is often more than offset by the ease with which accurate control can be achieved.

The need to reduce or eliminate motor wear, particularly in the brush assembly means that occasionally AC motors are used rather than DC. There are a great many types of AC motor but the most common are induction motors, AC brushless motors, and synchronous motors. These are all smaller than their DC equivalent but are not so easy to control, requiring encoder or resolver feedback to give accurate position regulation. They are, however, ideal if a constant velocity is required.

Each type of AC motor has special properties, being generally classified by

application, construction, principle of operation, or operating characteristics.

Induction motors which are the most common type of AC motor form a large family, operating by inducing current in the windings. Squirrel-cage induction motors are the simplest and cheapest of all the AC types, requiring the least maintenance because there are no commutators or brushes. The starting torque is high, but generates large currents which mean that in all but the smallest motors a reduced starting voltage must be used, hence reducing the torque [Fitzgerald, 1945]. The basic design of a induction motor is shown in figure 2.12.

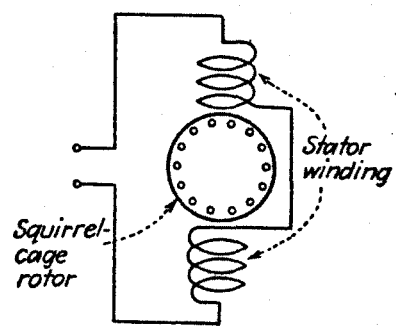

Figure 2.12. Schematic diagram of a Single-Phase Induction Motor [Fitzgerald, 1945].

Within the induction motor family the type is defined by the method of starting which is used, with the design and performance characteristics being slightly different for each case [Fitzgerald, 1945].

The *shaded pole motor* has salient poles with half of each pole surrounded by heavy, short circuited windings (shaded coil). The induced currents in the shaded coil cause the flux in that half of the pole to lag that in the other half. This results in a periodic shift in flux from the unshaded to the shaded half of the pole, producing a low starting torque, figure 2.13a.

Split phase motors have two stator windings with their axes at 90° to each other. The auxiliary winding has a higher resistance - reactance ratio than the main winding so the currents are out of phase. These induced fields produce a rotating stator field which causes the motor to start. At about 75% of the

synchronous speed the auxiliary winding is cut out by a centripetal switch, figure 2.13b.

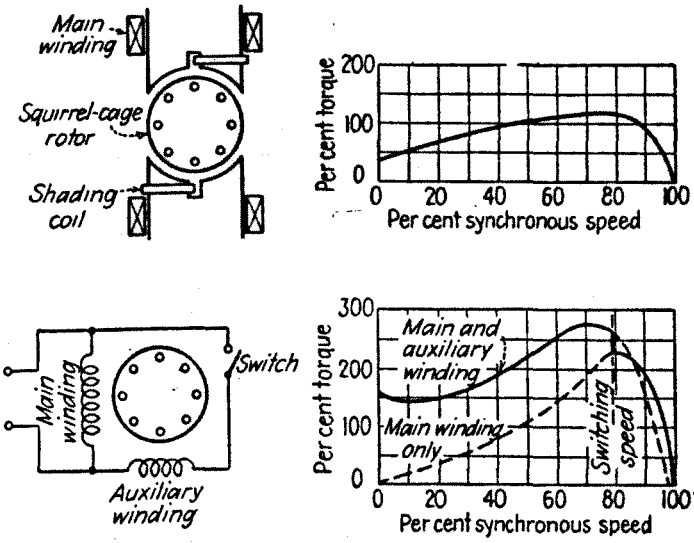

Figure 2.13a and b. Torque/Speed Curves for Shaded-pole and Split-phase Motors [Fitzgerald, 1945].

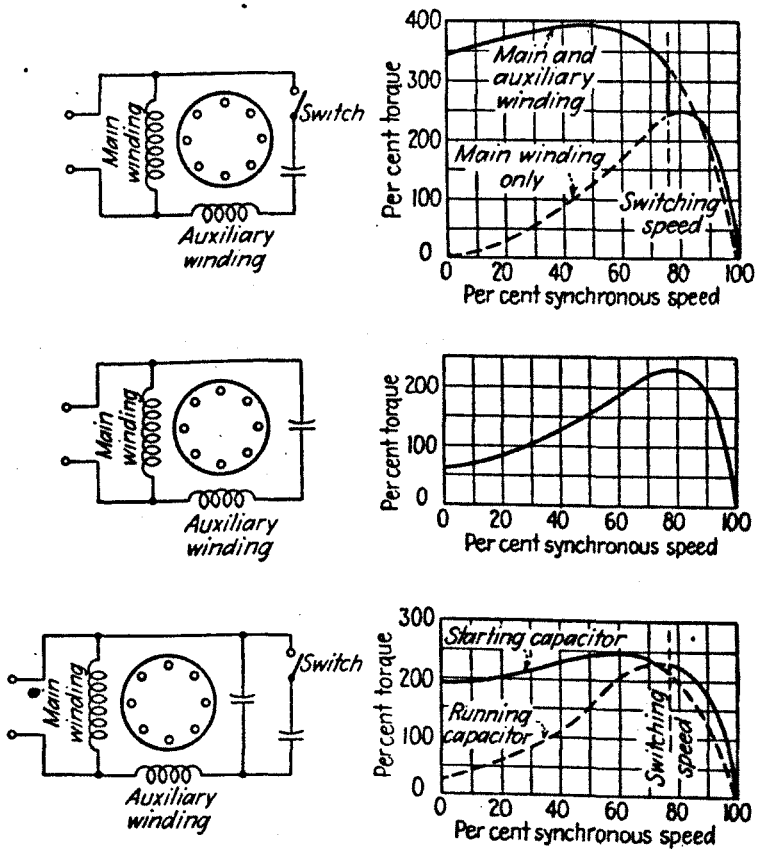

Figure 2.14a, Capacitor-Start, Induction-run Motor

b, Single value Capacitor Motor

and c. Capacitor Start, Capacitor Run Motor [Fitzgerald, 1945].

With the *Capacitor start motor* the design is a split phase arrangement as above, but in this case the phase displacement is a result of a capacitor in the auxiliary winding. This winding can be switched out at 75% as before, giving a motor with high starting torque, figure 2.14a. If the auxiliary winding is not cut out the running performance of the motor is improved although the starting torque is sacrificed because the capacitor value used is a compromise between the best running and starting values, figure 2.14b. If a twin capacitor system is used there is no need to compromise the settings and optimum starting and running performance are obtained, figure 2.14c.

The induction motors above cannot be speed or direction controlled, but the absence of sliding parts means that they can be very useful when the electrically driven robot is required for use in a flammable environment.

In the previous designs the rotor current is obtained by conduction from the stator. With repulsion motors, which are of similiar design to the series wound DC motor, except that the rotor and stator are inductively coupled, the rotor current is derived from the transformer action of the stator, figure 2.15. The brush axis is placed at an angle to the stator field. With the axes in line there is a current, but no force, while at 90° there is power but no current. This motor action can be used in two modes of operation where either, the repulsive force is used continuously (for start-up and running), or where the repulsive force is used to start the rotation, switching to induction principles when the motor has almost reached its operating speed.

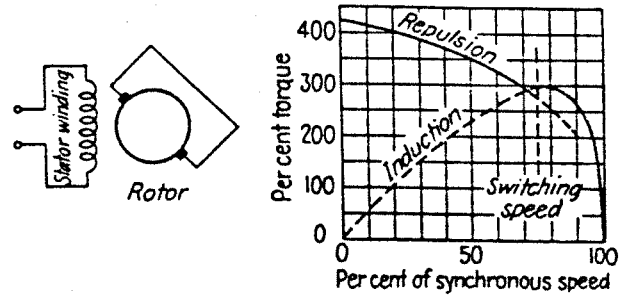

Figure 2.15. Repulsion Motor Schematic and Characteristic [Fitzgerald, 1945].

Where constant speed is essential synchronous motors are used. Large designs use DC fields in the rotor and three phase armature windings. For lower power requirements a design is used employing a number of copper bars in the pole face, with end connections; which effectively form a squirrel-cage. At start up the synchronous motor behaves like a squirrel-cage induction motor. As with the squirrel-cage motors the stator voltage must be reduced at start up to prevent the development of large currents. These motors are most often employed in tasks requiring fixed constant speed, with direction reversals being possible by changing the phasing on multi-phase motors.

In the previous motors only AC or DC can be used, but never both. One motor can, however, use either type of supply. The design used in the DC series motor, when supplied with AC; forms the AC series (universal) motor. If AC is applied to a series motor the stator and rotor field strengths will vary sinusoidally in magnitude, while having the same phase. This produces a motor with a high starting torque and a performance profile similar to its DC equivalent. Generally the response to AC will be poorer than for DC, figure 2.16, with commutator problems being increased. It does, nevertheless, have one advantage over other AC motors in that its speed can be controlled by varying the applied voltage.

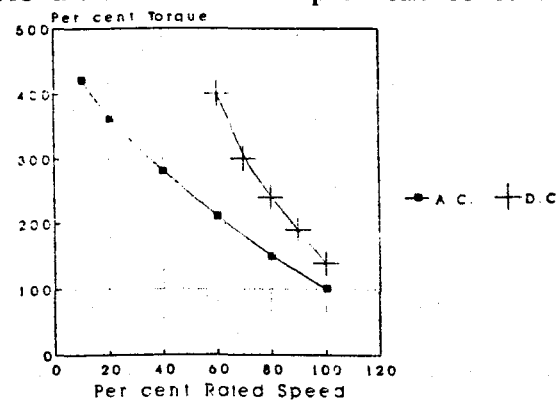

Figure 2.16. Typical Torque/Speed Profiles for a DC and an AC Universal Motor.

Generally speaking AC motors have not been used as extensively in robotics as DC mainly due to a lack of variable speed control.

2.5 Natural Muscle Power

As most robots are modelled on man or some other animal it is interesting to consider the power system which they utilize.

Animals use 'muscle' (skeletal) to exert forces and move objects including themselves. These muscles are biological machines of great complexity [Woledge, 1985], which convert chemical energy made available in the form of food, into forces and mechanical work. In higher animals the muscle content of the body can be up to or even above 40% [Wilkie, 1976], with a wide variation in the designs, contractile rates and power. These differences are mainly due to the functions that a specific muscle must perform.

Muscle action is triggered by electrical impulses transmitted through nerves from the brain (occasionally automotive responses are triggered from the spine). Chemical energy is then released by the conversion of ATP into ADP, with the filaments which form the muscle using this energy during their sliding motion. The actual physical forces which produce this sliding motion are not as yet understood by biologists.

As with other machines the power (force x velocity) which can be produced is dependent on the loading (light loads move quickly, heavy loads move slowly and may even prevent motion). This power output is produced by extremely small fibres (a few microns in diameter) which possess little strength on their own, and it is only when combined in bundles containing hundreds or thousands of fibres that large contractile forces can be generated.

Another factor of great importance in the design of muscles is that they can only pull; a pushing action is not possible. Hence to produce virtually any motion two muscles are required, the coordination of their movements being a complex task which must be solved by the brain.

If a muscle were to have its specifications summarised as for a typical robot actuator it might be described as;

1. A linear motor
2. Robust and dependable with a working life in excess of 65 yrs.

3. Wide range of models.

4. Direct chemical to mechanical energy conversion. Efficiency varies with speed of contraction but generally ranges from 45% up to 70% [Woledge, 1985].

5. In built servo feedback giving accurate control.

6. Rapid response (<5ms), and fast controllable motion.

7. High stress generation (15 - 40N/cm^2) [Wilkie, 1976].

8. Excellent power/weight ratio, typically from 40W/kg up to 225W/kg, but may have a very short peak of 1kW/kg [Wilkie, 1976].

9. Good Repeatibilty and accuracy.

10. Modular and expandable.

11. Environmentally Safe.

2.6 Direct versus Indirect Drives

Power generated by the many types of actuators considered above is transmitted by either direct or indirect drives. With the direct drive, there is no mechanical linkage between the actuator and the driven joint. Hydraulic and pneumatic motors and cylinders and to a lesser extent rare-earth permanent magnet motors can take advantage of this method because of their high force/torque capabilities. This means that an actuation system with much greater accuracy can be incorporated into a compact design which can easily be accommodated in the robot linkages. The simplicity of this technique means that maintenance is relatively easy.

With the indirect drive mechanism mechanical linkages are included generally to increase the force/torque output, although a second benefit can be the removal of heavy actuators from the joint extremities reducing loading. These linkages (gears, ball screws, harmonic drives, belts, chains, etc) have the effect of increasing the backward stiffness, which means that the effects of loading changes on the drive are small, but the introduction of non-linearities tends to increase the system control difficulties. Generally, if it is possible mechanical

linkages are avoided, to reduce costs, complexity and aid control.

2.7 Compliance Control

Compliant motion occurs when the position of a manipulator is constrained by a task or object. This constraint can be handled in two basic ways, either by a passive compliant device built into the manipulator or through active compliance (force) control implemented in software.

The use of controllable compliance in certain insertion tasks led to the development of the remote centre compliance (RCC). The RCC is an elastic mechanism used to control the stiffness of a grasped object. By placing the centre of compliance of this object at the tip of the object, insertion was possible without jamming, a vital technique when two parts must be mated [Drake, 1979].

The software approach to compliant control has been studied by a number of researchers. Whitney [Whitney, 1977] formed an admittance matrix to study the problems of arm force control, with Gerelle [Gerelle, 1978] extending this work and identifying conditions for stability and symmetry in this matrix. In many cases a compromise was sought [Paul, 1976; Raibert, 1981] where some of the joints were under force control while others remained under position control. This often meant a careful analysis of the motions had to be made to determine which joints should have which type of control. Development of these 'hybrid' controllers led to the stiffness controller [Mason, 1985], in which the stiffness of each of the joints could be specified by the programmer. By sensing the position and forces acting, the system could determine which point the task had reached and hence change the compliance as required. Methods have recently been proposed based on observation of human skeletal muscle, whereby the stiffness of each joint is regulated, giving 'Direct Compliance Control' [Kaneko, 1988]. This design suggests that the natural system might be a good starting point.

Compliance control in animal muscle is defined as the instantaneous change in

length with tension (dl/dT). When unstimulated, the muscle is very compliant (little stiffness) and it is believed that this is because the fibres can move past each other with little restraint [Woledge, 1985], but when stimulated stiffness increases significantly, following the same time course as the tension.

Clearly good control over the compliance would be very beneficial and is at present not easily achieved using any of the common power sources.

2.8 Experimental Actuation Systems

Although the previous sections cover the main factors governing the utilization of the three power units most commonly used in robots, a number of new techniques are being developed to try to overcome the constraints imposed by these systems.

It is possible to improve some of the control characteristics associated with pneumatics power by using a device known as a McKibben muscle [Wolff, 1970]. This is a tubular piece of netting closed at both ends enclosing an inflatable rubber sack. When the sack is inflated, the diameter increases and this shortens the length of the net bag so imitating the action of a real muscle.

A second actuator based on controlled air flow has recently been developed with:

1. Accurate smooth motion from start to stop.
2. Low hysterisis and friction.
3. Low cost, yet powerful actuation from a light weight compact device.
4. Rotation as well as longitudinal motion using the same basic driving principle.

This actuator has been applied to the lifesize puppets in the television series 'Spitting Image' with considerable success.

The system uses lengths of flexible flat hose and it is the behaviour of these devices when filled with air which provides power for actuation. The arrangement of the hose controls the motion which can be achieved. When wrapped around a shaft, inflation produces rotation, while linear action is

produced by passing a tendon over the bag. On inflation the tendon is effectively shortened giving motion, figure 2.17.

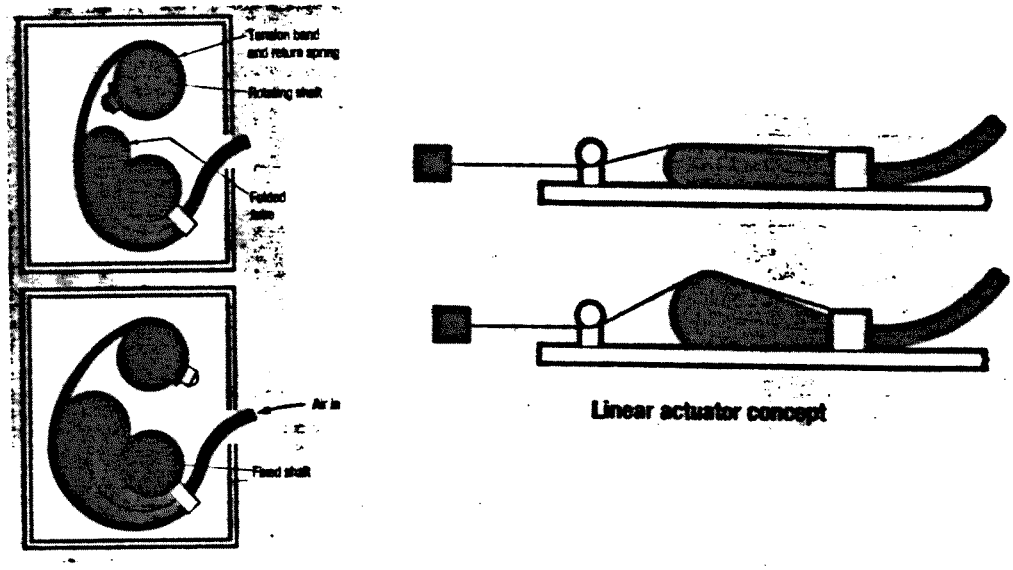

Figure 2.17. Pneumatic Actuators used by 'Spitting Image' Puppets [Findlay, 1988].

Simple electromagnetic actuators have been developed using solenoids. These give a compact, linear actuation unit with the potential for quite large force generation, although this is dependent on the length of the stroke. The major drawback with this unit is the poor control possibilities with only bang-bang motion being available, hence poor speed and position regulation.

Also using electrical generation but working on totally different principles are the piezo-electric actuators. There has been a tremendous surge in interest in these motors co-inciding with the development of new materials, such as PZT (lead zirconate titanate) and PMN (lead magnesium niobate). Actuators of this type can be divided into two categories depending on the strain used. A rigid displacement is induced by a constant applied field while a resonating strain is caused by application of an AC field. The full mechanism causing these changes has been described in many texts [Takahashi, 1987; Muller, 1986].

At present the main applications of this technology are as micro-actuators. A typical range of specifications is [Takahashi, 1987];

1. Controllability in the displacement range up to several tens of μm, with accuracy better than 0.01 μm.

2. Fast response speed (10μsec.).

3. Generates high forces (440N/cm^2).

4. Driving power a magnitude smaller than electro-magnetic motors, because of a capacitive type dielectric condenser.

As they are primarily designed for very limited motion, piezo-electric motors are not likely to be used in large robot joint motors, but they may find applications in micro-manipulation tasks.

Recently there has also been a considerable interest in the use of shape memory effect actuators. Shape Memory Alloys exhibit a peculiar property called the shape memory effect (also known as thermoelastic martensitic transformation). The alloys (most commonly Nickel-Titanium although other alloys are available) are formed at low temperatures, followed by annealing at a temperature higher that the 'austenite finish' (A_f) temperature. When deformed from this original shape at a temperature below the 'austenite start' (A_s) temperature, (with apparent plastic deformations of up to 10%), and then heated above (A_f), a complete reverse transformation occurs. Thus with shape memory alloys a relatively large recovery stress (up to 500 Mpa) can be obtained within relatively small spaces, and there is a possibility of using this stress as a power source for small sized actuators. These actuators can be made from different alloys which can be formed into wires, rods, or sheets, and have a range of transition temperatures [Dario, 1987].

At present the major drawbacks with this unit are;

1. Relatively slow rates of heating and cooling which limit the cycling time, with the low resistivity of the SMA making electric heating difficult.

2. Nonlinearities in the SME and the complex thermodynamic relationships make control difficult.

3. The efficiency is low (<10%).

4. Degradation of the SME occurs because of changes in the metal, and

elongation.

Research in Sheffield [Scott, 1985], has focused on the uses of Electro-Rheological Fluids; finely divided particles suspended in a non-conducting base liquid. Under the influence of an externally applied electric field (up to 5000V/mm) reversible changes in viscosity can be produced, to an extent that the liquid can change to a solid and back again. An ERF based actuator has been formed from a hydraulic valve arrangement having an extremely wide piston/cylinder separation of 1mm, figure 2.18.

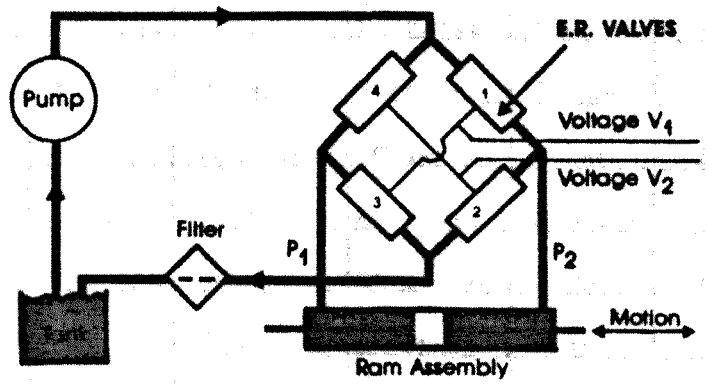

Figure 2.18. Electro-Rheological Fluid Actuator.

With no applied electric field the fluid which is circulated using a hydralic pump has a low viscosity and flows easily between the piston and the cylinder wall. Increasing the electric field produces viscous drag which moves the piston. The thrust which can be produced by this system is proportional to the applied voltage (using the viscous drag) and hence the strength of the piston stroke can be accurately controlled. The developers believe that this may be useful in robotic applications.

2.9 Evaluation of Presently Available Actuators

To give an idea of the use of actuators in modern robotic systems a table, table 2.1, has been prepared showing the specifications of a number of robots available today [Automation 1987].

Supplier	System	Robot Type	Actuators	Repeat-ibility	Max. Load Kg	Max. Tip Speedm/s	Cost £
Asea	IRB 1000	Polar	DC servo	0.1mm	4	-	-
	IRB 8200	Polar	DC servo	0.4mm	125	-	-
Cinncinnati	T3 300	Cylind.	AC servo	0.05mm	50	1	-
Milacron	T3 786	Polar	DC servo	0.25mm	90	1	-
	T3 800	Gantry	DC servo	0.25mm	90	1	-
GEC Robots	L. Giant	Polar	Hydraulic		30	-	-
IBM UK	IBM 7576	Scara	DC servo	0.05mm	10	4.4	32.5K
LJ Elec.	Atlas II	Polar	Stepper	1.0mm	1	-	2.6K
Lamberton R		Spherical	DC servo	0.5mm	2000	12	90K
Meta Mach.	Adept	Scara	AC servo	0.025mm	9	9	30K
Syke Auto.	Syke 600	Spherical	DC servo	0.25mm	2	1.6	15K
Texas Inst.		Scara	Stepper	0.1mm	1.6	1.2	8K
UK Auto Tec	Speedy	Cartesian	Pneumatic	0.01mm	30	4	6K
UMI	RTX	Scara	DC servo	0.5mm	4	1.5	7.2K

Table 2.1 A Representative Sample of Presently Available Robots.

This table clearly shows the dominance of electrical motors in all areas of modern robot design, primarily due to their availability and ease of use. The hydraulic and pneumatic systems by contrast appear to be being driven out of the robot market, and are now most often used in special purpose robots and in older machines.

But just how well do the actuators meet the actual specifications set by the robotics industry and how do they perform relative to each other. Clearly this is difficult to quantify because of the wide range of possible actuators using each of these power sources, Nevertheless seven key areas will be considered.

1. *Stalling*. Stalling of hydraulic and pneumatic actuators or motors does not

cause overheating or damage. With all types of electric motors this is a major problem and must be avoided.

2. *Size and weight (Power/weight ratio).* The power/weight ratio of electric motors is very dependent on the motor size. Small motors have power/weight ratios as low as 20W/kg [Radio-spares, 1989], but with increasing size this can rise to over 100W/kg. For hydraulic motors power/weight ratios range from 330W/kg - 3.3kW/kg [Patton, 1980]. The power/weight ratios for pneumatic systems are very dependent on the pressure of the air supply, but they are normally intermediate between those of the electrical and hydraulic units.

3. *Starting Torque.* Generally electric motors have a high starting torque which cannot be matched by either hydraulics or pneumatics.

4. *Inertia.* The large sizes and masses of electric motors produce large inertias which make rapid stopping and reversal difficult. Hydraulic and particularly pneumatic devices have low inertias and can be stopped and reversed in a fraction of a second.

5. *Efficiency.* Efficiency is a factor which varies widely within each power grouping. Generally electric motors have efficiencies of 80% or more. With hydraulics the efficiency may be as high as 90% for piston motors, but drops to 70% for inexpensive gear motors. The pneumatic drives have typically lower efficiencies than their hydraulic counterparts because of pressure losses and lower tolerances in construction [Patton, 1980].

6. *Cost.* Hydraulic motors are generally the most expensive due to the high tolerances demanded, while the light construction and low tolerance requirements of pneumatic devices makes them the cheapest. Electric motors vary greatly in cost, but generally their prices are intermediate between those of pneuamtics and hydraulics.

7. *Speed Control and accuracy.* Speed control and accuracy are easily achieved using DC motors and are relatively simple in hydraulic units. With AC motors similiar control can be expensive, while accurate control of pneumatics is extremely difficult.

These are probably the most important factors when considering which actuator to use, but obviously certain other parameters mentioned previously (such as cleanliness) may have a strong bearing on the choice. It should also never be forgotten that the abilities of actuators using the same power source and often the same design philosophy will vary markedly from manufacturer to manufacturer. Clearly the choice of the best actuators for robotic uses requires much consideration.

Chapter 3
Artificial Muscle Systems

3.1 Introduction

There are clearly a great variety of techniques for converting energy in its many forms into mechanical motion, but one method has been virtually ignored by technology although it forms the basic system used by most plants and animals. The direct conversion of chemical energy into mechanical energy is routine in muscles, but is very rare in man-made machines. Isothermal mechanochemical processes, underlie the motility of living organisms, forming a fundamental distinction between the motion of living matter and that of technological devices. This direct conversion of chemical to mechanical energy gives an organic cycle; intaking food and outputting useful work, that can be greater than 50% efficient [Wilkie, 1976]. Steam turbines and internal combustion engines are by comparison only about 40% and 20-30% efficient respectively.

These mechanochemical cycles are driven by biogels of pronounced polyelectrolyte nature, which vary in both type and organization. The different organisms also use different gel mechanisms to provide their motility. The amoeboid's movement is based on progressive solution-gel transformation, the movement of plants is founded on reversible swelling and shrinkage of protoplasm, while the great majority of higher animals and many protista use an intricate and very effective contractile gel mechanism. Recent investigations [Woledge, 1985] of muscular contractility have made the contractile machanics

of these gels amenable to physio-chemical research by reducing it to elementary molecular components.

The possibility that some form of muscle-like actuation could be produced using synthetic polymers was discovered independently by Kuhn and Katchalsky [Kuhn, 1949; Katchalsky, 1949] in the late 40's. Tests were conducted on the contractile potential of polyacrylic acid (PAA) and polymethylacrylic acid (PMAA) when thermally crosslinked with polyvinyl alcohol (PVA), figure 3.1. These materials are still used extensively today, although it has since been shown, [Osada, 1985] that most polymers and copolymers containing ionizable groups can undergo marked contractions.

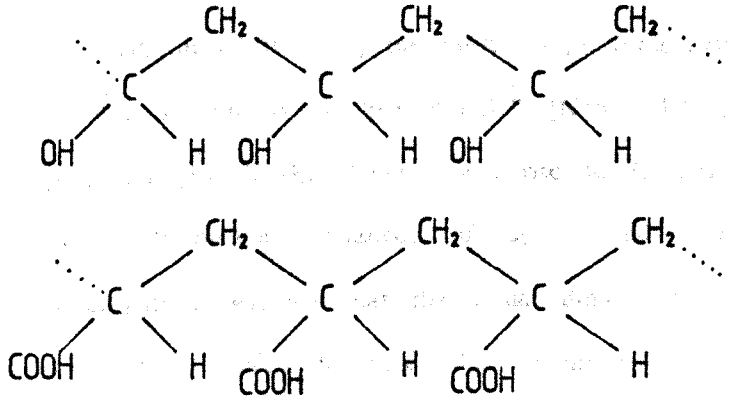

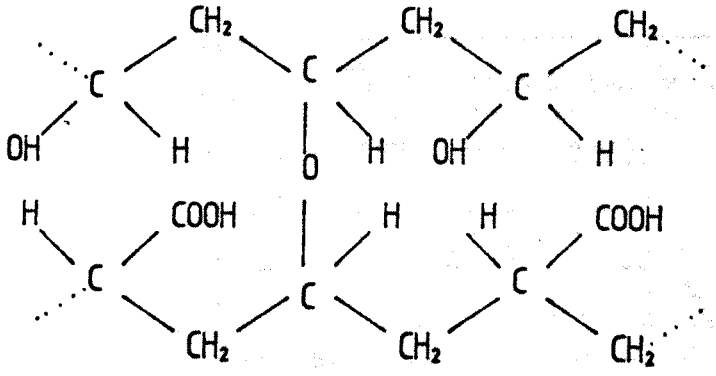

Figure 3.1 Polymers used to form muscle fibres.

This chapter outlines the significant developments which have occurred in the field of mechanochemical actuation. A number of stimulatory techniques (pH, reduction-oxidisation, electrical, thermal, photo-sensitive, and ion exchange),

that can produce the dimensional changes required in a pseudo-muscular actuator are studied (sections 3.2-3.7), with the mechanisms which induce each of these responses being subsequently considered in detail in section 3.8. This leads to a fuller understanding of the processes involved, and how these effects may be enhanced or modified to produce new actuators and sensors.

3.2 The "pH Muscle"

These first artificial muscles operated on the principle of reversible ionization of the constituent polyionic sidechains, with stimulation by acids and alkalis producing dilation and contraction respectively. Since the response is produced by variation of the pH, the muscle replicating system based on this technique became known as a "pH muscle" [Kuhn, 1960]. The polymer when fully prepared [Katchalsky, 1949], gave rise to fibrous strips which could undergo linear dimensional changes of up to 60% without destruction. Further investigation revealed that the actual dimensional changes and responses were strongly influenced by production conditions such as the temperature during crosslinking, the crosslinking period and the presence or absence of applied stress during this annealing.

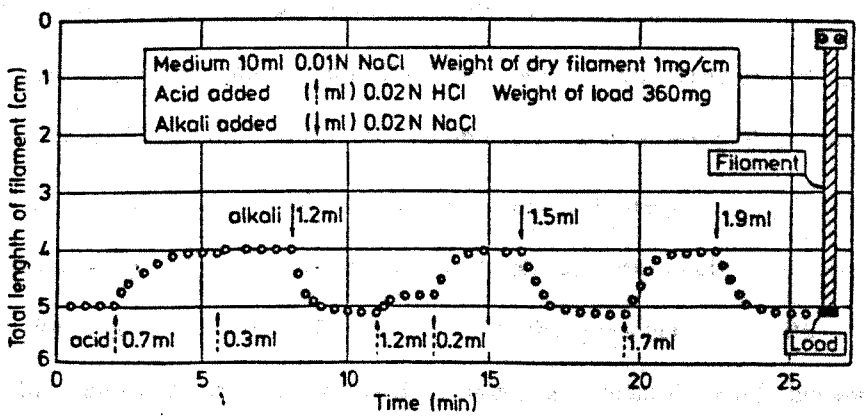

Figure 3.2. Reversible lifting and lowering of a load under pH stimulus [Kuhn, 1950].

These unloaded strips could now be chemically stretched by the addition of alkali and contracted using acid. In tests conducted at the time it was

discovered that strips (thickness 0.1mm) loaded with a weight 5000 times the mass of the dry fibre underwent contractions of up to 30%. These results were repeated over 1750 times, with a period for each complete contraction/expansion cycle of less than 5 minutes [Kuhn, 1950], as shown in figure 3.2.

Clearly these initial experiments demonstrated the potential of pH stimulated polymers, while there was an obvious feeling that other polymers could be found with equal or superior qualities to those originally tested. This belief was borne out when Katchalsky and Eisenberg produced fibres of polyvinyl phosphate (diameter 0.15mm) which contracted to half their original length in under 1 second, the expansion was slower but was still described as returning 'rapidly to its original length' [Katchalsky, 1950]. Although the response is many times faster than for other systems its mechanical properties (strength and contractile force) were reported to be poor and further tests were not conducted.

A problem which was associated with these attempts at replicating muscle action was that the swelling/deswelling was three dimensional, where one dimensional motion would have been preferred. Kuhn [Kuhn, 1960], overcame this problem by preparing two different foils of approximately equal thickness. The first foil was made solely from PVA that was heavily crosslinked to permit only very limited swelling, while the second foil was a PVA-PAA copolymer prepared as described previously. This was only relatively weakly crosslinked. Circular discs were cut from these foils and placed alternately one on top of the other forming a sandwich, figure 3.3a. In the presence of a PVA bathing solution this sandwich was compressed forming a pressure bond between the leaves, before being heated under light pressure to increase the inter-leaf bonding strength. This heating also increased the crosslinking in the PVA-PAA layers preventing dissolution during swelling, and further reduced the swelling potential of the PVA layers.

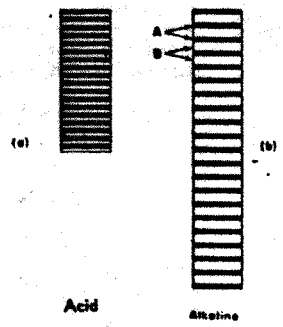

Figure 3.3a and b. Contractile and non-contractile layers of polymer [Kuhn, 1960]. Black layers - pure PVA; White layers - PVA/PAA copolymer.

When saturated in water the swelling of the PVA layers is very limited, while that of the PVA-PAA layers is substantial. This produces longitudinal swelling in the block, but swelling in any other direction is virtually eliminated by the rigid nature of the PVA layer, hence achieving the desired one dimensional effect, figure 3.3b.

Further research into pH stimulated responses has continued slowly, with the major effort being made by Belyakov [Belyakov, 1985] in the Soviet Union, where work has been directed towards finding applications of pH-type muscles and pH activated devices.

Since these first tests a number of other methods of initiating a response have been discovered. The actual mechanisms which produce these dimensional changes are studied later in section 3.8.

3.3 The "Redox" Muscle

Observation that the energy output in natural muscle was obtained by oxidation of glucose, prompted Kuhn to investigate the possible stimulation of the contractile reaction in polyelectrolyte gels using oxidising and reducing agents. This new system used a new copolymer prepared from vinyl alcohol and allylalloxan [Kuhn, 1960], which was crosslinked with PVA in equal parts as described before, figure 3.4.

Addition of reducing and oxidising agents produced a completely reversible cycle with contractions of about 20% on reduction.

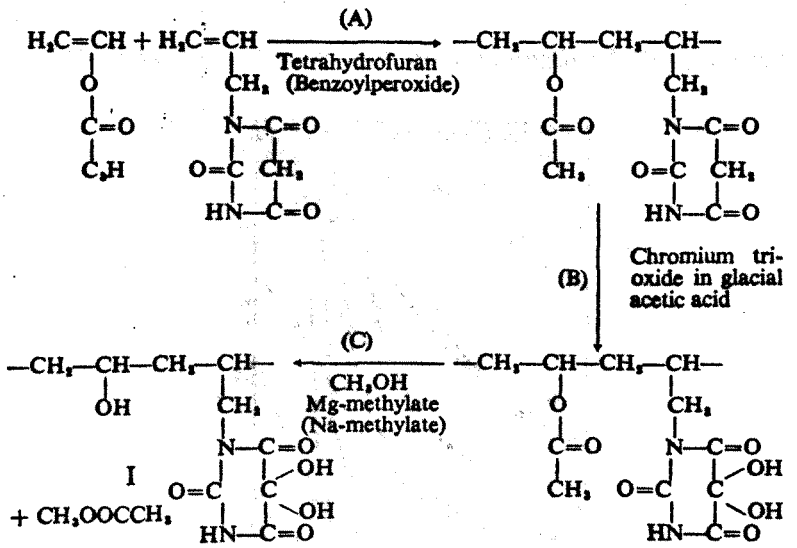

Figure 3.4 Preparation of Redox Muscle Polymer [Kuhn, 1960].

Oxidation restored the strips to there original length. Since the motions in this polymer were induced by an oxidation/reduction reaction this has been termed a "Red-ox muscle".

3.4 The "Ion Effect Muscle"

In 1955 Katchalsky [Katchalsky, 1955] showed that mechanochemical responses could be produced when polymers were subjected to ionic stimulation. It was found that when a sodium salt of a polyacid was converted into a calcium or barium salt there was a critical point at which a violent contraction occurred. This process was fully reversible on addition of a monovalent salt to replace the divalent salt. The reaction mechanism is given by [Katchalsky, 1955];

$$R(COO^-Na^+)_n + {}^n/_2\ Ca^{2+} \rightleftharpoons R(COO^-Ca^{2+}/_2)_n + nNa^+ \qquad (3.1)$$

Hojo [Hojo, 1971] later studied the contractile effects of specific ions and found that the degree of contraction decreased along the series:

$$Cu(II) > Cd(II) > Co(II) > Fe(II) > Ca(II) > Al(III) > Zn(II) > Ba(II) > K^+$$

This mechanism has not found much success when applied to polyionic gels

because of the sluggish response and poor strength of the materials.

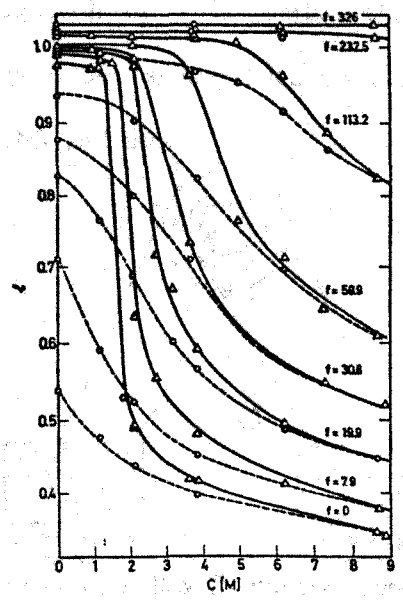

Figure 3.5. Equilibrium length v Conc. for KCNS stimulated collagen fibres [Katchalsky, 1955].

In 1956 Flory [Flory, 1956] pointed out that considerable forces could be produced during phases transitions, encouraging Katchalsky and his coworkers to experiment with a range of other materials that they felt might show these phase transitions. This eventually lead to tests on reconstituted collagen which undergoes 'chemical melting', figure 3.5, when interacting with a variety of compounds, both electrolytes and non-electrolytes.

In these tests stimulation by LiBr or KCNS produced rapid contractions, with forces 10 times those generated in muscles of equal cross-sectional area. These contractions could be reversed by treating the collagen fibres with water.

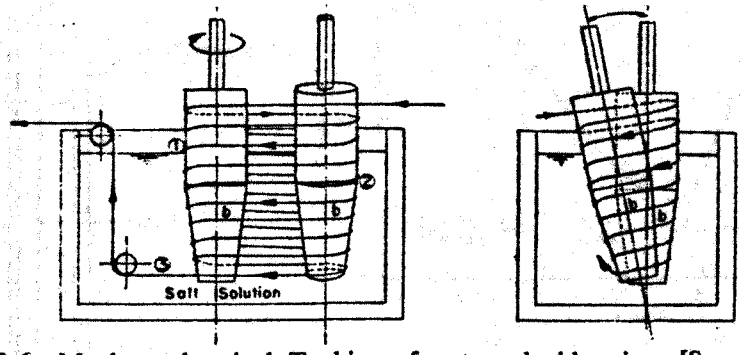

Figure 3.6. Mechanochemical Turbine, front and side view [Sussman, 1970].

Sussman [Sussman, 1970] and Steinberg [Steinberg, 1966] have used this principle in the construction of their mechanochemical motors and turbines, figures 3.6 and 3.7, which can be stimulated by a range of compounds such as, LiBr, CaCl, MgCl, KCNS and urea.

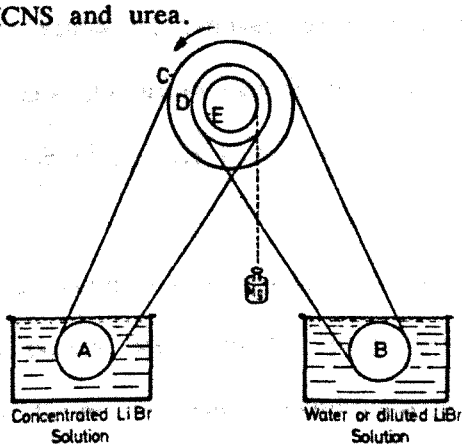

Figure 3.7. Mechanochemical Pulley [Steinberg, 1966].

Using these engines masses several thousand times that of the fibre could be lifted, generating tensions in excess of 125kg/cm^2 [Steinberg, 1966], (maximum muscle tension is approximately 2–4kg/cm^2) while a maximum power output of 0.03W/g was attainable, equalling that for the sartorius muscle in a frog.

3.5 Electrically Stimulated Muscle

Artificial muscles have also attracted the attention of researchers hoping to use electrical stimulation to trigger a response in much the same way that electrical pulses are used in animal muscular control.

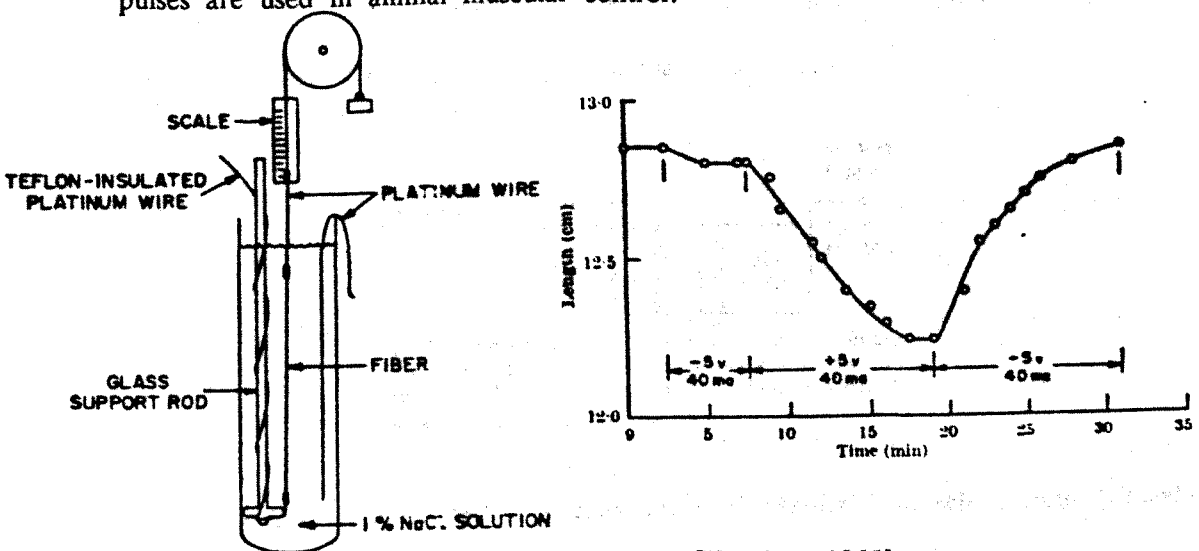

Figure 3.8. Apparatus and Time Response [Hamlen, 1965].

The first system of this type was proposed by Hamlen et al. [Hamlen, 1965], Figure 3.8. This "electrical muscle" used platinum electrodes to electrolyse the solution producing alternately acid and then alkali environments. The use of electrolysis to produce acid/alkali changes means that the response rate is low. It is also perhaps a little zealous to classify this as new form of stimulation as it is merely an extension of the pH technique.

Work in this area has continued, however, with Fragala et al. [Fragala, 1972] producing a refined system based on the properties of cationic and anionic exchange membranes, figure 3.9. These membranes are formed in three layers, the central membrane being the actual muscle fibre. There are two compartments on either side of this muscle each initially containing HCl and NaCl solutions of equal concentration. The muscle membrane is in an undissociated (less swollen) state. When current flows in the circuit, the electrolyte concentration in the central compartment containing the muscle decreases, due to differences in permselectivity of the ion exchange membranes. The more mobile H^+ ion concentration decreases most rapidly. When this concentration is less than that of the muscle membrane dissociation constant, the acid groups in the polymer ionize producing muscle dilation. Contraction is achieved by reversing the direction of current flow. This method although exhibiting some very interesting features, gave dimensional changes of less than 1%, and was obviously not a good actuator candidate.

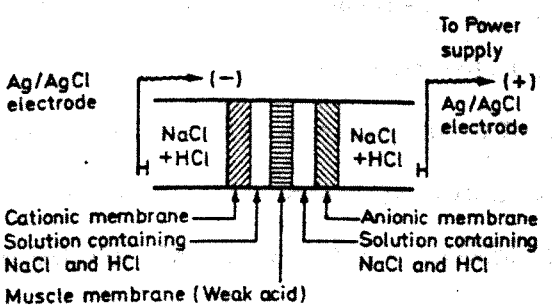

Figure 3.9. Scheme of Electrically-activated Artificial Muscle system [Fragala, 1972].

Recently Tanaka [Tanaka, 1982], using partially hydrolysed polyacrylamide gels (PAM) reported that infinitesimal changes in the electric potential across the gel produced a discrete, reversible volume change, the volume of the collapsed gel being several hundred times less than that of the swollen gel, figure 3.10.

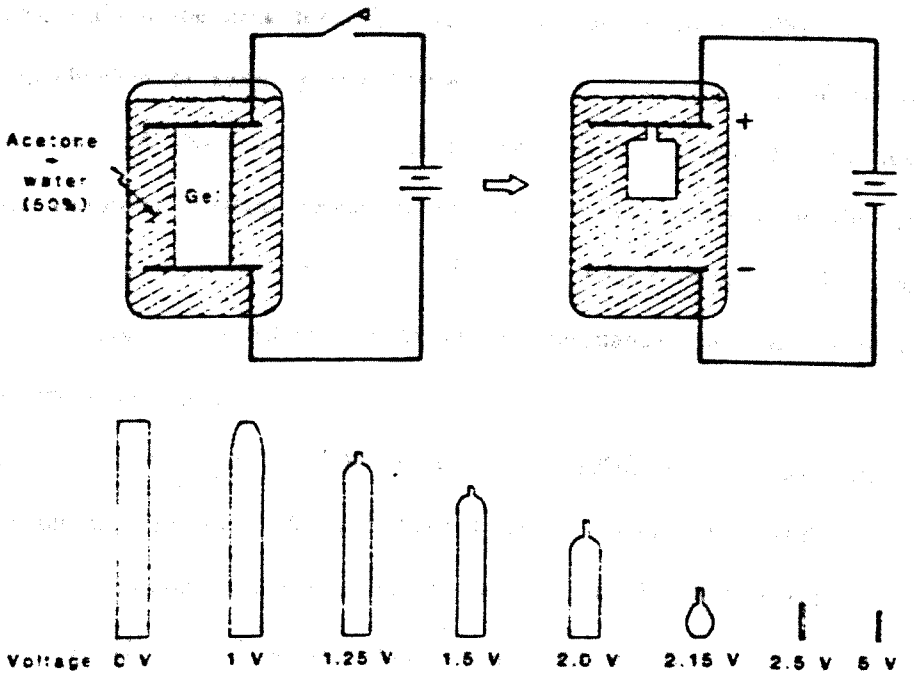

Figure 3.10. Electrical Stimulation producing Phase Transition [Tanaka, 1982].

Osada [Osada, 1985] using water swollen poly(2-acrylamido -2-methyl-1-propanesulfonic) acid (PAMPS), reported similar results, concluding that reversible volume changes can be produced under electrical influence in all polymers; synthetic or natural, which contain ionizable groups. The rate of water release from these PAMPS gels is described as 'high' with a strip of material weighing 1g when dry and 2250g in water reducing its weight by 70% due to water loss under the influence of a 12V/cm (0.7mA) DC field applied for 20 minutes. To date the poor mechanical properties of this material have prevented its use in actuator design. Similar tests [Osada, 1985] conducted by Osada on a number of other gels produced a series of anomalous results when lifting a load. It was found that initially increasing the loading reduced the contraction rate, but this trend was then reversed with increasing loads being

lifted at increasing speed. Increases of a factor of 6 in the power output have been recorded. This unusual behaviour is believed [Osada, 1985] to be due to spontaneous ionization of the ionizable groups, leading to an increased current flow when the gel is stretched. It is felt that this may be useful as a form of controlled feedback with the polymer increasing the energy absorbed as the load increases, without the need for any external stimulus [Osada, 1988].

The mechanism of swelling and deswelling under the influence of an electric field as described above has, however, not been fully clarified. Tanaka describes a phase transition whereas Osada states that no critical point of the electric field induces a sudden substantial shrinkage. These inconsistencies will be addressed in section 3.8 when considering the mechanism involved in producing dilation and contraction.

In Italy, De Rossi et al. [De Rossi, 1985, 1986, 1988a] have also been working on the use of PAM and PAA-PVA polymers. The artificial muscles used in this research are stimulated by an electro-chemical effect similar to that used by Hamlen. The apparatus being used in their tests is shown in figure 3.11.

This electro-chemical stimulation technique produces contractions of 8% in 86 seconds (≈0.1%/sec.) in a PVA-PAA strip 100μm thick [De Rossi, 1988b]. During these contractile cycles the forces generated have been measured at up to 10N/cm^2.

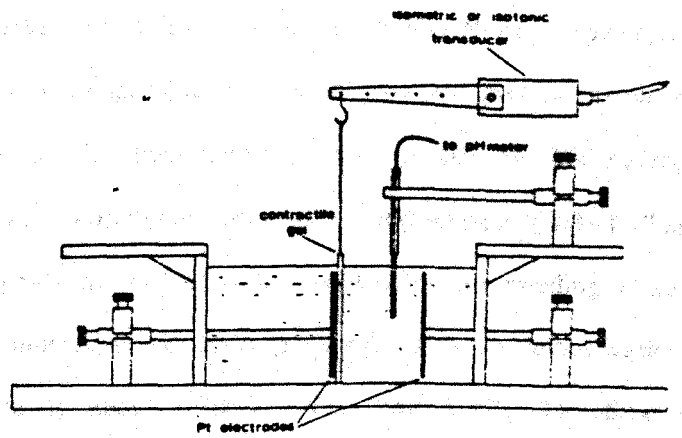

Figure 3.11. Force and Velocity Measuring Apparatus [De Rossi, 1986].

It is claimed that by increasing the PAA content this force can be increased, although at the expense of making the polymer less robust [De Rossi, 1988b].

It has been stated that the major objective of this research is the development of physical and mathematical models of the mechanism, with attempts being made to improve the response characteristics under electrical stimulus by incorporating the electrodes into the body of the polymer. These electrodes are introduced into the PVA/PAA strips during a doping process involving conducting fibres made from Polypyroll, figure 3.12.

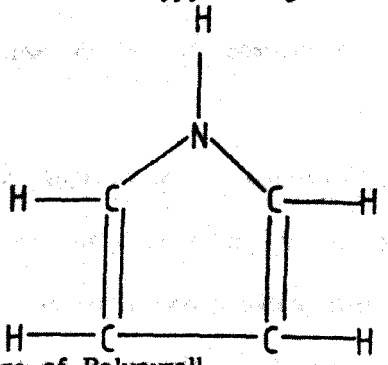

Figure 3.12. Structure of Polypyroll.

The main applications of this research are in the biomedical field with hopes of producing an artificial sphincter muscle and perhaps an artificial urinary system.

3.6 Thermo-sensitive Polymers

Studies [Bae, 1987, 1989] into methods of drug delivery and release have highlighted the properties of crosslinked poly(N-isopropylacrylamide) (PNIPAAm) which shows a remarkable change in aqueous swelling when the temperature is varied. Due to the poor mechanical properties of this hydrogel it is generally synthesised in a copolymer with butyl methacrylate (BMA). Temperature changes result in significant variations in the equilibrium swelling ratio (weight of water uptake per unit mass of dried polymer), with an initial ratio of almost 7:1 at 10°C reducing to about 1.5:1 at 60°C [Bae, 1987]. The time response is shown in figure 3.13,

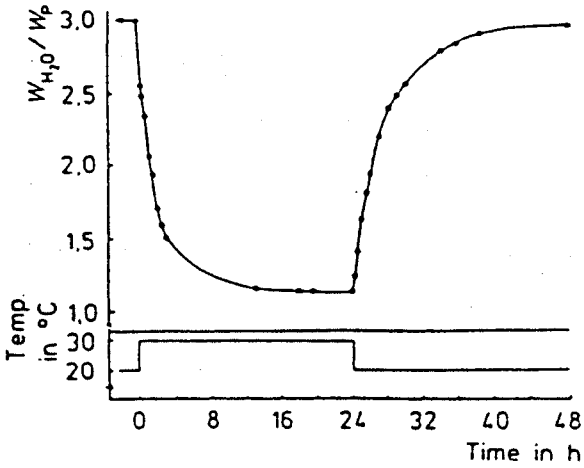

Figure 3.13. Response of Thermo-sensitive Polymers [Bae, 1987].

and although slow, appears to be consistent and reversible. At present this method of control has only been applied to drug release problems, but the development of new materials may mean that a thermo-sensitive actuator is conceivable. This technology could equally be applied to sensor design where it may be of additional value.

While not being truly a 'thermo-sensitive' reaction the author discovered during subsequent research into methods of stimulating contraction that motions can be produced by thermal stimulation (drying) of the material. This method will be studied in detail in Chapter 4 where it will be shown that very high contractile forces can be generated. The actual internal mechanism producing these contractions will be considered in section 3.8.

3.7 Photo-sensitive Polymers

Contractions induced by light effects have been reported by a number of researchers [Smets, 1975; Avriam, 1978; Ishihara, 1984]. Substances which contain groups such as spirobenzopyrane, azobenzene, stilbene, and thioindigo undergo cis ⇌ trans isomerization on irradiation and by incorporating the groups into polymers a photo responsive reaction can be produced. Three types of photocontraction are considered below.

Smets [Smets, 1975], using a crosslinked poly(ethyl methacrylate) -

spirobenzopyrane copolymer observed dimensional changes of 2.3% (in a polymer with dimensions of 3.97mm x 5mm x 0.48mm having a 115g load) in under 2 minutes when exposed to ultraviolet light. These changes were dependent on the stress, temperature, degree of crosslinking and nature of the photocontractile component. This contraction was completely recoverable when the polymer was placed in the dark, figure 3.14.

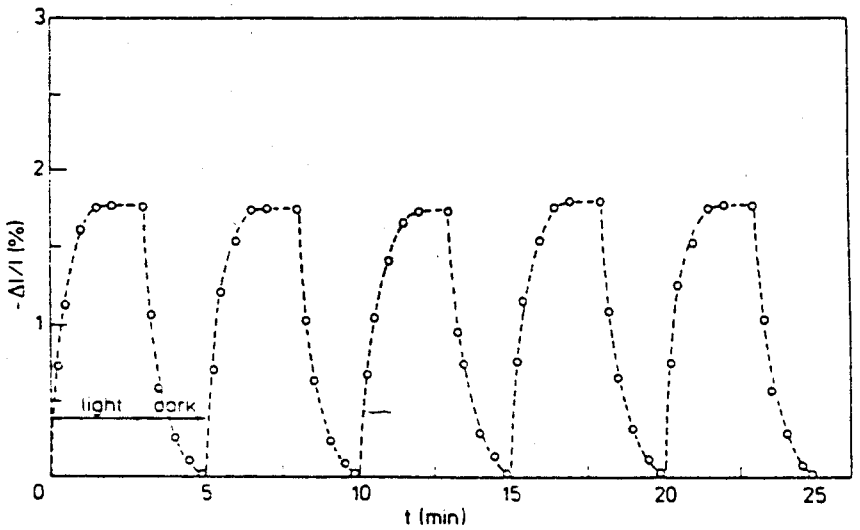

Figure 3.14. Light Stimulated Contraction–Dilation [Smets, 1975].

Aviram [Avriam, 1978] synthesized poly (γ–glutamic acid) membranes with active N,N – dimethyl amino groups which react when irradiated by UV light in the presence of CCl_4 or CBr_4 figure 3.15.

Other researchers [Ishihara, 1984] have prepared polymers which when irradiated change their water wettability characteristics. This can be used to induce swelling under irradiation by light of different frequencies or in darkness depending on the exact nature of the polymer.

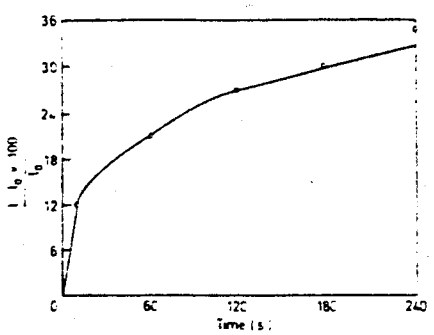

Figure 3.15. Photo–mechano–chemical Response [Avriam, 1978].

These changes can be fully recovered by placing the polymer in darkness or by appropriate irradiation.

3.8 Dilation/Contraction Mechanism

PVA-PAA copolymers gels are neither solid nor liquid. To understand what causes the contraction/dilation response in these materials it is necessary to understand the forces at work. Three key forces have been identified, the rubber elasticity, the polymer - polymer affinity and the hydrogen ion pressure (electro-repulsive effect). By combining these forces in the body of the gel the muscle-like motions are replicated.

3.8.1 Rubber Elasticity

The rubber elasticity of the gel is the elasticity of the individual chains, or the resistance of the strands to stretching or compression. A single strand may be represented as a rigid chain of freely jointed segments, which are in constant motion due to thermal agitation. If such a chain has its ends extended almost to its full length, thermal energy gives rise to a force which on average tends to pull the ends inward, a contractile force. If on the other hand the ends are held close together the random motion on average uncoils the chain. At a point between these extremes is a position were the strand is neither in tension nor compression. In any particular configuration the rubber elasticity strength depends on the activity of the fibres. Being a thermally induced activity the motion is dependent on the absolute temperature, hence the restoring force is proportional to temperature, but temperature has no effect on the direction, figure 3.16.

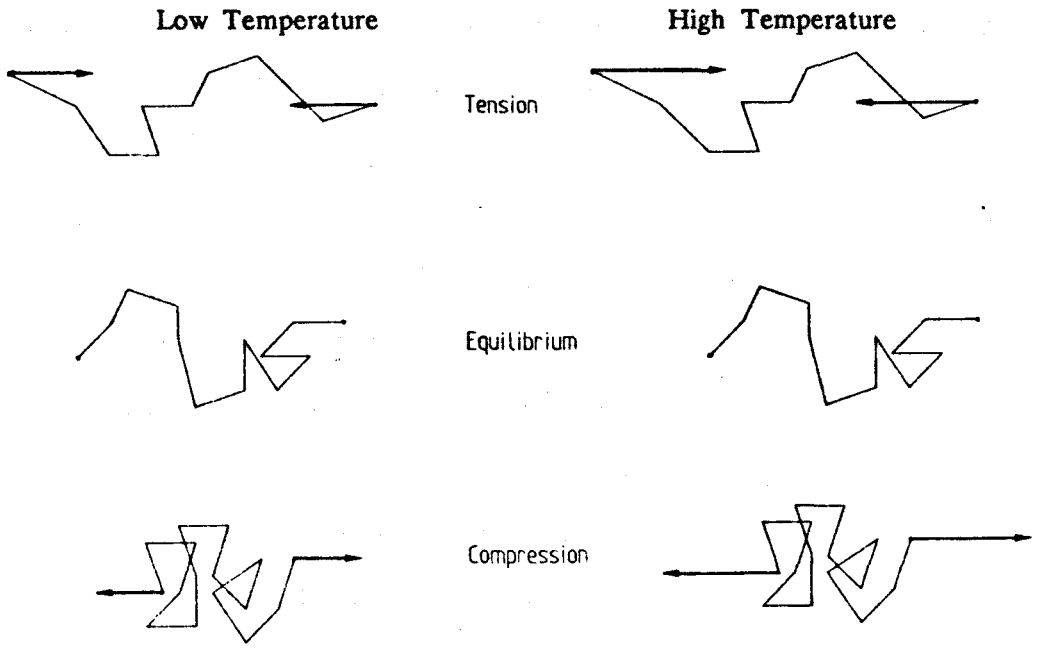

Figure 3.16. The Rubber Elasticity Component of the Osmotic Pressure.

It has been shown that equilibrium is attained at an intermediate distance such that the root mean square (rms) value of the distance r between the ends of a polymer chain containing n links with bond lengths l_0 is given by [Treloar, 1975];

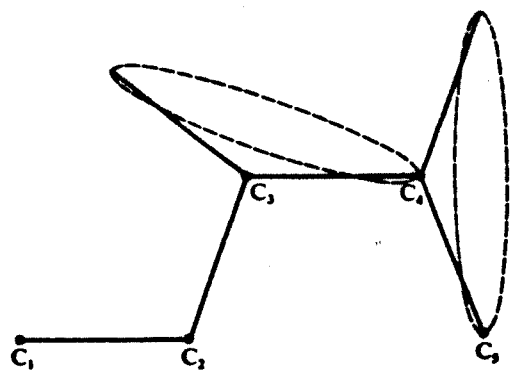

Figure 3.17. Bond Orientation [Treloar, 1975].

$$(r^2)^{\frac{1}{2}} = l_0 n \{(1+\cos\theta)/(1-\cos\theta)\} \qquad (3.2)$$

where θ is the supplement to the valence angle which for an ideal model on

a long chain polymer having complete freedom of rotation, figure 3.17, is given as; valence angle = $109\frac{1}{2}^{\circ}$, $\theta = 70\frac{1}{2}^{\circ}$, giving;

$$(r^2)^{\frac{1}{2}} = l_0(2n)^{\frac{1}{2}} \qquad (3.3)$$

The elasticity of the material can now be formulated using the theory of statistical thermodynamics [Treloar, 1975], involving calculation of the relative number of configurations as a function of deformation. This will reveal the relationship between the temperature and the elastic force.

If a strip of polymer is extended, the work done against tension F to increase the length from l to l+dl is equal to the free energy G at constant temperature. This may be defined as:

$$F = (dG/dl)_T \qquad (3.4)$$

Assuming free rotation of the links (subject to constant values for their lengths and valence angles) is equivalent to the thermodynamic condition that the internal energy U is independent of length. Therefore using G = U − TS (2nd law of thermodynamics), where S is the entropy, it follows that:

$$F = -T\,(dS/dl)_T \qquad (3.5)$$

This result has been proven experimentally by Meyer [Bawn, 1948]. It has further being shown that thermodynamically, the entropy S and the internal energy U are related to the tension and the length by [Bawn, 1948];

$$F = (dU/dl)_T - T(dS/dl)_T \qquad (3.6)$$

$$= (dU/dl)_T + T(dF/dT)_l \qquad (3.7)$$

Meyer [Bawn, 1948] has also shown that for a rubber this relation becomes:

$$F = bT \quad (b = \text{constant}) \qquad \{3.8\}$$

Raising the temperature of the system clearly increases the tendency for the expanded gel to collapse, and the collapsed gel to expand. This gives rise to a pressure which, by convention, is positive if the tendency is to expand the gel, and negative if it makes it shrink.

Generally the force is not calculated because the configuration is not known. However, by measuring the swelling, force predictions can be made. The elastic force component of the osmotic pressure associated with the swelling of the polymer has been given by a number of sources as [Treloar, 1975; Bawn, 1948];

$$\Pi_r = \rho RT \left(\tfrac{1}{2} v_2 - v_2^{1/3}\right)/M_c \qquad \{3.9\}$$

Where Π_r is the swelling/deswelling force induced by rubber elasticity, v_2 is the volume fraction (volume fraction is the ratio of the unswollen to the swollen volumes, which for swelling is ≤ 1) of the polymer, R is the gas constant, T is the absolute temperature, ρ is the density of the unswollen polymer, and M_c is the molecular weight.

For materials with large molecular weights (>10,000) subject to relatively small swelling (<200%), $v_2^{1/3} \gg \frac{1}{2}v_2$, and equation {3.9} is often simplified to [Flory, 1953];

$$\Pi_r = -(\rho RT\, v_2^{1/3})/M_c \qquad \{3.10\}$$

Thermal stimulation as mentioned earlier produces high contractile forces on drying and it is believed that these forces are produced as a result of the

rubber elasticity effect. Heating causes the swelling solvent (water) molecules to evaporate from the surface of the polymer, leaving this dry. The water molecules within the polymer now move to the surface because of the imbalance, reducing the internal concentration resulting in contraction. These molecules are subsequently removed by evaporation and the cycle continues until all the water has been removed and the polymer is in its unswollen state. By attaching these films to a joint, motion can be produced during contraction.

3.8.2 Polymer – Polymer Affinity

The second force acting on the gel, the polymer–polymer affinity, can be traced to an interaction between the polymer fibres and the solvent [Flory, 1953]. Such interactions can either be attractive or repulsive depending on the electrical properties of the molecules. When the interaction is attractive the polymer can reduce its total energy by surrounding itself with solvent molecules. Where the interaction is repulsive the solvent is excluded, figure 3.18.

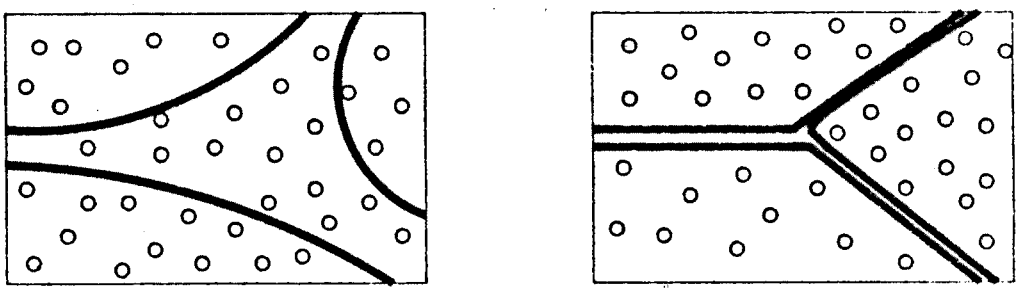

Low Polymer Affinity High Polymer Affinity

Figure 3.18. Polymer – Polymer Affinity

If a polymer has greater affinity for another fibre than the solvent, it coagulates, and creates a negative pressure which in the absence of any other forces would cause the gel to collapse. This negative pressure is temperature

independent, but does depend on the composition of the solvent. Volume also plays a part in determining the strength of the polymer – polymer interaction. Polymer affinity is a short range force and is only fully effective if two fibres are touching. The probability of such contact is inversely proportional to the square of the volume. Therefore, as the gel contracts, the attractive (negative) pressure increases, but as the gel expands the resistance to further expansion abates.

The most important feature in the understanding of polymer – polymer affinity is the connection between the energetics of the polymer and the swelling/contracting solvent. Gee [Gee, 1942] believing that the interaction was a result of the field forces between neighbouring atoms developed the theory of 'cohesive energy density' (C.E.D). C.E.D is defined as the energy required to separate all the molecules in a given material from one another, which for non-polar solutions is the heat of dilution ΔH_1. It was suggested in this theory, that for a polymer swollen in a solvent maximum swelling will occur when ΔH_1 is a minimum, ie when the C.E.D of the liquid equals that of the polymer. This theory is more widely applied in terms of the solubility parameters (δ) which are defined as [Gee, 1942];

$$\delta = (C.E.D)^{\frac{1}{2}} \qquad (3.11)$$

Solubility parameters for an extensive range of solvents and polymers are available in chemical texts, and by judicious choice of solvents the swelling and deswelling can be maximised. While this theory appears to be universal with non-polar solvents, polar, and hydrogen bonded solvents cause anomalies due to ionic interactions. Favourable interactions as before cause swelling, while unfavourable interaction produce no swelling and perhaps contraction. Unfortunately for these polar solutions no overall theory or list of solubility effects is available.

As with the rubber elasticity the polymer – polymer affinity component of the

osmotic pressure can be found [Treloar, 1975];

$$\Pi_p = (RT/V)[v_2 + \ln(1-v_2) + \chi v_2^2] \qquad (3.12)$$

where V is the molar volume of the solvent, and χ is the Flory – Huggins parameter.

3.8.3 Electro–repulsive Effect

The electro–repulsive effect (hydrogen ion pressure), is the third factor contributing to the swelling and deswelling pressure. This force is associated with the ionization of the polymer network, increased ionization results in the displacement of positively charged hydrogen ions into the gel fluid, with electro – repulsion between the ionized groups on the polymer chain causing dilation, figure 3.19. A reduction in ionization, causes the H^+ ion to reassociate with the carboxyl groups; reducing the repulsion and producing a contraction. The situation thus arises of [Treloar, 1975];

$$\text{Expansion:} \quad R(COOH)_n + nA^+B^- \rightarrow R(COO^-A^+)_n + nH^+B^- \qquad (3.13a)$$

$$\text{Contraction:} \quad R(COO^-X^+)_n + nH^+Y^- \rightarrow R(COOH)_n + nX^-Y^+ \qquad (3.13b)$$

Hence the electro –repulsive effect although maintaining electrical neutrality because of the presence of a balancing number of positive and negative ions, produces a significant force with a pressure which is directly proportional to the absolute temperature, and inversely proportional to the volume.

The pH muscle uses the electro– repulsive effect as its driving force. Adding an alkali increases the pH, inducing ionization of the long chain molecule, this ionized system repels strongly causing dilation. Addition of an acid reduces the ionization, hence reducing the repulsion and allowing the polymer to contract.

Addition of a salt uses the electro – repulsive effect in a different way to produce similar results. Positively charged metal ions from the salt displace the

hydrogen ion from the polymer, the H^+ combining with the free radical associated with the metal. The presence of the metal ion results in screening of the polymer ions reducing the repulsion and the system collapses. Introduction of a large quantity of a metal ion with a lesser ionic strength causes displacement of the original ionic species. This second metal ion has a reduced screening effect and thus swelling ensues.

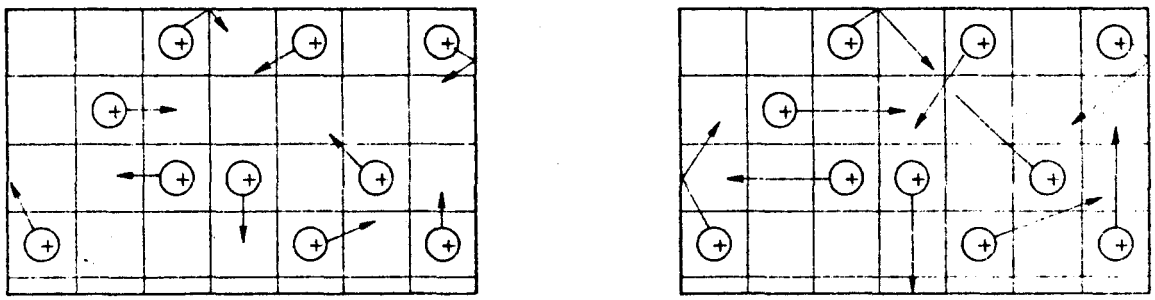

Low Temperature High Temperature

Figure 3.19. Electro-repulsive Force (Hydrogen Ion Pressure)

The electric field effect observed by Osada and Tanaka can also be explained in terms of the electro - repulsion. Application of an electric field affects both the negatively and the positively charged ions in the gel. The hydrogen ions flow towards the negative electrode forming part of a closed electrochemical circuit with the number of ions remaining constant. The negative ions on the carboxyl groups cannot move, which means that the polymer as a whole is drawn to the positive electrode. This gives rise to a negative pressure, which is most strongly negative adjacent to the positive electrode and zero at the other end of the gel.

The osmotic pressure component produced by electro - repulsion is given by [Tanaka, 1980];

$$\Pi_e = (\rho RTf/M_c)v_2 \qquad (3.14)$$

where f is the number of dissociated hydrogen ions per chain.

By combining these three forces the factors which produce swelling and deswelling in polyelectrolyte gels can be explained. In particular the mechanisms whereby the various stimulation techniques produce contractile responses can be understood.

3.8.4 Combined Intra-polymer Effect

The effects of each of these osmotic pressure components can easily be seen in isolation, but in a pseudo-muscular polymer it is the interaction of the effects which produces the dilations and contractions required to induce motion. By analyzing these factors it may be possible to explain why certain researchers [Tanaka, 1980] have emphasised a phase transition while others [Osada, 1985], have said that no discrete changes occur. The essential feature is that whenever possible the polymer will try to adjust its volume so as to minimize the osmotic pressure and the internal energy. If this pressure is negative the polymer expels liquid and shrinks, while a positive pressure induces the uptake of liquid and swelling occurs. These actions continue until an equilibrium is reached, the total osmotic pressure Π_t being given by [Tanaka, 1980]:

$$\Pi_t = \Pi_r + \Pi_p + \Pi_e \qquad (3.15)$$

Changes in the osmotic pressure are caused by addition of one of the stimulants considered above. Depending on these conditions, contraction or dilation will occur, but the changes in the three pressure components which accompany any volume change are not equal. It is the relative pressure changes which give a series of equilibrium positions which are not directly proportional to the strength of the stimulus. Tanaka [Tanaka, 1980] has shown that these component pressure equations are critically defined by factors set during the

production of the gel. By redefining the relationship between the pressure components during expansion and contraction, a variety of profiles can be obtained, figure 3.20.

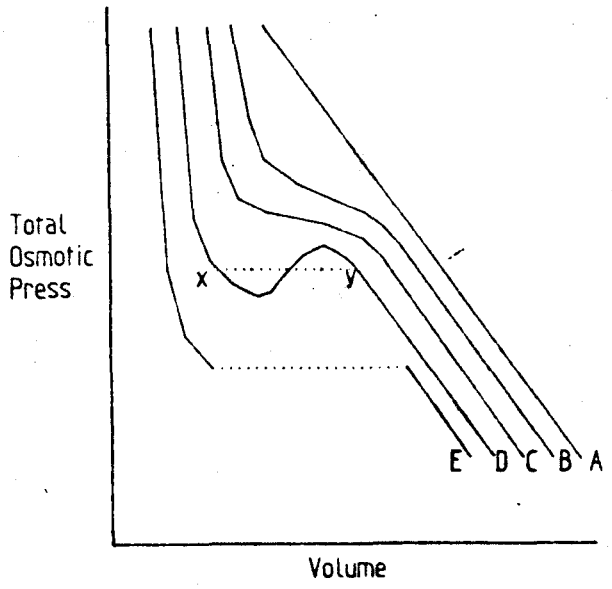

Figure 3.20 Phase Transition Effects.

Thus a muscle strip prepared under one regime may give the input stimulus–swelling curve A, while new conditions give curves B, C, D and E. It will be noticed that curves B and C have developed inflection points because of these variations, while for D and E a point is observed were an infinitesimal input change causes a large volume change. This is the point of phase transition.

This region is believed to develop because of particularly large discrepancies between the rates of changes of the pressure components [Kuhn, 1960], which produce an inversion region, ie contraction is preferred in a system which would be expected to dilate or vice versa. Rather than following the inner curve (x–y) produced by this inversion, a straight line response is observed. This is due to the instability of this region. With extremely small stimulus changes, the material 'jumps' from a low to a highly swollen condition (during swelling) and from a high to low swelling state (during contraction). This jump constituents a phase transition the exact nature of which can be varied by

production effects to give different curves such as D and E.

It is the author's opinion that the disagreement over whether a phase transition is causing the changes would now seem to be resolved, since both phase and non-phase transitions can be observed depending on the production conditions, which determine the relationship between the various osmotic pressure components.

3.9 Evaluation of Stimulation Techniques

As the object of this research is the production of an actuation system to be used in a dextrous hand, the primary consideration at this point is to produce a mechanism with rapid, strong movements.

A number of the methods outlined in this chapter are ruled out almost immediately. Thermo- and photo- sensitive polymers are at present too slow and have only limited dimensional changes. Thermal stimulation (drying) may be worth pursuing because of the large forces which can be generated and the possible application to high vacuum, high thermal radiation environments (space).

The ideal mechanism would be one which could be controlled electrically using chemical energy as the storage medium, much as muscles do. This will be investigated, but it is believed that at the moment the response is too slow, while materials having more rapid responses are too weak.

PH and chemical stimulation will also be tested as these are felt at present to be the methods which have the optimum response, and hence are the best way to prove the feasibility of this pseudo-muscular actuation sysytem.

The salient point which emerges from this evaluation is that there is considerable scope for improvements in the materials available, and the physical properties which they possess.

Chapter 4
Development and Characterisation of Polymer Properties

4.1 Introduction

It is theoretically possible to produce a contractile response in many types of polymer. Tests were conducted on three such materials, gelatin, gum arabic, and a polyvinyl alcohol/polyacrylic acid co-polymer, to determine which if any produced the best (most muscle-like; rapid strong contractions on application of a stimulus) response.

In this chapter, synthetic muscles (particularly PVA–PAA) are stimulated using a number of techniques including saturation with acetone and water. The strength and power output profiles obtained are then compared with profiles obtained from natural muscle. The production processes are also considered as a number of factors set at this stage are believed to have a significant bearing on the final pseudo-muscular performance.

4.2 Testing of Potential Muscle Materials

Gelatin and gum arabic are naturally occurring long chain polymers. Gelatin is produced by thermal degradation of collagen and as such has many of the properties of collagen, while gum arabic is used mainly as an adhesive.

The gelatin used in these experiments was a high purity edible type, while the gum arabic was a commercial grade adhesive used in the paper industry. Test films of both materials were produced using identical processes.

The polymers in powder form, were dissolved in hot water forming a saturated solution. On cooling these solutions formed gels of no great strength

which were left for 72hrs to evaporate, forming solid films of high tensile strength at the end of this period. Since these films were still water-soluble, some method of preventing dissolving was required. This was achieved by thermal crosslinking.

Strips of both materials were annealed in an oven at 100°C for 10, 20, and 30 minutes. At the end of these periods the strips were removed and it was observed that in all cases the material had expanded and now had a honeycomb structure. The gelatin was observed to have changed colour from almost colourless to amber or brown, while the gum arabic had changed from cream to a dark brown or black. The deepening of colour is related to the period of treatment. The samples (thickness = 0.3mm, width = 20mm) were expanded in water and the percentage dilation and breaking stress were tested and recorded, Table 4.1.

Material	Crosslinking	Swelling	Breaking Stress	Thickness	X-sectional Area
Gelatin	100°C;10min.	50%	0.05N/cm²	0.25mm	5mm²
Gelatin	100°C;20min.	28%	0.11N/cm²	0.23mm	4.6mm²
Gelatin	100°C;30min.	19%	0.2N/cm²	0.24mm	4.8mm²
Gum Arabic	100°C;10min.	63%	0.01N/cm²	0.25mm	5mm²
Gum Arabic	100°C;20min.	31%	0.02N/cm²	0.26mm	5.2mm²
Gum Arabic	100°C;30min.	20%	0.03N/cm²	0.24mm	4.8mm²

Table 4.1. Effects of Crosslinking on the properties of Gelatin and Gum Arabic

These results indicate that increased exposure to heat, which increases the crosslinking, reduces the potential for expansion, while increasing the breaking stress. In all instances the load which could be sustained was not large. This is believed to be due to the weakening effect of the honeycomb structure. The

values for gum arabic proved to be particularly poor in this respect. These results highlight the effect of crosslinking which is to reduce the freedom of movement of the molecules by increasing the strength of inter-molecular binding.

Observation of the gelatin when being vulcanised showed that bubbles were produced by expulsion of water vapour and air. Some of these bubbles did not manage to escape and formed the honeycomb structure. It was felt that if this could be prevented the strength of the gelatin films would be increased. To test this theory new films were crosslinked using Iron (III) Chloride [Kruyt, 1949].

A gelatin film was immersed in a 10% solution of $FeCl_3$ for one hour, after which the saturated film was found to have expanded and changed colour to dark brown. This sample was left as before to evaporate to dryness. At the end of this period, the material had shrunk to form a thin film which in this dry condition was very strong. On addition of water the film formed a plastic-like material with no measurable tensile strength.

While the experiments as outlined so far have dealt with the failures of gelatin and gum arabic, it should be remembered the these tests were designed to test if muscle-like movement could be produced artificially. To demonstrate this action a final test on thermally crosslinked gelatin strips produced at 100°C for 20 minutes, with the same dimensions as before, was undertaken. Swelling/deswelling was produced by water saturation and drying respectively, while it was shown by attaching loads to the fibres that useful work could be produced, Table 4.2.

Load	Expansion Rate	Contraction Rate	Area	Power
0g	0.75%/sec.	0.04%/sec	4mm²	0mW
5g	0.95%/sec.	0.03%/sec	4mm²	.0015mW
10g	0.105%/sec.	0.01%/sec	4mm²	.001mW

Table 4.2. Swelling/deswelling of Loaded Gelatin Strips

With no load, rapid, repeatable swelling/deswelling was produced at rates of up to 0.75%/sec. and 0.04%/sec. respectively. Loading caused an increase in the swelling rate and a decrease in the contractile (active cycle in muscle) rate. During these loaded tests, stresses of up to $0.2N/cm^2$ were supported. In conclusion it can be stated that while gelatin and gum arabic are unsuitable for use as an artificial muscle because of their lack of strength, the response shows that a synthetic process resembling muscle contraction/dilation is a possibility.

4.3 PVA-PAA Co-polymer Synthesis

The previous experiments with gum arabic, and particularly gelatin have demonstrated that it is possible to produce films which will do useful work when expanding and contracting. So far these materials have generally proved to be too weak for use as an artificial muscle, but, a study of the properties of polyvinyl alcohol (PVA) has shown that this material has a high tensile strength and can be combined with other polymers such as polyacrylic acid (PAA) to produce a material with substantial swelling /deswelling variation [Kuhn, 1949; Katchalsky, 1949].

PVA having a degree of hydrolysis of 86%-89% and an average molecular weight of 100,000 and PAA with a molecular weight of 500,000-1,000,000 (Fluka AG, Buchs, Switzerland) were separately dissolved in hot water forming 10% solutions. These solutions were then mixed and thoroughly stirred for 20 minutes. This homogeneous solution was poured into a clean, smooth container, where gelation occurs. These gels were then left for a period of 48-72hrs to evaporate to dryness. When thoroughly dry, the still soluble film was removed from their original container and heated in a thermostatically controlled oven producing the crosslinked co-polymer.

When combined in a co-polymer, polyvinyl alcohol (PVA) and polyacrylic acid (PAA), crosslink to create a tangled network immersed in a liquid medium, with the properties of the gel depending strongly on the interaction of the

polymer with the fluid medium. The chemical nature of the polymers and the effects of crosslinking have been shown in figure 3.1.

Control over the thickness of the strips is exercised by varying the amount of material used and the area of the drying vessel, with the thicknesses used in subsequent tests being detailed in the relevant section.

4.4 Thermodynamics

To fully understand the physical factors which produce swelling and deswelling (particularly in PVA–PAA), it is necessary to study the thermodynamics of the interactions. The starting point for an analysis of this type is the Gibbs equation [Kuhn, 1960]:

$$dU = TdS - pdV + fdl + \sum \mu_i dn_i + \psi d\epsilon \qquad (4.1)$$

where

dU is the change in internal energy (U);

TdS is a heat term composed of the product of absolute temperature and the entropy added to the system; (thermal energy).

-pdV is the energetic contribution of compression; (mechanical energy)

fdl is the work done in stretching a fibre of length l to l+dl using a force f; (mechanical energy).

$\sum \mu_i dn_i$ is the increase in energy produced by the introduction of dn_i moles of component i, the specific increase being the chemical potential μ_i. The summation is necessary if more than one chemical component must be added; (Chemical energy).

$\psi d\epsilon$ is the electrical work term due to a change in the charge $d\epsilon$ at an electrostatic potential ψ; (Electrical energy).

The potential for converting energy from a mechanical to a chemical form and vice versa can be clearly seen from this equation.

Information on the exact changes which are occurring cannot, however, be obtained from this equation since any energy changes could be produced in a number of ways; e.g. variation in the internal energy or entropy, or volume expansion of the fibre. Useful information can nevertheless be obtained by taking the cyclic integral of the total differential and equating this to zero ($\oint dX=0$) [Katchalsky, 1971]. Therefore since dU, dS, and dV are total differential for a reversible process, these integrals over a cycle (expansion - contraction) vanish.

Applying this cyclic integration to a transduction from chemical to mechanical energy, while keeping the temperature and pressure constant gives;

$$\oint dU = \oint TdS - \oint pdV + \oint fdl + \oint \sum \mu_i dn_i + \oint \psi d\epsilon \qquad (4.2)$$

however, as both T and p are constant and since a cyclic integral of dU is present;

$$0 = 0 - 0 + \oint fdl + \oint \sum \mu_i dn_i + \oint \psi d\epsilon \qquad (4.3a)$$

or

$$-\oint fdl = \oint \sum \mu_i dn_i + \oint \psi d\epsilon \qquad (4.3b)$$

this gives the mechanical work performed by the engine (muscle) as $\oint fdl$, which is known as the elastic or mechanical free energy (F_{elast} or F_{mech}). The chemical energy in the system $\oint \sum \mu_i dn_i$ is known as the chemical free energy F_{chem} or the energy of mixing F_{mix}, while F_{elect} ($\oint \psi d\epsilon$)is the electrical free energy. It can thus be stated that in a reversible mechanochemical cycle all the free chemical/electrical energy input into the process may be converted into mechanical work.

$$-F_{elast} = F_{mix} + F_{elect} \qquad (4.4)$$

The Gibbs integral equation now shows that if the chemical potential remains constant during conversion, no work is performed, because, if each μ_i is a constant and each dn_i is a total differential then ;

$$F_{mix} = \oint \sum \mu_i dn_i = \sum \mu_i \oint dn_i = 0 \qquad (4.5a)$$

A similar relationship is true for constant electrical potential;

$$F_{elect} = \oint \psi de = \psi \oint d\epsilon = 0 \qquad (4.5b)$$

Hence, to convert chemical/electrical energy into mechanical energy, there should exist a difference in the chemical/electrical potential of at least some of the substances participating in the work cycle. This shows a basic comparison with the thermal work cycles developed by Carnot [Reynolds, 1977]. The comparison of the chemical work cycle with the Carnot cycle will be dealt with later in this chapter.

The free energy change ΔF which occurs in swelling/deswelling reactions can be divided into three parts that have already been considered {4.5}, giving;

$$\Delta F = \Delta F_{mix} + \Delta F_{elast} + \Delta F_{elect} \qquad (4.6)$$

Using the Flory-Huggins expression [Flory, 1957] gives ΔF_{mix} as;

$$\Delta F_{mix} = RT\{(\ln(1-v_2)+(1-1/x)v_2+\chi v_2^2) \qquad (4.7)$$

with χ - Flory-Huggins parameter.

x - number of segments in chain.

R - Gas constant per mole.

If the number of segments is large, $1/x$ is very small, and the equation reduces to [Flory, 1957];

$$\Delta F_{mix} = RT((\ln(1-v_2)+v_2+\chi v_2^2) \qquad (4.8)$$

By reference to gaussian network theory [Treloar, 1975], with isometric expansion $\lambda_1 = \lambda_2 = \lambda_3 = v_2^{1/3}$ (where $1/v_2$ is the volume swelling ratio) the elastic energy is;

$$\Delta F_{elast} = (\rho RTV_1 v_2^{1/3})/M_c \qquad (4.9)$$

where ρ is the density of the polymer; V_1 is the molar volume of the solvent; and M_c is the average molecular weight of the segments. Equating this with the Flory–Huggins expression F_{mix}, gives the total free energy of dilution of a non–electrolyte gel;

$$\Delta F = RT(\ln(1-v_2) + v_2 + \chi v_2^2 + (\rho V_1 v_2^{1/3})/M_c \qquad (4.10a)$$

which at equilibrium, where $\Delta F=0$, gives

$$\ln(1-v_2) + v_2 + \chi v_2^2 = -(\rho V_1 v_2^{1/3})/M_c \qquad (4.10b)$$

With polyelectrolyte gels such as PVA–PAA these energy balance equations must additionally contain an electro–repulsive component. The nature of this electrostatic effect is so complex that it is not open to thorough mathematical analysis, but it has been shown that the energy associated with this parameter is of the form [Tanaka, 1980];

$$\Delta F_{elect} = \rho RTf v_2/M_c \qquad (4.11)$$

Under these cicumstances the energy balance equations {4.10a} and {4.10b} are modified as follows;

$$\Delta F = RT\{ \ln(1-v_2) + v_2 + \chi v_2^2 + (\rho V_1 v_2^{1/3})/M_c + \rho RTf v_2/M_c \quad \{4.12a\}$$

$$\ln(1-v_2) + v_2 + \chi v_2^2 = -(\rho V_1 v_2^{1/3})/M_c - \rho RTf v_2/M_c \quad \{4.12b\}$$

Chapter 3 gives a feeling of how these various chemical, mechanical and electrical effects influence the behaviour of the polymer. By applying the thermodynamic relationships outlined in the above analysis the effects of the energetics of swelling can be understood. Further details on the thermodynamic effects will be outlined in the relevant sections.

4.5 Relationship between Molecular Weight and Equilibrium Swelling

The equilibrium swelling is a very important component which can be used to give an indication of the effects of variations in the production parameters, based on the response achieved. Flory and Rehner [Flory, 1943], have demonstrated that the polymer chains in non-polar gels have a swelling equilibrium which can be encapsulated in a formula. Although the gels which are being used to mimic muscle are polar, this is still believed to give a fair estimate of the degree of polymerisation. The application of this theory to this study seems particularly valid when considering that it is not the actual degree of polymerisation which is being sought, but the chain length relative to other samples of the same material. The approximate equation which is used for the evaluation of Z (the degree of polarisation) is [Huggins, 1943];

$$Z = \frac{V^{5/3} - \frac{1}{2}V}{\frac{1}{2} - \chi} \quad \{4.13\}$$

Using this equation the degree of polymerisation of the samples prepared above can be obtained for comparison, so that the results of the crosslinking

effect can be quantified to some extent.

By considering the changes in the free energy the effects of crosslinking on swelling can also be studied.

From equation {4.4}:

$$\Delta F_{elect} + \Delta F_{mix} = -\Delta F_{elast} \qquad \{4.14\}$$

where the total free energy ΔF has the dimensions of pressure, ΔF_{mix} is the osmotic swelling pressure, while ΔF_{elast} represents the resistance of the network to swelling or deswelling, and ΔF_{elect} is the ionic repulsion effect within the network. By plotting the energetics of mixing, electro-repulsion, and elasticity the effects of these parameters on swelling can be observed, figure 4.1 [Lloyd, 1962].

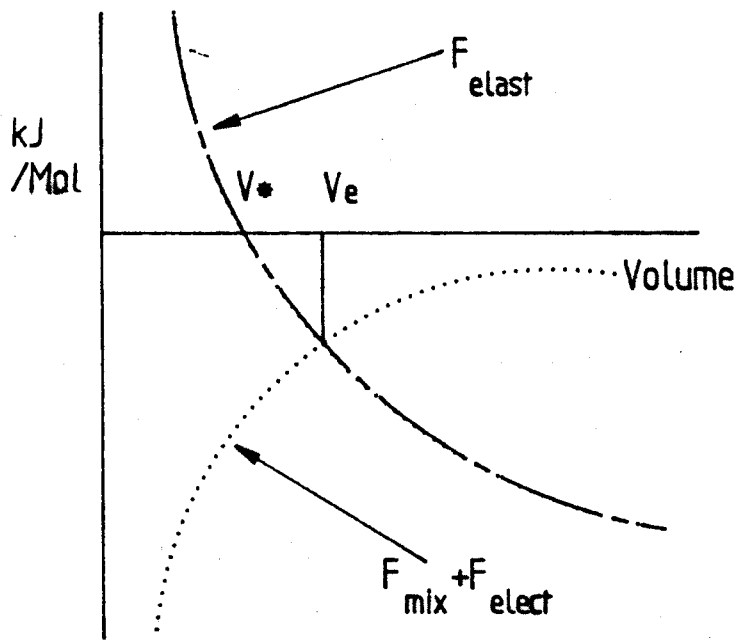

Figure 4.1. Energetics of Equilibrium Swelling

In the unswollen state, V^*, the elastic component is zero, while the mixing component is at negative infinity. Swelling induces changes in the energies of all these components and at the intersection of the curves, equation {4.14} is satisfied; the equilibrium value point being designated V_e.

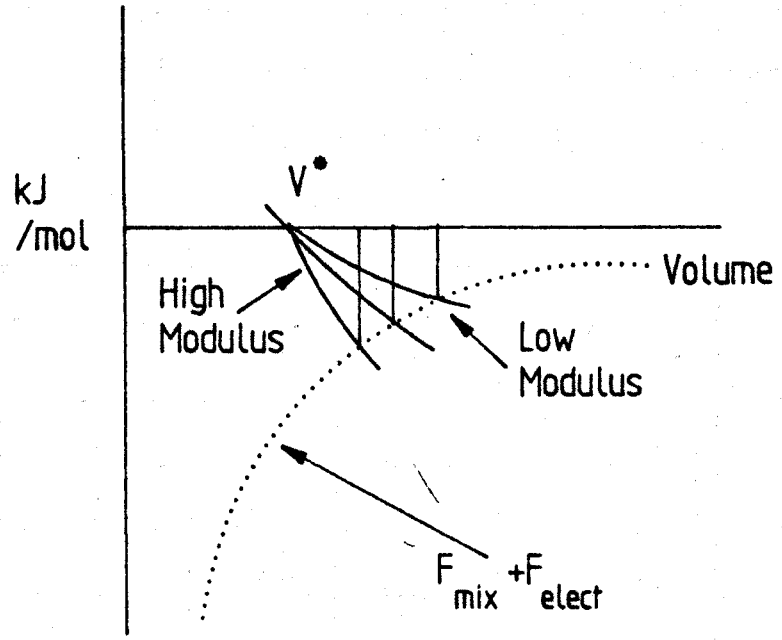

Figure 4.2. Modulus Effects on Swelling.

The effect of varying the crosslinking is to change the modulus values K, which changes the elastic equation, producing F_{elast} curves of greater steepness when the crosslinking is increased and less inclined curves when the crosslinking is reduced. Plotting these results, figure 4.2, shows that the intersection points have been moved, giving new equilibrium swelling values. This observation agrees with the theory that increased crosslinking decreases the swelling and vice versa.

4.6 Production Variable Effects

The thermodynamic analyses completed above have indicated that the production conditions have a significant bearing on the mechanical and chemical properties of the polymer. To further investigate these factors, polymer films were prepared subject to the variations listed below:

1. The relative proportions of PVA and PAA in the films ranged from 50–80% and 50–20% respectively.
2. The crosslinking temperature ranged from 100°C–200°C.
3. The crosslinking period ranged from 0–100 minutes.

Strips were prepared under different conditions the production parameters for each sample being recorded in Table 4.3. Future reference to productions conditions or samples prepared subject to a given procedure will relate to the manufacturing conditions in this table.

Sample No.	PVA/PAA Ratio	Thickness (μm)	Vulcanisation Period/temp	% Swelling at Equilibrium
1	100:0	130	0 min @150°C	Dissolved
2	100:0	130	30 min @150°C	100%
3	100:0	130	60 min @150°C	76%
4	75:25	140	0 min @150°C	Dissolved
5	75:25	140	30 min @150°C	61%
6	75:25	130	60 min @150°C	50%
7	75:25	140	100min @150°C	42%
8	"	130	0 min @150°C	Dissolved
9	"	130	0 min @150°C	Dissolved
10	"	140	30 min @150°C	59%
11	"	140	60 min @150°C	52%
12	50:50	130	0 min @150°C	Dissolved
13	50:50	140	30 min @150°C	51%
14	50:50	130	60 min @150°C	44%
15	75:25	130	60 min @100°C	Dissolved
16	75:25	140	60 min @200°C	15%
17	25:75	150	0 min @150°C	Dissolved
18	"	150	30 min @150°C	26%
19	"	140	60 min @150°C	17%

Table 4.3. Preparation Details of Test Samples

In order that the chemical and physical reactions involved in the production of these copolymers could be explored, and that the structure of the material

could be more fully understood, infra-red and X-ray spectrum tests were conducted.

4.6.1 Infra-red Spectroscopy Tests

To try to determine the composition and internal structure of the polymer it was necessary to ascertain the types of chemical bond which were present. It was expected that the heating would produce crosslinking within the PVA chains {4.15} (ether) and between the PVA and the PAA {4.16} (ester).

$$2\ ROH \rightarrow R\text{-}O\text{-}R + H_2O \qquad (4.15)$$

$$RCOOH + R'OH \rightarrow RCOOR' + H_2O \qquad (4.16)$$

where R is a free radical grouping.

This would result in the formation of ether and ester bonds respectively. By analyzing the relative quantities of these bonds it was hoped that the degree of crosslinking could be quantified, giving a comparison of the production effects on the polymer, and permitting comparison with the swelling tests considered later. This was to be achieved by quantitative I.R. spectroscopy.

Strips of polymer were prepared as outlined in Table 4.3. Due to the thickness of the polymer the testing was done (by the Chemistry Dept.) using the A.T.R (attenuated total reflectance) method rather than the more usual absorbence technique [Brugel,1962], the resulting I.R. profiles are shown in Appendix I.

The results which were produced by these tests proved to be much less useful than would have been hoped, with bond groups being observed at frequencies were none were expected. Examples of this are the grouping at $1740cm^{-1}$. Later tests showed that this grouping was present in the original PVA powder obtained from the manufacturer. Tests conducted on strips cut from the same batches to ascertain the interbatch consistency proved to be equally unproductive with the relative proportions of the bonds varying extensively. It is not known

why the results should be so poor, but the thickness of the materials which made normal test methods impossible may be a significant factor. Due to the poor quality of the results only a very limited analysis was possible.

Samples 1-3 and 17-19 (where the controlled variable was the period of annealing) show a general trend to increased ether formation ($1025cm^{-1}$), indicating shorter bond lengths. This is in agreement with the theory on the effects of increasing the curing period.

The effects of the curing temperature are demonstrated quite nicely by samples, 11, 15, and 16 which show a substantial rise in the ether bond content with temperature.

Comparisons based on the PVA-PAA ratio were impossible to make due to the poor quality of the results.

These tests in general agree with the original theory but are of such poor quality that they are of only very limited practical use.

4.6.2 X-ray Diffraction Tests

The object of this series of tests was to try to find the nature of the polymer and if any structural changes occurred during saturation which would account for the transition from a rigid leathery material when dry to a very elastic rubber material when saturated. Using these tests it was hoped to determine if a change similar to thermal glass transition (change from a glass to a rubber induced by rising the temperature) was occuring.

It was hoped that X-ray tests would give some indication of any internal restructuring that may be occuring during swelling and deswelling. Two samples of 75:25 PVA-PAA heated for 60 minutes at 150 °C (type 6) with thickness 0.13mm were used in the tests, which were conducted by the 'X-Ray Diffraction Unit' in the Physics Dept, producing several plates for both wet and dry samples, figures 4.3-4.6.

Fig.4.3

Fig.4.4

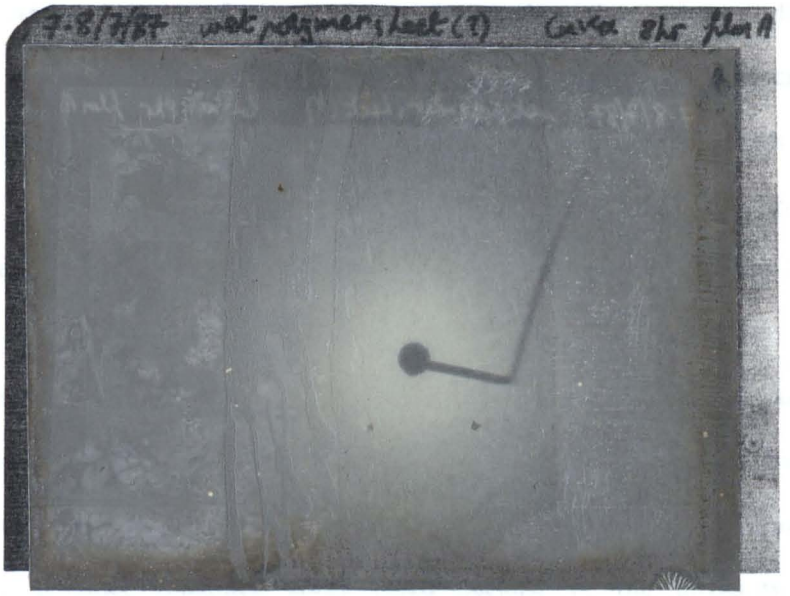

Fig.4.5

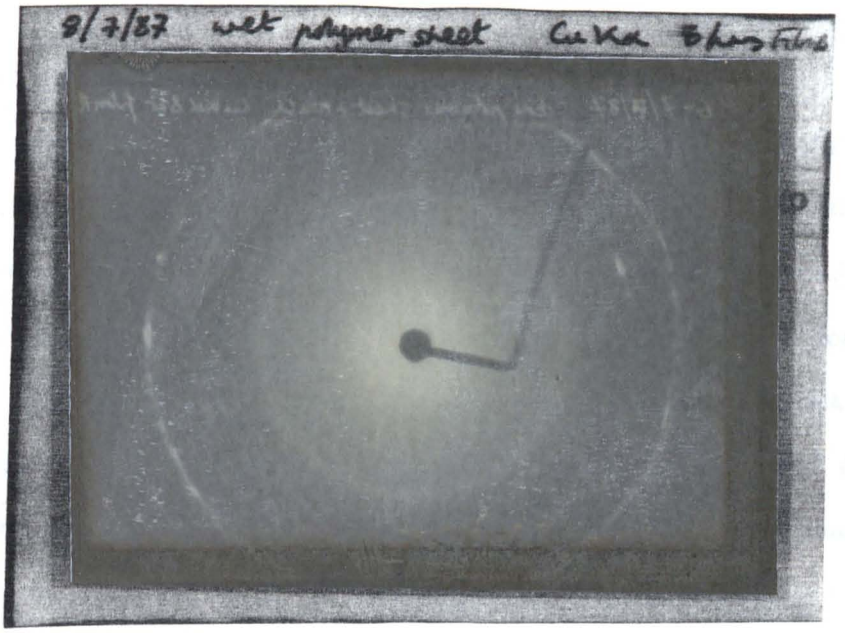

Fig.4.6

Figure 4.3–4.6. X-ray Diffraction Tests

The banded nature of these plates shows that the polymer does possess a degree of crystallinity, although it is by no means totally crystalline. No indication of the extent of the crystallinity could be obtained from these results, neither does there appear to be a increase or reduction in the number or strength of these bands when comparing the dry sample with the moist case. It is not certain, however, that some changes did not occur, for the long time scale required for the tests (because of the thickness of the polymer) meant that keeping the swollen polymer moist was difficult, and this may mean that the results for the moist test are in actual fact not valid. Attempts to ensure that the polymer remained moist failed because of the difficulty in placing a water reservoir within the X-ray apparatus. Until a more detailed study can be made of these results ensuring that the polymer remains moist, only the knowledge that the structure is partially crystalline when dry can be taken as reliable.

4.6.3 Equilibrium Swelling Tests

As disclosed earlier, the equilibrium swelling is a very useful method of determining the extent of crosslinking in the polymers, with the strips prepared as shown in Table 4.3 being used for these tests. The dry dimensions of these materials were accurately recorded using a vernier microscope for the length and width, while a micrometer screw was used to measure the thickness.

These samples were then swollen in distilled water and allowed to equilibrate during a period of 24 hrs. At the end of this time all three dimensions were again measured.

A second set of strips prepared and measured as in the above instance were carefully mounted in a tensometer (Hounsfield), their lengths being obtained from the tensometer's initial setting. Using this apparatus the elastic modulus and breaking stress of each strip was measured.

The results obtained in these experiments for specific production parameter

variations are detailed in the relevant sections listed below.

4.6.4 Isotropic or Non-isotropic Response

Close examination of the dimensional changes experienced by selected strips (3, 5, 6, 7 and 14), demonstrates that the swelling is approximately equal in all three directions, with any discrepancies being so small and random that it is reasonable to state that under the above range of production conditions the material is isotropic. This result appears to be valid regardless of the temperature, period of annealing or the component ratios.

Production Conditions	Original Dim.(mm) Lg. Wd. Th.	Final Dim.(mm) Lg. Wd. Th.	% Change Lg. Wd. Th.
3	30.0; 5.5; 0.12	47.0;8.75;0.19	57%; 59%; 58%
5	30.0; 5.0; 0.12	48.0; 8.0; 0.19	60%; 60%; 58%
6	30.0; 5.2; 0.13	45.0; 7.8; 0.20	50%; 50%; 53%
7	30.0; 5.2; 0.12	42.0; 7.4; 0.17	40%; 42%; 42%
14	30.0; 5.4; 0.13	43.0; 7.7; 0.19	43%; 43%; 46%

Table 4.4. Tests for Isotropic Swelling.

As these polymers are to be used to replicate a muscle which uses mainly one dimensional (longitudinal) motion, it was felt that if some method of limiting the width and thickness changes could be found while permitting the present or increased length changes this would be very beneficial. It must also be ensured with such a mechanism that there is no degradation of the mechanical properties.

A strip of polymer cut from film prepared according to production procedure 6 was later tested in a rig, figure 4.7, which maintained a undetermined longitudinal stress during the curing period.

When this stressed test sample was swollen in water it was found that the length and thickness increased by only 11% while the width increased by over 90%. At the same time the material was still found to have good mechanical integrity. It should perhaps be observed that the volumetric change in this instance was in actual fact less than that for the isotropic swelling.

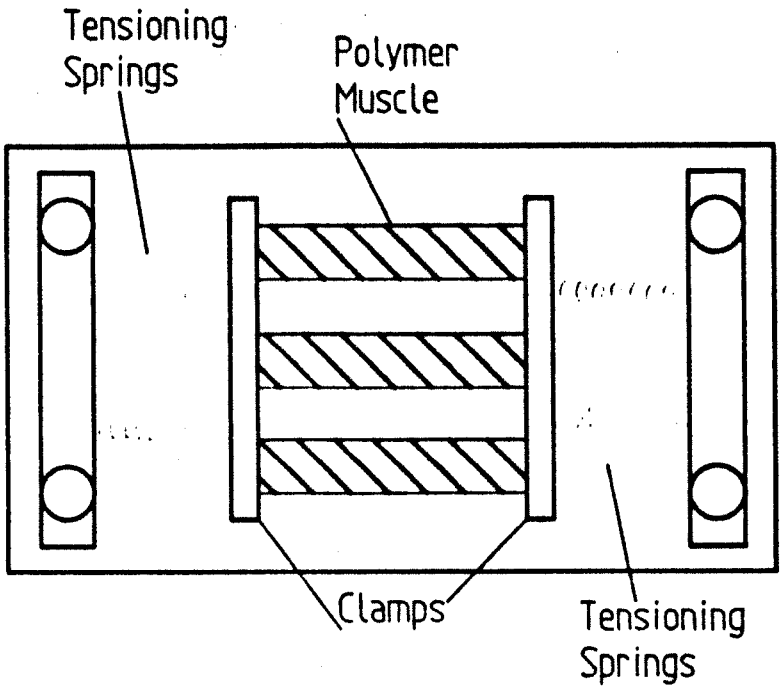

Figure 4.7. Production of Non-isotropic Strips.

This phenomenon is believed to be due to orientation of the longchain molecules during the stressed curing. It is also thought that further increases in the length:width and length:thickness swelling ratios can be obtained if higher annealing stresses were used.

This technique has, however, not been applied to the polymer when used as muscle because of problems maintaining a constant force and orienting the material in such a way that the major axis of swelling is longitudinal. Under commercial production conditions this would not present a major problem and this method would seem to form by far the best means of producing muscle replicating fibres.

Other benefits which are obtained from this solely or almost solely one

dimensional swelling are, reduced size for the containing vessel and an almost cube root reduction in the volume of solvent required to produce a specific swelling factor.

4.6.5 Annealing Period Effects

Strips 4, 5, 6, and 7 were used to demonstrate the effect that varying annealing periods have on the swelling potential and the mechanical strength, figures 4.8 and 4.9.

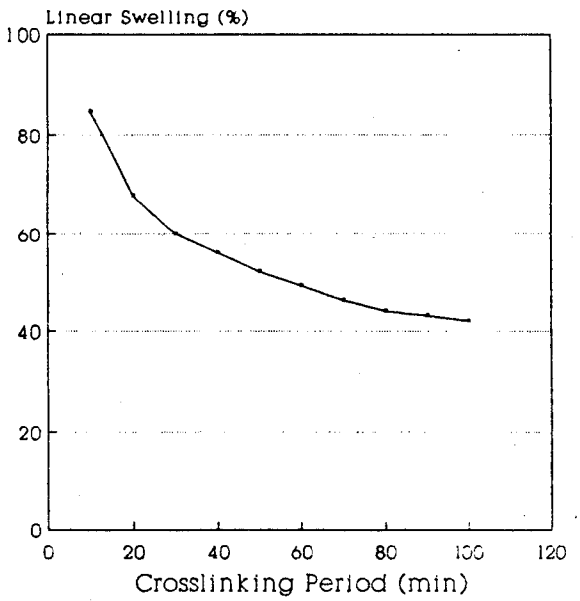

Figure 4.8 Annealing Period effect on Swelling.

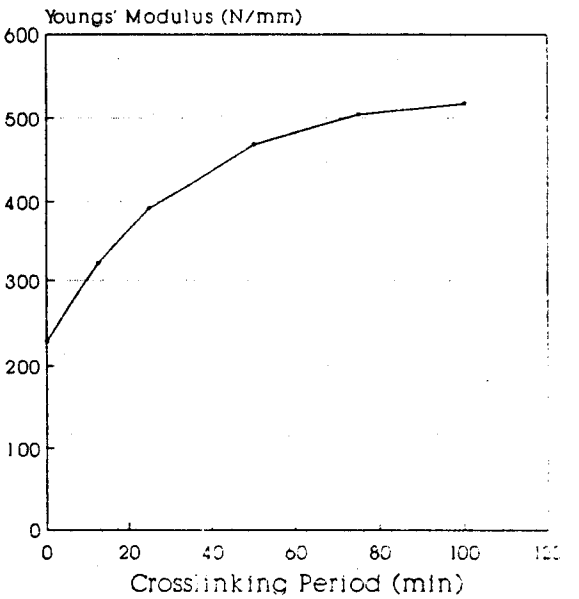

Figure 4.9 Annealing effect on Mechanical Strength.

These results show that, as expected, increasing the period of curing decreases the expansion, while increasing the strength (elastic modulus), with the uncrosslinked strip (type 4) dissolving. Clearly the properties of the polymer are very much dependent on the curing period. It has been predicted [Treloar, 1975] for non-electrolyte polymers that the modulus is related to the chain length by;

$$G = \rho RT/M_c \qquad (4.17)$$

where G is the elastic (Young's) modulus. As the bond length cannot be accurately determined the validity of this equation for PVA-PAA copolymers cannot be tested.

These properties are due to increased inter-chain bonding. With increased exposure to heat more bonding between the long chain polymer links can occur. This increased binding results in more rigidity within the structure and less mobility, hence the reduction in the equilibrium swelling. This swelling - bond length relationship can be quite easily explained by referring to equation {4.13}, where the equilibrium swelling volume is actually used to determine the extent of crosslinking. This increased bonding also means that the structure is more stable possessing greater mechanical strength and a higher value for Young's modulus. The coupling of increased modulus with reduced swelling has been shown from a thermodynamic viewpoint in section 4.5.

4.6.6 Annealing Temperature Effects

The effects on the equilibrium swelling of variations in the curing temperature are shown in figure 4.10, for strips prepared from films 6, 15,and 16. As in the previous section results are also obtained to show any changes in the mechanical properties of strips produced by these variations, figure 4.11.

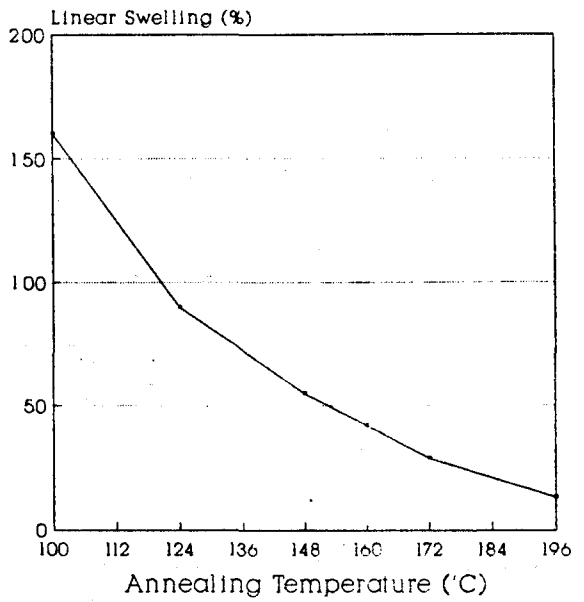

Figure 4.10 Annealing Temperature effect on Swelling.

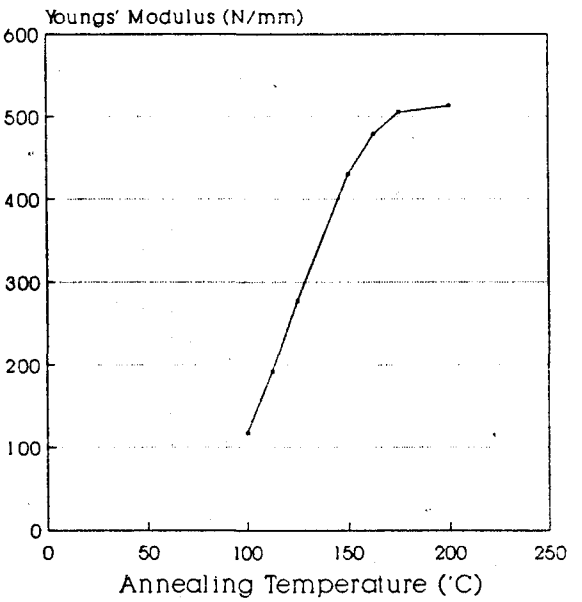

Figure 4.11 Annealing effect on Material Strength

Increasing the curing temperature enhances the degree of crosslinking and as such gives rise to similar effects to those discussed in the previous section. Hence similar conclusions are drawn with regard to the effects of crosslinking. It is also worth noting that these results suggest that the bond lengths set during annealing can be achieved through a coupled interaction between the temperature and the period, giving a wide range of preparation conditions that can produce a specific degree of crosslinking.

4.6.7 PVA-PAA Ratio Effects

Figures 4.12 and 4.13 show the effects of PVA-PAA on the swelling and mechanical properties of samples from films 2, 5, 13 and 18.

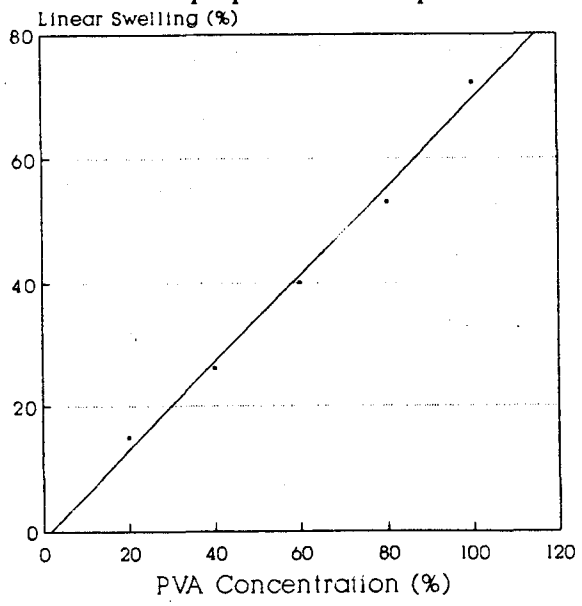

Figure 4.12 Co-polymer Ratio effect on Swelling

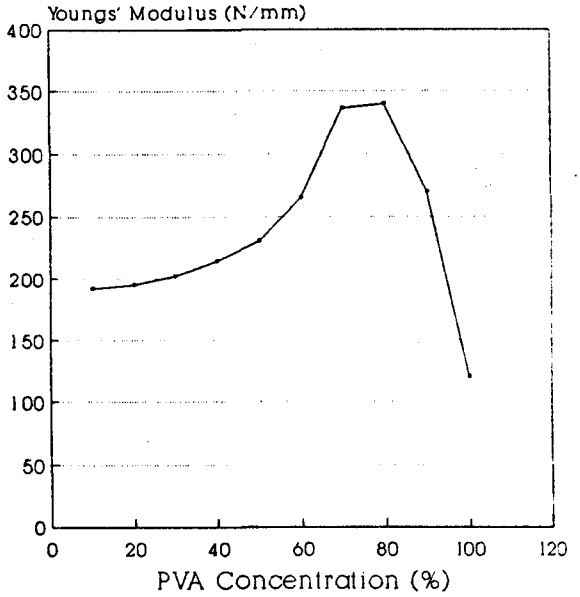

Figure 4.13 Co-polymer Ratio effect on Mechanical Strength

The results produced show that the samples with a high concentration of PVA swell more than those with a high PAA content. An interesting point that was observed was that as the PAA concentration increased the strength of the material at first increased (to a PVA:PAA ratio of 3:1) and then slowly decreased. This factor and the knowledge that increased PVA content enhances

the swelling will clearly influence the later designs for muscle replication.

4.7 Relationship between Water Content and Swelling

The dry dimensions and masses of freshly prepared samples of polymer cut from films produced according to procedures 5 and 6 were measured using a Stanton Instruments Unimatic balance and a vernier microscope. The polymer strips were then placed in water for several hours and allowed to come to equilibrium At the end of this period their surfaces were dried to remove excess moisture and their masses and dimensions were again measured and recorded. This gave an increase in mass from the dry state to the saturated state of up to 400%. These swollen materials were placed in a glass container and allowed to evaporate. To ensure that distortions did not occur because the surface layers were drying more quickly than the centre, the evaporation rate was kept very low. At one hour intervals the strips were then removed from the container and their dimensions and masses recorded, figure 4.14, repeating the procedure until no changes were measurable. Typically this procedure lasted 8–10 hours.

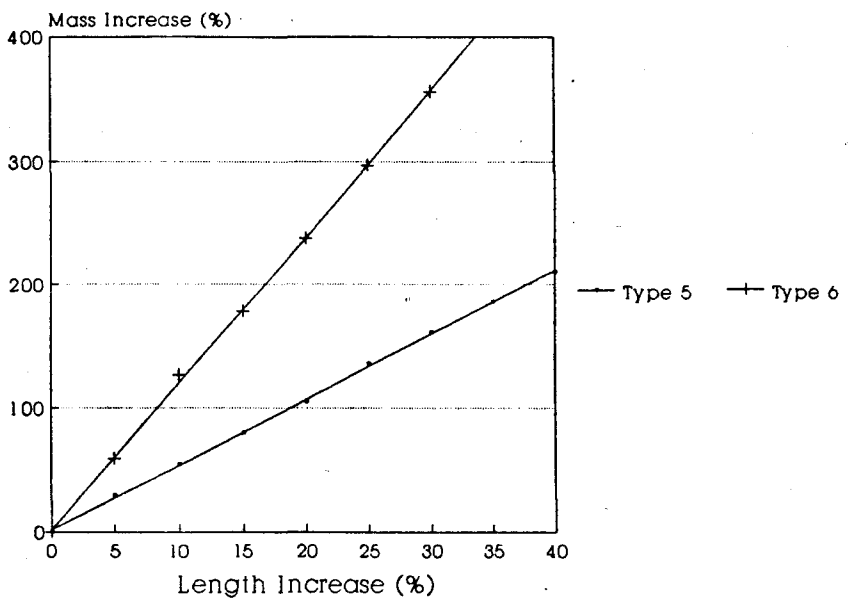

Figure 4.14. Relationship between Water Uptake and Swelling

The relationship between the percentage elongation (or volume change) and mass of water absorbed; the swelling absorbance ratio (ratio of volume or

longitudinal swelling to mass of water absorbed), is linear under all crosslinking conditions. This swelling absorbance ratio is, however, observed to be crosslinkage dependent, with a reduction in the coefficient value as the degree of crosslinking is increased. The reduction in swelling capacity with crosslinking is due to increased inter-chain bonding which reduces molecular mobility. A swelling absorbance ratio of 0.2 which is the value obtained for strips prepared using procedure 6 is used for future testing as this gives a good balance between the strength of the material and contraction/dilation cycle range.

4.8 Swelling Effects on Young's Modulus

A strip of polymer muscle cut from a film produced according to parameters 6 was measured when dry and then placed in water until fully swollen (50%). This test sample was then stretched using a Hounsfield tensometer and the elastic modulus was calculated from the stress-strain curves. This process was repeated several more times with strips cut from the same film but having different swelling fractions (ratio of the volume or length of the swollen polymer relative to their dimensions when dry). The change from a very strong glass-like material when dry, to a rubbery material when moist is shown very clearly, figure 4.15, by the rapid decrease in the modulus during the initial stages of swelling.

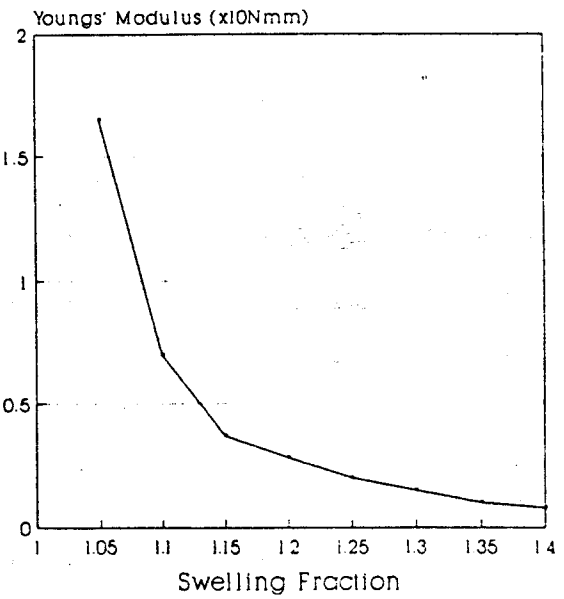

Figure 4.15. Modulus Variation with Swelling Fraction

The relationship between the Young's modulus G and the linear swelling fraction S_w (ratio of the swollen to dry polymer lengths), is found to be:

$$G = K_1/(S_w^3 - C_1) \qquad (4.18)$$

where K_1 and C_1 are constants set in the production of the polymer. This is in very close agreement with the equation for the swelling of rubbers in non–polar solvents [Treloar, 1975].

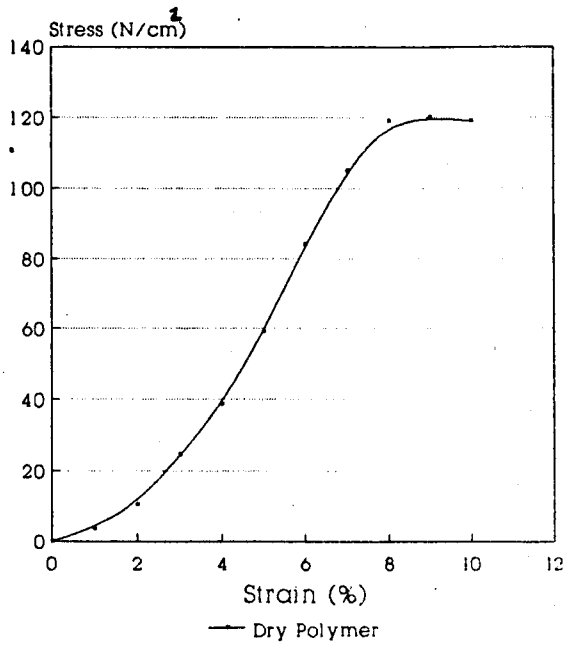

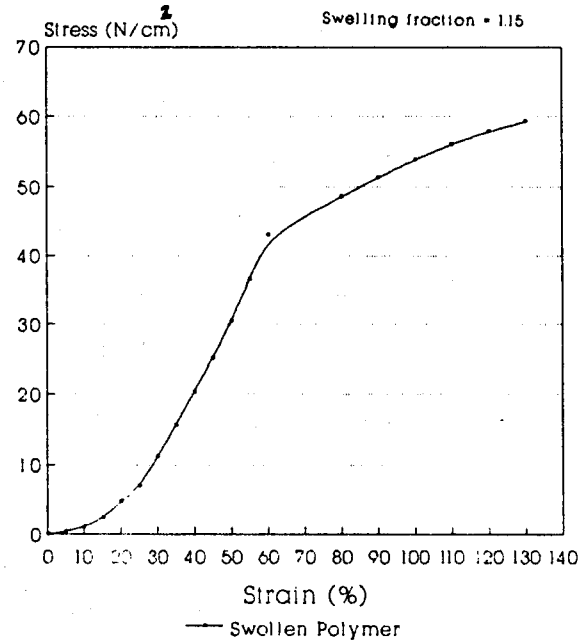

Figure 4.16a and b.

Typical plots of the stress–strain curve produced in these tests, figure 4.16a and b, show that the presence of water in the polymer causes a distinct change in the profiles. When dry, the material behaves much like a glass with very little extension before breaking, while when the material is moist, the curve is typical of that obtained for rubbers. This suggests that the swelling may induce a form of glass transition similiar to that obtained on heating rubber/glass materials.

4.9 Stimulating Muscle Response

The study in the previous chapter of the mechanisms producing contraction

and dilation showed that there is a great range of activating methods. There has, however, been no absolute comparison of the relative merits of these systems. To determine the best technique for use in a robotic actuation systems these different methods were tested, the results of these investigations being included in the following sections.

4.9.1 pH Stimulation

The effects of pH variation on the swelling of PVA-PAA films has been widely studied in the past [Katchalsky, 1960; Kuhn, 1951]. Polymer strips prepared according to procedure 6 were soaked in water and allowed to come to equilibrium, at which point their dimensions were measured. This gave a increase of 52% in any one dimension relative to the unswollen size. When immersed in 1M HCl the film contracted slowly to give a final length of 30% (relative to the unswollen dimensions), giving a cyclic change from swollen to contracted of 22%. When 1M NaOH was added the strip expanded to it's original swollen length.

Problems with relatively small dimensional changes, slow rates of contraction and the deposition of salts from the acid - alkali reaction meant that a better method of activation was sought.

4.9.2 Electrical Stimulation

Previous tests by other researchers have suggested [Hamlen, 1965; De Rossi, 1985] that electrical potential can be used to stimulate muscle contraction. Using a freshly prepared strip of polymer (procedure 6), water was electrolysed using a 5V supply rated at 0.5A. This slowly produced a change in pH which resulted in a reduction in the dimensions of the polymer. As this is basically a variation on the pH method discussed above the dimensional changes observed were of a similiar scale to those recorded for the pH muscle, but the rate of response was even slower.

This method was discounted for the same reasons given for the pH effect,

particularly the slow response rate.

Unfortunately the electrical contraction technique based on electrostatic repulsion was not tested as the necessary polymers could not be obtained. It was, however, subsequently revealed [Osada, 1988] that the strength of these materials was low preventing there use as artificial muscles even if good dynamic rates could be achieved.

4.9.3 Thermal Stimulation

The poor response observed when the polymer was stimulated electrically or by changing the pH, meant that other methods of activation were sought. Noting that contraction occurred when the polymer was left to evaporate to dryness in air, thermal activation was considered. Initial studies showed that considerable effort would need to be directed towards improving the drying rate which controlled the contractile rate, but it was felt that this might be worth investigating.

The first method considered for increasing the evaporative drying rate was to pass a stream of hot dry air over the polymer strips. The air supply was obtained from a compressed air point available on-site. To ensure that the muscle was fairly strong it was necessary to construct the unit in several (typically 5) thin layers (increasing the cross-sectional area), but the drying of these layers presented a second set of problems which had to be overcome before a muscle-like response could be reproduced.

To hydrate and dehydrate these layers some method of pumping air between the muscles fibres was required. This could not be achieved by simply blowing heated air through the layers and hence it was necessary to explore methods of improving this dehydrating effect. Three such methods were eventually tested;

1. Small thin films of aluminium which were heated (turning the water in the polymer into steam) were inserted between the polymer layers. Air was then blown into the system driving the steam from the polymer producing a contraction, figure 4.17a. The major failings of this method were uneven

heating of the films, and poor air distribution between the layers.

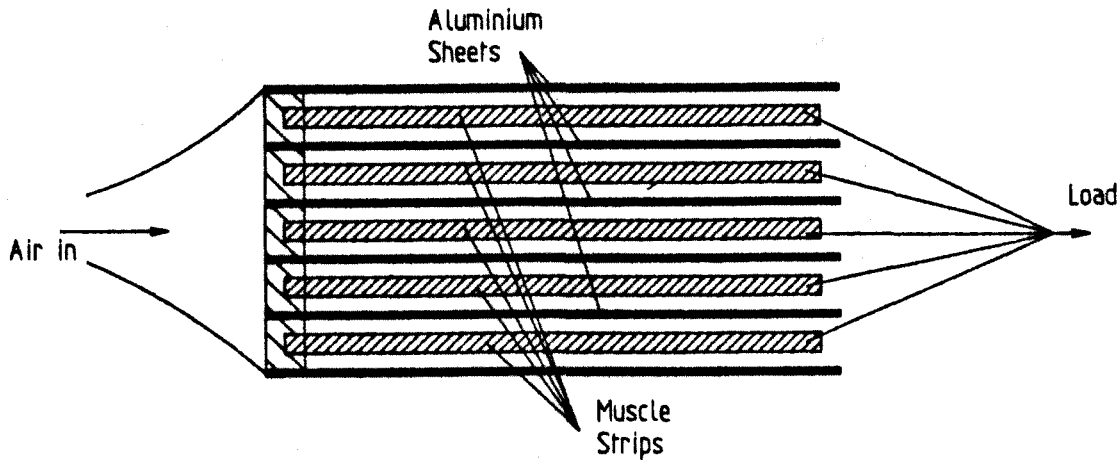

Figure 4.17a. Aluminium Hot Plate Drying System

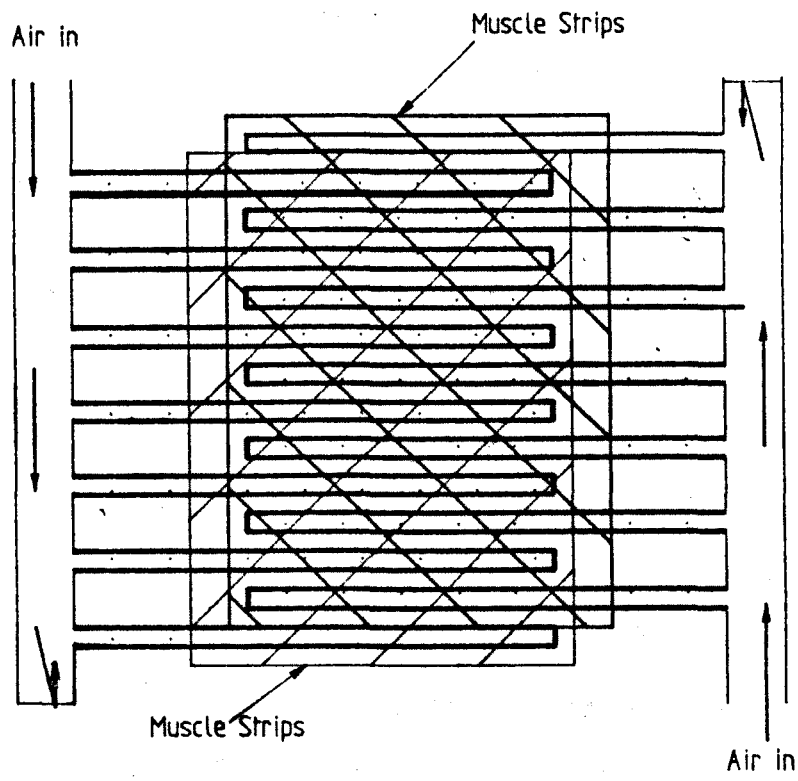

Figure 4.17b. Conceptual Circulating Air Design.

2. An air distribution system was then tried were pipes were fed between the layers at spacings of approximately 10mm. Small holes were cut in these pipes allowing hot air to escape causing evaporation and contraction, figure 4.17b.

It was hoped that this system would act much like blood circulation, but it was abandoned due to the construction complexity.

3. A structure based on the circulating system suggested above but simplified by having the piping replaced by porous sacks was finally used, forming the basic design unit. In this system air was pumped into the sacks which were placed between the polymer layers, Figure 4.18.

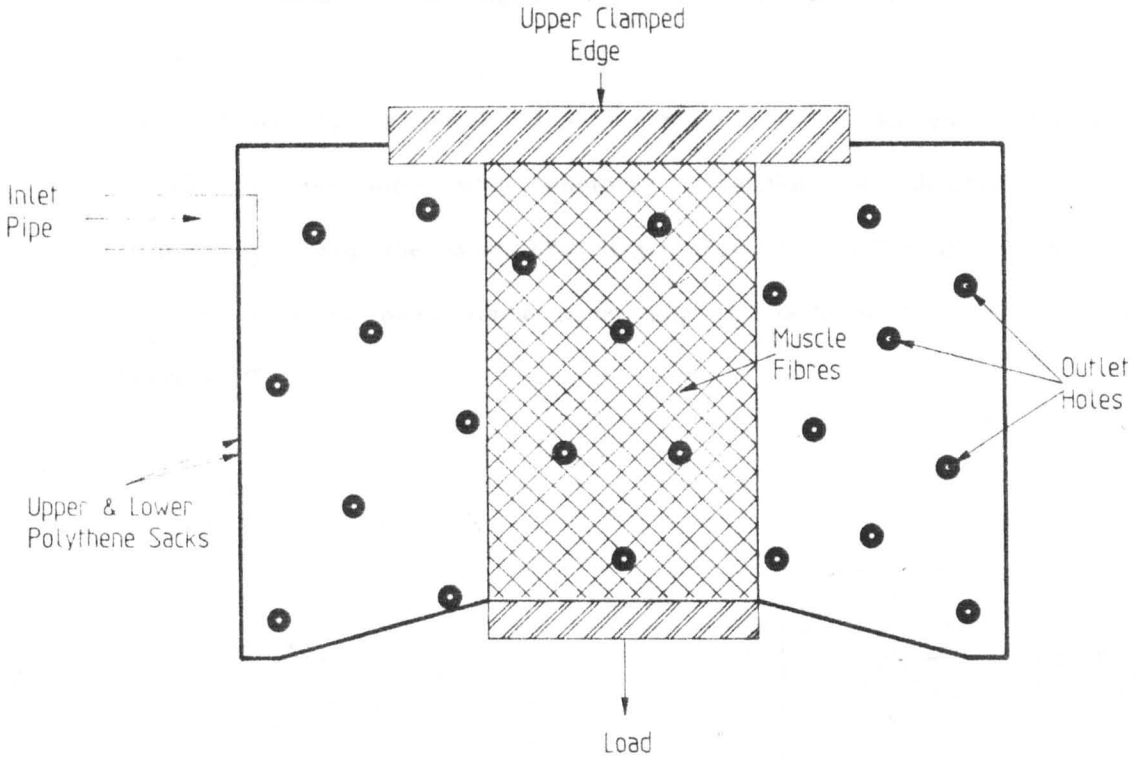

Figure 4.18. Air Distribution through Air Sacks.

The air circulates within these sacks before escaping through the pores. This heats the polymer, removing moisture from the muscle strips and causing contraction. The air distribution system was originally constructed using a polythene sack, with air outlet holes cut at regular intervals. This was later replaced by a nylon 'stocking' which, could withstand higher inlet temperatures, gave a more even air flow, and did not 'wet' easily. This nylon design was

itself eventually replaced by a water repellent material, in which moisture did not collect easily between the pores. The most readily available of these water repellent fibres are those used in 'nappy liners'.

The air supply was pumped into the unit through heated copper pipes which were formed into a coil to increase the exposure of the flow to the gas heat. While this did dry the muscle fibres, it also revealed that the circulation was still poor. Improved circulation is obtained by having inflow jets at opposite ends of the muscle unit with the jets 'flared' to enhance the distribution. These initial designs were still found to be unsatisfactory because the air pressure within the sacks caused bulging which prevented good air flow between the layers.

By incorporating a metal frame which held the sacks under tension, the bulging was prevented, while improved circulation and flexible motion was ensured by having the sacks 20% larger than the swollen dimensions of the polymer, with the metal frame penetrating the sacks in the longitudinal axis, figure 4.19.

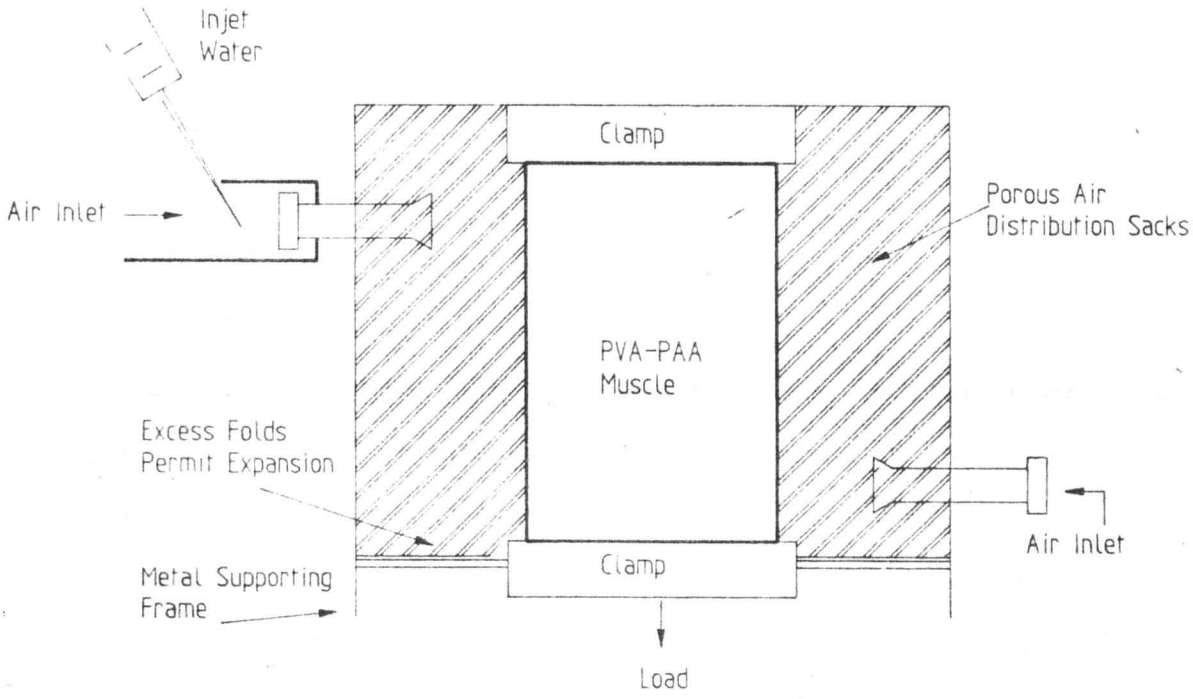

Figure 4.19. Design of Thermal Muscle Cell

Tests could now be conducted on the contractile behaviour under thermal stimulation. 5 strips of polymer prepared according to procedure 6 with dimension 70mm x 50mm x 0.2mm were clamped between air distribution sacks. The upper edges were held securely and a 5g mass attached to the lower edge, figure 4.19. Water was introduced into the system and the strips were allowed to swell to their maximum state during the next 10 minutes. Once in this swollen state a heated air supply was directed into the unit. During the following 180 seconds the movement of the load was recorded, figure 4.20. These tests were repeated 10 times so that a measure of the repeatability could be made. Observation of the contractile motion of the muscle was made using a sliding microscope.

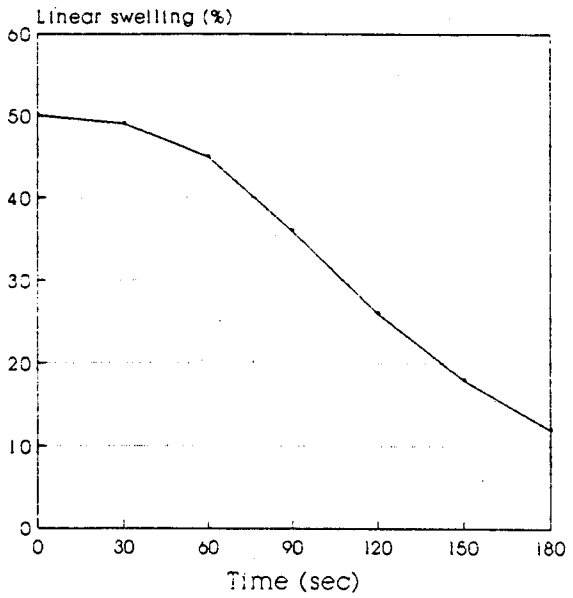

Figure 4.20. Profile of the Thermally Stimulated Contraction

The rate profile shows that during the first 45 sec. there is a very little motion. Following this, the motion during the subsequent 60 sec. is almost constant at a substantially increased rate, with the contractile rate being measured at up to 0.36%/sec. Beyond this time, the response rate gradually decreases according to a log relationship. The strength of the material in these tests is good, lifting more than 30 times its own mass. This series of tests shows repeatibility to be within 15% which seems very reasonable considering the crude construction.

Two possible causes for the sluggish initial response have been suggested;

(1). The muscle fibre surface has excess moisture which requires drying before the water contained within the polymer layers can be removed. As this response is due to the evaporation of the water contained within the body of the polymer only when the surface moisture has been removed can the contraction be maximised.

(2). Retention of moisture in the fibres of the containing vessel is believed to be significant problem reducing the rate of contraction because the liquid contained in these pores must be removed first before rapid drying of the muscle can begin.

The reduction in rate of response as the excitation time rises beyond 100 secs. is believed to be due to a drop in the moisture available for evaporation. The surface no longer remains permanently moist since the diffusion from lower layers is reduced due to a lack of water. With slower removal of the solvent, the contraction rates obviously decreases.

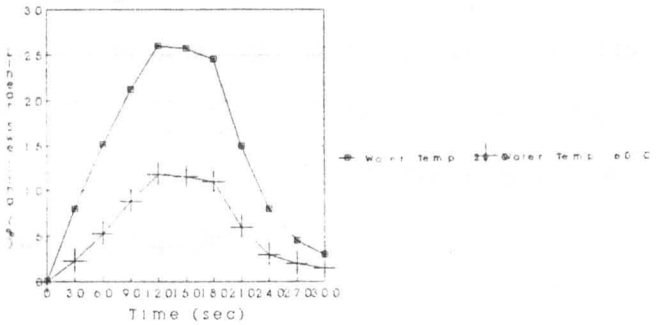

Figure 4.21. Expansion/Contraction Profile.

Since this system was required to operate as a muscle, it must be capable of dilation as well as contraction. The previous tests have dealt with expansion and contraction in isolation, but it was now appropriate to integrate these features to produce the muscle-like action required. The experiment was set up using the basic design indicated above, but in this instance the saturation of the muscle was produced by direct spraying of a heated water jet into the cell using the same mechanism as that employed for distributing the air. The temperature of this inlet water ranged from 20°C to 60°C with a spraying period of 120 secs. This period of water induced swelling was followed by 180

sec. of thermal stimulation producing contraction, figure 4.21.

The measured expansion of 22% occurred fairly slowly, but the increased temperatures helped to increase this dilation rate. Tests were later conducted on the strength of the contraction produced under these conditions and it was measured at in excess of 50N/cm^2.

There still remained several problems which must be overcome in this design.

(1). The quantity of solution supplied is many times greater than that absorbed by the muscle, and this excess must be disposed of somehow.

(2). Much of this excess is retained between the strands of the containing vessel and must be expelled before rapid contraction can obtained.

This method of stimulation clearly shows that an artificial muscle using thermal stimulus is a possibility although the response rate is not exceptional. There is, nevertheless, excellent contractile strength and good potential, especially if more rapid drying is possible, by perhaps using microwave heating. These initial tests had not suggested any method of producing an actuator which was felt to be responsive enough to be applied in robotics, but it was believed that in view of the contractile forces available during drying that it might be worth investigating the use of other dilation inducing solvents having a lower boiling point and heat capacity.

4.9.4 Chemical Stimulation

Polymer muscle samples (type 6) were prepared, measured, and immersed in a number of solvents for several hours, with any responses being noted, Table 4.5. These tests which were conducted using ammonia, ethanol, formic acid, toluene, chloroform, acetone, distilled water, tap water and carbon tetrachloride, revealed that highly polar solvents and those containing hydrogen bonds caused swelling. The non-polar, and low polarity solvents caused no discernable swelling. It was also noticed that certain of the non-polar solvents seemed to cause changes in the dry polymer although not producing swelling. These generally related to changes in clarity and apparent rigidity.

Solvent	Swelling	Comments
Ethanol	No	No Noticeable Change
Ammonia	Yes	Relatively rapid swelling
Formic Acid	Yes	Rapid Swelling
Toluene	No	Becomes more Rigid
Choloroform	No	Slightly more Pliable
Acetone	No	No Noticeable Effect
Distill.H_2O	Yes	Slow Swelling
Tap Water	Yes	Rapid Swelling
Carbon Tet.	No	More Translucent and Rigid

Table 4.5. Solvent Effects on Co-polymer

Subsequently, when a water swollen strip was immersed in acetone rapid contraction was observed. This contraction/dilation cycle was found to be reversible and it was felt that this might be a suitable candidate for testing as a artificial muscular actuator. These tests will be outlined later in this and subsequent chapters.

To understand why the different solvents should produce expansion and contraction, it is necessary to study the factors which are causing this swelling /deswelling reaction. Chemical stimulation produces muscular movements because of polymer - solvent affinity, and the effects can be explained by considering the solubility parameters of the components involved in the processes. PVA has a solubility parameter value of 12.6 $(\text{cal cm}^{-3})^{\frac{1}{2}}$, while that of PAA is 8.8 $(\text{cal cm}^{-3})^{\frac{1}{2}}$. The best swelling solvents are those with a solubility parameter equal to that of the copolymer, which would appear to disqualify water with a value of over 23 $(\text{cal cm}^{-3})^{\frac{1}{2}}$. There is, however, a second factor influencing

the swelling and in this case this is more significant. Hydrogen bonding associated with some solvents causes interaction with the charged longchain polymer molecules, which is why high polar solvents such as methanoic acid produce swelling. Having produced a swollen material using water, what induces the contraction?

Contraction is caused by replacing the water with a solvent for which the polymer has little or no affinity. The high external concentration of this solvent causes the water to move out of the polymer due to osmosis but the external solvent cannot move into to replace the water as this is not energetically favourable. Hence the specifications for a solvent to produce contraction are;

1. A solubility parameter different from the copolymer by more than 1.0 (cal $cm^{-3})^{\frac{1}{2}}$ (the greater separation the less the affinity and the better the changes of contraction).

2. Little or no polar effect.

3. Being completely immiscible with water so that osmosis is favoured.

Clearly, a number of solvents fulfil these requirements.

A number of candidates were tested, with the contractile reaction induced by these solvents being much faster than any which had been previously observed. Of these solvents acetone was chosen as it has a good response, it is readily available, is cheap, and is relatively safe.

Since acetone has a contractile effect and water causes elongation with rapid reversible changes, it was now conceivable that an actuator could be built based on an artificial muscle response, with this chemically stimulated actuator being capable of powering a robot or any other mechanical device.

4.10 Response to Acetone Concentration

Having decided that chemical stimulus was the best way to produce the rapid responses needed to replicate muscle, it was necessary to test the effects which acetone has on the polymer. Since most of these effects relate to the motions produced they will be dealt with when considering the dynamic response in the

next chapter, but it is also important to characterize any equilibrium factors influenced by the acetone.

4.10.1 Development of Acetone Sensor

The first requirement when attempting to test the effects of acetone stimulus on the polymer was to be able to measure the actual acetone concentration in any activating solvents.

This monitoring was achieved using a system based on the conductance bridges outlined in many chemical texts [Palin, 1969], with the operating conditions stated in these tests being observed. The design of this circuit is included in Appendix II.

Calibration of the sensor was achieved by measuring the conductance of carefully prepared solutions of acetone and water, ensuring that the relative proportions of each solvent was accurately known. The calibration curve is shown in figure 4.22. During these tests it was important to ensure that parameters such as the electrode separation and solution temperature remained constant.

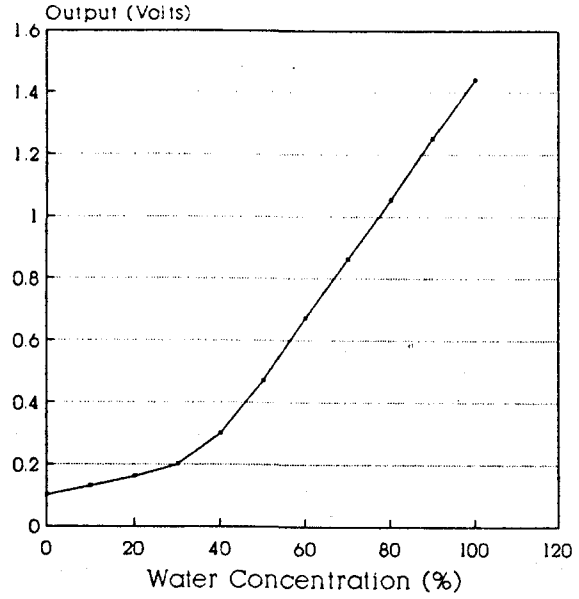

Figure 4.22. Calibration of Acetone Sensor.

Although the sensor is not linear over the whole test range the fact that repeated tests showed the results to be reproducible with no hysteresis, and the ability to program the response curve into the computer means that this device

was acceptable. With the calibration tests completed, this sensor was used in a study of the variation in the polymer length as the acetone concentration changed.

4.10.2 Effects of Acetone Concentration on Muscle Size

Two strips of polymer prepared according to procedures 5 and 7 were treated with water/acetone solutions of varying concentrations for 5 minutes, during which time equilibrium was attained. The lengths of the strips after immersion in the various solutions (concentrations were measured using the apparatus described above) were measured using a sliding microscope, giving extension/concentration plots for each strip, figures 4.23. These tests were repeated while both increasing and decreasing the concentration of the acetone in the stimulating solution.

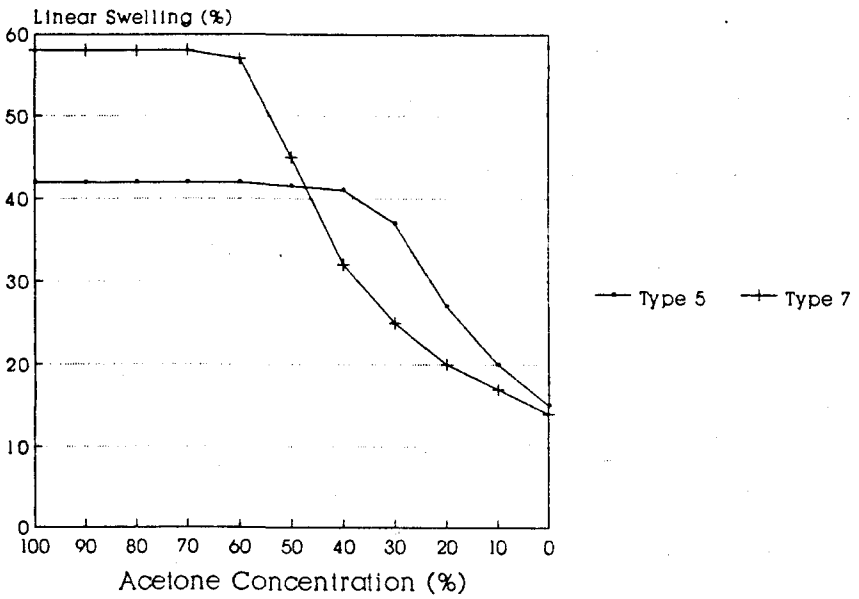

Figure 4.23. Acetone Concentration effect on Swelling.

There are three striking points about the results observed in these tests.

1. The responses are non-linear. There is in fact a distinct S-shape to the curves. When increasing the acetone concentration from zero there is initially very little contraction. Similarly at high acetone concentrations there is very little contraction. In the middle concentration region the change in length with concentration of the now shrunken polymer is very dramatic, and bears

comparison with the phase transition effects mentioned in the previous chapter.

2. The difference between the maximal swelling observed for the two strips was expected due to the differences in crosslinking, but the lower swelling limit of 12% to 15% is most peculiar. No explanation of this effect is as yet satisfactory. Later testing showed that this limit still remains when contraction is stimulated using ethanol and ethanoic acid. It may be that this is an equilibrium point for removal of water (contractile limit) just as there is a equilibrium point for absorption (swelling limit). At present the only way to further contract the polymer to its initial unswollen dimensions is through drying.

3. Although the overall pattern for the two plots is similar with the three distinct regions, the point of on-set varies, as does the gradient in the region of change and the production conditions are clearly having an effect. Increased crosslinking increases the ionisation, leading to an on-set of contraction at a lower acetone concentration. It is again worth comparing this with the phase transition theory for it may be that a very high crosslinking levels a discrete change would be observed.

4.11 Evaluation of Results

In this chapter a co-polymer was produced which when stimulated would respond by swelling and deswelling. A number of methods of stimulating this response were considered and it was discovered that the most effective of these was chemical stimulation using acetone to produce contraction and water to induce dilation. Using thermodynamic analysis the mechanism underlying these movements was uncovered. This chapter has demonstrated the existence of a material which may have potential as a pseudo-muscular actuator. This must now be further tested to determine if the dynamic response, power/weight output, work potential and contractile forces are adequate for the proposed task.

Chapter 5
Dynamic Properties of Artificial Muscle Fibres

5.1 Introduction

The physical, chemical and equilibrium (static) properties of mechano-chemical materials have been studied in detail in the previous chapter. It is now important to consider the factors producing motion and generating forces. The dynamics of electrical [De Rossi, 1986], pH [Kuhn, 1960], and thermal [Caldwell, 1987a] systems have been considered and discarded because of their relatively poor responses, although these schemes proved the possibility of building a muscle replicating actuator. It has subsequently been noted that chemical stimulation using acetone for contraction and water for dilation produces movements which are significantly faster. In this chapter the dynamic properties of chemically stimulated pseudo-muscular fibres are tested and analyzed.

5.2 Dynamic Mechanochemical Properties

Since the dynamic rates of contraction/relaxation, and the forces generated during a contractile stroke are the critical factors in determining the feasibility of an artificial muscle, all properties which might have a bearing on this response must be fully documented. As with the measurement of the static properties of the polymer, the conditions under which the muscle was manufactured have a strong bearing on these properties. These factors which so strongly influence the dynamic rates will be studied in detail in the following

sections.

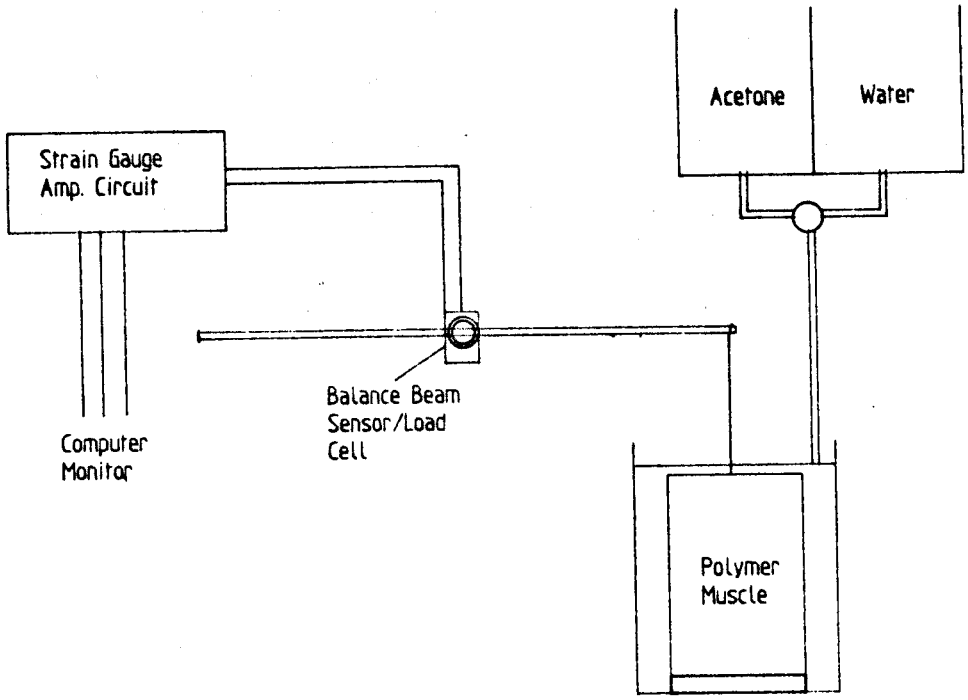

Figure 5.1 Dynamic Response and Force Generation Test Mechanism

The standard experimental setup was as follows: strips of PVA-PAA (the type and dimensions being detailed in the relevant section) were anchored at one end to the base of a water-tight 'muscle cell', figure 5.1. Their free end was connected through a 'tendon' (made from non-elastic cord; nylon covered with a spun-glass core) to the monitoring sensors which measured the rates of muscular contraction/dilation, and muscle forces.

5.2.1 Crosslinking Effects on Dynamic Rates

Several polymer strips prepared according to procedures 5, 6, and 7 (as outlined in chapter 4) and having thickness, 0.15mm, and width 15mm, were tested to determine the effects on the dynamics and the contractile force of varying the degree of crosslinking. These samples were connected into the muscle unit as outlined above. Water (at a temperature of 21°C) was rapidly added to the system and the swelling was monitored using a rotary potentiometer sensor on the balance beam, figure 5.1. When the polymer was fully swollen, the water was removed from the cell and acetone (temperature

17°C) was added, contraction followed. Alternate draining and addition of water or acetone to this system produced muscle-like expansion/contraction cycles. The outputs were recorded using a microcomputer, (the interface and program used to monitor the movement and display the results are given in appendix III). The traces produced by the various strips are shown in figures 5.2.

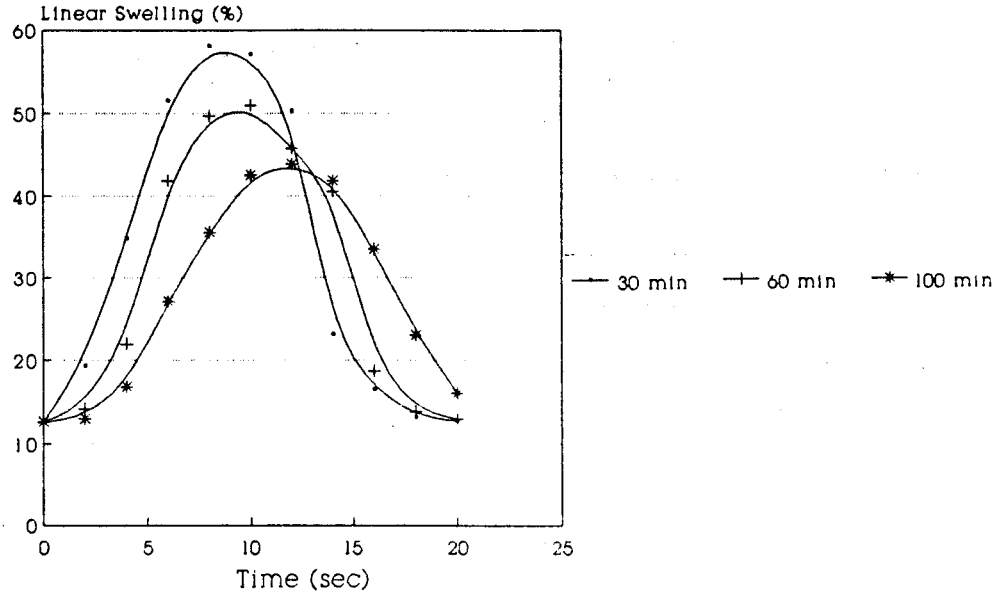

Figure 5.2 Effects of Crosslinking on the Dynamic Response

The rotary beam sensor was then replaced by a beam load cell which had been previously calibrated, appendix III. The swollen polymer was connected to the load cell so as to produce no initial loading.

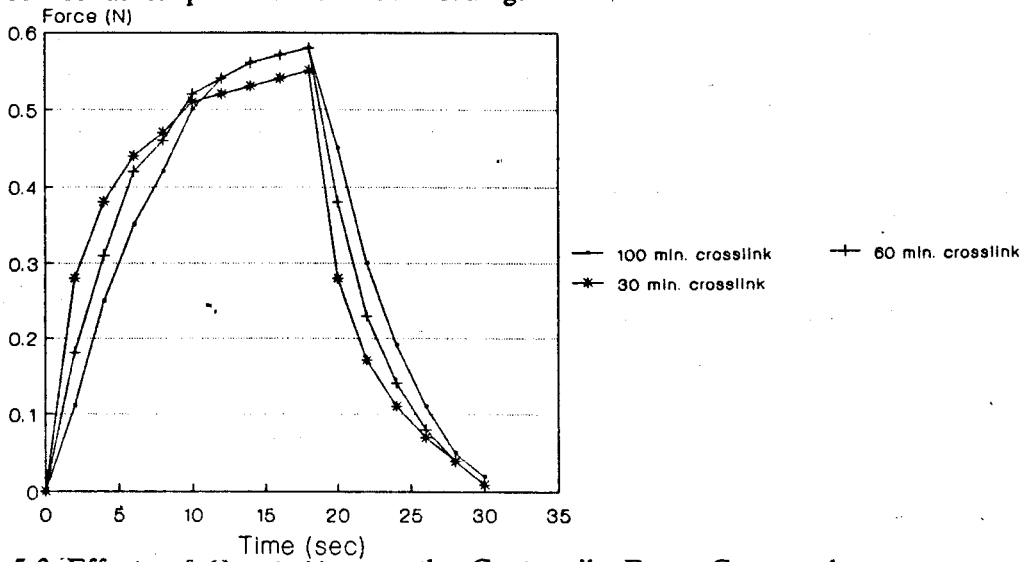

Figure 5.3 Effects of Crosslinking on the Contractile Force Generated.

Addition of acetone produced the expected contraction, while adding water to

the contracted system resulted in rapid relaxation of contractile tension. The forces generated during these sequences were measured and recorded on the computer, figure 5.3.

These results show that crosslinking, which reduces the equilibrium swelling ratio of the muscle as the amount of inter-chain bonding increases, also reduces the dynamic rates. Two factors contribute to this reduction.

1. The amount of solvent required to produce a specific volume expansion/contraction increases as the crosslinking increases, i.e. the material has an reduced swelling coefficient.

2. Additionally, increased crosslinking causes a tighter meshing of the fibres within the network. With a more restrictive material the flow of solvent molecules is reduced. This factor is equivalent to a reduction in the diffusion coefficient with increasing crosslinkages.

The forces generated during contraction are also found to vary with changing crosslinkage values. The first factor that can be observed is that the rate of force buildup and relaxation reduces as inter-fibre bonding increases. The differences in the contractile force although not as large as the rate changes are still important and as expected tend to increase with increasing crosslinking, despite the reduction in the upper swelling limit.

5.2.2 Effect of Film Thickness on Dynamics

For this test three strips of polymer of different thicknesses (0.1mm, 0.2mm and 0.4mm), but uniform width (20mm), were prepared under the same conditions (type 6) with constant PVA-PAA ratios and degrees of crosslinking. These dimensions were accurately measured using a micrometer screw. The strips were tested in the cell described above with the dynamic rate and force generation experiments being conducted as previously outlined.

A study of the dynamic rate results, figure 5.4, indicates that the thickness has a very significant effect on both the rate of dilation and contraction (with reduced fibre thickness increasing the dynamic rates), although the overall

response patterns are similar.

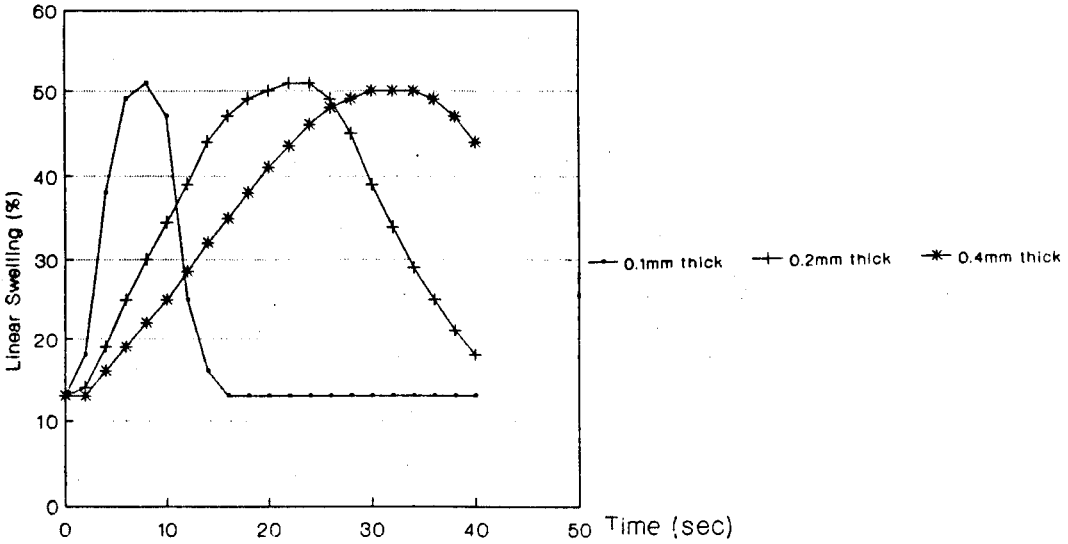

Figure 5.4. Effect of Thickness on Dynamic Response

The measured increases in the maximum contractile rate versus thickness are recorded in figure 5.5.

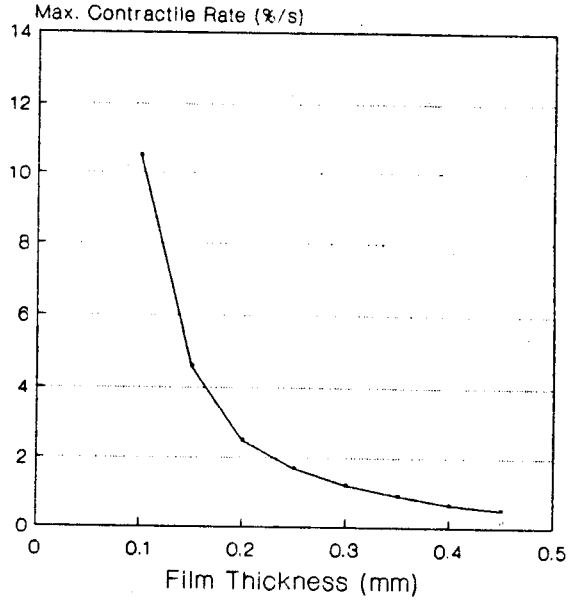

Figure 5.5 Dynamic Response versus Thickness.

Despite these large ranges in the dynamic response rate it was found that in all instances the equilibrium swelling and deswelling values were identical.

It has been predicted that the polymer dynamics will vary as the inverse square of the thickness [Tanaka, 1979]. Based on these results this appears to be a valid relationship which can be expressed mathematically as;

$$\Phi = K_0/\Delta^2 + C_0 \qquad (5.1)$$

Where Φ is the contractile rate, Δ is the thickness and K_0 and C_0 are constants set during the production of the polymer.

This film thickness effect shows that although the present maximum contractile rate (under no loading) is 10.5%/sec. with strips 0.1mm thick; considerably less than values recorded for animal muscle (24% -1800%/sec depending on the muscle), it should be possible to increase the rates in the artificial muscle to values similar or higher than those in natural muscle through the use of thinner films.

The measurements of the forces generated during contraction also show significant changes as the thickness varies, with lower stresses being recorded as the film thickness is reduced. By calculating the contractile force relative to a constant cross-sectional area it was observed that in actual fact the stresses were approximately equal. This suggests that by using multiple thin strips connected in parallel large contractile forces can be generated without sacrificing the rapid dynamic response.

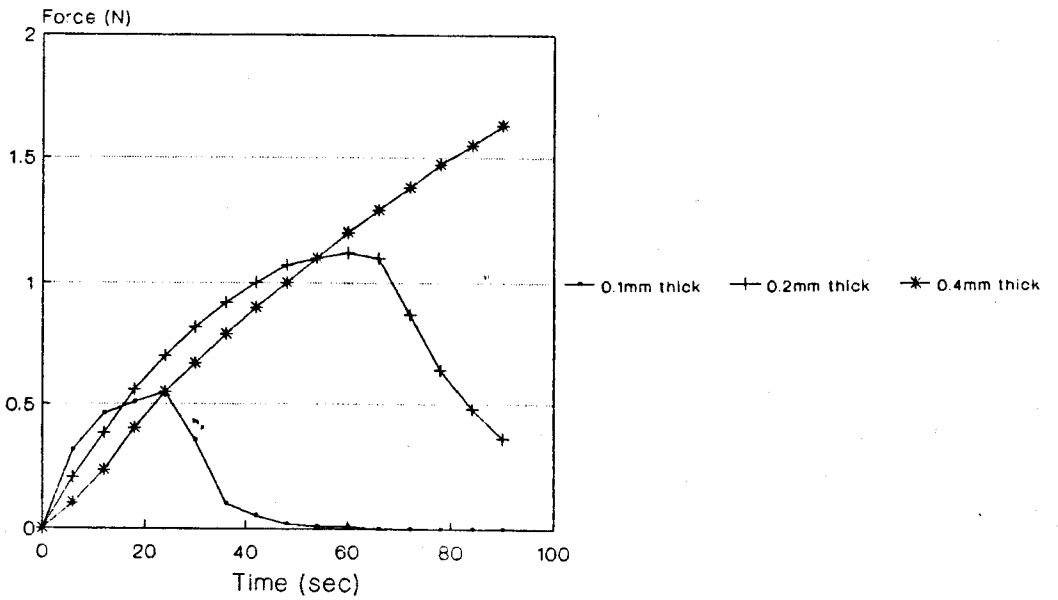

Figure 5.6. Effect of Thickness on Contractile Force

A overall view of the force profiles shows that apart from the relative rates of force build-up and relaxation (faster for thin strips) and the actual maximum

forces generated, the patterns are identical.

5.2.3 Effect of Temperature on Dynamics

Strips of polymer prepared according to procedures 6, and 7 (thickness 0.5mm and width 20mm) were used in testing the effects of temperature on the dynamics. The experiments were conducted using the cell arrangement outlined above, with water temperatures ranging from 21°C to 65°C and acetone in the range 17°C to 45°C.

Measurement, figure 5.7, of the maximum contractile rate at each temperature for both swelling and deswelling shows that temperature variations have a profound effect on the dynamics. Interestingly, the relative changes are almost constant for the both polymers tested.

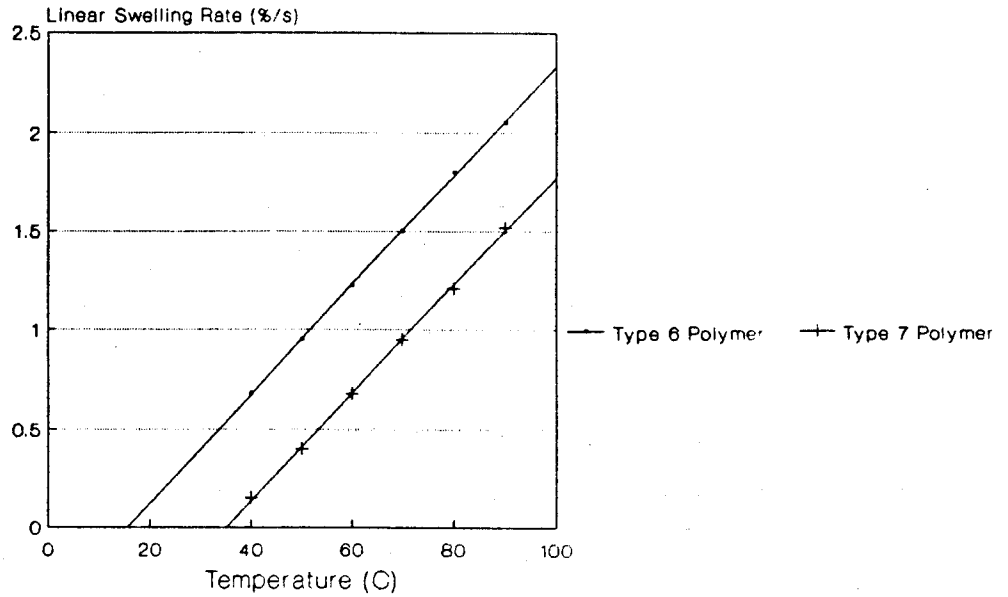

Figure 5.7 Effect of Temperature on Dynamic Response

The increase in the dynamic rates observed when increasing the solvent temperature is given by equation;

$$\sum = \sum_{20} + K'T_{\rho} \qquad (5.2)$$

where $\sum$ is the swelling rate, $\sum_{20}$ is the swelling (contraction) rate at 20°C, K' is a swelling (deswelling) rate coefficient equal to 0.0275°C for swelling in

this instance) and T_ρ is the temperature above 20°C. The production effects appear to be the main cause of variation in these tests. These parameters set the initial swelling/deswelling rate at room temperature.

That the dynamic rates increase by almost equal amounts as the temperature rises is not so unexpected. These increases are caused by an increase in the diffusion coefficient which, being a temperature dependent factor, will be equal or approximately equal in both test samples.

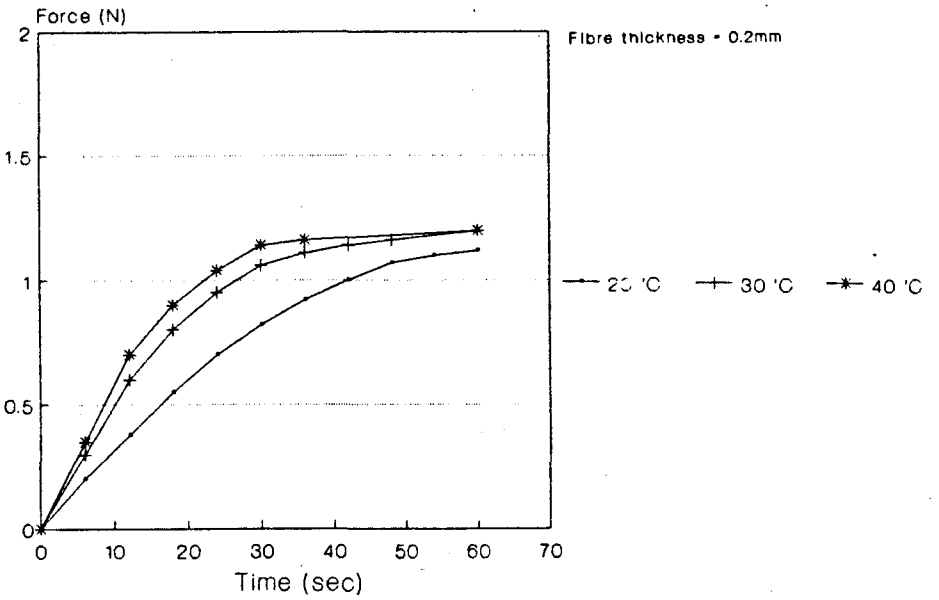

Figure 5.8. Effect of Temperature on Contractile Force

The force generation results, figure 5.8 show that heating has little actual effect on the maximal stress which can be produced, although obviously faster contractions produce faster stress build-ups. It was also observed during these tests that at higher temperatures (>50°C), there appears to be a softening of the polymer which permits deformation and could be detrimental to the mechanical performance. For this reason a maximum working temperature of 40°C was set which gives excellent response rates without compromising strength.

5.2.4 Effect of Salt Concentration on Dynamics

Strips of newly prepared polymer types 5, 6, and 7 (thickness=0.5mm and width 20mm) were used to test the effects of salt concentration on the dynamic

rate and the forces generated. Using the previously described test rig the material was swollen in water solutions with salt concentrations (NaCl) ranging from 0M (distilled water) to 2M (M = molar). The dynamics and forces were recorded in figure 5.9.

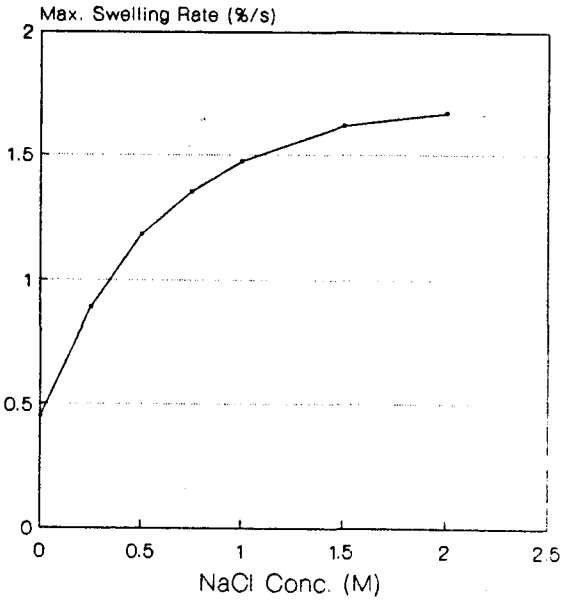

Figure 5.9. Effect of Salt Concentration on Dynamics.

Overall consideration of these results shows that as the sodium ion concentration was increased the swelling rate increased. The change in salt concentration does not, however, seem to have any bearing on the contractile rate, and as a result has no effect on the contractile force generated.

5.2.5 Stimulant Solvent Concentration Effects

During some of the experimental tests it was discovered that contamination of the solvents (acetone in water or vice versa) meant that the dynamic rates dropped substantially. This effect was in addition to the already measured concentration dependent equilibrium swelling results. This suggested that the swelling was dependent on the concentration of the external solution.

This experiment using the apparatus specified above was designed to determine the relationship between the dynamic rates, the contractile forces and the external solvent concentration.

Fully swollen polymer strips prepared according to procedure 6 were

contracted in solutions with known proportions of acetone and water, the resultant plots being displayed and recorded on the computer. From these results a graph, figure 5.10, showing the relationship between the maximum rate of contraction and the solvent concentration was produced.

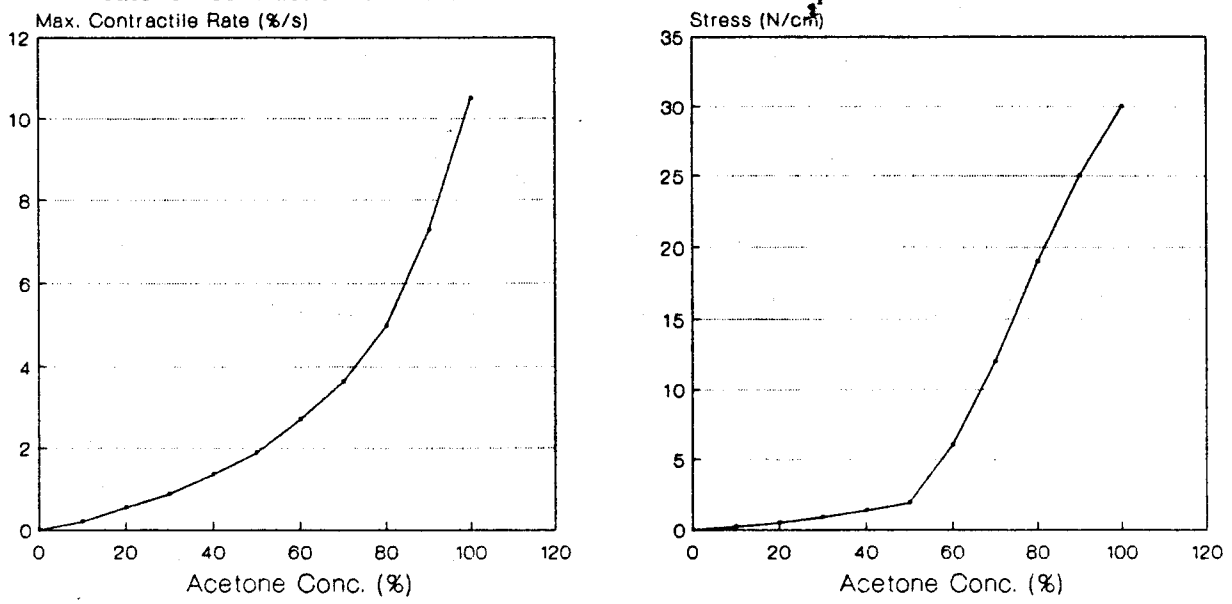

Figure 5.10. Effect of Concentration on Dynamics and Stress.

This can be represented by;

$$\Phi = a_1 e^{(-b_1 x_1^2)} \qquad (5.3)$$

where Φ is the contractile rate, x_1 is the contaminant (water) fraction in the solution and a_1 and b_1 are production parameters, which for this sample are 1 and 23.5. A similar profile was found for dilation, with x_1 in this instance being contamination of the water with acetone. Clearly for maximum response it is very important to ensure that all residual liquid has been removed from the cell before refilling with the second stimulant.

With regard to the force profiles and measurements, figure 5.10, two factors have been noted. First the presence of contamination reduces the contractile force and second the relationship between the force reduction and contamination is non-linear. It is believed that the reduced stress and nonlinear response result from reduced contractile motions, since it has previously being shown that the relationship between polymer length and purity is non-linear, figure 4.23.

5.2.6 Diffusion Coefficient Effects

Chemical stimulation of dilation and contraction is produced by movement of solvent molecules into and out of the polymer. The more rapidly these molecules move the more rapid the response. Clearly it is the diffusion coefficient which governs the rate of movement of these molecules. No specific tests were actually conducted at this stage to measure the diffusion effect since most of the factors influencing the diffusion coefficient value, such as, crosslinking, temperature and the solvents used in activation have been considered previously in this and other chapters. It is nevertheless important to realise the vital role which the diffusion coefficient plays in all the muscle emulating responses being tested here.

5.2.7 PVA-PAA Ratio Effects

The final factor which was considered important in the determination of the responses of the polymer was the PVA-PAA ratio.

Strips of polymer prepared according to procedures 3, 6, 14, and 19 (thickness 0.1mm and width 20mm) were tested using the force and response rate measuring apparatus.

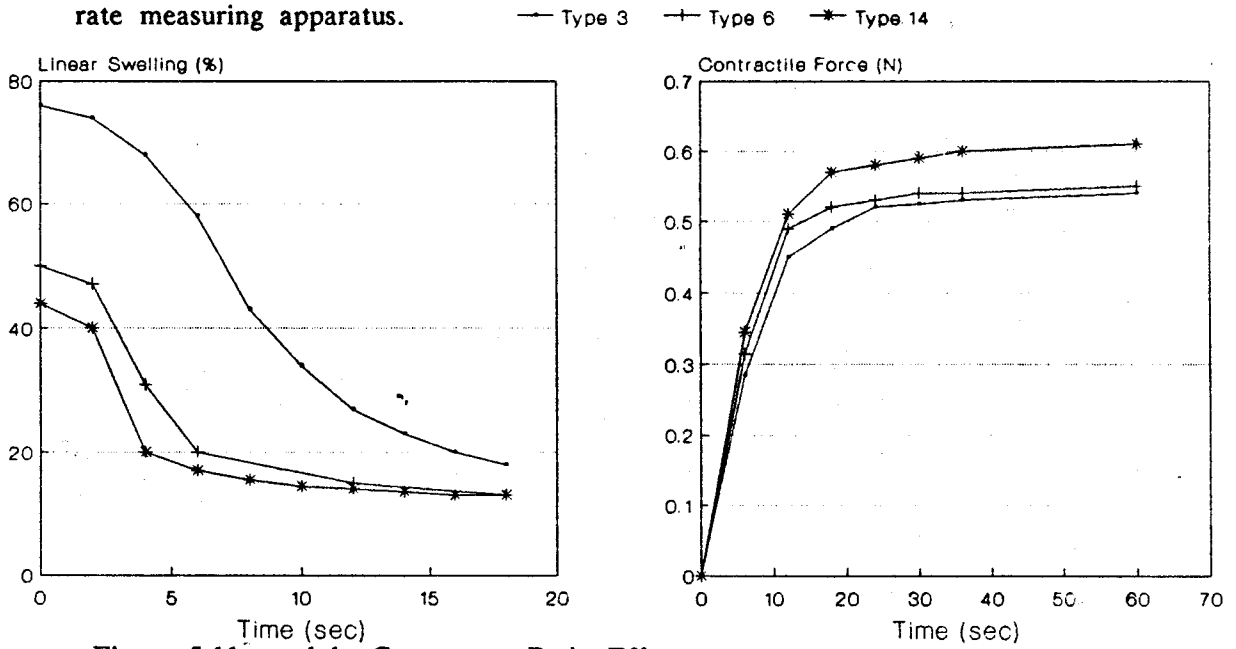

Figure 5.11a and b. Component Ratio Effects.

From these results, figure 5.11a and b, it was observed that the ratio has a

small effect on the contractile force generated, with increases in the ratio causing a small increase in the stress. At these higher PAA levels the material was very brittle. Variation in the component ratios similarly have an effect on the dynamic responses, with increased PAA content increasing the rates, but as with force generation the decrease in robustness must always be considered.

5.3 Muscle Fibre Performance Tests

Having determined the factors which effect the dynamic response and how this response can be varied to give specific characteristics. It was then possible to construct the 'best' polymer for use as an artificial muscle. The first criteria that had to be determined were, what were the optimum characteristics for this synthetic muscle?

It was felt that rapid contraction and dilation were of the upmost importance and as the most critical parameter in this instance was the film thickness, the strips were to be made as thin as possible. The fact that these strips were to be produced in the laboratory meant that thicknesses of less than .100mm were impossible to make with any accuracy or repeatability.

The dimensional changes between fully swollen and fully contracted were the second factor in determining the muscle constitution. These changes were mainly dependent on the amount of crosslinking, so this was obviously the most important factor to consider in this case. Since crosslinking reduces the response rate of the muscle, excessive crosslinking must be avoided, at the same time with too little crosslinking the material is very weak, and also the large dimensional changes which follow mean that the volume of the containing vessel will be large. For these reasons, the crosslinking was set to give an equilibrium linear swelling of approximately 50%. This gave a range of about 35% between the lower limit of 12-15% and the upper limit. A material meeting these dimensional swelling/deswelling requirements can be produced as a result of annealing at 150°C for 60 mins. under no strain.

The need to produce a strong resilient material has been partly dealt with

when considering the degree of crosslinking. The PVA:PAA ratio was, however, also known to have an effect. With high PAA content the contractile force was increased but the material became very brittle, while high PVA content gave a flexible material with greatly reduced contractile force. The best compromise values for use as muscle appeared to be when a PVA–PAA ratio of 3:1 was used.

Now that the material for a pseudo-muscular actuator had been defined and constructed it was necessary to examine its abilities. A series of tests were devised which would help to characterize the properties of the device and allow comparison with other actuators, particularly natural muscle.

Tests were conducted to determine;

1. Polymer swelling from dry.
2. The contraction/elongation rates under no loading.
3. Isotonic (constant load) effects on rates.
4. Isometric (constant length) effects.
5. Contraction/elongation rates in a multilayered muscle.

These tests were an extension of the dynamic tests completed previously, and use the same apparatus, monitoring equipment, and software, figure 5.1. Each of these tests is considered in detail in the following sections.

5.3.1 Polymer Swelling from Dry

Polymer samples prepared as outlined above were mounted in the test cell and water (at room temperature) was introduced. The response profile during the next 5 mins. was then recorded, figure 5.12.

This profile shows that initially (i.e. swelling <15%) the material dilates very slowly. This rate of dilation gradually increases and peaks at about 20–30% swelling. There-after the dimensional changes follow the typical first order pattern expected from diffusion based process.

There are two reasons for this exceptionally low initial rate of expansion.

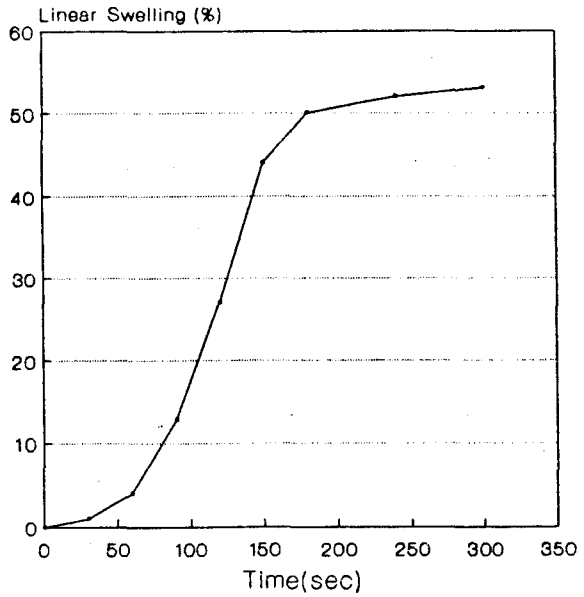

Figure 5.12. Polymer Swelling Profile from an Initial Dry State.

1. A relatively long period of time is required for the penetrant to diffuse into the core of the polymer which is initially in a 'glassy' state. Once some solvent reaches the core this becomes rubbery (plasticizes), and longitudinal expansion is possible.

2. The second factor relating to this initial very sluggish response is due to the diffusion rate being concentration dependent, a feature which is quite common in diffusion processes within polymers. This diffusion effect will be studied in more detail in the next chapter.

5.4 Force/Velocity Relationship

Since this polymer actuator is designed to simulate the movements and action of natural muscle it seems reasonable to try to ensure that valid comparisons can be made between the two materials.

When muscle is stimulated the amount of force it produces depends on whether, and how, its ends are constrained. If the ends are completely free to move, no force is produced and contraction occurs at the maximum rate. If the muscle is immoveably attached at one end and the opposite end has a constant loading, then motion occurs at a speed which is less than the maximum. Larger loading forces increasingly reduce the rate of contraction. If a sufficient force is used in the load to prevent motion, then the maximum contractile force is

obtained.

These properties are generally summarised in a force–velocity curve first used by Hill [Hill, 1938; Hill, 1970] which shows the relationship between the forces generated and the rate of contraction.

In the following experiments the isotonic and isometric properties of artificial muscle are investigated to determine if force–velocity curves of a form similar to natural muscle can be produced for the synthetic version. It is hoped that in this way a fairly direct comparison of the relative merits of the artificial muscle can be made.

5.4.1 Muscular Response under no Loading

A strip of muscle prepared as described in section 5.3, (this will now be termed the 'standard' muscle fibre), with dimensions 50mm x 25mm x 0.1mm was mounted in the cell with one end clamped and the other attached to the unloaded sensor beam, figure 5.1. The polymer was initially brought to equilibrium in water, before being drained and refilled with acetone which caused contraction. Pure water could then be added to the shrunken fibre, causing dilation, figure 5.13. This cyclic process was repeated over 60 times to ensure that the muscle could be operated repeatedly without being destroyed and that no short–term deterioration in performance occurred.

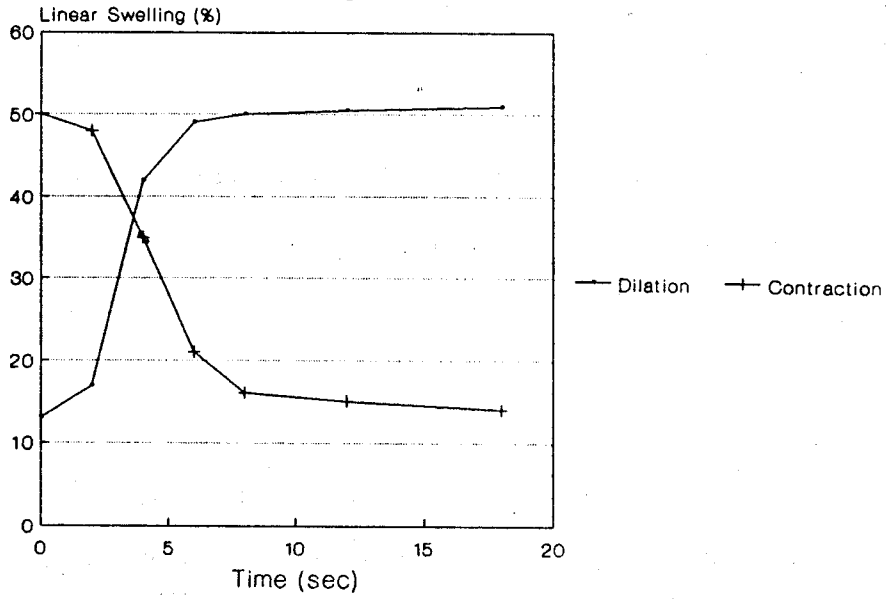

Figure 5.13. Pseudo–muscular Response under Zero Loading.

During initial testing a number of unexpectedly poor responses were obtained. Use of the acetone concentration sensor (chapter 4.10.1) showed that this occurred when the new input solvent was diluted by residual liquid left in the container. To prevent this, as much of the 'spent' solvent as possible was removed. Monitoring using the sensor meant that the purity of the input solvent was never less than 98%, and this gave consistent response readings.

From the response plots the maximum rates of dilation (11%/sec) and contraction (10.5%/sec) can easily be calculated. That these rates are not equal is mainly due to slight differences in the diffusion coefficient when the molecules are moving into the polymer as opposed to the rate when diffusing out. These response rates may alternatively, be quantified as time constants for the material to reach 63% of the terminal value. For this test, values of 5.3 sec. for relaxation and 4.8 sec. for contraction where recorded. Beyond this point of maximal swelling the responses slowed and finally stopped once the equilibrium swelling limit was reached. As in the tests in chapter 4.10 it was noticed that there was a lower deswelling limit of about 12–15%.

Observing the overall response of the fibres it was noted that as in the case of swelling from dry there is a short delay before the maximum rate of change is experienced. In these instances this is believed to be primarily due to the penetration delay period, rather than the concentration dependence of the diffusion coefficient.

Repetition of the results showed that after in excess of 60 cycles (limited by the availability of acetone), the responses were still comparable with those obtained in the first cycle.

5.4.2 Isotonic Response

Isotonic tests were conducted to determine the ability of the muscles to respond under loading. Two different strips were tested in this instance as it was necessary to determine if the thickness of the film had an effect on the

lifting ability per cm^2 of the muscle. The 'standard' muscle fibre was used along with a strip prepared under the same conditions, but having double the thickness (0.2mm). The tests were conducted using the cell test apparatus previously described. Constant loadings were produced by suspending weights from the counter balancing arm of the beam sensor.

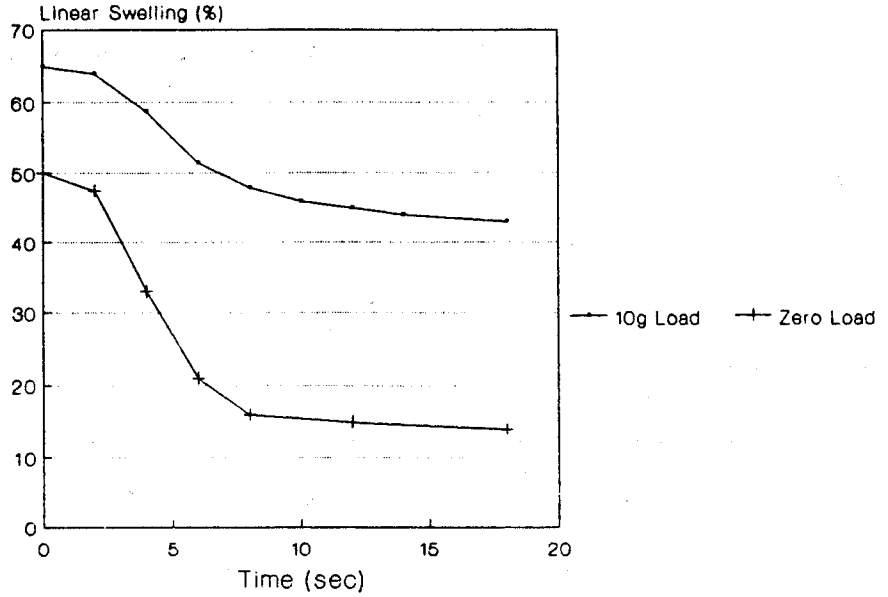

Figure 5.14a. Effect of Loading on Contraction Profiles.

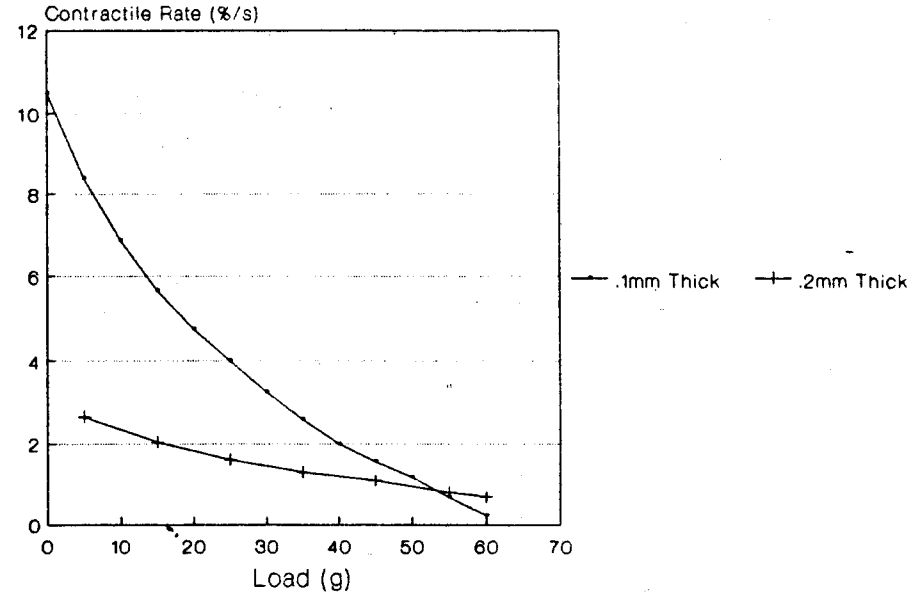

Figure 5.14b. Variation in Contractile Response with Loading.

The effect of loading on the maximum contractile rate (the active component in a muscle based system), is shown by the results in figure 5.14a and b. Using these results it can be seen quite clearly that the increased thickness does

improve the response under loading, with the thicker fibre having approximately twice the contractile potential, of the standard strip. However, when these loading and contractile velocity values are calculated in terms of loading per cm^2 it is found that the abilities of both muscles are constant across the test range.

An analysis of the range of movement of the loaded strips, figure 5.14a, shows that free motion is greatly reduced. This observation is expected.

Repeated tests on the ability of the polymer to lift loads shows that the results were reproducible provided plastic deformation did not occur. This means that a upper 'safe' loading limit needs to be defined, which for these muscle fibres is under $42N/cm^2$. This plastic deformation while obviously being undesirable does not in fact destroy the muscle, which is still capable of lifting loads up to the 'safe' limit at speeds comparable with those of the undamaged model. The main effect is a stretching of the strip (with greater extension as the overloading is increased) relative to its resting dimensions. Beyond the region of plastic deformation the muscle tore under the effects of excessive loading ($>60N/cm^2$). A stress-strain curve showing the effects of this loading is produced below, figure 5.15.

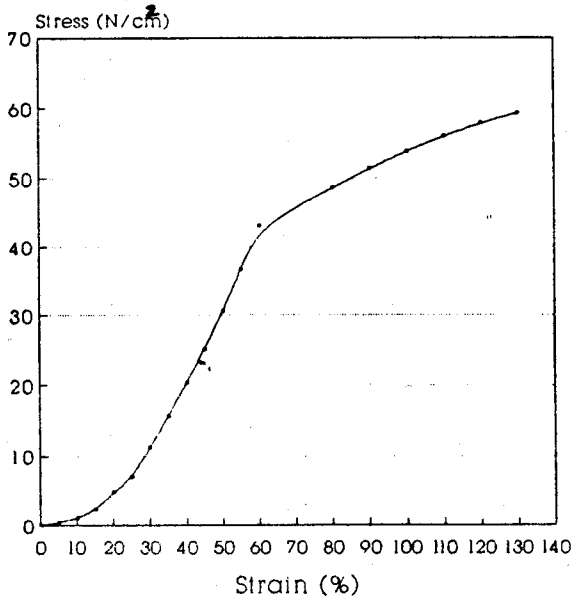

Figure 5.15 Stress-Strain Curve for Muscle Fibres.

5.4.3 Isometric Response

Measurements of the isometric forces generated by the muscle are required to complete the force/velocity profile. It is this ability to exert a force while not physically shortening that is critical in actually grasping and holding an object firmly once initial contact has been made. Using a 'standard' muscle fibre of length 50mm and width 20mm the test cell was set up as before but with the beam sensor replaced by load cell which measures the stresses generated during contraction. The muscle fibres were attached to the load cell through the tendons in such a way that the fully swollen film was fully extended, but no tension was being generated. The forces generated during stimulated contraction and dilation were recorded on the computer and the results shown in figure 5.16. The test was repeated several times to ensure the repeatability of the results.

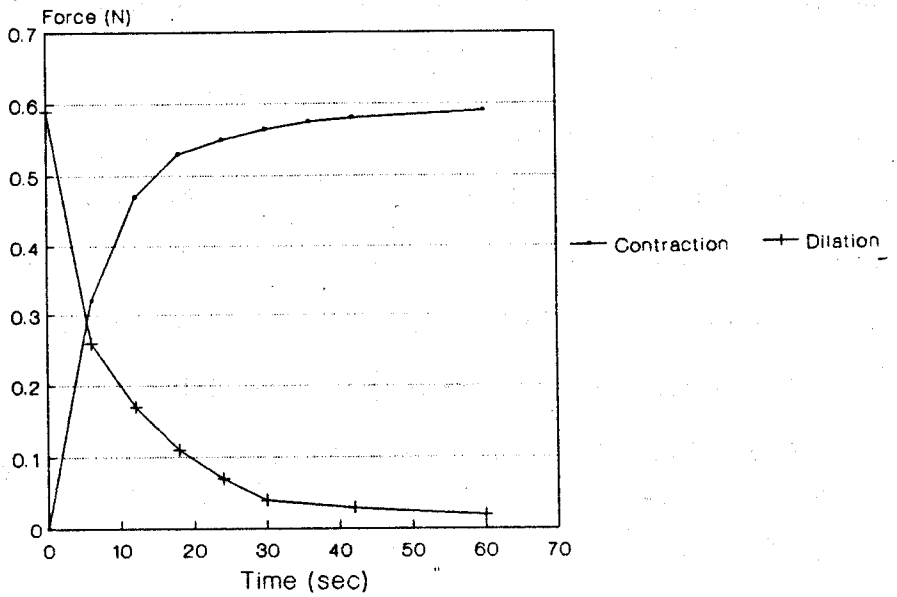

Figure 5.16. Isometric Force Generation.

At constant length, the forces on contraction rapidly build up, the greatest changes being recorded in the first few moments when it was previously determined that the rate of contraction was at or near its maximum. The contractile forces developed by this muscle under these conditions were up to 0.59N which in terms of the force per cm^2 of contractile material is just under $30N/cm^2$. This compares very well with the forces generated by natural muscle

which range from 20N/cm²–40N/cm² depending on the animal and the muscle chosen [Woledge, 1985; Pedley, 1985]. Muscular relaxation on the addition of water is found to be even more rapid, with the initial change being particularly fast. The repetition of the experiment showed the performance to be reproducible (to within ±0.02N i.e. ±1N/cm²) over up to 15 cycles with no degradation. The number of cycles tested was again limited by the availability of acetone.

This test clearly demonstrates that polymer actuators are capable of generating the high forces required when gripping an object, while the rapid relaxation means that any gripped object can be quickly released preventing damage. At the same time the force can be accurately regulated by controlling the stimulus, stopping contraction at any desired instant. The compliant nature of the polymer muscle is also of benefit in these tasks, preventing damage to sensitive objects.

Using the results produced by the no load, isotonic and isometric tests, a force/velocity diagram can now be constructed showing the variation in contractile velocity with loading. The maximum contractile velocity is obtained under no loading and is specified as V_{max} which for these artificial muscle fibres was just under 11%/sec.. The maximum force, obtained from the isometric experiment is F_o, which for an artificial muscle is 29.5 N/cm².

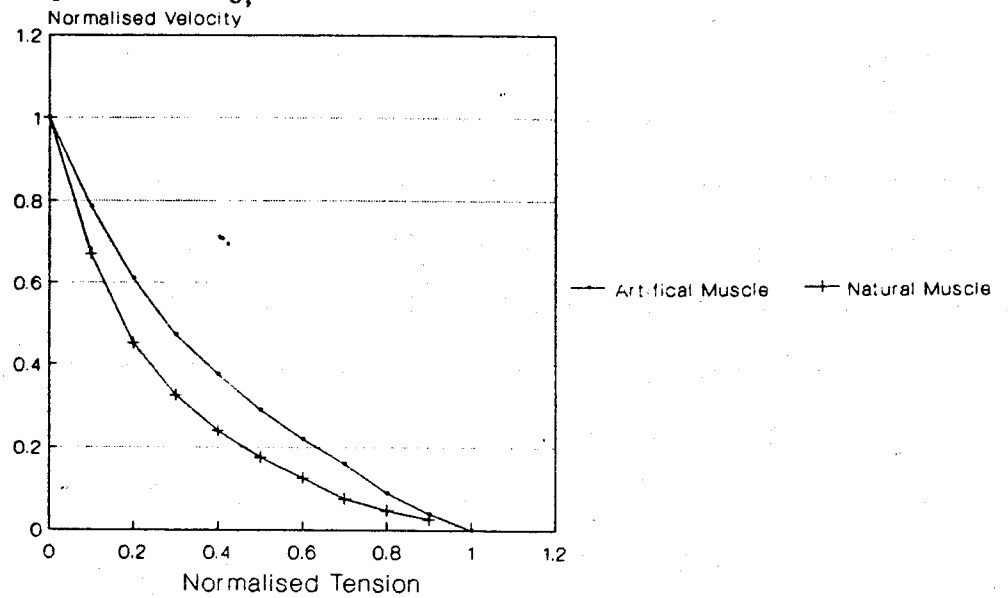

Figure 5.17. Force/Velocity Relationship for Artificial Muscle.

Figure 5.17 shows the force/velocity relationship obtained using the isometric and isotonic data obtained in the preceding sections. This may be approximated by a rectangular hyperbola with equation;

$$(F+ a)(V + b) = (F_o+a)b \qquad (5.4)$$

where F is the force during shortening at velocity V, F_o is the force during isometric contraction, and a and b are constants. This pattern is of the same form as that produced by Hill [Hill, 1938] in his tests on animal muscle.

5.5 Multilayered Muscle Dynamics

The previous tests have shown the potential of a single polymer strip to respond to chemical stimulus quickly and strongly. But to develop a system capable of powering a robot gripper the total gripping strength and contractile force must be increased significantly. The simplest way to do this would be to use strips with increased cross-sectional area, hence just as in nature, limbs with heavy loading have larger muscles.

To ensure rapid responses were retained during this thickening process the fibres must remain thin and to achieve the desired overall thickness, 10's (or perhaps 100's) of fibres must be connected in parallel. Producing and testing such a muscle 'bundle' was the object of this experiment.

The contractile force and rate experiments previously conducted on a single fibre were repeated using 10 'standard' strips of length 50mm and width 20mm connected in parallel forming a muscle bundle. Since small variations in film thickness and crosslinking are known to have a significant effect on the response rates, particular care was taken to ensure that the fibres were as uniform as possible. The results obtained are used to construct a new normalised, multi-muscle, force/velocity profile, figure 5.18, which can be directly compared with the single muscle equivalent.

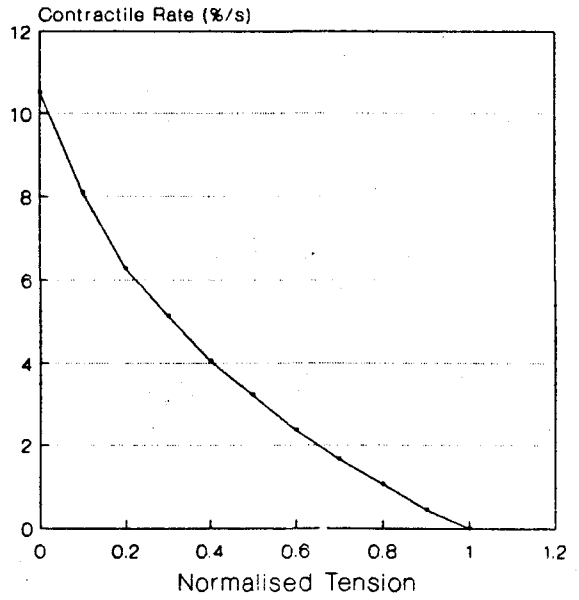

Figure 5.18. Multi-fibred Force/Velocity Profile.

These results show that the use of a multi-layered muscle bundle produces no reduction in the rates of contraction and dilation. The isometric and isotonic responses of the muscle bundle, monitored as in the case of the single fibre, show the multi-layered muscle generates greatly increased contractile forces with substantial increases in the safe loading limit, these values increasing to 6.1N and <7.9N respectively. When normalised this gives values of 30.5N/cm^2 for the contractile force and <39.5N/cm^2 for the safe loading limit. The slight difference between the values for the single (29.5N/cm^2) and multi - fibred tests is probable due to errors in reading the values and small non-uniformities in the strips forming the muscle bundle.

A comparison of the normalized force/velocity profiles for the single and multi- layered muscle systems, figure 5.17 and 5.18 indicate that the use of several hundred or thousand polymers strips is a viable long-term objective and with such a system a very powerful actuator will be a possibility.

5.6 Muscular Power Output

When measurements of the mechanical performance of muscles (both natural and synthetic) are to be compared, it is often desirable to eliminate variations due to size, shape, and arrangement of the contractile components.

Many arrangements are possible, but in this study the films are arranged into bundles with the fibres connected in parallel between the binding points. This basic model is applicable to some forms of natural muscle as well as synthetic muscles and this permits comparison. Since the shortening velocity being measured adds up along the length of the fibre, it is proportional to the muscle length, and the normalized contractile velocity can be given by [Woledge, 1985];

$$V_{norm} = V/l_f \qquad (5.5)$$

where l_f is the muscle fibre length, V is the velocity of shortening and V_{norm} is the normalised velocity of shortening per unit length. With the fibres in parallel, the force generated is proportional to the total cross–sectional area of the fibre, and the normalized force is [Woledge, 1985];

$$F_{norm} = F/A \approx Fl_f/vol \qquad (5.6)$$

where vol is the volume of the dry muscle fibre, F is the force generated, A is the cross–sectional area, and F_{norm} is the normalised force per unit volume. The power of this actuator can now be obtained from the velocity and force values. The normalised power output P_{norm} being;

$$P_{norm} = F_{norm} V_{norm} = FV/vol \qquad (5.7)$$

This power output equation is valid for all other possible arrangements of the fibres although the velocity and force measurements may vary considerably [Woledge, 1985; Pedley, 1985]. The power produced by any muscle, natural or artificial can now easily be obtained using the information contained in their force/velocity profile, figure 5.17 or 5.18, to give a power/force relationship, figure 5.19.

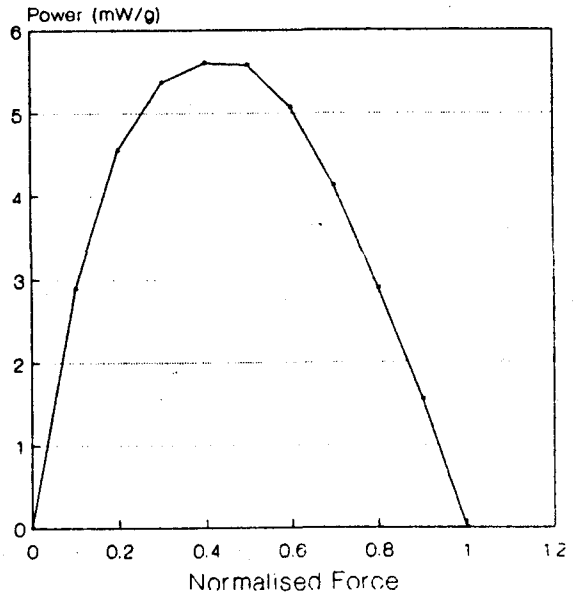

Figure 5.19. A Power/Force Profile for Artificial Muscle.

This clearly shows that maximum power is generated at medium shortening velocities and low contractile forces. It can in fact be proved mathematical that the maximum power is generated when $P_{norm} = F_{norm}$ (Appendix IV).

The maximum power/weight ratio obtained in these experiments using an artificial muscle is 5.8mW/g which is considerably less than that for natural muscle, which may vary from 40 to 200mW/g depending on the muscle being considered [Woledge, 1985; Wilkie, 1976]. This is not, however, a major cause of dismay since the power output is a product of the force generated times the contractile velocity. Hence by using thinner fibres (<0.1mm) improvements in the power output comparable with those already predicted (and obtained) for contractile response rates are possible. For example using the contractile rate versus thickness theory it is predicted that polymers strips 0.01mm thick would have a power/weight ratio of 580mW/g.

Although the power output of natural muscle is at present much greater than for the artificial muscle, it is interesting to note that the total energy available from both systems is comparable at 0.6–0.8J/g for natural muscle [Woledge, 1985] and 0.4J/g for the synthetic muscle.

5.7 The Carnot Cycle and System Efficiency

Thermodynamic analyses conducted in previous chapters have tended to deal with the energy balances during swelling and deswelling. Now that it has been demonstrated that the polymer can perform work it may be useful to consider the work cycle which is involved and the potential efficiency of such a system. These analyses will be based on the thermal work cycles developed by Carnot (idealised gases), Otto (combustion engines) and Diesel (diesel engines). Using methods developed for these thermal engines, the work cycle and thermodynamic response of polymer muscles will be studied.

For the mechanochemical cycle the driving force is the chemical potential of the stimulant solvents, with the variation being plotted as changes in the polymer length and force. As with the other cycles a four stroke operation is required, figure 5.20.

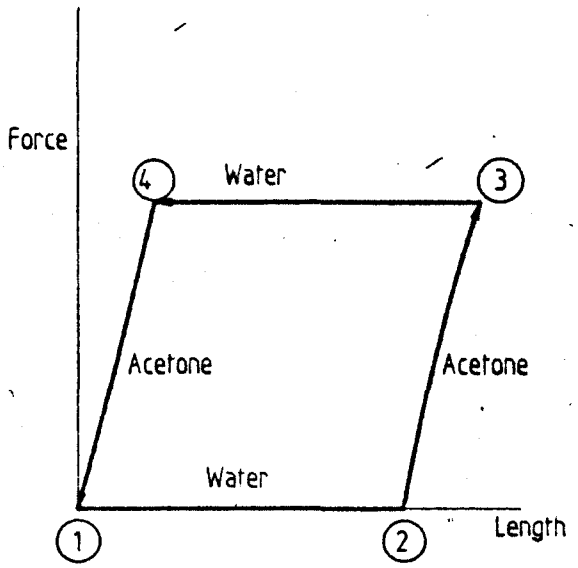

Figure 5.20. Mechano-chemical Work Cycle

The operation of this device as an engine can be explained in the following way. Starting at {1}, water is added to the system which causes expansion against no external forces {1} - {2}. At {2} the water is removed from the system and an external force is applied, causing obviously an increase in the force and also extension, {2} - {3}. The force is kept constant at {3} - {4} but the chemical potential is changed by the addition of acetone. Here

contraction occurs against a constant load. Finally the external force is reduced to zero once more and the force/extension relationship returns to its original position by {4} - {1}.

The energy changes for each steps can be given as;

$$[dH]_{(1)-(2)} = [\mu_{H_2O}\, dn_{H_2O}]\ (1)-(2) \qquad (5.8a)$$

$$[dH]_{(2)-(3)} = [fdl]_{(2)-(3)} + [\mu_{H_2O}\, dn_{H_2O}]\ (2)-(3) \qquad (5.8b)$$

$$[dH]_{(3)-(4)} = [fdl]_{(3)-(4)} + [\mu_{Ace.}\, dn_{Ace.}]\ (3)-(4) \qquad (5.8c)$$

$$[dH]_{(4)-(1)} = [fdl]_{(4)-(1)} + [\mu_{Ace.}\, dn_{Ace.}]\ (4)-(1) \qquad (5.8d)$$

where μ is the chemical potential, dn is the number of ionic groupings in the solvents, H is the Helmholtz energy, and dl is the displacement change in the material under an external force f.

From these results it is seen that steps {1}-{2}-{3} represent the work done on the fibre to cause dilation, while {3}-{4}-{1} is the contractile work which the system performs.

The absolute work developed by a mechanochemical material is then given by [Tatara, 1972a; Tatara, 1972b];

$$W = \Delta\mu dn = \mu dn + \mu dn = (\mu_1 - \mu_2)\Delta n \qquad (5.9)$$

where μ is the chemical potential before (μ_1) and after (μ_2) swelling.

The effective mechanical work of the material is then given as [Tatara, 1972b];

$$E = -ofdl = f\Delta l \qquad (5.10)$$

where Δl is the contractile length of the material. Thus the work efficiency of a mechano-chemical material is [Tatara, 1972b];

$$\eta = E/W = -fdl/\Delta\mu dn \quad (5.11)$$

Sussmann and Katchalsky reported that the mechanical efficiency of such mechano-chemical systems (using collagen as the active material in this instance) was up to 40%. While experiments conducted by Tatara [Tatara, 1972b] gave efficiencies of up to 30% for fibres made from contractile polymers, and up to 60% efficiency for cationic resins swollen in water.

5.8 Conclusions

In this study it has been demonstrated that an artificial muscle made from a polyvinyl alcohol/polyacrylic acid copolymer can be chemically stimulated, using acetone for contraction, and water for dilation, producing an output which can be coupled to a load giving a effective actuator response. The performance profile of this pseudo-muscular actuator is comparable on a macroscopic scale with natural muscle giving strength, contractile force and energy outputs which very similar.

As this device is to be used an actuator to power a robot gripper (although it could be used in a multitude of other actuator applications) a number of design parameters need to be maximised. The most basic of these are the rate of response and the force which can be generated.

With the polymer muscle various factors involved in the production processes are known to have a strong influence on the properties and responses. Increases in crosslinking reduce the swelling ability and the rate at which expansion and contraction occur, at the same time the strength of the material is enhanced. Increasing the PAA content gives a muscle with greater contractile force generation, but unfortunately this system is not robust. With only a little PAA the resilience is increased, but the stresses generated are lower and a compromise value which is suited to the specific situation is required. Increasing the salt concentration of the water enhances the swelling rate, but can result in

salt deposition due to salting out. Temperature increases raise both the contractile and the dilatory rates but must be limited to prevent damage, while for optimum response it must be ensured that the water and acetone are uncontaminated. Finally, and perhaps most importantly is the thickness of the fibres. They must be made as thin as possible to provide rapid response, with the reduction in mechanical strength and contractile forces which accompany the thickness reduction being offset through the use of multilayered muscle bundles with many fibres connected in parallel.

In terms of the power/weight ratio the synthetic muscle is at present, much poorer than the natural muscle and provides only about one sixth of the power/weight performance of electric motors [Radio-spares, 1989]. These figures are in terms of the mass of the dry muscle and also do not include the mass of the muscle cell or fluids. These factors will obviously reduce the power/weight ratio still further.

While the power output at present is poor, the potential use of thinner fibres could substantially enhance this performance. This combined with a number of other important features such as;

a). rapid response, again through the use of thinner fibres,

b). total energy storage and contractile forces comparable with natural muscle,

c). direct compliance control,

d). and linear direct drive,

shows the scope that exists for the development of an new actuator to rival present systems.

Chapter 6
Mathematical Modelling and Simulation

6.1 Introduction

The potential power made available through the use of chemically stimulated artificial muscles has recently come under renewed investigation [Osada, 1985, De Rossi, 1986; Suzuki, 1987], but to date modelling of the processes has been very limited. The development of muscle-like actuators depends on the ability of polymer gels to convert chemically stimulated microscopic motion into macroscopic volume and force changes, and it is vital to the future progress of this technology that accurate simulation models are developed so that muscular control strategies can be tested.

This study is aimed at investigating the causes of this contractile behaviour and simulating the motions produced following the diffusion of the activating chemicals into the fibre network. Using the models derived for the contraction and dilation of the fibres, control strategies for these muscular actuators can be tested before being implemented on experimental systems to be considered in chapter 7.

6.2 Mathematical Model

In analyzing and describing the transient mechanical behaviour of a polyelectrolyte gel element in response to chemical stimulus, it must be remembered that this is basically a concentration controlled diffusion problem. Models of penetrant diffusion in solids have been available for many years

[Thomas, 1982; Peppas, 1984], but while these analyses are very thorough, it is desirable to develop a simplified approach which can be adapted for numerical solution and yet retains the required accuracy. The mathematical model developed here was designed to incorporate the effects of volume changes due to penetrant diffusion, but local stresses are not considered.

Being primarily a diffusion controlled reaction the processes involved are basically governed by Fick's diffusion equation [Casey, 1962]:

$$dC/dt = d\ (D\ dC/dx)\ /\ dx \qquad (6.1)$$

where C is the concentration at time t and at distance x from the centre of the strip along the normal to the face, D is the diffusion coefficient. The driving force for the swelling/deswelling is the penetrant concentration difference between the polymer gel at equilibrium, and at time t. This concentration may be expressed as a ratio of water to polymer in a giving volume. As a first order approximation this gives the swelling rate as [Freundlich, 1926];

$$Sr = dA_\tau / d\tau = K_c(A_\infty - A_\tau) \qquad (6.2)$$

where A_τ is the amount of penetrant absorbed at time τ, and A_∞ is the amount absorbed at equilibrium. K_c is a coefficient depending on the solvent, temperature,and production factors.

This model is, however, too simple and the presence of a number of system non-linearities and secondary factors must be considered if an accurate simulation is to be developed. These factors as they relate to the mathematical model will be dealt with in the subsequent sections.

6.2.1 Diffusion Coefficient Effects

The diffusion coefficient controls the rate of movement of the chemical molecules within the polymer strips and as the dynamic rates are dependent on

the chemical properties, this is clearly a very important parameter.

This diffusion coefficient is not a fixed quantity, but varies with a number of factors having a significant influence, such as; solvent used, internal solvent concentration, crosslinking, and temperature. The exact nature of these effects will now be considered.

1). Solvent used. The solvent used has a very significant bearing on the diffusion coefficient, hence, methanol has a different diffusion value from distilled water or a solution of NaCl. Unfortunately, due to the polar nature of the polymer, it is not possible to predict accurately how a particular solvent will affect the coefficient value, and this can only be determined by experiment.

2). Internal solvent concentration. The diffusion coefficient is subject to changes as the concentration of the solvent within the body of the polymer increases or decreases. These types of concentration dependent diffusion variation are typically modelled as [Buckley, 1962];

$$D = D_0 \exp^{\beta V} \qquad (6.3)$$

where D is the diffusion coefficient, D_0 is the diffusion coefficient of the unswollen polymer, β is parameter defining the concentration dependence of D, and V is the swelling fraction of solvent penetrating the polymer at time τ.

3). Crosslinking. Previous testing has demonstrated the effects of crosslinking on the contraction - dilation dynamics. Two factors can be identified:

i) The variation in bond length effects the ease with which a solvent can move between the long-chain molecules.

ii) The bond strength governs the swelling ratio (swelling produced relative to the amount of solvent imbibed).

Again as in (1) the effects of these parameters can only really be determined experimentally.

4). It has been shown experimentally in the previous chapter that the

dilation/contraction rates are temperature dependent, with a relationship given by;

$$\sum = \sum_{20} + K' T_\rho \qquad (6.4)$$

where $\sum_{20}$ is the dilation/contraction rate at 20°C, K' is a dynamic rate coefficient depending on the production parameters, and T_ρ is the temperature above 20°C. This rate increase is due to an increase in the energy of the solvent molecules as the temperature rises, that in turn leads to more rapid molecular motion. Clearly the effects of temperature variation must be taken into account in the development of an accurate simulation model.

6.2.2 External Solvent Concentration Effects

A second important effect which has been observed in dynamic tests conducted in the previous chapter is the change in the rate of dilation and contraction when the stimulant chemicals are contaminated, (traces of water in acetone or vice versa). Modelling of these responses in the muscle simulator allows an analysis to be made and an equation to be found relating the dilution to the reduction in dynamic response. This is given by;

$$\Phi = \Phi_0 \exp(-\gamma(C_x^2)) \qquad (6.5)$$

where Φ is the dynamic rate, Φ_0 is the dynamic rate when using pure chemicals, γ is a parameter defining the dilution dependence of Φ, and C_x is the concentration of the external solvent.

6.2.3 Plastizing of Core

A third factor which causes distortions in the output is the finite diffusion period. During the initial stages of solvent absorption the polymer has a 'glassy' core which remains rigid and restricts longitudinal motion. When solvents

reaches the core this 'softens', and motion is possible. The time delay associated with the diffusion into this central region will, however, always mean that the core's reactions to stimulii will lag behind those of the surface regions.

During contraction similar delays occur, but in these instances the central region remains swollen while the surface layers contract rapidly. This occurs because the diffusing solvent (water) is now being drawn out-of, rather than in-to the polymer.

Tests on the polymer have also revealed that the solvent content also has a significant effect on the elastic modulus of the material. Swelling produces considerable reductions in the fibre strength, with this effect being particulatly apparent during the initial stages of solvent absorption. These effects are modelled by incorporating the Young's modulus into the calculation, with the relationship between swelling fraction and modulus having been obtained in chapter 4;

$$G = K_1/(S_w^3 - C_1) \qquad (6.6)$$

where G is the Young's modulus, S_w is the linear swelling fraction (ratio of the swollen to dry polymer lengths) and K_1 and C_1 are constants set in the production of the polymer. Using this equation it becomes a simple process to calculate the modulus value (material strength) at any penetrant concentration. The length change in the z-direction, (the power stroke) is then calculated by combining knowledge of the plastizing of each element due to diffusion in the χ-direction, with the modulus at any swelling fraction and the rate at which stimulant chemicals are input into the muscle cell.

These effects are particularly important because by using these variations and by controlling the percentage solvent content and external solvent concentration, the stiffness of the gripper can be varied producing a gripper with variable compliance controlled directly by the actuator.

6.2.4 Dimensional Change Effects

The primary characteristic of this polymeric muscle is its ability to expand and contract, and these dimensional changes lead to non-linearities which clearly must be considered when attempting to formulate a model of the system. This expansion and contraction is modelled by permitting the elemental volume within the fibres to vary according to;

$$\Delta x_\tau^3 = \Delta x_0^3/(1-K_4A_\tau)^3 \qquad (6.7)$$

where Δx_τ the elemental volume at time τ, Δx_0 is the initial volume and K_4 is a coefficient set during production.

6.3 Film thickness

The final and perhaps most important parameter that has not been considered in the preceeding modelling is the film thickness. Previous experiments have demonstrated that the dynamic rates are related to the thickness by an inverse square relationship [Tanaka, 1979];

$$\Phi = K_0/T^2 + C_0 \qquad (6.8)$$

Where Φ is the contractile rate, T is the thickness and K_0 and C_0 are constants set during the production of the polymer.

This effect has been modelled into the final simulation model and its inclusions means the estimates on the response of very thin fibres can be made. It is fibres of this design that will be required if response rates comparable with natural muscle are to be achieved.

6.4 Determination of the Diffusion Coefficient

The swelling of these polymer fibres is due to polymer/solvent attraction/repulsion and results in the uptake and expulsion of solvents

depending on the nature of this force. It is vital to obtain a value for the diffusion coefficient in order to be able to predict the response of the muscle when chemically stimulated. The problem of obtaining diffusion data is resolved by using a method based on the equilibrium swelling parameters, as devised by Crank [Crank, 1956] and Buckley [Buckley, 1962].

With this technique, the swelling profile is divided into sections and the coefficient for each test section is obtained. The driving force for this swelling/deswelling is the difference between the present swelling/deswelling condition and the equilibrium state, according to equation {6.2}.

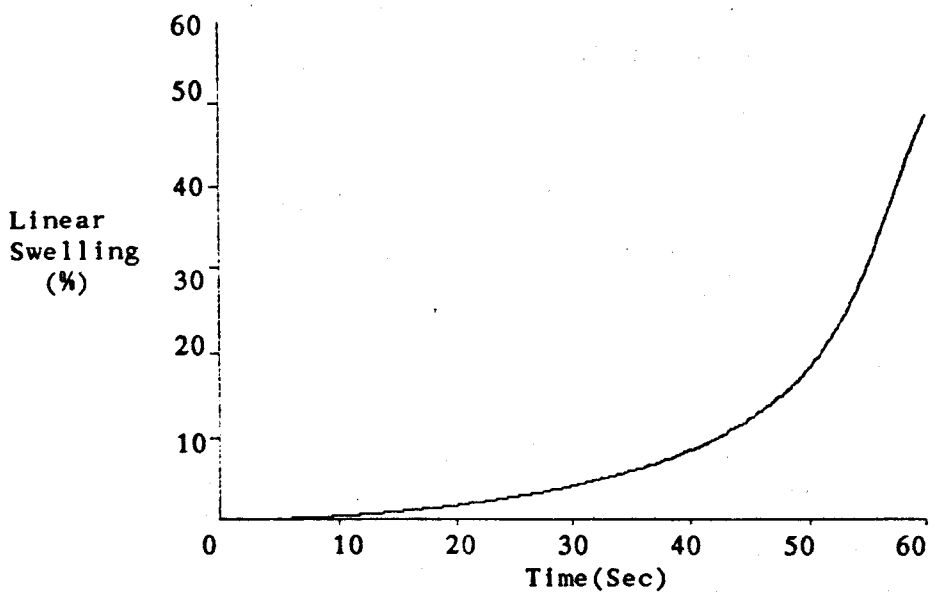

Figure 6.1a Time Response/Equilibrium Swelling Curves

Using the time response/equilibrium swelling curve, figure 6.1a, the diffusion coefficient $D_a{}^B$ (relative to the unswollen sheet) can be calculated from the following equation (Buckley);

$$D_a{}^B = 0.049/(t/41^2)_{\frac{1}{2}} \qquad \{6.9\}$$

where $D_a{}^B$ is in cm^2 /sec., $t_{\frac{1}{2}}$ is the time at which the swelling is half the equilibrium value, and $l_{\frac{1}{2}}$ is half the sample thickness.

This equation is valid for constant rates of diffusion, but where the diffusion rate is concentration dependent $D_a{}^B$ represents some mean value $D_{(bar)}$, $D_a{}^B$

= $D_{(bar)}$. By making the test sections sufficiently small the true diffusion coefficient may be estimated.

To permit the effects of concentration differences to be estimated the diffusion coefficient $D_{(bar)}$ must be modified by the driving force equation {6.2} giving

$$D = (D_{(bar)}\ \epsilon_\infty) / (\epsilon_\infty - \epsilon_\tau) \qquad \{6.10\}$$

where D is the concentration dependent diffusion coefficient, and ϵ_∞ and ϵ_τ are the swelling at equilibrium and time τ respectively. From the test sample the results were divided into swelling sections representing a change of 5%. The resultant table is shown below, table 6.1. The results have been obtained from a strip of polymer .12mm thick, with a PVA:PAA ratio of 3:1 and crosslinked at 150°C for 60 mins., i.e. the conditions for a 'standard' strip.

V_0(%)	$t_{\frac{1}{2}}$ sec.	$D_a B$	D
0-5	90	5.44e-8	0.11e-6
5-10	30	1.98e-7	0.25e-6
10-15	15	4.32e-7	0.61e-6
15-20	11	6.41e-7	1.06e-6
20-25	9	8.51e-7	1.70e-6
25-30	7½	1.10e-6	2.76e-6
30-35	6	1.49e-6	4.96e-6
35-40	8	1.20e-6	6.00e-6
40-45	10	1.03e-6	10.3e-6
45-			

Table 6.1 Swelling Time Response Results.

From these results by extrapolation the diffusion coefficient of the unswollen polymer D_0 can be determined, figure 6.1b.

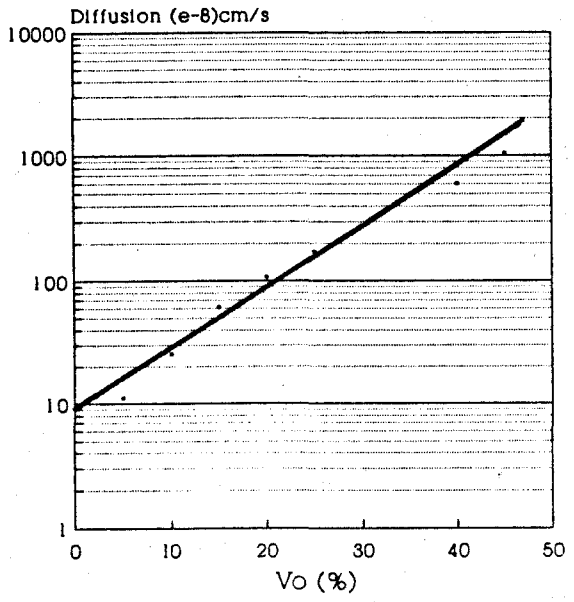

Figure 6.1b. Determination of the Diffusion Coefficient Parameters.

For this material a value of 9E-8 $cm^2/sec.$ is obtained. Further analysis of these results gives a value of 11.6 for the β parameter. Hence this relationship may be expressed in the form given in {6.3} as;

$$D = 9E\text{-}8 \exp^{11.6V} \qquad \{6.11a\}$$

The coefficient value obtained in the above equation is solely for diffusion of water into the material, i.e. the sequence causing dilation. For contraction a new diffusion coefficient must be sought using the method outlined above. In this instance the equation for the relationship is;

$$D = 9E\text{-}8 \exp^{9.4V} \qquad \{6.11b\}$$

D_0 is constant as the swelling coefficient of the polymer does not change, while β varies to reflect differences in the ease with which the diffusing solvent can pass through the polymer network. A number of factors can have an

influence. During dilation the network fibres are close together and penetration is more difficult, while during contraction the polymer attempts to retain water molecules to prevent acetone penetration. Clearly slight differences in the diffusion coefficient when swelling and deswelling are expected.

The stage has now been reached were it is felt that the modelling of the muscle should be fairly accurate and it is worth designing and building a dedicated muscle simulator.

6.5 Algorithm Development

To model the molecular processes involved in the contraction and dilation of the fibres it is necessary to consider a two-dimensional model, Fig. 6.2. The strip is divided into small elements in the χ and z directions, with the element boundaries being represented by nodes. The elements in the χ direction emulate the swelling of the polymer lattice when the penetrant diffuses through to the core from the outer layers. Motion of the elements in the z plane simulates the longitudinal motion of the muscle and will be used as the measure of the muscular dynamics. The dimensional changes in the z-direction are calculated by combining knowledge of the plastizing of each element due to diffusion in the χ-direction, with the modulus at any given swelling fraction. The swelling calculations are repeated for each of the nodes within the polymer array.

Diffusion and swelling in the third dimension, y, is not considered as this is very slow relative to that in the χ-direction, and it is not used in the power stroke as is motion in the z plane.

As the critical criteria for this system is the motion of the polymer, a finite difference technique has been used for the numerical solution. This gives the movement of the specified nodes and the overall dimensional changes during expansion and contraction. The actual finite difference technique employed was that developed by Crank and Nicolson, the advantages of this method having been well documented [Caldwell, 1986].

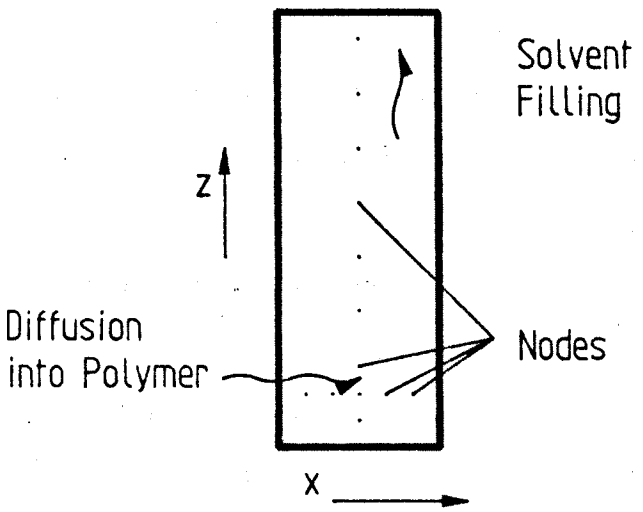

Figure 6.2 Diffusion of Solvents within the Polymer.

Calculations were performed on a Victor VPC II using Turbo Pascal. An algorithm outlining the steps involved in the production of this software is shown below;

1. Input the data relating to the polymer strip to be tested; muscle thickness, diffusion coefficient, swelling ratio, etc.

2. Initialize the polymer parameters;
   (i). Set the water concentration to zero.
   (ii). Initialize nodal water concentrations.
   (iii). Initialize Crank-Nicolson matrices A and B.
   (iv). Determine the normalised diffusion value for each node (p).
   (v). Configure matrices A and B based on the related p value.
   (vi). Solve for matrices A and B by gaussian elimination.

(vii). Calculate the nodal swelling based on the water concentration.

(viii). Repeat (iv) to (vii) for each node.

(ix). Sum for the total longitudinal swelling.

3. Input required simulation period and stimulant to be used.

4. If stimulant = water Then

(a). Set water concentration to 0.8. (Concentration of water in polymer when fully swollen.

Else

(b). Set water concentration to 0.5. (Concentration of water in polymer when fully contracted (not dried)).

5. Set external nodes to water concentration.

6. Set the diffusion value p for each node based on the water concentration.

7. Configure the matrices A and B based on these p values.

8. Solve for matrices A and B by gaussian elimination.

9. Calculate the nodal swelling based on the water concentration.

10. Repeat (6) to (9) for each node.

11. Sum for the total longitudinal swelling.

12. Display graphical results.

13. Repeat (5) to (11) until the simulation period is completed.

14. Repeat (3) to (12) if a cycle with a different stimulant is required.

A listing of this program is given in Appendix V.

Should non-pure solvents be used as the input stimulants the algorithm must be amended to take account of this. Section (3) of the algorithm should then read in the water concentration of the stimulant, and hence modify the diffusion coefficient (at (6)) according to equation {6.5}.

6.6 Simulator Test Sequence

In order that the mathematical model and the simulation can be validated it is important to test the results of a series of test runs against previously obtained experimental results. These tests have been conducted specifically to determine if there is good agreement in three primary conditions; initial swelling, polymer thickness variation and variation in the concentration of the activating solvent. Clearly other features can be considered, such as the crosslinking, but as these factors have already been included indirectly through such parameters as the swelling ratio and the diffusion coefficient this is not considered to be necessary.

Following experimental tests the period for filling of the containing vessel was set at 2 sec.

6.6.1 Initial Swelling and Dilation/Contraction Profile

The object of these simulations was to obtain a comparison between the simulation model and the experimental results subject to the condition of concentration dependent diffusion. This effect can best be observed when the polymer is initially swelling from its dry condition, since this gives the widest

range of concentration variations.

The results produced in this first sequence, on polymer fibres 0.1mm thick, figure 6.3, shows the slow initial swelling expected from the polymer. This response increases following the typical profile obtained experimentally.

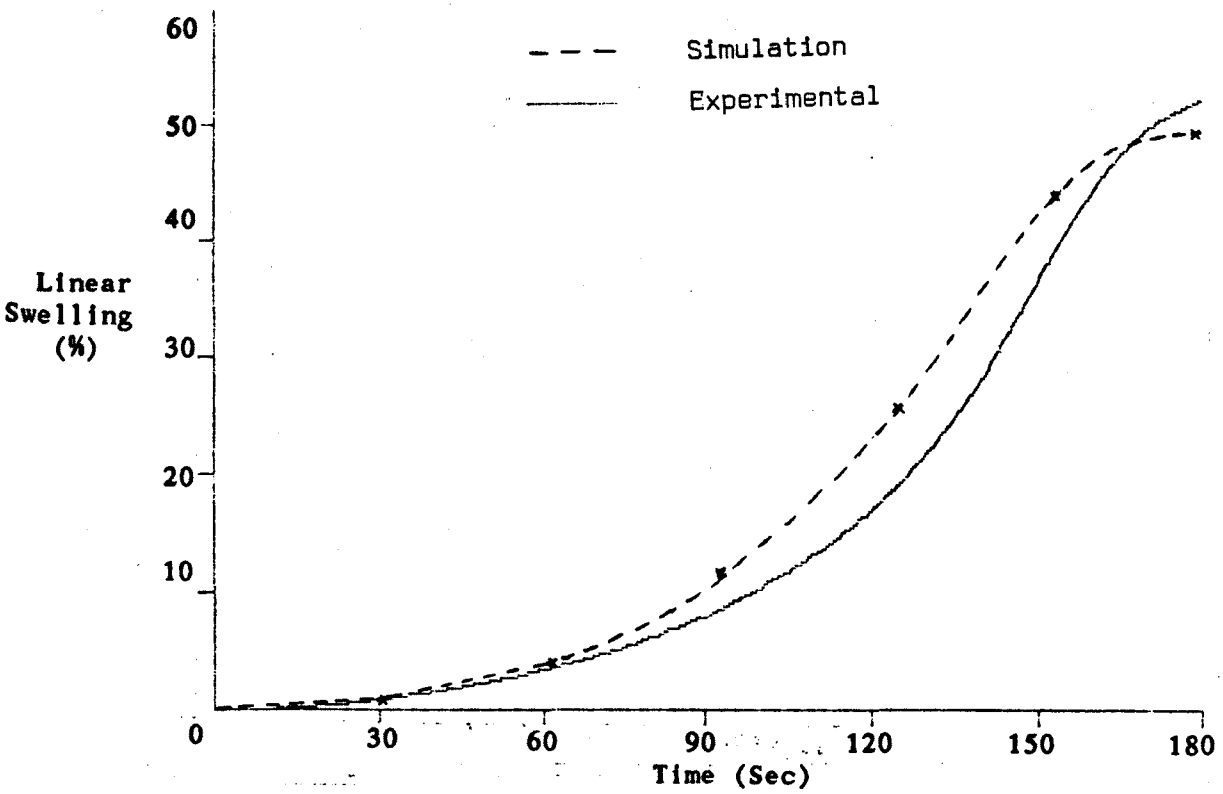

Figure 6.3 Initial Swelling from Dry.

6.6.2 Polymer Thickness

Particular attention has been paid to the effects of thickness as theory has predicted that there is an inverse square relationship between the dynamic rates and the thickness. These results were prepared for muscle strips of thickness 0.1mm, 0.2mm, 0.3mm, and 0.4 mm when both dilating and contracting.

The effect of reducing the polymer thickness is quite clearly demonstrated in figure 6.4, with sharp reductions in the response rates. Only the contractile motions have been recorded as they are the vital power generating cycle in this system, but similar rate reductions are produced in the dilatory cycle.

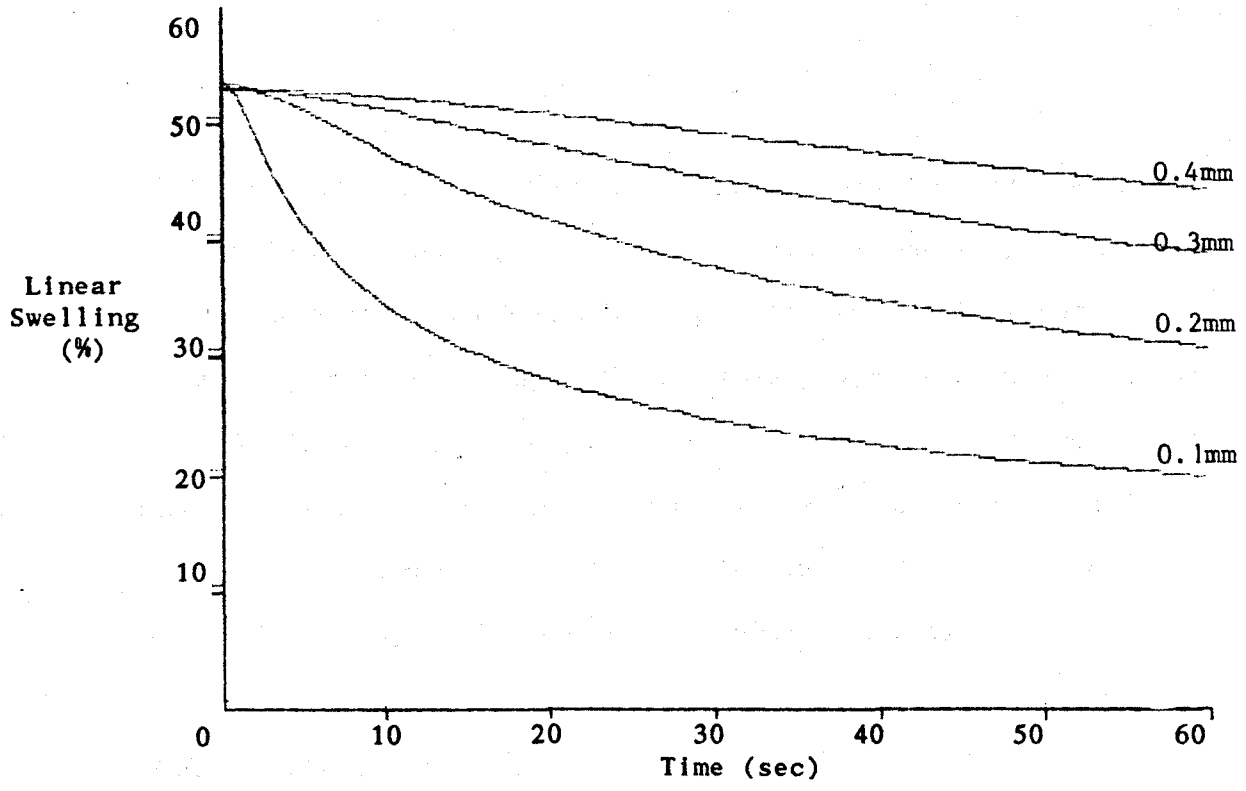

Figure 6.4 Polymer Thickness Effects.

Observation of the maximum rates of contraction over a range of thicknesses shows the predicted inverse square relationship.

6.6.3 Activating Solvent Concentration

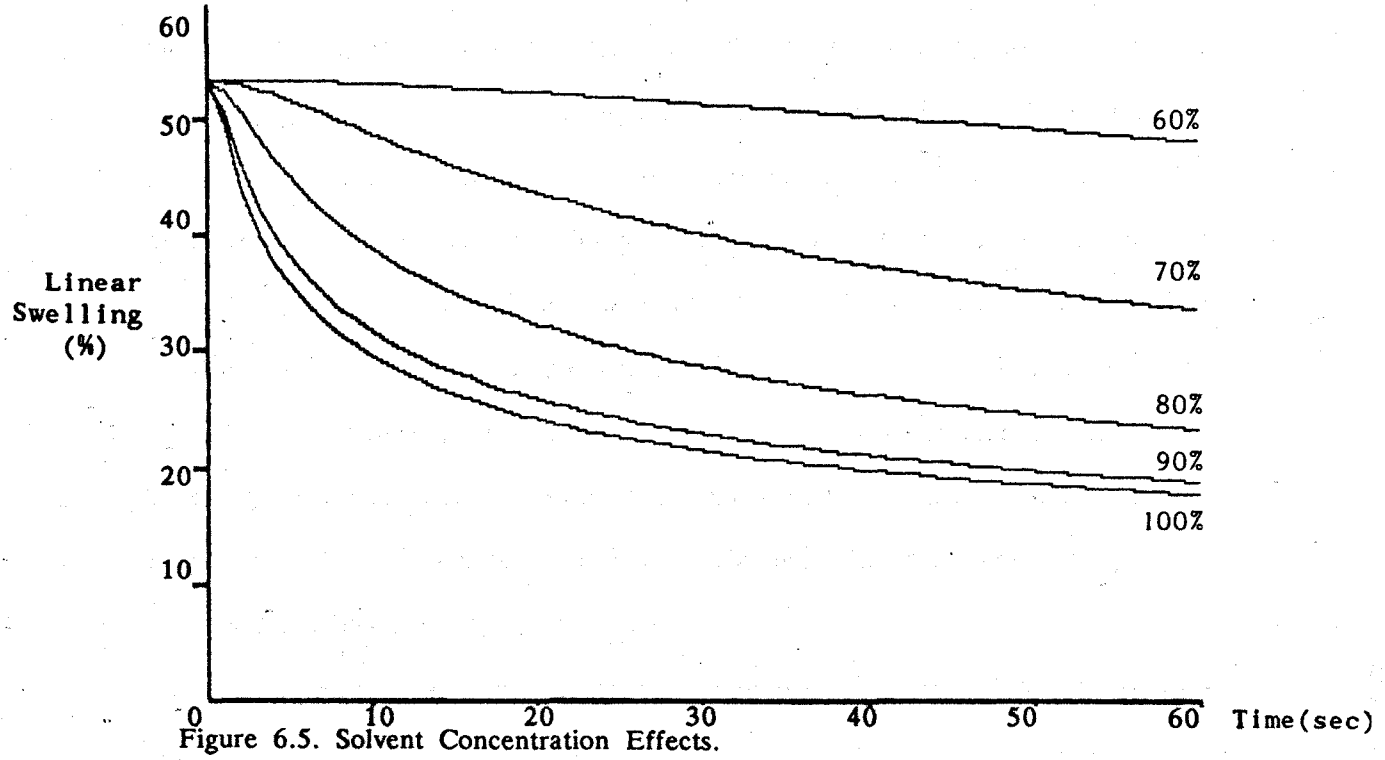

Figure 6.5. Solvent Concentration Effects.

It is important that the relationship between the external solvent concentration and the dynamic rates (equation {5.3}) be accurately simulated; this was the object of these tests. As before, strips of polymer 0.1mm thick were used.

The changing of the strength of the activating solvents is demonstrated in figure 6.5, with the twin effects of reduced response rates and also reduced deswelling limits. Again only contractile responses have been rcorded but similar effects can be observed during dilation. As with all the previous tests the results compare very favourably with the experimental profiles.

6.7 Flexor/Extensor Actuation System Design

Having produced what appears to be a fairly valid simulation of the pseudo-muscular dynamics, the next stage in the development can be considered. This involves producing a muscle actuator pair with controllers designed to optimise (or at least enhance) the system response characteristics. These characteristics will be defined later.

This type of artificial muscle has been developed for use in robotic grippers and as such it is important to test the feasibility of any design before implementation. Since a muscle-type actuator only provides power during its contractile cycle, two complementary muscles are required, the flexor and the extensor. A system based on these principles has been suggested for development, figure 6.6, but it is necessary to test a number of control methodologies before any implementation on a full experimental model. The following sections deal with the design of a series of control systems which have been considered for use with the flexor/extensor muscle actuator pair. These systems will then be tested using an actuator simulator built using the knowledge of the muscular response obtained in the previous polymer swelling/deswelling simulations.

The development of this actuator pair and the design thinking involved are considered in chapter 7.

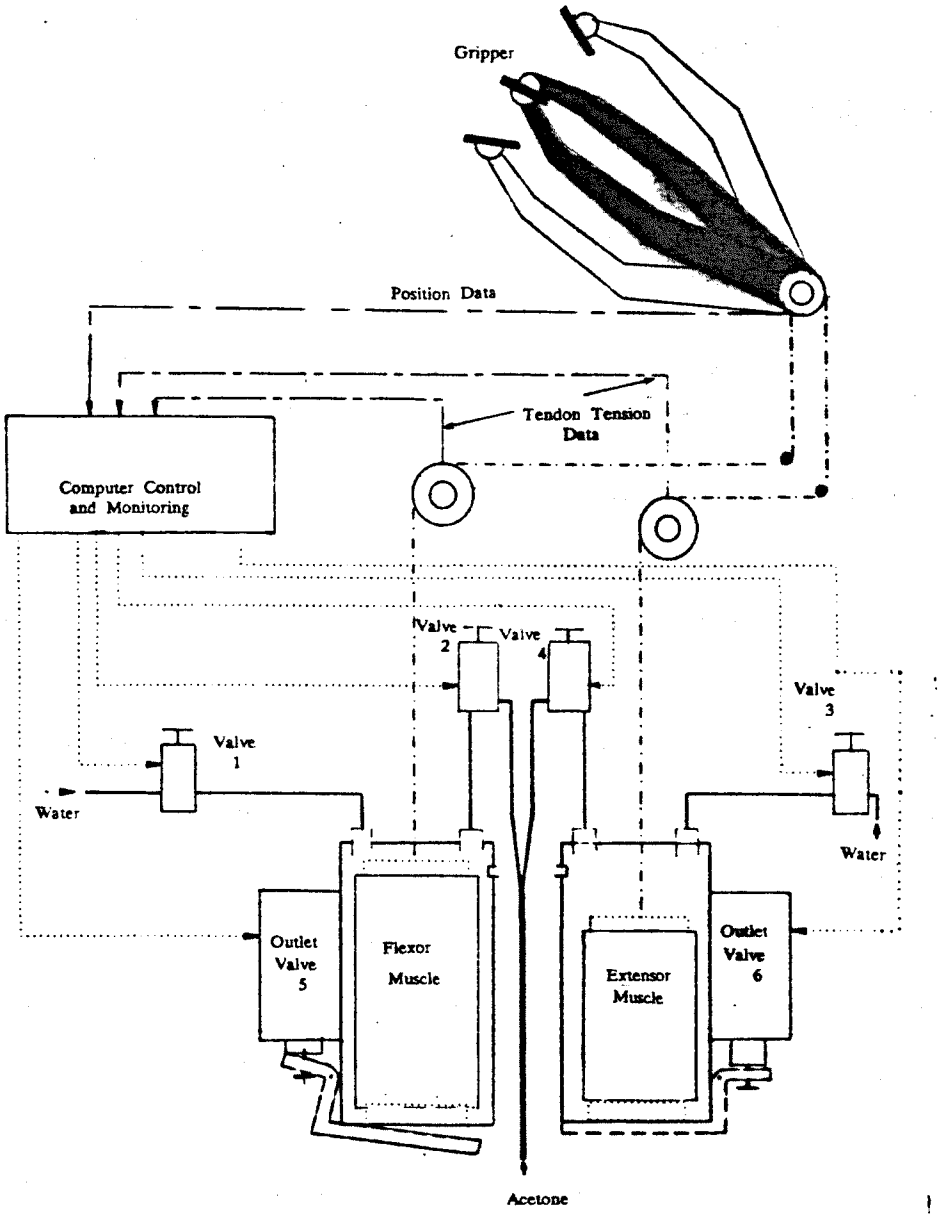

Figure 6.6 Muscle Actuator Pair Design.

6.7.1 Control System Design

A control model for the muscle cell described above, figure 6.6, will now be developed and tested, and the response to the different control systems measured and recorded.

The control requirements (as specified in detail in the next chapter) are; to move the gripper as quickly as possible between its desired end-points, without oscillation and with over/under shoot of less than 2°. A PID controller was originally considered for installation but due to the fact that no oscillation must

occur and the tolerance of a small steady-state error (2°), no integral action was required. The three control strategies which were developed are considered in the following subsections.

6.7.2 Position Control

The first control method consists simply of closed loop position feedback on the contracting muscle alone, with the muscle cells being filled with pure (undiluted) acetone or water according to the demands of the control law, and hence producing contraction and dilation. The basic control law governing the filling and emptying of these cells is set by a single PD controller monitoring the error signal from the contracting muscle.

When the rate of change of position is too rapid, the contraction and dilation velocities can be reduced by dumping solvent from the cells. This effectively reduces the muscle stimulation signal. When the final end-point is reached all the solvents are removed from both cells and the motion terminates. A system control model is shown in figure 6.7. The detailed structure of this model will be explained in section 6.7.4 when considering the position/force control strategy. At present only the dynamic responses obtained using this controller will be considered in depth.

With this controller it is important to realise that the position signal being monitored is only a reflection of the motion of the contracting muscle and hence over-relaxation may be occurring in the dilating muscle without any sensory indication of this condition. This will affect a gripper joint response in two ways.

(1) Upon reversing the cycle there will be a delay before the contracting muscle can produce any finger movement.

(2) Since only one muscle is under tension, a random disturbance may cause the finger to 'flop'.

The lack of feedback information also means that it is difficult to determine the condition of the modulus of the material, or operate the muscles in

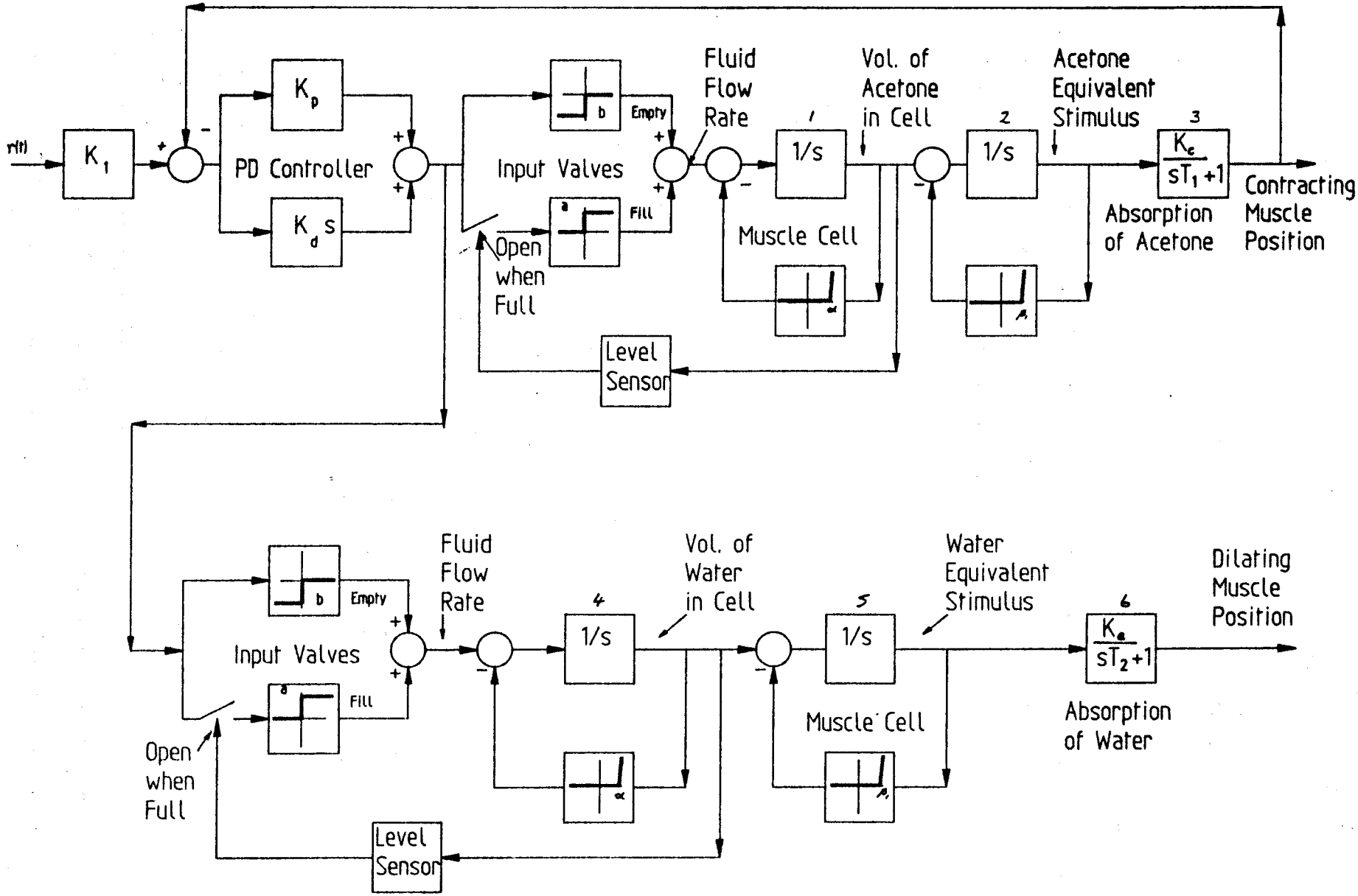

Figure 6.7 'Position' Controller Design

opposition. These techniques are vital if some control of the compliance is necessary.

A typical response curve (gripper motion between 50° and 100°) for an actuator with strips 0.1mm thick in both the muscle cells is shown in figure 6.8. The K_p and K_d values are 1.0 and 0.5 respectively. These results demonstrate that the response rate is rapid but cannot give any indication of the system over-relaxation. The over-relaxation can be seen indirectly in the slow pick-up at the reversal points (50° and 100°).

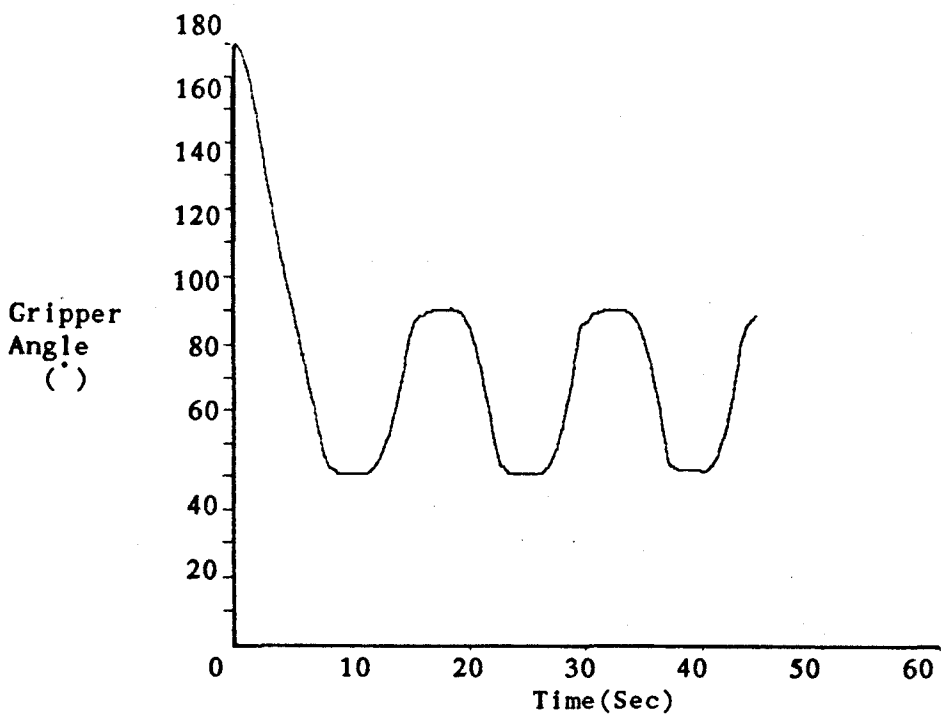

Figure 6.8 System Response using the 'Position' Controller.

Due to these relatively poor control responses and the poor compliance regulation abilities this technique was discarded.

6.7.3 'Solvent Concentration' Control.

The design used for the 'solvent concentration' controller is quite different from that for the 'position' controller, with the new control model being shown in figure 6.9a. Two major differences in the design philosophy have been identified.

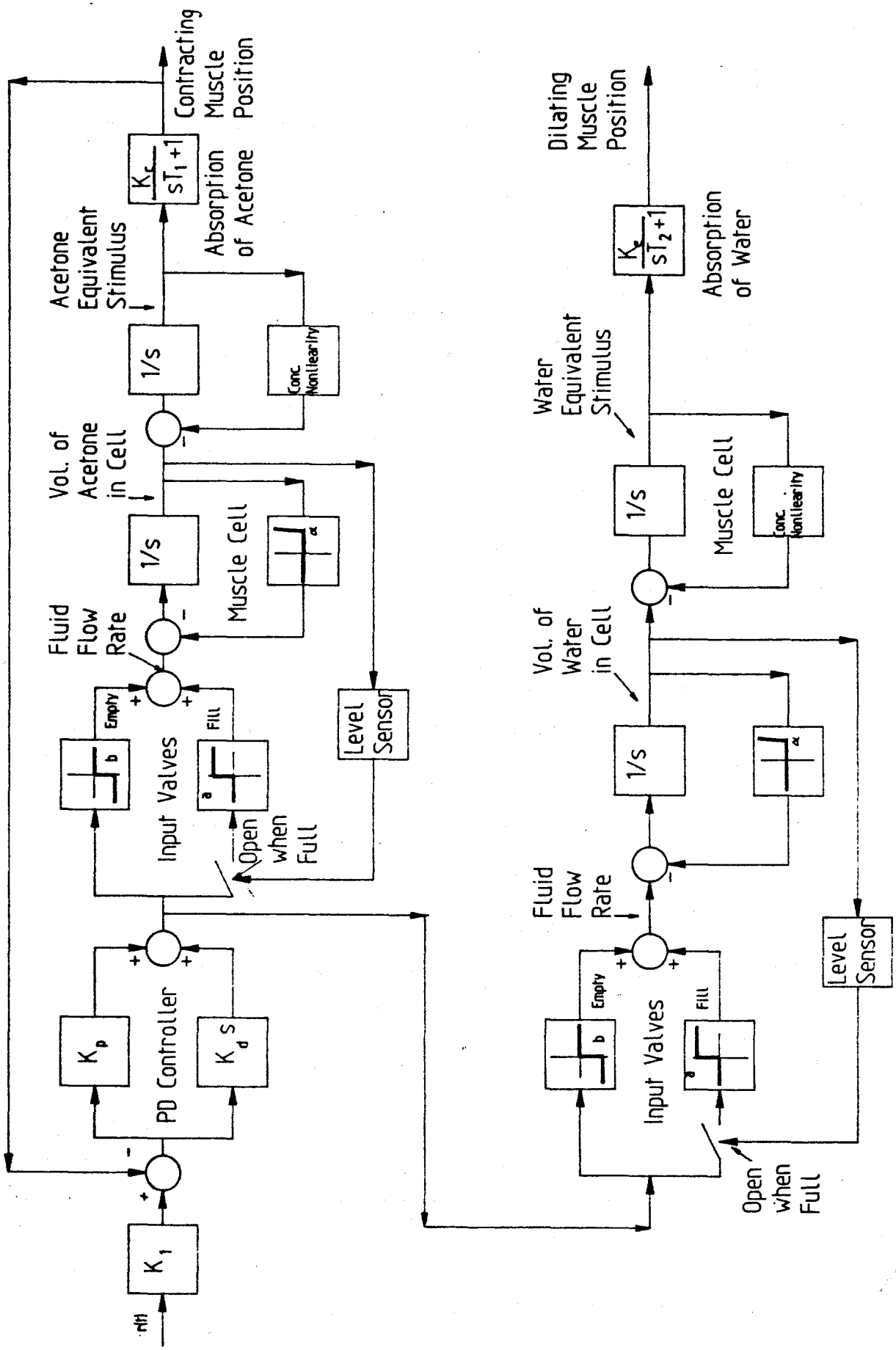

Figure 6.9a 'Solvent Concentration' Controller Model.

1. In the previous design the muscle cells are filled and emptied according to the demands of the control law, whereas in the 'solvent concentration' system the cells remain permanently full of liquid at all times. Any inflow is countered by an equal outflow with the effect that the concentration of the fluid within the cells varies, but the fluid levels remains constant.

2. The 'position' controller uses 100% (undiluted) water or acetone as the stimulant, but with the 'concentration' controller motion is initiated by varying the concentration of the solvent in the cells. This variation in fluid concentration then regulates the motion and the final end position of the joint.

Within the control model these 'new' effects are modelled using the concentration nonlinearity feedback term in integrators 2 and 5. β_1 is retained as in the 'position' control model but this value is now variable to permit the swelling/deswelling limits to be set subject to the different stimulant concentration conditions. Contamination reduces the β_1 value with the relationship having been explored previously in 4.10. The second term to be included in this nonlinearity is to control the rate of contraction/dilation. Using pure solvents there is no feedback until saturation (β_1) is reached, so the most rapid response possible is produced, but as the contamination increases so the feedback signal increases until no motion at all is observed. All other factors such as the PD control of the solvent inputs are identical to the position control design. The nonlinearity is shown in figure 6.9b, with arrows indicating the changes which occur when using non pure solvents. The remainder of the control model and its effects will be studied in the following section.

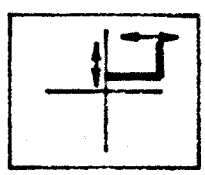

Figure 6.9b Concentration Nonlinearity Term

This second method permits monitoring of the concentration of the solvent in the cells, using the acetone sensor developed in chapter 4, with the result that the actual modulus of the polymer at any instant will be known. Compliance control can thus be achieved by either (or both) varying the water content of the polymer fibres or by having the extensor and flexor working in opposition.

The system response when moving between 50° and 100°, figure 6.9c, shows the slow dynamic response caused by the dilution of the stimulants.

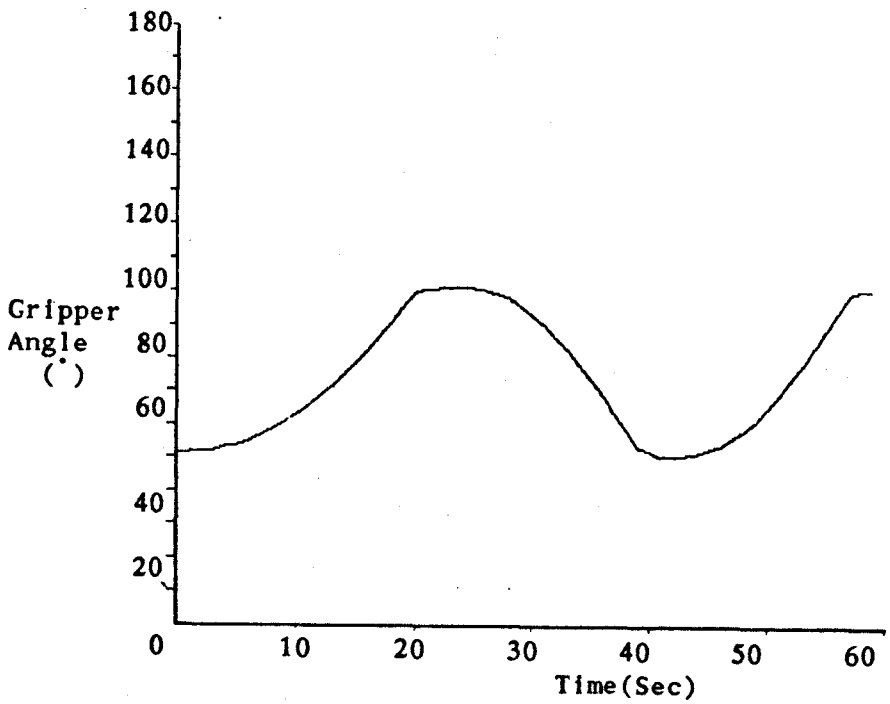

Figure 6.9c. Dynamic Response using the 'Solvent Concentration' Controller.

Despite giving good compliance control potential and positional accuracy (with careful adjustment of the parameters better than ±0.5° is possible) this method was abandoned due to the extremely sluggish dynamics produced as a result of the use of non-pure stimulants.

6.7.4 Position and Force Control.

This controller combines positional information from the contracting muscle with knowledge of the tensions being developed in the inter-connecting tendons. The basic concept is similar to the position controller with improvements to

attempt to eliminate the problems associated with over relaxation. Where this method differs is in the additional information available through monitoring of the tension (using strain gauges) being developed in the tendons connecting the artificial muscles to the joints. This tends to mimic the sensor information produced in animal muscle control systems. The control system design is shown in figure 6.10.

In this design the initial chemical stimulant is only applied to the muscle which will be contracting. This single muscle stimulation continues until an increase in tension is detected in the inter-connecting tendons at which point both muscles are stimulated similtaneously, the solvents being added (or removed) so as to maintain the tendon tension at a very low level indicating coupling. When the joint reaches its desired end-point deflection, the solvents are removed from the cell as was the case for the 'position' controller. To move the joint in the opposite direction the stimulants added to each cell are reversed, i.e. acetone replaces water and water replaces acetone. This continual joint tension prevents over-relaxation and ensures that there is always muscular support.

By referring back to the mathematical model for the motion of the muscle derived previously in this chapter it can clearly be seen that a great many non-linearities are present. When this is further developed to form a muscle flexor/extensor pair with the input of the solvents to the cell under computer control the complexity is still further increased.

The remainder of this section will be devoted to the analysis of a complete system model for a flexor - extensor muscle actuator, figure 6.10.

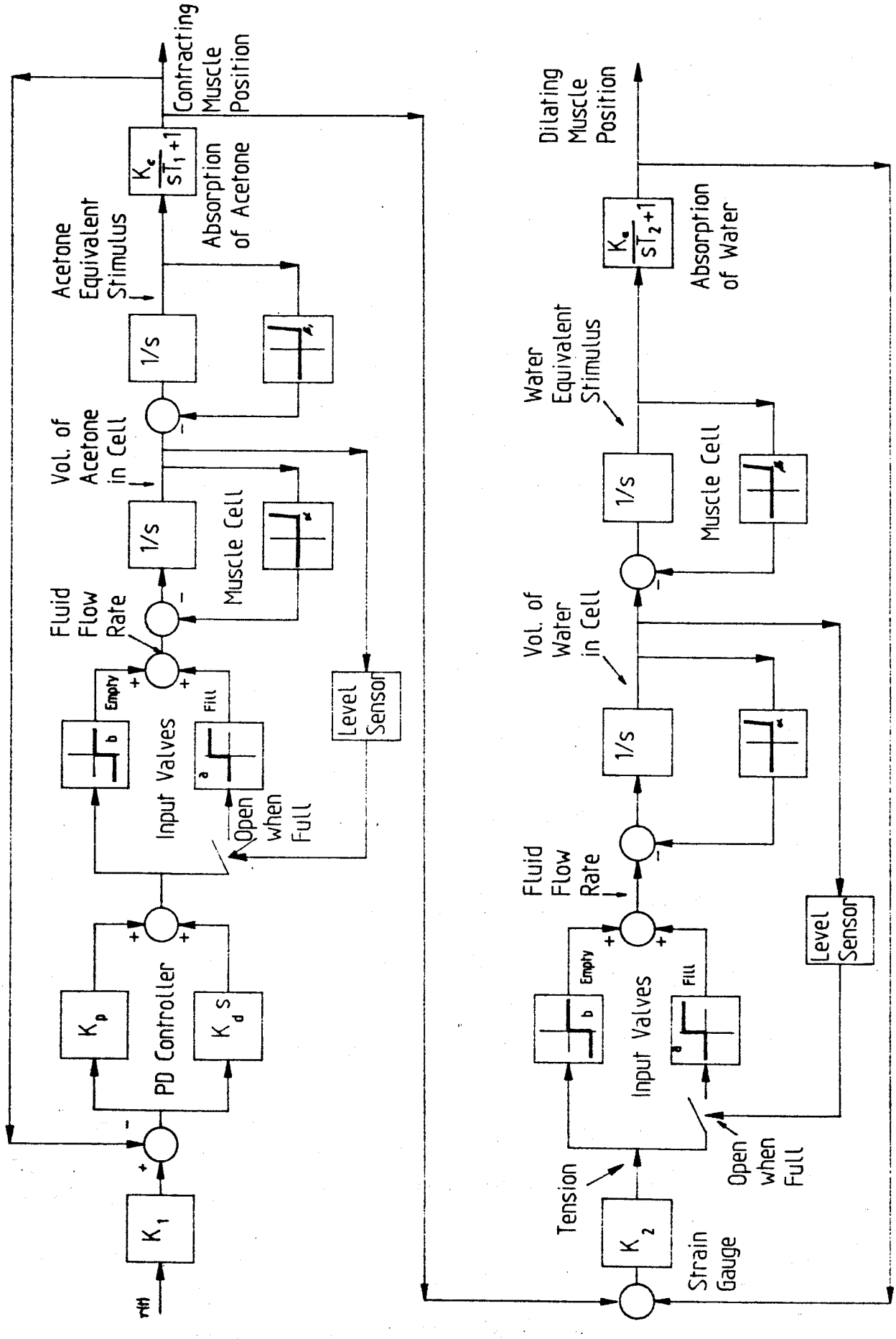

Figure 6.10. 'Position and Force' Controller.

where τ_1, τ_2 = the swelling and contracting time constants which are dependent on the production conditions.

β_1 = the saturation factor determining the amount of water absorbed by the polymer. This parameter is again subject to production conditions and effectively governs the extent of equilibrium swelling.

α = the amount of liquid which the cell can contain before overflow occurs. This value is chosen in conjunction with the swelling factor and the material time constant such that $\tau_1 \alpha \approx 0.6\beta_1$, i.e after τ_1 sec. of input α the material will be swollen by approximately 60%.

a,b = set the cell filling and emptying rate respectively, these values not being necessarily equal. The filling (emptying) time F_t, is set according to;

$$F_t = {}^{\alpha}/_{a} \qquad \{6.12\}$$

The input relay simulates the flow - no flow action of the hydraulic valves which can assume only one of two states. The relay function is duplicated in both the flexor and extensor arms of the system permitting independent control of the filling and emptying of the cells. The A and B values set for this relay determine the cell filling and emptying periods respectively.

The input of solvent to the contracting muscle is regulated by the PD controller in this loop. This determines if acetone should be added to, or removed from the muscle cell and hence coordinates the rate of movement. Solvent input to the dilating muscle is indirectly controlled by the PD function. Strain in the tendons caused by slower relaxation than contraction induces the dilating muscle cell to fill with water. If there had been no muscle tension, the cell would have started to empty, reducing the relaxation rate, and maintaining joint rigidity. Should these cells become completely full during the process, the filling is stopped when a level sensor detects this condition.

Integrators 1 and 4 are both simply ramp functions to replicate the filling of

the cell with solvent. The feedback loops of these integrators contain a saturation function, which effectively limits to α, the amount of liquid which may be introduced into the cells.

Two more simple integrators are introduced into the design at 2 and 5. These are used to give an accurate measure of the quantity of solvent which has been made available for absorption by the polymer. This is effectively the chemical stimulus acting on the polymer. A saturation function β_1 has again been introduced to limit the swelling or deswelling. During dilation this sets the upper swelling limit, while during contraction a lower limit is set, which has been previously shown to be approximately 12–15%. This saturation is based on the absorption curve determined in Chapter 4.

The contraction and dilation of the polymer is simulated by integrators 3 and 6, which have a 1st order response (in a simple model of this system, ignoring the non–linearities, this 1st order system would represent the muscle response). The time constants (which are a reflection of the diffusion delays) are set according to whether the muscle is relaxing or contracting and the physical properties of the strip of material being used (eg thickness and temperature). During the initial swelling phase (the swelling from dry) a third time constant τ_3 is used as this phase is very slow due to the low concentration of water in the polymer reducing the diffusion coefficient.

The outputs from both muscles are fedback for comparison with their respective demand signals, which for the contracting muscle is set externally and for the dilating unit is set by the strain in the inter–connecting tendons. This coupling between the muscles ensures that the rates of contraction and dilation are equal, and emulates the tension monitoring systems available to animal muscle.

This model is a valid representation of the actuator pair if there is no loading on the muscle, since the dimensional changes on solvent uptake are extremely rapid relative to the rate of uptake.

Under loading, however, there are additional effects to consider. When being

loaded the moist polymer can be compared to a helical spring, with a modulus of elasticity and a damping factor. This system can thus be modelled as 2nd order system of the form [Casey, 1962];

$$\ddot{x} = -B'\dot{x} - G'x \qquad (6.13)$$

where G' is a modulus component and B' is a damping component. Where this mechanism differs from a normal spring is in the coefficients which are variable depending on the water content of the fibres.

As small errors in the final position were to be tolerated and as a reversal of the cycle would be difficult because of the delays inherent in emptying and then refilling the cells, proportional plus derivative control was used. It was found that when this design was implemented, the combination of PD feedback with the relay input produced a switching line similar to that defined for VSS controllers. The gradient of this switching line was set by the values of the PD controller.

Consideration of the system equation which can be derived for this unit shows how this effect can be achieved.

The initial stage of each muscle controller uses a PD based unit which defines a switching line according to :

$$S = K_d \dot{e} + K_p e = 0 \qquad (6.14)$$

where K_d is the derivative gain, K_p is the proportional gain and e and $\dot{e}$ are the error and the derivative of the error respectively. This defines a control signal for each muscle as:

$$u = \begin{cases} U_h & S>0 \\ U_l & S<0 \end{cases} \qquad (6.15)$$

Where U_h is greater than 0 and U_l is less than 0. These control signals

determine the state of the relay functions which open and close the valves and in turn control the in or out flow of solvent.

Using this method the problems of over-relaxation and lack of muscle support for the joint are overcome while use of pure chemicals gives the maximum possible response rates.

At times it may be advantageous to have both the muscles operating against each other for this condition combined with changes in the polymer modulus creates a system with variable compliance. Compliance control is achieved by monitoring the position of the gripper and adding the chemical stimulants at rates which ensure that contraction in the flexor is balanced by contraction in the extensor. During this simultaneous contraction (or dilation) tension is generated in the inter-connecting tendons. This increase in tension manifests itself as an increase in the overall system stiffness. This is the way in which limb stiffness is controlled in animals.

With the pseudo-muscular mechanism there is also a second compliance regulating method. The Young's modulus of the polymer can also be varied by controlling the water content within the fibres, as demonstrated in previous performance tests. Hence by combining this system with the technique mentioned above a relatively simple but effective compliance control mechanism can be produced.

The results for an extended range of motions using this controller are considered later in this chapter (section 6.9). The controller was implemented as described in the following section.

6.8 Muscle Actuator Simulation

Some modifications must now be made to the muscle simulator of section 6.5 to take into account the design of the actuator pair. Since there are now two groups of muscle fibres, the flexor (closing the gripper when contracting) and the extensor (opening the gripper when contracting), the muscle simulation algorithm (1) to (14) must be repeated for each grouping. Additionally this

design is intended to demonstrate the effect of a muscle pair as an actuator and unfortunately a new modelling problem is presented due to the different rates of expansion and contraction. This is a coupling action between the muscles through the gripper and it requires the development of a separate section of program to cope with the interaction. In this routine the elasticity in each muscle is assessed by calculating the modulus (using the water content/modulus relationship) and hence the equilibrium joint position is set.

15. If interaction is present Then

    (i). Calculate the modulus of flexor

    (ii). Calculate the modulus of the extensor

    (iii). Use bisection method to determine the balanced extensions caused.

    (iv). Calculate the new flexor and extensor lengths.

    (v). Calculate the gripper position.

The algorithmic implementation of the position/force controller can now be included, giving a full actuator system simulation.

Points (3), (4), (13) and (14) from the previous algorithm which are used for manual control of the input solvents must be removed to automate the processes.

Additionally the following sections of code are required to complete the algorithm for position/force control.

3.(modified). Input the gripper demand position.

16. If the gripper angle > the demand position Then

    (a) close the gripper, i.e. fill the flexor with acetone (water–concentration = 0.5) and the extensor with water (water–concentration=0.8).

Else

(b) open the gripper, i.e. fill the flexor with water and fill the extensor with acetone.

17. Determine the PD signal based on the demand specified in (3) and the present position obtained in (15).

18. If the gripper position with 2 of the demand value Then

(a) empty both cells.

Else

(b) If the error signal >0 Then

(i) continue filling contracting muscle with acetone.

Else

(ii) stop filling contracting muscle cell.

(c) If tension is present in the tendons (indicated by (15)) Then

(i) continue filling the relaxing muscle cell with water.

Else

(ii) stop filling the relaxing muscle cell.

19. Repeat (3) to (18) until simulation is finished.

The program for the implementation of this algorithm is contained in appendix VI.

6.9 Force/position Simulation of Actuator Pair. Test Results.

The cell filling and emptying times which were of paramount importance in determining the response and controllability of the actuator, were set using experimental test data to 2.5 and 0.4 sec. respectively. The simulation tests

were conducted for samples of thickness 0.1mm (this was the standard thickness defined previously for use in all experimental tests), with a sampling frequency of 10Hz.

In these tests the polymer strips were stimulated producing motion between sets of predefined gripper limits, (defines how fully open or closed the gripper will be, with 180° being fully open and 0° being fully closed). These limits were set as 0°-180°, 45°-135° and 60°-120°. It is in these latter ranges that motion will most commonly occur. Using the simulator the K_p and K_d values of the controller were carefully tuned to give the most rapid response while still retaining the required accuarcy. These results obtained for a number of different PD settings have been recorded in Table 6.3.

End Point Degrees	Optimum PD Values	Cycle Time Sec	Compromise Cycle Time
40°-70°	K_p=1; K_d=.25	6.25s	7.0s
40°-120°	K_p=1; K_d=.5	11.5s	12.25s
50°-100°	K_p=1; K_d=.4	9.0s	10.0s
80°-100°	K_p=1; K_d=.5	4.75s	5.25s

Table 6.2 PD control Parameters and Response Rates.

From these simulations it was discovered that the nonlinearity of the muscle response meant that the optimal PD values varied as the operating limits changed. Compromise values of K_p = 1.0 and K_d = 0.35 were used to obtain the gripper motion plots shown in figure 6.11a, b, and c. For each of the sequences the relative fluid level in the flexor and extensor cell was also recorded.

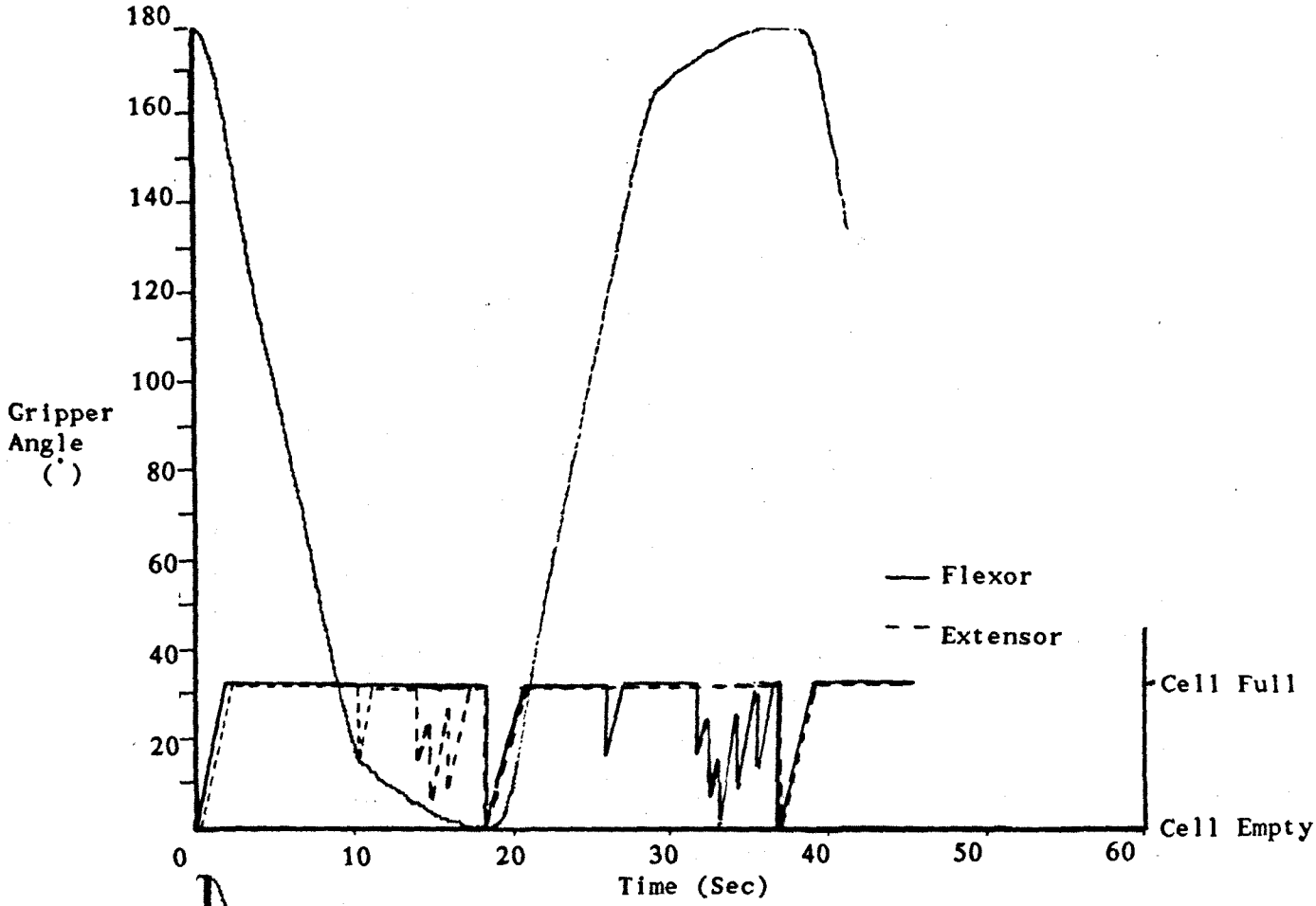
180
160
140
120
100
80
60
40
20
Gripper Angle (°)
Flexor
Extensor
Cell Full
Cell Empty
0
10
20
30
40
50
60
Time (Sec)

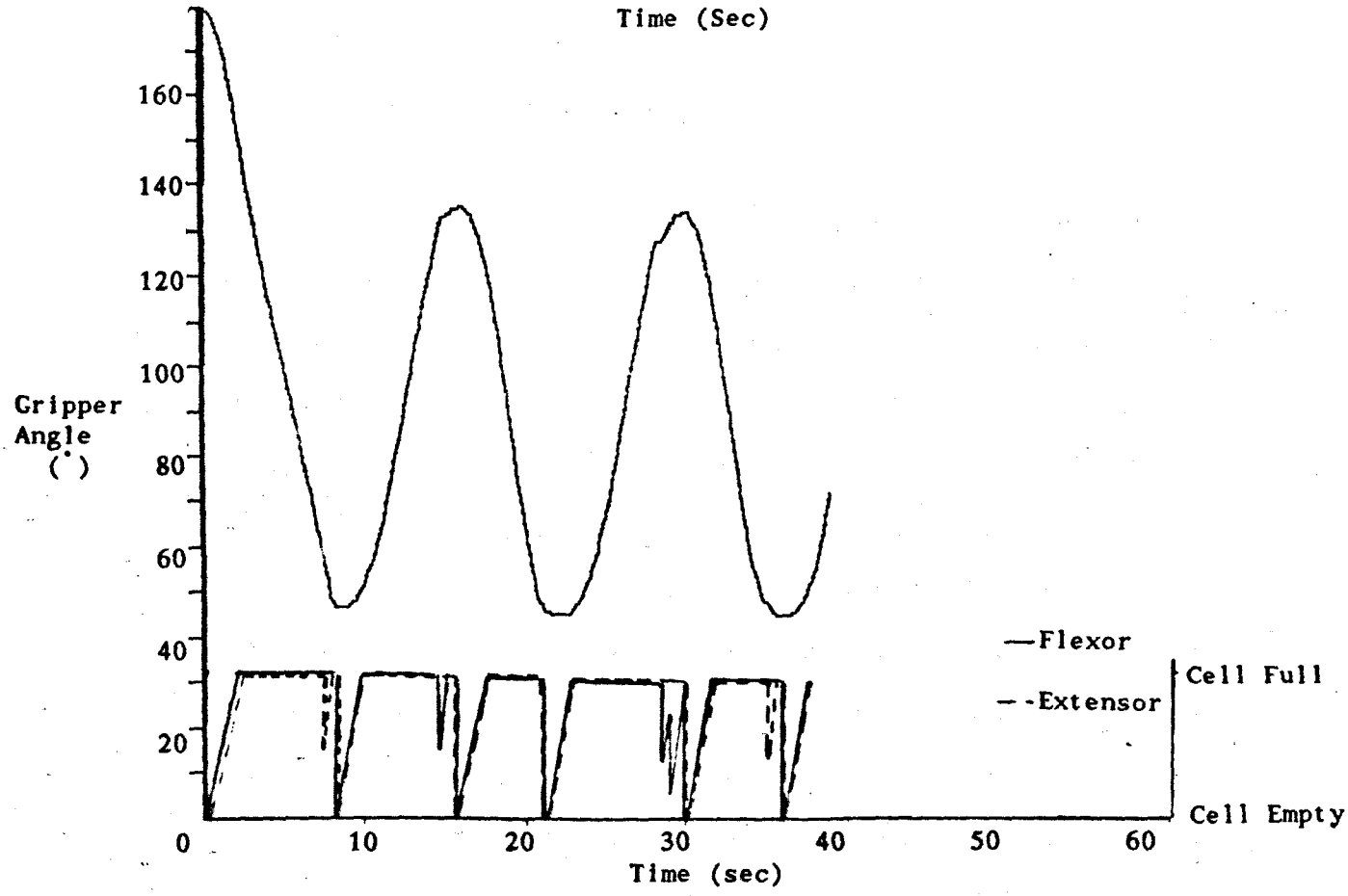
160
140
120
100
80
60
40
20
Gripper Angle (°)
—Flexor
--Extensor
Cell Full
Cell Empty
0
10
20
30
40
50
60
Time (sec)

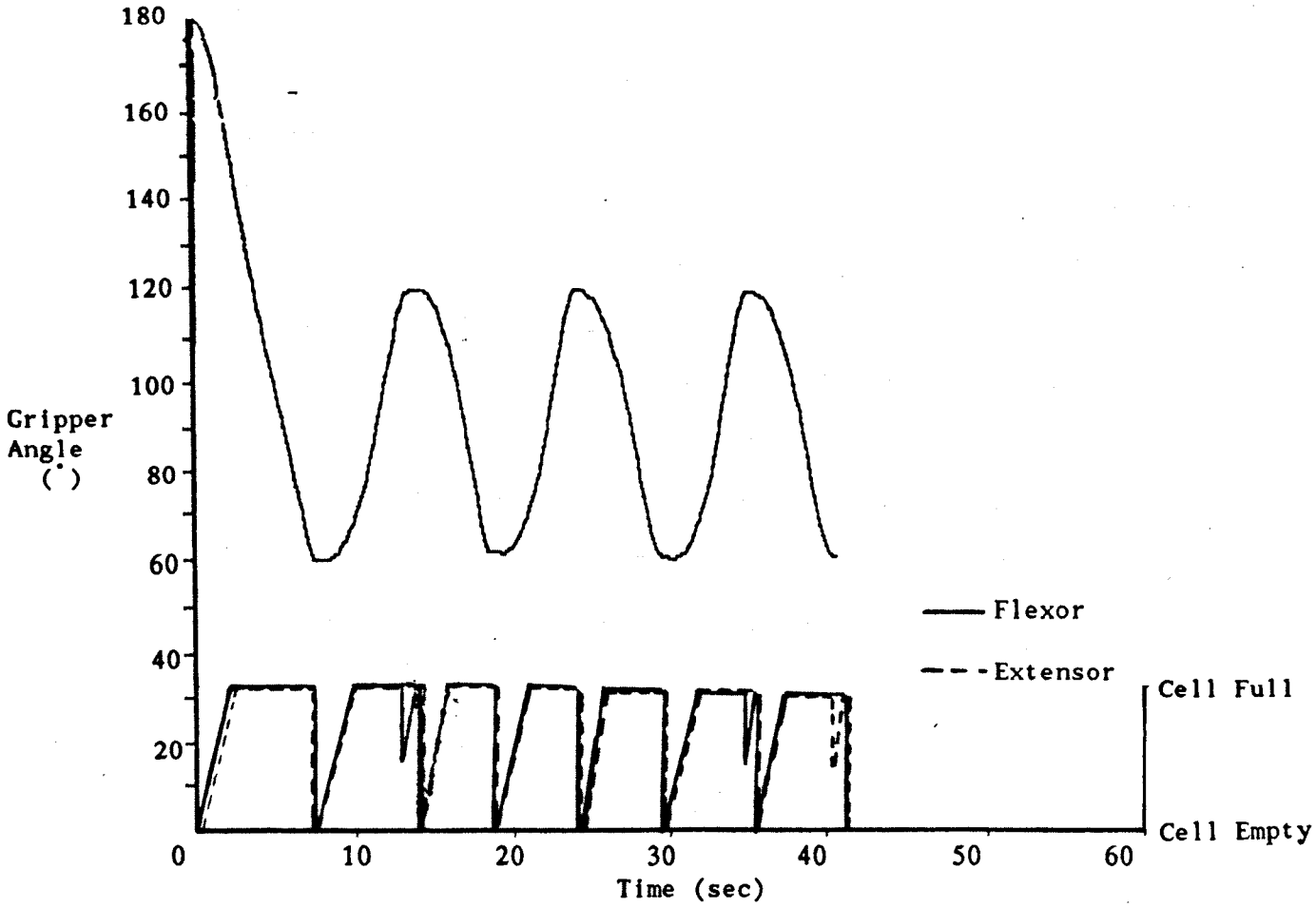

Figure 6.11a, b, and c. Gripper Dynamic Response Simulations.

Observation of the gripper movement profiles discloses a number of interesting points. A characteristic of these results is the nonlinear nature of the responses, with the closing and opening of the gripper not being symmetrical. This action is due to the fact that both muscles are not necessarally operating between the seem expansion/contraction limits. It has also been noted that at initial start-up and when the direction of motion changes, there are short delays as the solvents diffuse into the core of the material. At the end of each sequence small overshoots occur due to chemical transport delays (equalising of concentration levels within the muscle and surface residual liquid). Nevertheless, the simulated actuator responses have positional accuracy which is better than the 2° specified at the start of the experiment and the cycle times of 38 sec., 13.6 sec. and 10.9 sec. for motions between 0°-180°, 45°-135°, and 60°-120°

are felt to be quite respectable.

6.10 Conclusions.

From these results it was concluded that the mathematical models and computer simulations that were developed were a good representation of the dynamics of an artificial muscle, at least on a macroscopic scale.

Using these models strategies for the development of a flexor/extensor muscle pair were prepared, and a force/position controller chosen for the regulation of the gripper movements. It is believed that this will produce a feasible actuation system with relatively rapid response rates and good positional accuarcy. Experimental testing of this mechanism will be studied in the next chapter.

Chapter 7

A Pseudo—Muscular Actuator Pair

7.1 Introduction

The results provided by the tests on polymer fibres, and simulations of the physical and chemical processes involved in the dilation and contraction of a synthetic muscle, have suggested that an actuation system could be constructed which would supply the power necessary to drive and control a robot gripper.

Using the information derived from the simulations, controllers have been implemented which monitor the motion of a gripper and accurately control its movement.

At the same time as providing a useable power source, artificial muscles have a secondary benefit. By varying and controlling the liquid content of the polymer the modulus values can be varied quite dramatically which allows a degree of control over the system compliance to be exercised directly from the actuator.

This chapter investigates the development of artificial muscle cells which respond to controlled inputs. In particular an artificial muscle pair composed of a flexor and an extensor is considered. Under controlled stimulus this unit can provide the power and variable compliance required by a robot gripper.

7.2 Initial Muscle Control Design Structures

Obtaining an efficient means of delivering the acetone/water stimulants to the muscle fibres was the first design problem to be addressed.

A method of control was suggested in which a fine stream of solvent was sprayed directly onto the surfaces of the fibres. In this way the activating solvent can be quickly changed, giving rapid dynamic responses, and good control while only using a limited volume of liquid.

This process is automated, with hydraulic valves under computer control being used to regulate the flow of the solvents. Compressed air is used to generate the spray which is directed onto the muscle, figure 7.1a.

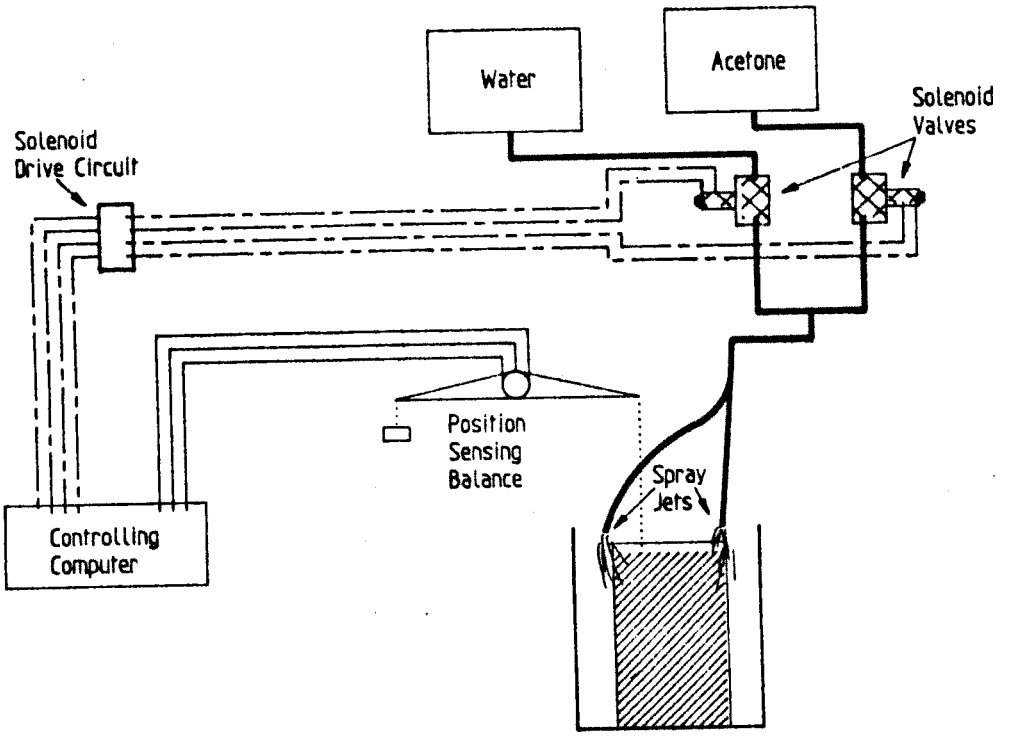

Figure 7.1a. Spray Jet Stimulation Technique.

The control algorithm used in this initial study is very basic being intended mainly to find out if the spray jet technique can provide the stimulus required. It consists of a simple on-off flow regulator, with the spray action being stopped when the required muscle extension/contraction is reached. This tends to give overshoot errors, but once a steady state is reached the output is very stable, figure 7.1b. By providing a short pulse of the opposite solvent it is found that this overshoot can be reduced or eliminated with little effect on the response rate or the stability.

PAGE NUMBERING AS ORIGINAL

considered in the following section.

7.3 Muscle/Gripper System Design

Since a muscle-type actuator, whether artificial or natural, only provides power during its contractile cycle, two complementary muscles are required, the flexor and the extensor. The coupling action of the muscles means that the activation of a joint is a combination of the relaxation of one muscle and the contraction of the second. Relaxation of the grip is produced by a reversal of the stimulants being applied to the flexor and the extensor.

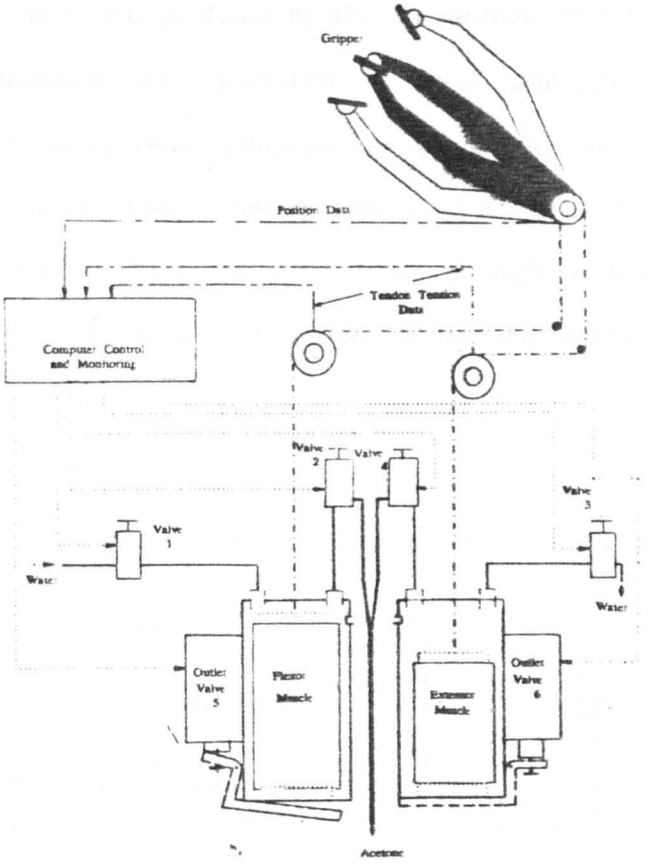

Figure 7.2. Actuator Control, Monitoring and Circulatory System.

A gripper/muscle system was designed and built to permit monitoring and control of the movements of the gripper and the muscles, figure 7.2. One muscle cell consisting of a water-tight chamber containing several strips of

'standard' (0.1mm thick, 30mm wide, and 45mm long) polymer muscle is attached to one side of the gripper. This muscle, which closes the gripper on contraction is the flexor. A second muscle cell - the extensor - is attached to the opposite side of the gripper. While the flexor is contracting, the extensor is relaxing and when the extensor is contracting, opening the gripper, the flexor is relaxing. To achieve the optimum contractile velocities 'very thin' polymer strips are used (0.1mm). This, however, reduces the cross-sectional area and hence the contractile force. These forces can, nevertheless, be enhanced by forming a muscle bundle consisting of tens or hundreds of thin polymer strips connected in parallel, all of which are contained within the 'muscle cell'.

Movements are produced by the introduction of the required chemicals, with the circulation and application of these stimulants being effected through hydraulic valves under computer control. Outflow occurs when the cell bottom plate is opened using a sprung solenoid. The solenoid valves used in controlling these chemical flows are each driven through a series of power transistors, figure 7.3, which are themselves under the direct control of the central micro-computer.

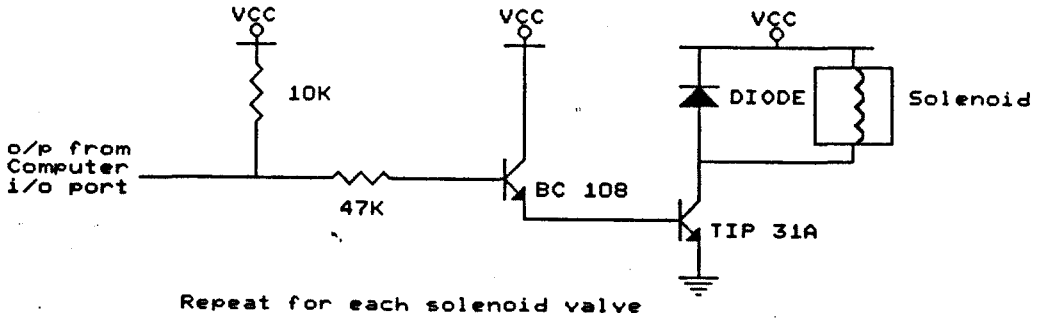

Figure 7.3. Solenoid Drive Circuitry.

The 'gripper' was initially a balanced beam mechanism, but once the design was proven experimentally, this was replaced by a more conventional gripper

which was formed from scissor jaws balanced to permit freedom of motion and limit loading effects caused by the mass of the gripper. Transmission of the power from the muscles to the end effector is by way of metal wire tendons. A strain gauge is connected to one of these tendons passing information to the computer on the tension being developed by the actuators. The outputs from the strain gauge are processed through a very sensitive bridge amplifying circuit, figure 7.4, before being sent to the computer, permitting accurate force control of the relaxing muscle.

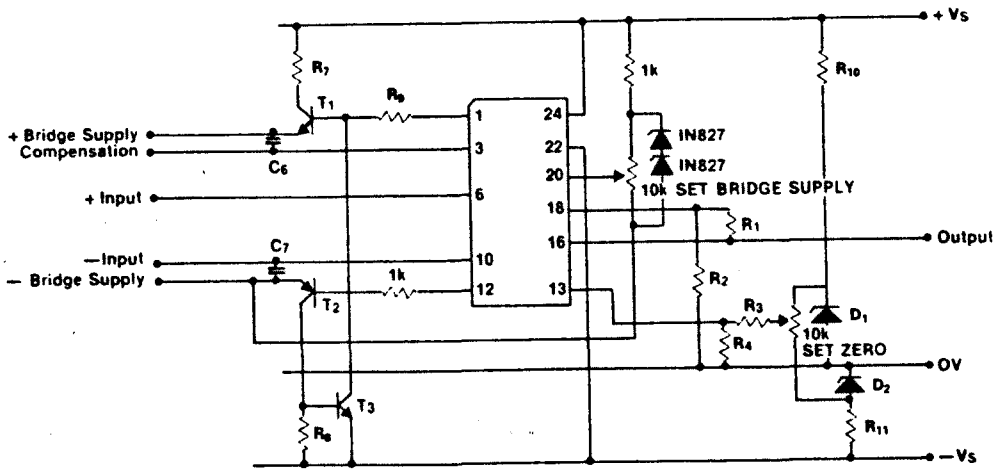

Figure 7.4. Strain Gauge Bridge Amplifier

Information on the gripper position is obtained by computer analysis of the output from a rotary position sensor connected at the gripper pivot point.

The filling of the cells is obviously a major factor in the control of the motion, with some method of determining when the cells are full being required to prevent overfilling. Solid state liquid level sensing switches use differences in the total internal reflection at the glass/liquid interface to determine if a solvent is present. When the liquid reaches the level of the sensor the inflow is stopped. The circuitry controlling this aspect is shown in figure 7.5.

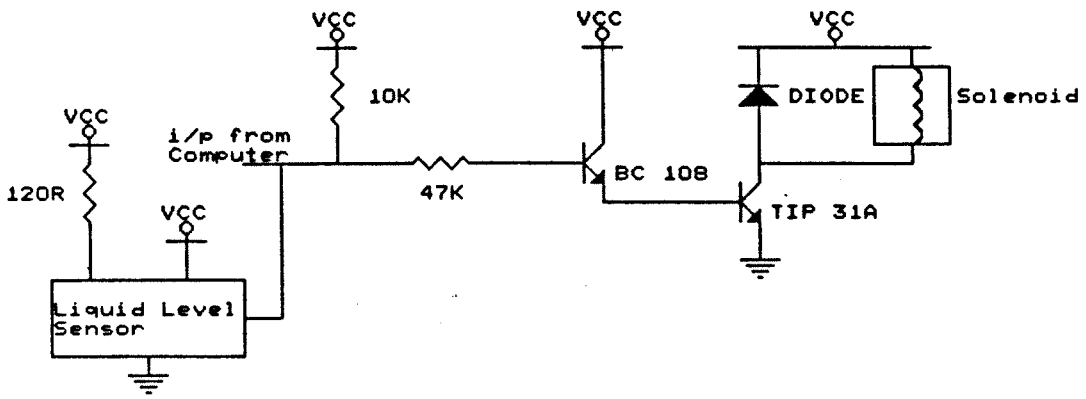

Figure 7.5. Liquid Level Monitoring Circuitry

Solvent diffusion effects within the polymer have been shown to give rise to delays before any motion occurs; similarly, delays are caused by the filling and emptying periods and the presence of residual liquids on the fibres. This all means that the movements cannot be started, stopped or reversed easily. For these reasons and because of the time taken for a stimulant to reverse a cycle, excessive overshoot ($<2^{\circ}$) must not occur.

Control over the system compliance can be achieved while monitoring the state of the solvents in the flexor and extensor cells by one of two methods.

1. When the gripper reaches the final set position, the normal response is to remove the liquid stopping the reaction. If, however, on reaching this final condition acetone (the contracting stimulant) is added to the relaxing muscle, tension will be generated. By balancing the tension in the extensor and flexor (as they now operate in opposition to each other) the compliance of the gripper can be regulated.

2. A simpler method involves direct solvent control over the polymer modulus. Using this scheme, when an object is gripped the strength of the grip, the compliance in that grip and the joint stiffness can be regulated by altering the solvent content in the contracting muscle cell.

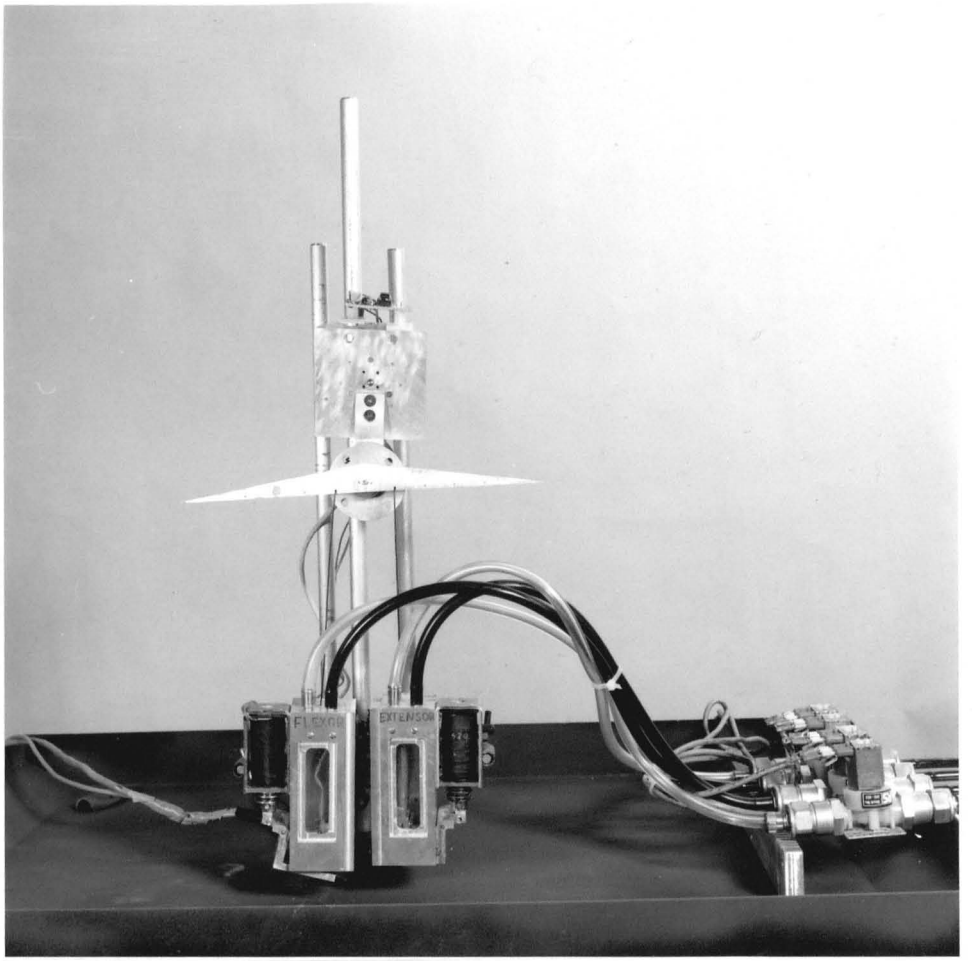
FLEXOR
EXTENSOR

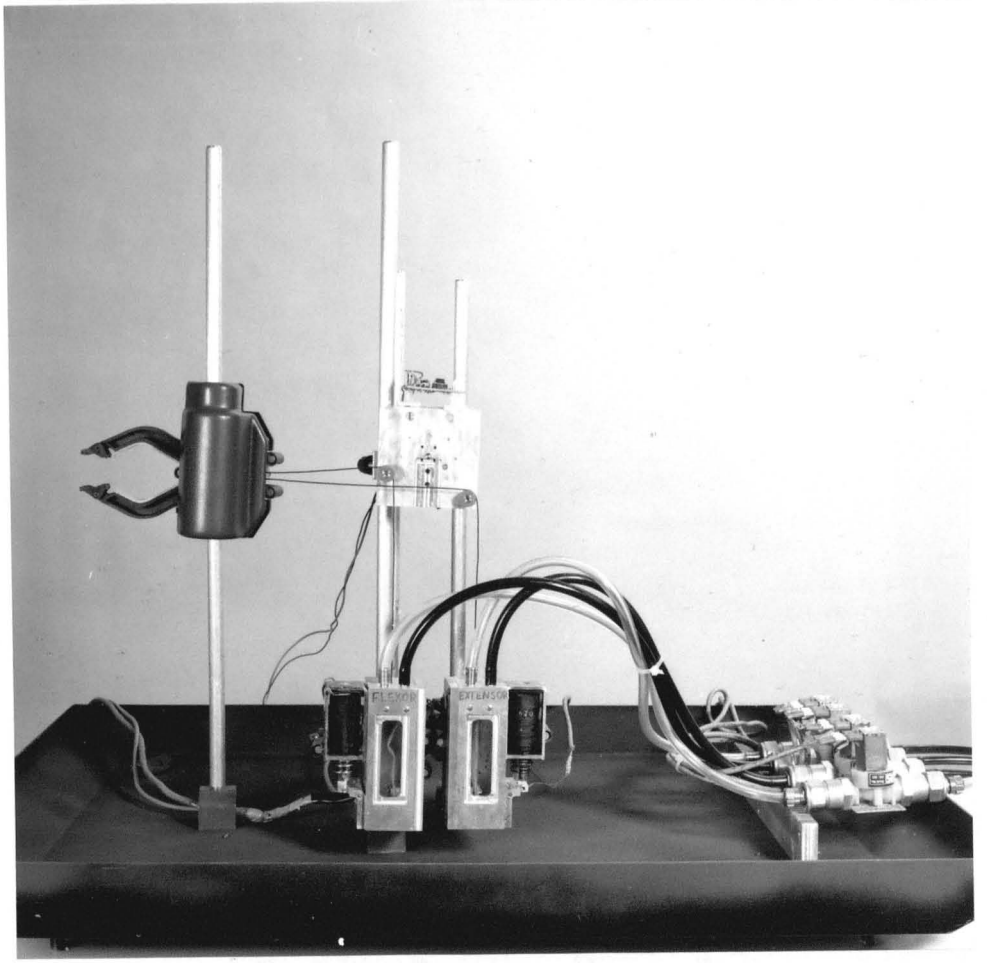
FLEXOR
EXTENSOR

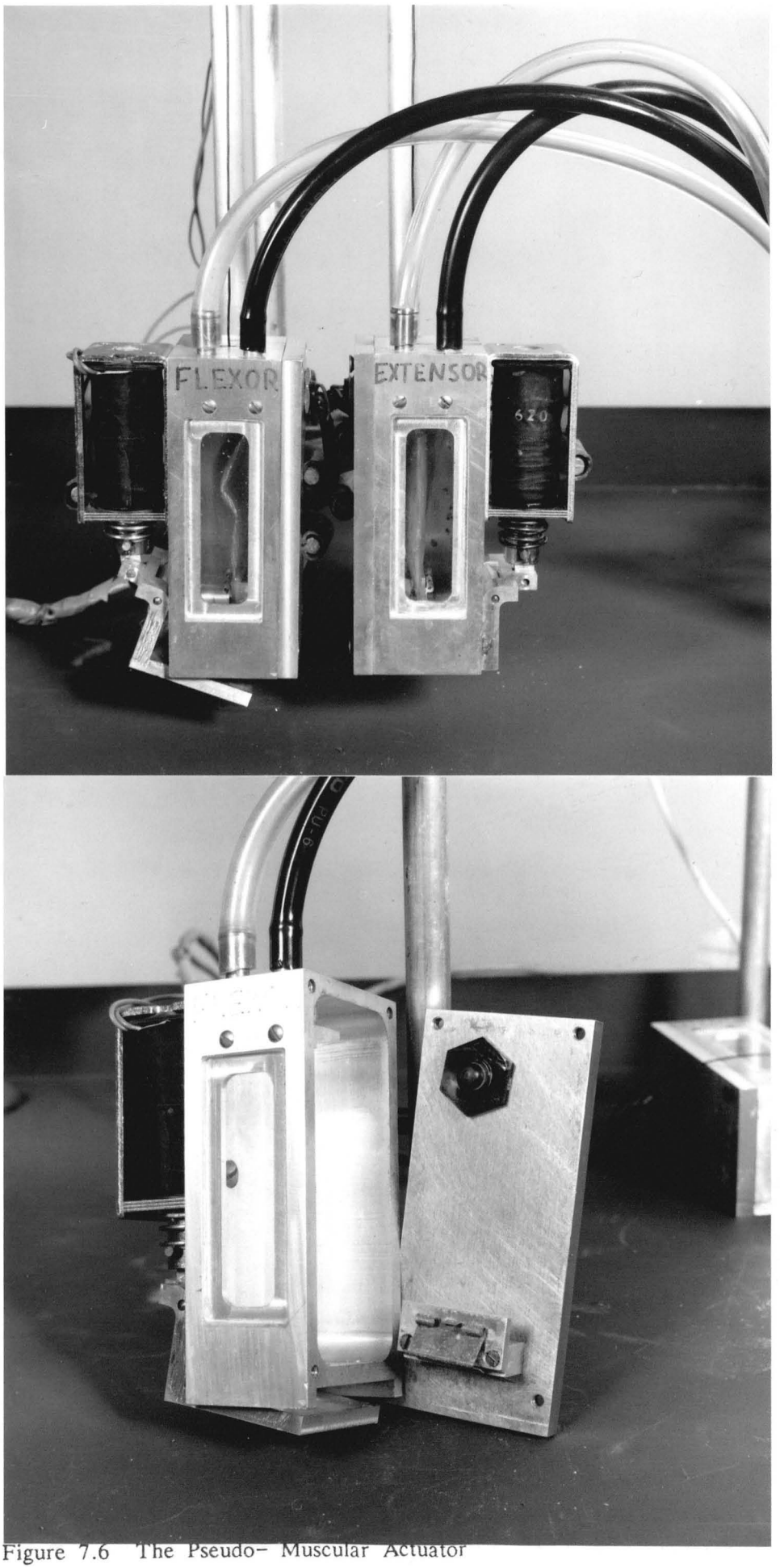

Figure 7.6 The Pseudo- Muscular Actuator

Such control over compliance is a significant advantage not only for insertion tasks, but also in general gripping were damage to the object, gripper, and actuator can be prevented.

The actual design which was implemented is shown in figures 7.6. These pictures show how the various parts of the system are constructed and how they fitted together to form the full mechanisms.

7.4 Control System Design

The control requirements are to move the gripper as quickly as possible between its desired end-points, without oscillation and with over/under shoot of less than 2°. A PID controller was originally considered for installation but due to the fact that no oscillation must occur and the tolerance of a small steady-state error (2°), no integral action was required.

The three control strategies which were developed for use with this system were initially tested on 'PHAS'. As a result of these tests, a PD based controller with position feedback regulating the contractile loop and force feedback regulating the flow of solvents in the dilating loop was chosen, figure 6.10. This control mechanism was included in an algorithm which provided a full simulation of the movements of the muscle fibres and the fluids contained within the flexor/extensor system. Using this algorithm the optimum PD values were determined.

The optimisation previously conducted using the muscle pair simulator suggested that the most flexible general purpose controller would be produced if K_p and K_d values of 1.0, and 0.35 respectively were used. It must be remembered that these are not the optimised values for operation over the whole range but simply reasonable compromise settings.

7.5 Muscle Actuator Operation

The operation of the muscle pair can be separated into a number of distinct phases depending on the action required and the conditions reported by the

sensors. This results in a need to coordinate the action of the valves to ensure the stimulants are introduced at the correct time and for the correct period. The valve conditions during each phase have been recorded in table 7.1.

Six valves have been used for the control of the motion, figure 7.2. Valves 1 and 2 control the flow of water and acetone respectively into the flexor, while valves 3 and 4 perform the same function for the extensor. Under normal conditions these valves are closed and no fluid flows into the cells. The fluid outflow from the cells is controlled by valve 5 for the flexor and valve 6 for the extensor, and these are initially open ensuring there is no solvent in the cells. During the operation the sensor outputs and valve control signals are updated every 0.15 sec., with the response rate and positional accuracy being continuously monitored and recorded.

At the start (phase 1) of the operation the gripper is open, the extensor being contracted and flexor relaxed. Stimulation of the flexor by the addition of acetone (phase 2) starts to close the gripper, the extensor remaining unstimulated until an increase in tension in the tendon is monitored. Fluid is then added to both the muscles simultaneously (phase 3), acetone to the flexor producing further contraction and water to the extensor causing relaxation. This process continues with the in and out flow of the solvents being governed by the switching line chosen, and the coordination of dilation/contraction needed to prevent over-relaxation which results in finger 'flop'. If the extensor were to relax too rapidly the flow of water to the relaxing muscle would be temporarily interrupted (phase 4). In this way slackness which would allow the finger to flop is not allowed to develop. While if the controller parameters are exceeded, solvent flow to both cells is stopped (phase 5).

This cyclic motion ensures that the gripper response remains on or near the switching line until the final end position is reached when all chemicals are removed (phase 6) and the gripper moves smoothly to the desired end-point position. Opening of the gripper follows the same procedure with the operations on the extensor and the flexor reversed (phases 7 to 11). The valves sequences

and positions at each of the phases within the opening and closing cycles are shown in table 7.1.

Phase	Valve State					
	1	2	3	4	5	6
1	closed	closed	closed	closed	open	open
2	closed	open	closed	closed	closed	closed
3	closed	open	open	closed	closed	closed
4			As for	phase 2		
5	closed	closed	closed	closed	closed	closed
6	closed	closed	closed	closed	open	open
7	closed	closed	closed	open	closed	closed
8	open	closed	closed	open	closed	closed
9			As for	phase 8		
10	closed	closed	closed	closed	open	open
11	closed	closed	closed	closed	open	open

Table 7.1. Solenoid Valve Control Sequence

At times it may be advantageous to have both the muscles operating against each other, which combined with changes in the polymer modulus creates a system with variable compliance. Compliance control is achieved by monitoring the position of the gripper and adding the chemical stimulants at rates which ensure that contraction in the flexor is balanced by contraction in the extensor. Changes in the system stiffness can be observed by noting the increase in inter-tendon tension during this coordinated contraction.

7.5.1 Actuator Control Algorithm

The control methodology for this system is based upon the algorithm

developed for the force/tension controller, as explained in the previous chapter. In this instance the routines have been developed on a BBC micro-computer using Basic. The algorithm detailing the sequencing of the various valves is as follows;

1. Initial Set-up routine.

   (i). Set user ports to output signals only.

   (ii). Energize acetone container.

   (iii). Turn all valves off (no fluid flow).

2. Specify the gripper demand signal.

3. Input values for proportional and derivative control.

4. Read initial gripper position (A/D converter).

5. If error signal > 0 And demand < gripper position Then

   (i). If cell level <>1 (not full) Then

      (a) Fill Flexor Cell with acetone. (Energize valve 2).

      Else

      (b) Do nothing.

6. If error signal > 0 And demand > gripper position Then

   (i). If cell level <>1 Then

      (a) Fill Extensor Cell with acetone. (Energize valve 4).

      Else

      (b) Do nothing.

7. If strain gauge tension >0 And demand < gripper position Then

   (i). If cell level <>1 Then

      (a) Fill Extensor Cell with water. (Energize valve 3).

Else

(b) Do nothing.

8. If strain gauge tension >0 And demand > gripper position Then

(i). If cell level <>1 Then

(a) Fill Flexor Cell with water. (Energize valve 1).

Else

(b) Do nothing.

9. Measure the gripper position.

10. If ABS(demand)gripper position) > permitted limit Then

(i) Repeat (5) to (9).

Else

(ii) Remove the solvents from both cells (Energize valves 5 and 6).

11. Turn all valves OFF.

12. Repeat (2) to (11).

A listing of this program is contained in appendix VII.

7.6 System Tests and Results

The rate of filling and emptying is of paramount importance in determining the response and controllability of the actuator. Tests on the fluid flow rates show that the cells (with an internal volume of 130cm^2) can be completely filled and emptied in 2.5 sec. and 0.4 sec. respectively.

With the rapid filling of the cell, fluid filling 'noise' and floatation effects are potential hazards which could have a serious effect on the results. Tests (using

the system and algorithm described above) on a heavily crosslinked sample (where the response relative to the filling rate is very slow) indicate that despite the high inflow rates there are no measurable effects, figure 7.7.

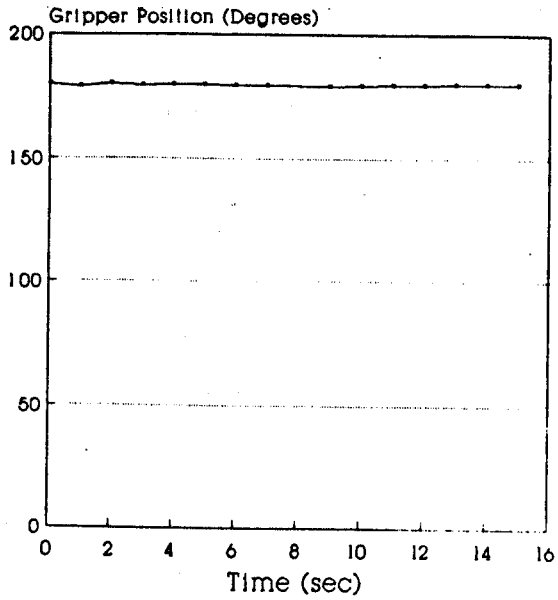

Figure 7.7. Flow Noise and Floatation Effects on Muscle Response

The system was constructed according to the design shown in figure 7.2. The response rate and contractile force for ten muscle fibres (fibre strip thickness 0.1mm) connected in parallel are measured, giving values for contractile rate of 10.5%/sec. at a contractile force of 29.8N/cm^2.

Having determined the response rate of the polymer strips being tested, the coupled muscle-pair actuator was fully implemented. Under computer control the gripper is driven between a series of different endpoint positions and the responses are recorded, figure 7.8a, b, and c.

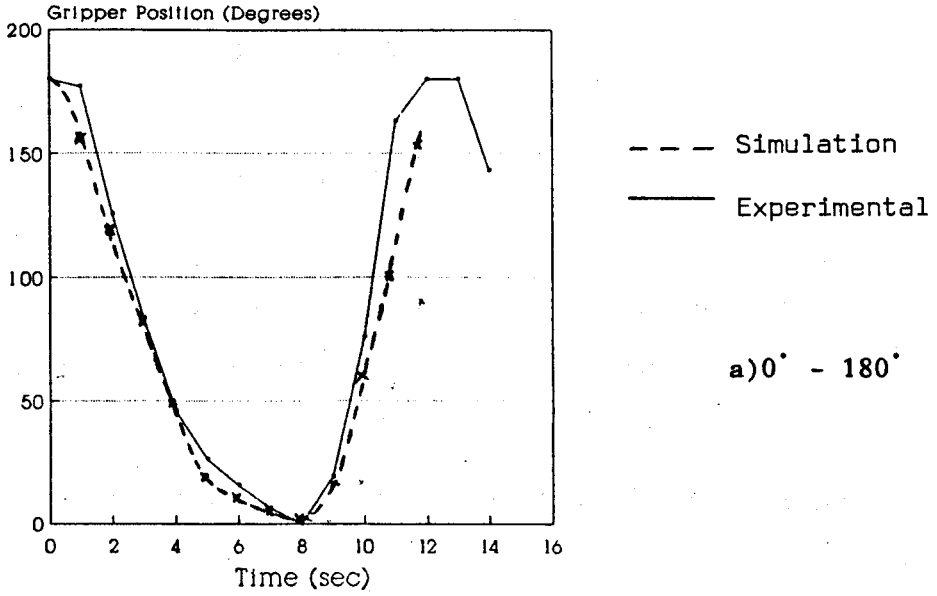

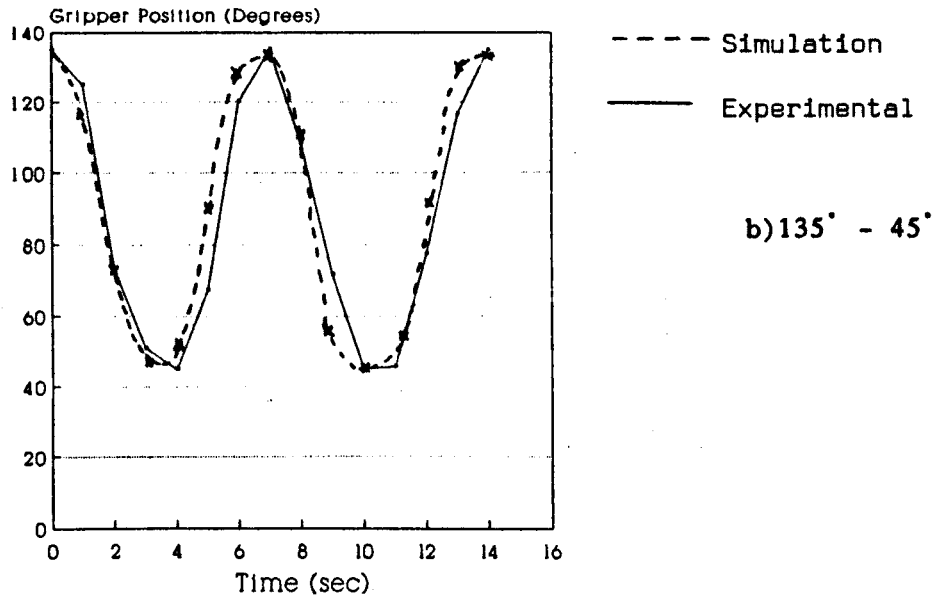

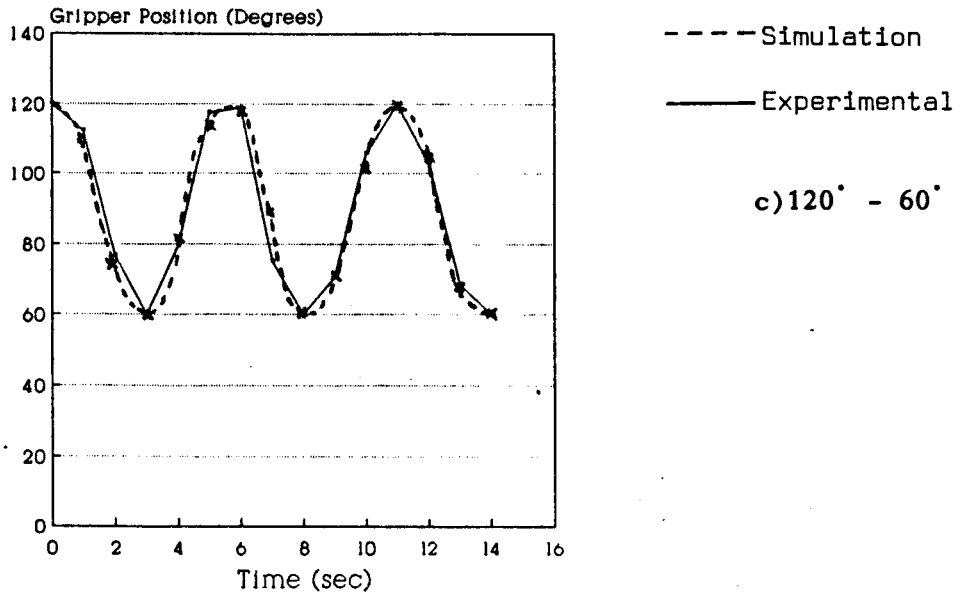

Figure 7.8a, b, and c. Operational Cycles Between.

a) 0° and 180°

b) 45° and 135°

c) 60° and 120°

Observation of the results discloses a number of facts about the operation of the muscle. At initial start-up and when the direction of motion changes, there are short delays as the solvents diffuse into the core of the material. At the end of each sequence small overshoots occur due to chemical delays (equalising

of concentration levels within the muscle and surface residual liquid). Finally, it can be seen that the response when opening and closing are not symmetrical. This is due to the non-linearity of the muscle response, and the initial set-up position. The symmetry could be improved while also optimising the response by ensuring that the muscles are operating at the centre of their range. Ideally this should be set to correspond to the 90° gripper position.

The open/close cycle time is clearly dependent on the extent of the motion required, but a movement from fully open to fully closed can be achieved in under 15 sec. Over this range of endpoint motions the positional accuracy is also found to vary slightly but at less that 1° it is always better than the 2° which was specified. Over the course of 20 tests on the system the results are found to be repeatable, being better than 1°.

A comparison of the results obtained in this chapter and the simulation results obtained in chapter 6 shows that there is very good agreement, as has been previously observed with other simulation/experimental comparisons, chapter 6.6.

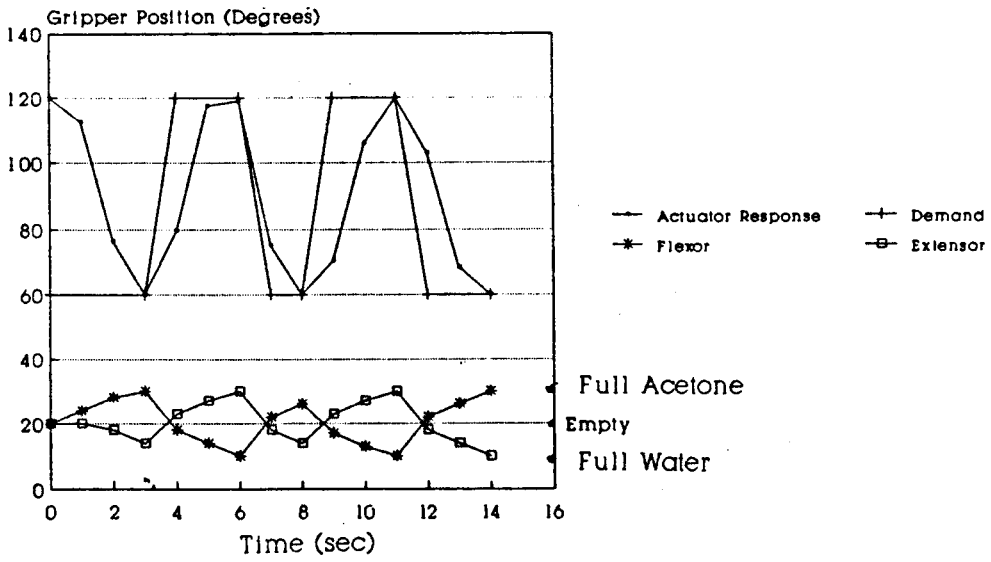

Figure 7.9 Demand and Solvent In/Out Flow Control Signals

The demand and control signals for a response between 60° and 120° are recorded in figure 7.9. The switching nature of the control system can be seen

for both the flexor and the extensor and it will be observed that the switching actions for each muscle is independent, although over considerable periods they are found to be in the same state (generally when the flexor is filling the extensor will be filling and similarly when emptying).

The ability to vary the compliance of the system can be tested by loading the gripper with a standard mass (5g) and measuring the deformation which occurs as the compliance is changed, both through opposal muscle actions and by chemically stimulated variations in the Youngs' modulus. These tests, figure 7.10, show that a standard mass can produce deformations greater than $10^{\bullet}$ when the actuator is very compliant, while at its most stiff the deformation is less than $1^{\bullet}$.

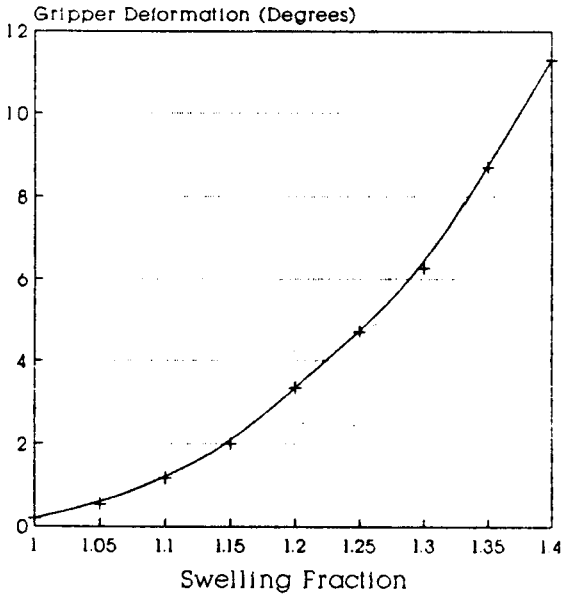

Figure 7.10 Control of Gripper Compliance

7.7 Conclusions

Chemical stimulation using acetone and water has been shown to be a new and effective medium for activating an artificial muscle constructed from strips of a polyvinyl alcohol - polyacrylic acid co-polymer. By monitoring the circulation and delivery of these stimulants the motion and position of a joint powered by this system can be accurately controlled.

A new actuator muscle pair has been developed and it has been demonstrated that controlled movement of a robot gripper is feasible.

In higher level organisms, control of muscle motion is controlled and coordinated by the brain, with special auto-motive processes under spinal control. In the artificial muscular environment these processes are undertaken by computer. Producing an effective method of transporting and delivering the chemical stimulants is not, however, a simple process.

Cycle times for opening and closing a gripper of under 15 sec. have been recorded, combined with good repeatability and positional accuracy better than the 2° specified. While these would seem to be barely acceptable rates of motion, micro-manipulation is an area which may be able to make use of this system in the short term. In the longer term the development of thinner fibres and perhaps new materials will lead to potential uses in large scale operations.

A secondary feature of this style of actuator design, which is nevertheless worth noting is that the system provides linear motion which can be used to drive a joint directly. Finally in terms of the physical properties of the material, the compliance control is a very useful parameter which could be of particular benefit in pick, place and insertion tasks.

The VSS controller used satisfies all the criteria set, with the angle accuracy always being within the required limits. It is, however, felt that by refining and improving the control algorithm it will be possible to achieve increased speeds, reliability and controllability. The most obvious upgrade would be the use of PWM to control the on/off action of the valves giving greater control of the liquid flow-rate. Additionally the non-linear nature of the actuator response means that the switching line has not been optimized over the range of motion, but rather uses a compromise value. By incorporating a form of adaptive or rule based learning controller into the design, the best switching line could be used for each movement as required. The usefulness of including some form of predictor is also being considered. This model would be based on that previously derived to simulate the system.

In this study it has been demonstrated that a chemical stimulated artificial muscle when used in conjunction with a VSS type controller monitoring

positional and muscle tension information, produces a feasible robotic actuator. Using this mechanism a new linear direct drive actuator with excellent power/weight ratios is a realistic long term possibility.

Chapter 8
Variable Compliance Tendons

8.1 Introduction

The object of the research in this thesis was stated at the outset to be the development of a new compact method of powering a dextrous manipulator. The work in the previous chapters has dealt with the development of an artificial muscle-type system, using the swelling/deswelling properties of the material to physically drive the joints in a gripper. Although these pseudo-muscular actuators have not progressed far enough to replace conventional designs in a gripper, it may be possible to use an application of this technology discovered during the research to circumvent one of the major difficulties encountered in the use of dextrous manipulators.

The work to be discussed in this chapter uses a second property of the polymer, its variable compliance, to control a dextrous manipulator. With the designs presently being used for flexible grippers, multiple fingers (which in themselves often have multiple joints) requires a great many motors (often 10 or more), and this adds significantly to the volume of the actuators and their mass.

Using the variable compliance tendon mechanisms, a rudimentary hand can be constructed which can be powered by a single conventional actuator (or perhaps at a later stage an artificial muscle), in this instance a linear stepper motor. By regulating the properties of the polymer strips, the distribution of power to the joints and hence the motion of the joints is controlled. In addition this design

gives the added advantage of increased control over the compliance of the gripper.

8.2 Factors influencing 'Variable Compliance Control'

It has already been demonstrated that when PVA-PAA co-polymers are swollen in water dimensional changes of 50% or more in any one direction (volume changes in excess of 300%) are produced. During this swelling the polymer changes from a very rigid, tough material, perhaps not un-like leather (dry condition) to a very flexible rubber-like material (when fully swollen). This change in stiffness can be clearly observed by a simple comparison of the elastic (Youngs') modulus when swollen and unswollen (see chapter 4.8), (unswollen modulus = 200-400N/mm^2; swollen modulus <1N/mm^2).

These modulus changes are fortunately not only observed at the extremes of swelling and deswelling. By carefully controlling the water content of the polymer, the swelling can be limited and regulated with the modulus being set to any value between these limits. The relationship between the water content and the modulus has also been given in chapter 4.8.

Two methods of inducing changes in the water content, and hence modulus, have been studied, thermal and chemical. When using thermal methods (drying) to alter the modulus it is possible to operate over the full range, but the rates at which the compliance can be changed are relatively slow. If more rapid responses are necessary this can be effected using chemical stimulation, although this doesn't give quite such an extended range of modulus values, since the upper stiffness limit is now reduced from 400N/mm^2 to 16-18N/mm^2. Both these methods of inducing parameter changes will be dealt with in detail in later sections, together with a number of techniques used for controlling these parameter changes.

8.3 Analysis of Hand Motion

One of the major facets of this work is the belief that only one actuator is

required to provide all the power and the flexibility of motion necessary in a dextrous manipulator.

If as a starting point the 16 working grip configurations defined by Cutkosky and Wright [Cutkosky, 1986] are considered as the minimum requirement for a dextrous gripper, then it is imperative that this single actuator system can operate in such a manner that each of these positions is obtainable. This is possible using this design, since the motion of each of the fingers can be independently regulated by controlling the stiffness and length of the connecting polymer tendon.

Clearly certain situations will create more problems than others. If, for instance, the required grip configuration is not known before movement starts there may be a need for several readjustment of the stimulus during motion. Although this may create a difficult control problem, the basic design and methodology is such that the problem can be overcome. In fact only one condition has been identified which this design, in its initial form finds difficult to solve. That is the opening of one finger or joint while another is closing. This limitation is simply due to the presence of a single actuator, which can only provide power in one direction at any instant. By using a semi-passive return system such as a spring, or if a second actuator stroke is available then this opening/closing dilemma is easily resolved.

That the moving of joints in this manner is not a trivial problem is demonstrated by the relative difficulty experienced when trying to achieve this motion in the human hand. In fact the only common events which appear to require this ability are playing musical instruments, and a great many people find this difficult.

Since these are the parameters within which the human hand operates, it is felt that the original hypothesis, that a dextrous hand could be powered from a single actuator, is valid.

8.4 System development

Polymer strips were prepared as outlined previously using the standard PVA-PAA ratio of 3:1 and a crosslinking period of 60 mins. at 150°C. Sections of polymer were then cut from these sheets forming strips 30mm long and 5mm wide and 0.1mm thick. The primary power source to be used in these initial tests was a stepper motor, but it is hoped that in future a pneumatic system could be used. The desire for a pneumatic system is inspired by the possible improvements which the compliance control mechanism could make in controlling pneumatic devices, combined with the knowledge that pneumatic sources provide a system with relatively good power/weight and power/volume ratios.

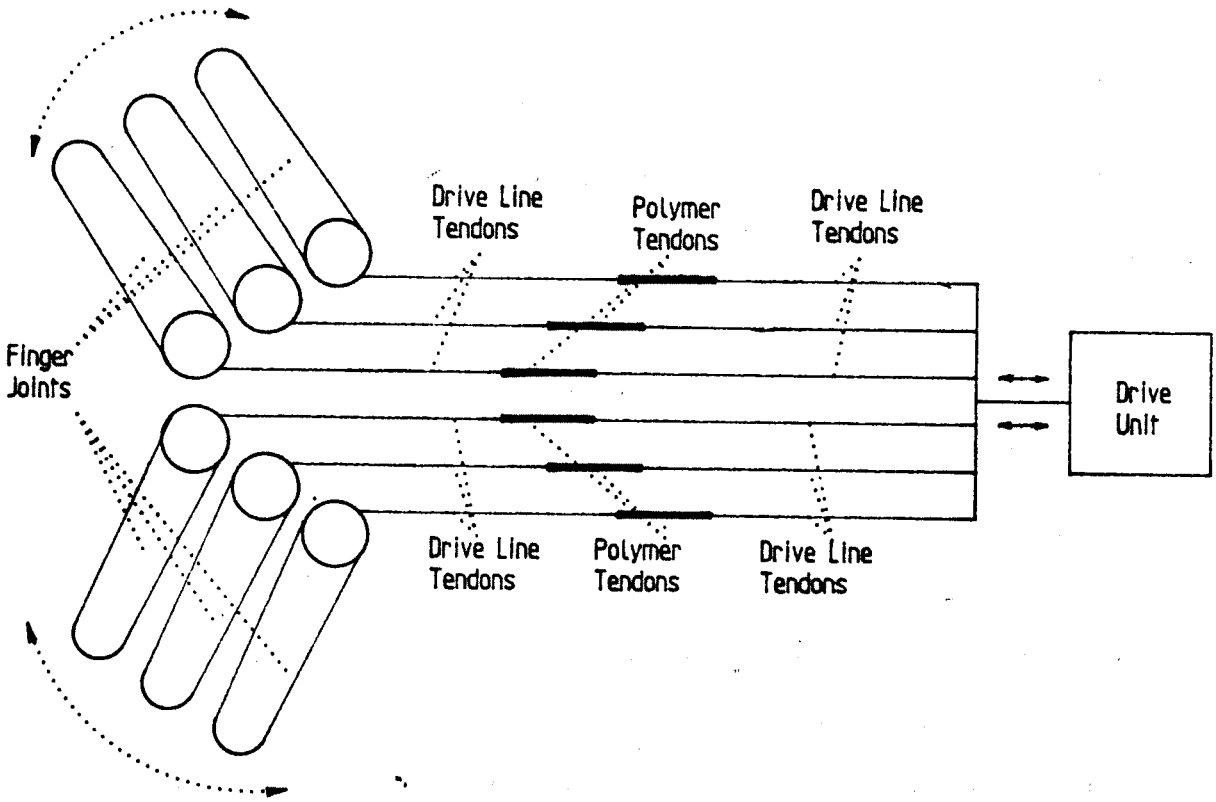

Figure 8.1. Compliant Actuator Mechanism

The controllable 'Variable Compliance Tendon' (V.C.T.) design mechanism shown in figure 8.1 can be divided into four major sections;

1. The drive unit. The present design uses a fairly large, powerful (starting

force 125N) linear stepper motor as its primary drive unit. This gives a system with a full stroke length of 170mm. Motion is controlled directly from a computer terminal through a stepper motor interface circuit (appendix VIII), giving control over the speed (up to 9.5mm/sec), direction, and distance moved by the motor. The power generated by this motor is distributed through a series of cables (via a number of intermediate stages which will be detailed in the following paragraphs), to the joints to be moved.

2. The joints. Although designed for use as a dextrous manipulator the gripper is a very simple device with three 'fingers' each having three joints, figure 8.1. Each of these joints has its own drive line (tendon) connecting it to the stepper motor. The finger joint design is shown in detail in figure 8.2.

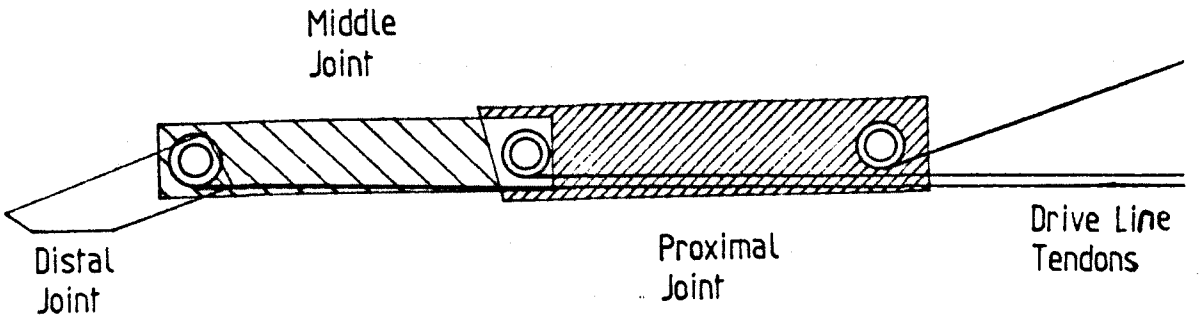

Figure 8.2. Design of the Finger Joints

The length of the first link (proximal phalanx) is 54mm, that of the second link (middle phalanx) is 35mm, and that of the third link (distal phalanx) is 22mm, these values are approximately equal to those in the human hand.

3. The drive line. This is the section of the mechanism which physically links the actuator to the gripper joints. There are in effect three sections in this linkage. The central polymer based unit which will be considered later, and the two outer tendons which are made from Kevlar to prevent extension on loading. These outer fibres are used to connect the central V.C.T. unit to the actuator at one end and the manipulator at the other end. The routing of these cables from the variable compliance unit to the joints is shown in figure 8.2.

4. The Variable Compliance Tendon (V.C.T.). This is the section of the

system which actually utilizes the variable compliance properties of the polyelectrolyte gel. Within this unit the polymer strips are used as a connecting line between the inextensible Kevlar tendons running to the joints and the motor. These strips are inside a containing vessel which is simply in place to store the compliance modulating chemical stimulant (water or acetone). This flow of chemicals can either be manual or automatic. A close-up view of the design of these tendons is given in figure 8.3.

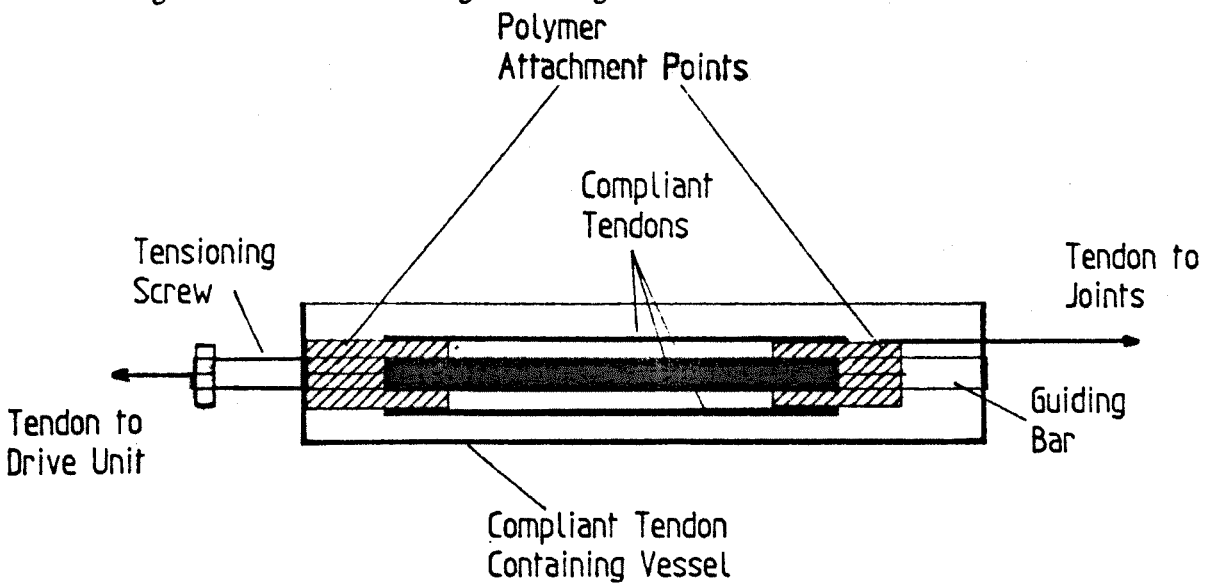

Figure 8.3 V.C.T. Controlling Unit

8.5 System Operation

Control of the motion of this system can be achieved using a number of different techniques, with varying degrees of complexity. These designs will be explored in the following sections, detailing the modes of operation and outlining the results obtained in experiments with these various strategies.

There remains one final construction detail which must be considered. With only one active actuation unit the problem of the return of the joint to its original starting point needs attention. Two methods of achieving this return action have been used and a third has been considered but as yet has not reached a experimental stage.

In the first design, a passive return mechanism, gravity, is used. The actuator

lifts the joint against gravity, closing the gripper. The opening of the gripper simply consists of the actuator moving in the reverse direction and letting gravity take effect. This mechanism can clearly only be used in a limited number of orientations.

To give a full range of motions and grasps, a spring was introduced into the return phase. Opening is produced by relaxation of the V.C.T. tension (addition of water) or by reversal of the motion of the actuator. This gives a gripper which can be used in any orientation, but it is by no means an optimum solution.

The third method which was considered but has not actually being implemented, involves using the energy of the stepper motor when both closing and opening. There would appear to be few problems with this design method, but because of a shortage of time no tests have been conducted.

8.5.1 Limit Control

This is the simplest mechanism tested for controlling the condition of the V.C.T. and the motion of the gripper. Prior to any motion, the V.C.T.s attached to joints which are not require to close are saturated in water. This produces dilation, the polymer tendon swelling to a new length of approximately 46mm, providing 16mm (50% dilation) of slack. The stepper motor is now energized and power is transmitted to those joints with untreated tendons. If the motion of the actuator is less than 16mm there will clearly be absolutely no motion in the treated tendon joints, as required. The return sequence can be effected by either of the mechanisms outlined above. To repeat the opening/closing procedure, but with different joint open/close settings, one of two possible methods may be chosen. To return the polymer tendon to absolutely its original length, drying is necessary. This may take several minutes although it is possible to increase this rate be using acetone to induce an initial contraction and then drying as before. Clearly if polymers were available with similar properties to PVA-PAA but using a more volatile liquid than water this

process would become more attractive.

The alternate mechanism which can produce contractions in periods from a few seconds upwards depending on the thickness of the polymer, is chemical stimulation. As before acetone draws the moisture from the polymer producing the modulus and dimensional changes required. Unfortunately with this method the final state is still slightly swollen relative to the dry condition and the maximum modulus value is less than that of the dry polymer, although still many times higher than that of the moist fibres. This 'incomplete' contraction will introduce an offset, but if all the fibres are swollen in water and then brought into equilibrium in acetone prior to use (the dimensions at this instance may be taken as the zero setting), no difficulties should be encountered. Once returned to their original or slightly swollen (offset) condition the tendons not required to transmit energy can be treated (swollen) with water. Motion of the actuator now distributes power only to the high modulus (unswollen) tendons, as before.

It is possible in fact to use all three of these states, dry, slightly swollen, and fully swollen, to achieve a simple graded compliance effect.

Experimental Results 8.5.2

To test the effectiveness of these theories three joints were connected via their respective V.C.T.s to the stepper motor. The experiments were repeated for tendons contracted by both chemical and thermal techniques, with a spring forming the return mechanism in proximal joint, and gravity return operating in the other joints. At each joint a rotary solenoid was used to monitor the angle of rotation by way of a microcomputer.

The following series of tests was conducted to determine the effectiveness of this mechanism.

1). In the first tests, all the joints were left untreated (fully contracted) and their motion was recorded as the stepper moved, figure 8.4a.

From the results a number of features can be observed, with many of these factors re-occurring in subsequent tests. The top trace shows the contracting and relaxing motion of the stepper motor, while the lower three traces show the resultant motions in the three joints. In each instance there is a short delay before any motion is detected. This is due to slack in the connecting cables, with some joints having more slack than others. It should also be noted that the freedom of rotation and the rate of rotation varies from joint to joint. These are simply constructional problems which have no effect on the response test results.

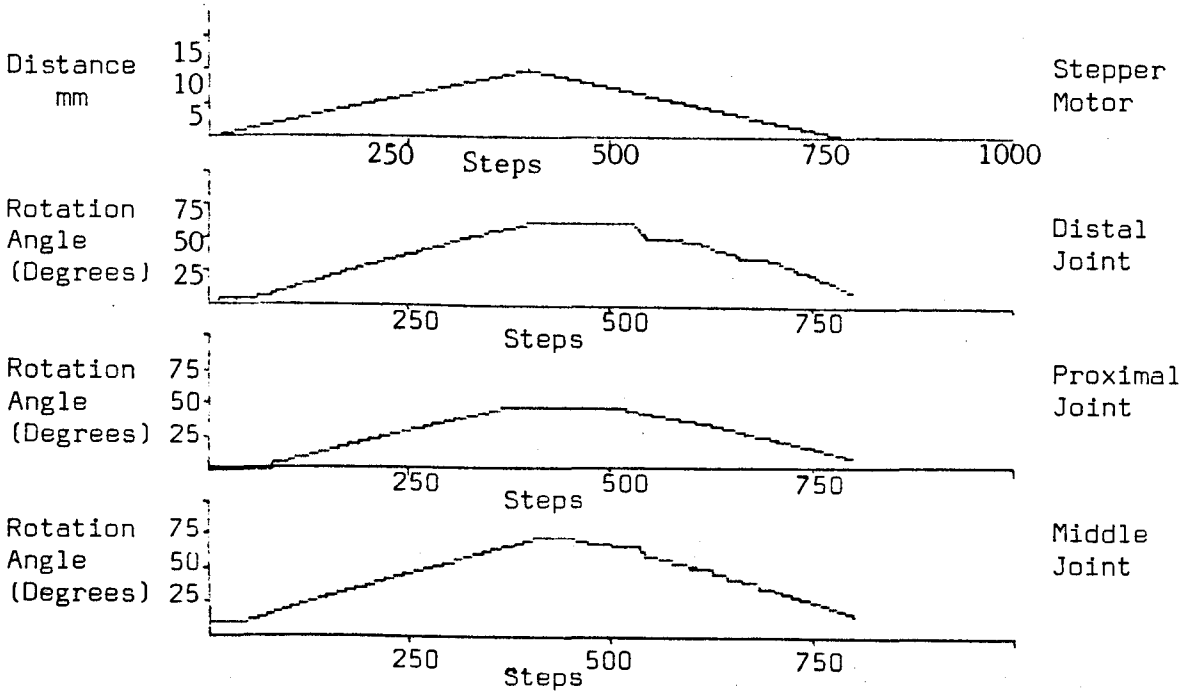

Figure 8.4a. Energy Transmission. All Tendons Untreated.

For each joints the contraction phase is very linear, but the relaxation of the middle and distal joints (which use gravity to reopen) is rather jerky. No such jerkiness is noticed in the proximal joint which uses a spring return system.

Basically the results show that the transmission of energy by the unstimulated tendons is very efficient as was hoped.

2). One of the V.C.T.s (distal) was now fully saturated and allowed to equilibriate. The motion of each of the three joints during the subsequent

opening/closing stepper motions is shown in figure 8.4b.

With the second series of results, the responses for the proximal and middle joints (which were unstimulated) are identical to those recorded in (1). With the distal joint which has been stimulated (fully swollen), no energy is transmitted and hence no motion is recorded.

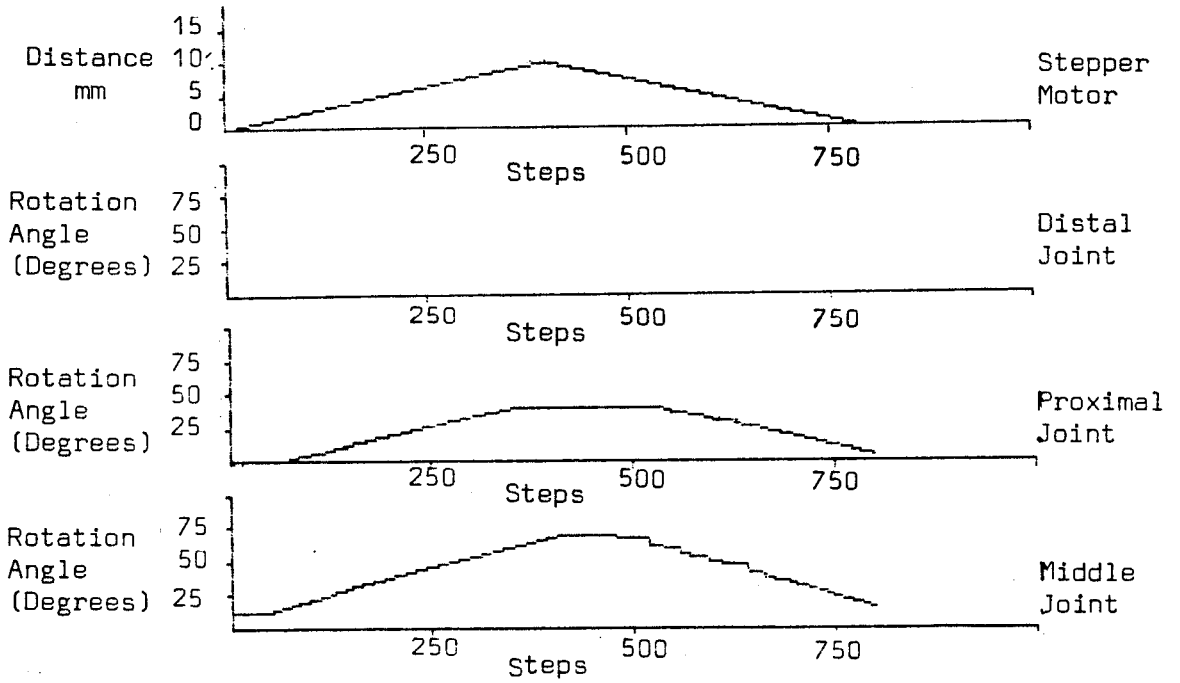

Figure 8.4b. Energy Transmission with One Joint Swollen.

3). This test was repeated with a second tendon (middle) being stimulated and brought to equilibrium before any actuator motion occurred. The results in this instance are shown in figure 8.4c.

The results for this test show that as before energy is transmitted effectively by the untreated proximal tendon, but there is no transmission of power by the swollen middle and distal tendons. In this case it will be noted that in the proximal joint the delay caused by slack has been reduced, since only the setting for this joint is crictical in this experiment. Results for the middle joint also show a slight offset from zero degrees. This will have been observed in all the previous and subsequent readings and is caused by an offset in the A/D converter, which does not effect the results.

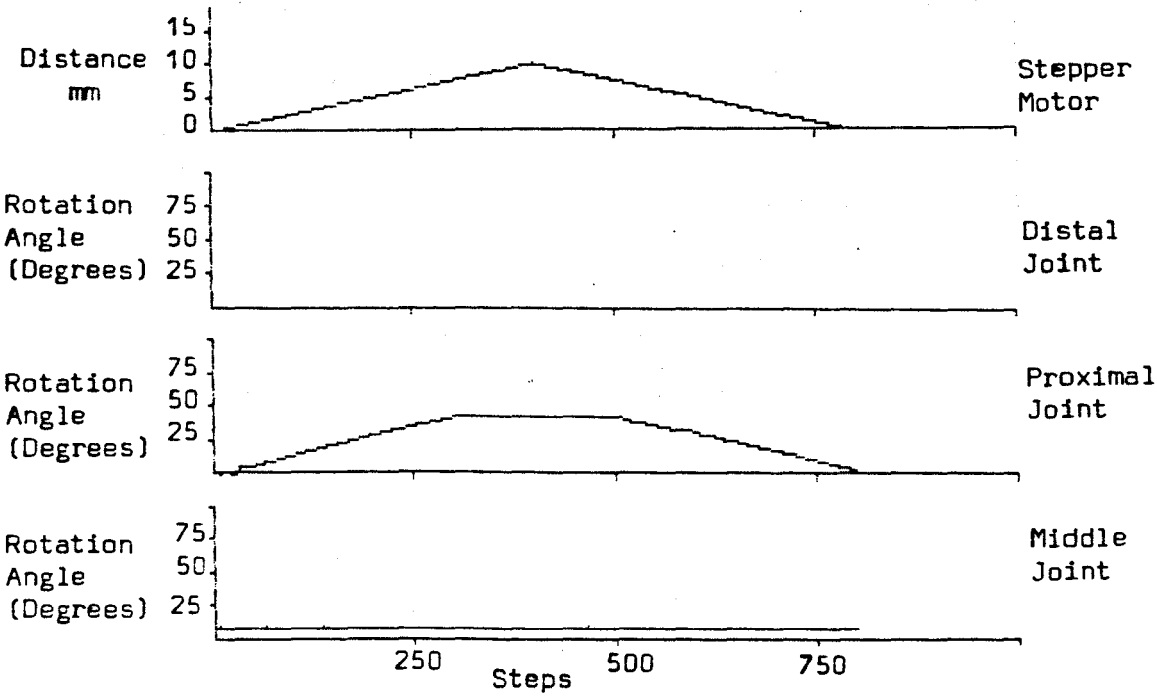

Figure 8.4c. Energy Transmission with Two Joints Swollen.

4). The swollen tendons were allowed to fully contract in air during the next 45 minutes, before repeating the measurments, figure 8.4d.

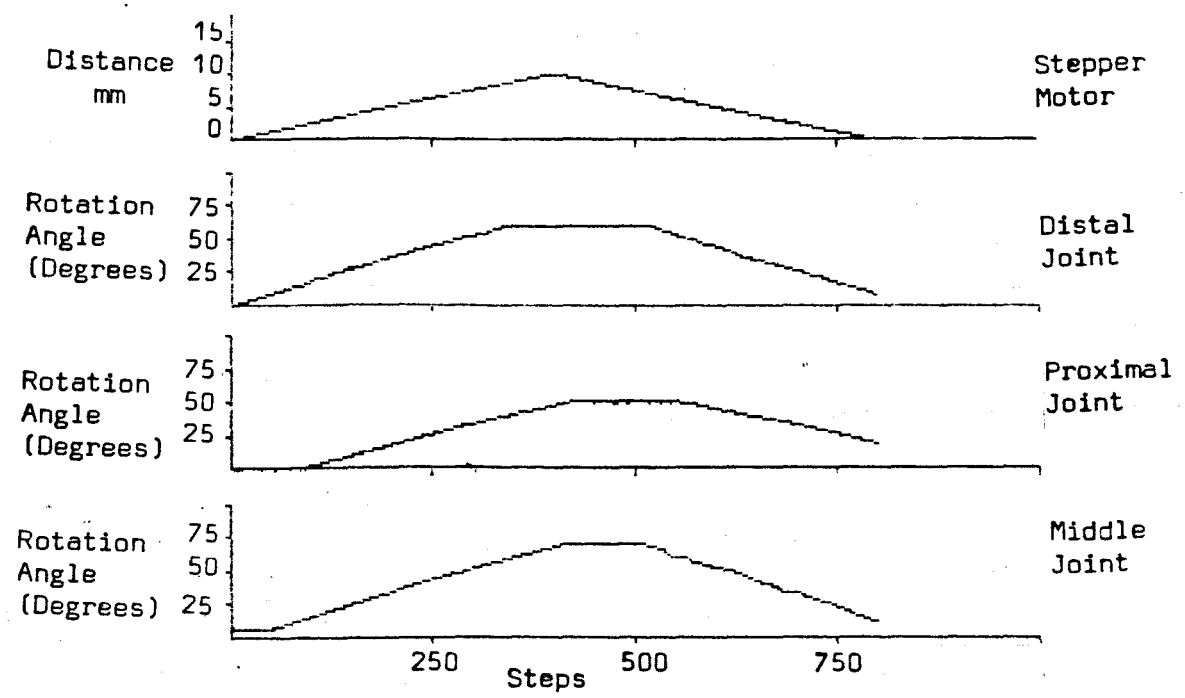

Figure 8.4d. Energy Transmission. All Tendons Restored.

These reults show that after contracting in air the tendons transmit energy as efficiently as in the original test (1), with the resultant plots bearing very close comparision.

5). Again a single tendon was swollen in water, but in this instance drying was rapid (<1 min. using a heated air flow to speed the drying). The results for this cycle are shown in figure 8.4e.

As with the slow drying technique, rapid drying appears to return the material to its original condition.

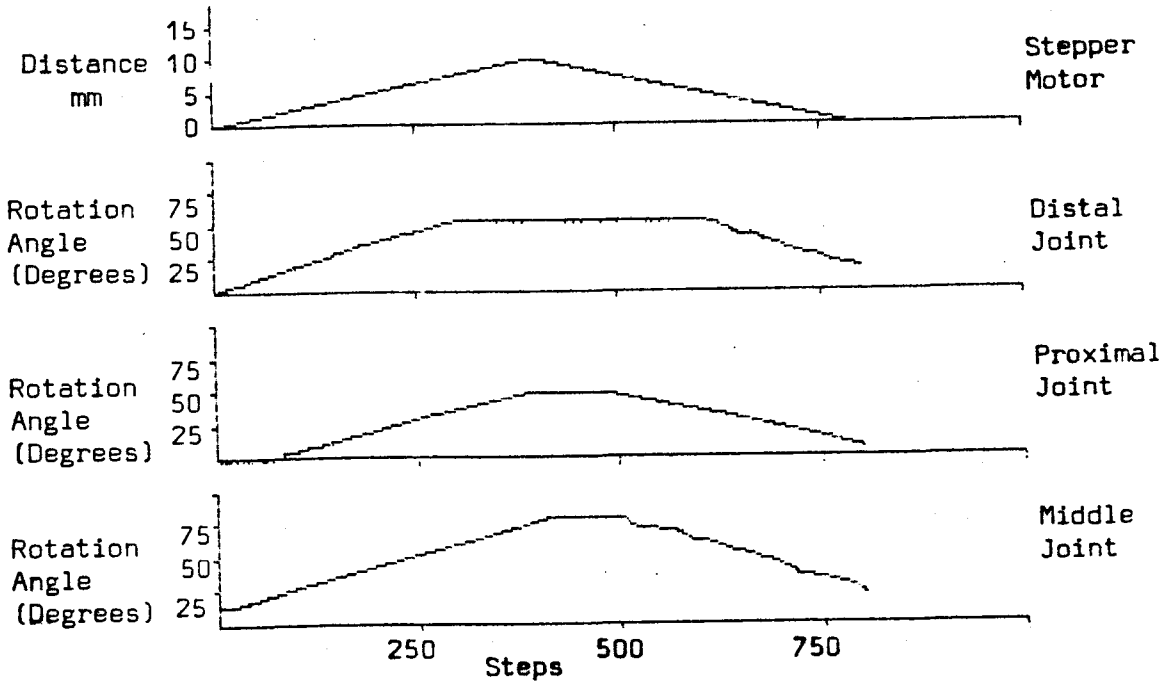

Figure 8.4e. Energy Transmission after Rapid Drying.

6). The swelling - rapid contraction cycle described in (5) was repeated a further 50 times to determine the effect of prolonged use. The results for the 50th cycle in the sequence are shown in figure 8.4f.

The results at the end of 50 cycles are almost identical to those obtained in the first test. This shows that the material has at least fair durability, although further tests will have to be conducted to determine if it is truely viable over very extended periods of testing.

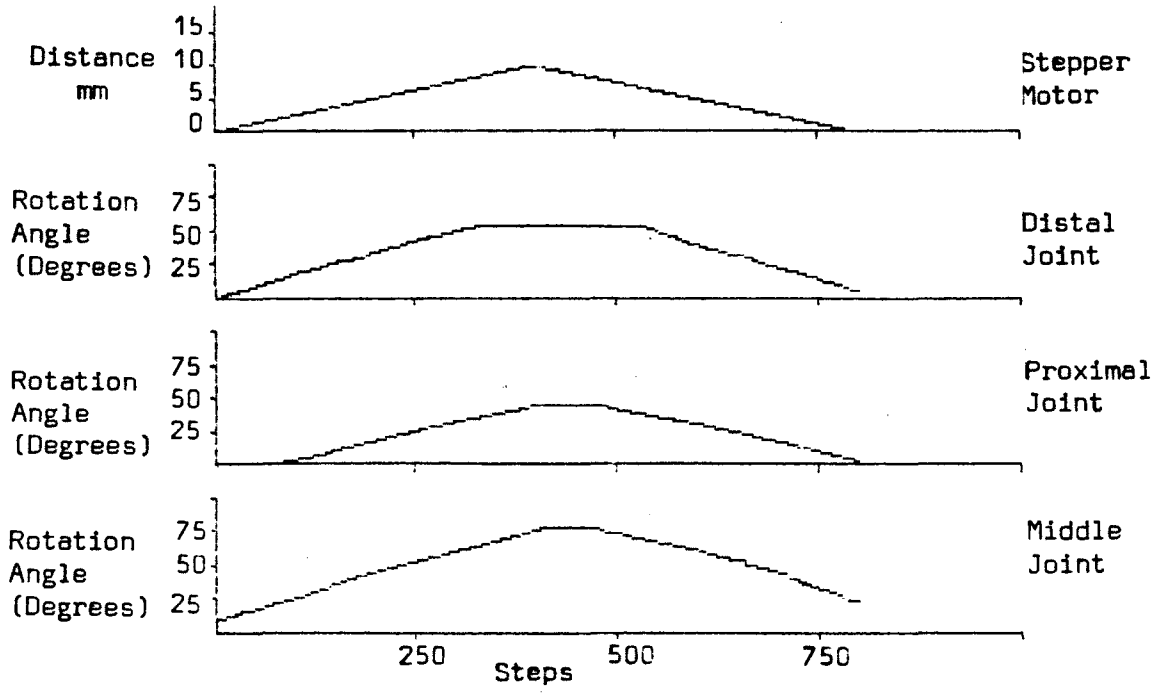

Figure 8.4f. Energy Transimission after 50 Cycles.

Having conducted a series of tests on the response of the thermal system, similar experiments were repeated using acetone as the contracting medium. For this second series of readings the tendons had been pre-swollen and then contracted (in acetone) to give an initial (offset) condition.

Three sets of results were recorded.

(a). The middle joint tendon is fully swollen in water. Power generated by the stepper is transmitted to the distal and proximal joints which move smoothly, but there is no motion from the middle joint, figure 8.4g. These results are obviously similiar to those recorded in (2), except that the proximal and distal tendons are in an acetone induced contractile state.

(b). The middle tendon is now contracted in acetone and the transmission of energy to all three joints is recorded, figure 8.4h. The tendon seems to have completely recovered giving the smooth joint rotation which was required.

(c). This expansion/contraction cycle was repeated for the middle tendon a further 50 times. At the end of this period the profile was again recorded, figure 8.4i.

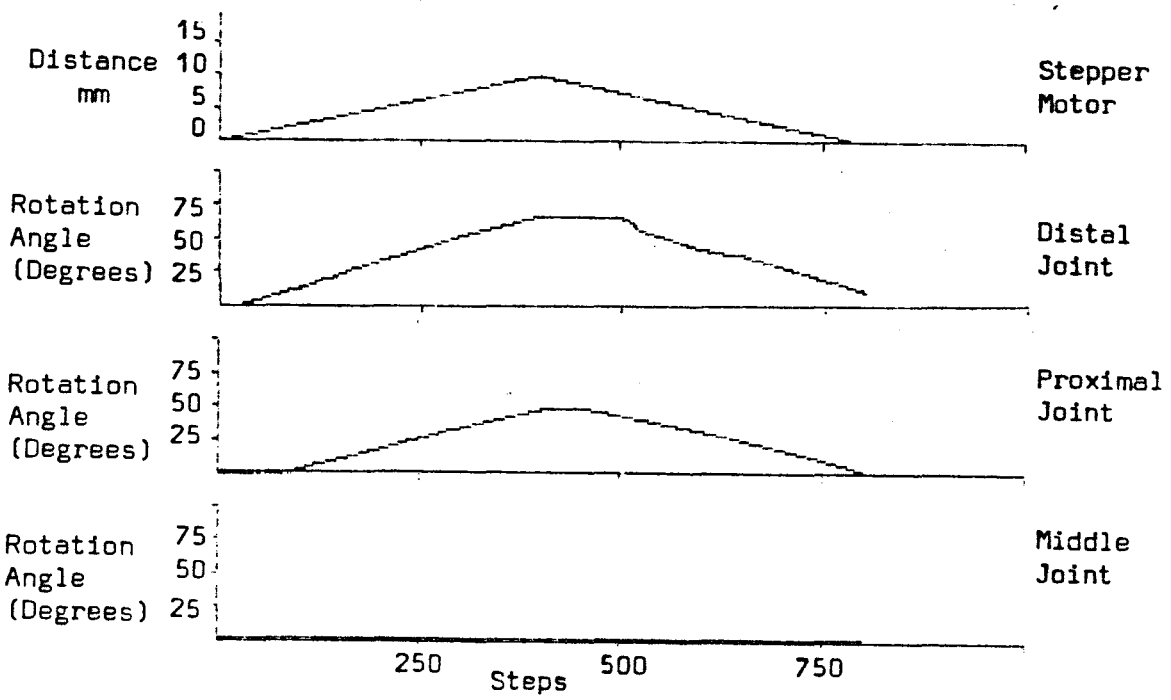

Figure 8.4g. Energy Tranmission using Acetone Contractor Stimulation.

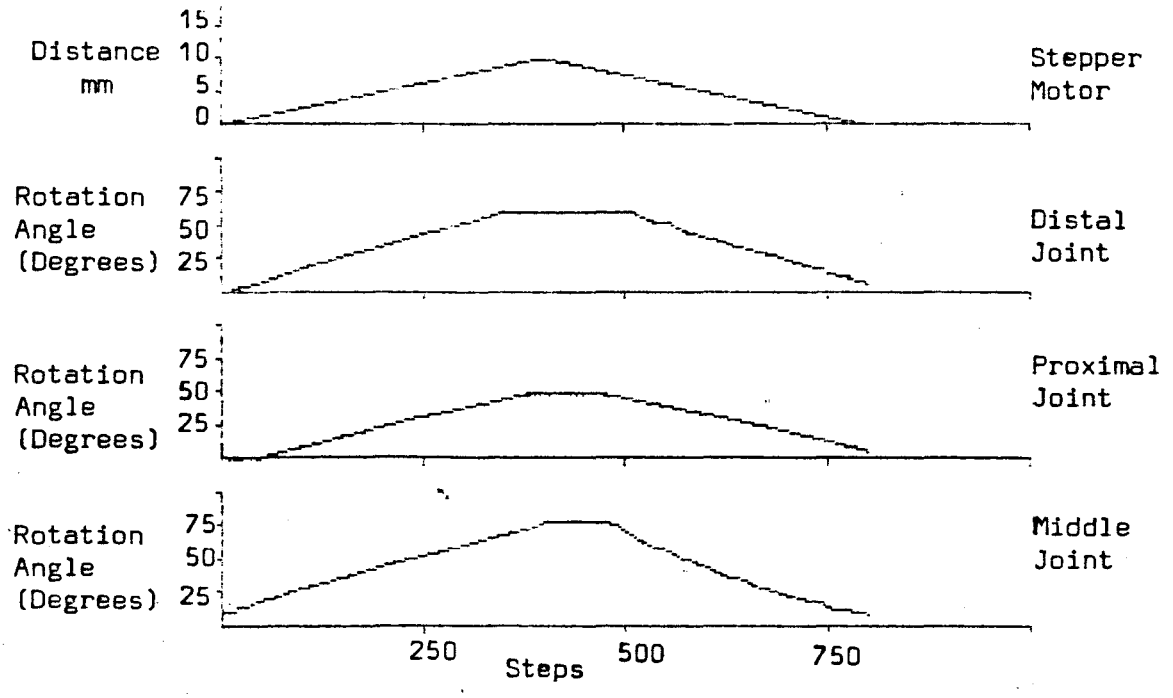

Figure 8.4h. Acetone Contraction; All Tendons Restored.

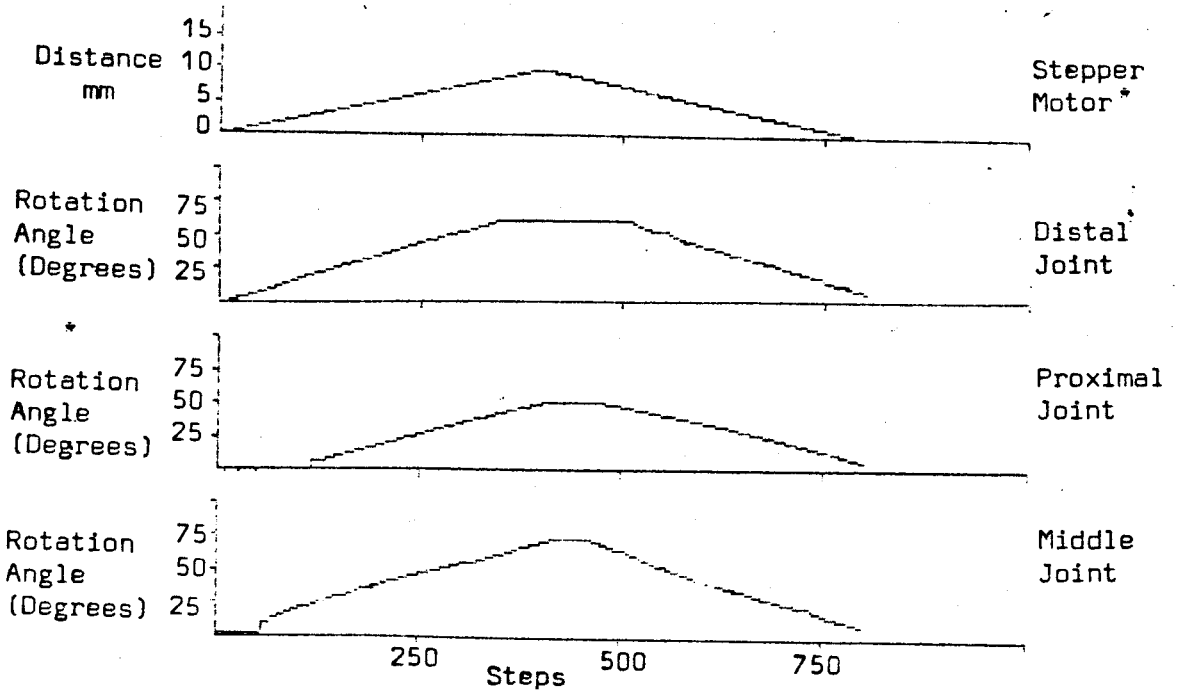

Figure 8.4i. Acetone System; Energy Transmission after 50 Cycles.

These results clearly show that the performance has not been noticabily degraded during the test sequence.

This series of tests also provided an opportunity to measure the response rate using this technique. As expected this was very rapid, with an almost instant reaction to stimulation, and the final water or acetone equilibrium states being reached in under 10 sec..

This method is indeed very promising.

8.6 Control System Enhancements

The control system described above is clearly very basic. In fact it is almost non-existant, simply consisting of a mechanism which follows the motion of the prime mover, or gives no motion at all. But what if each finger is required to close to a different final position? Two methods of achieving this aim have been explored.

8.6.1 Motion Control Effected by Varying the Point (time) of Stimulation

In the first of these methods the tendons which are not required to fully contract are completely saturated in water. The actuator now commences to close the gripper, as before. At a predetermined point or points (depending on the final position required) in this motion one or more tendons can be contracted, either by drying which is clearly going to make the process slow or by acetone stimulation.

Results for this type of test using three joints stimulated at different instances are shown for both the thermal and the chemical cases, figures 8.5a and b.

The distal tendon which was initially the only non-swollen connecting fibre responds immediately to the motion of the stepper. Fifty steps later the proximal tendon is dried (rapidly), and this joint starts to rotate as power is transmitted from the motor. Finally after 300 steps the middle tendon is stiffened and energy is distributed to this joint. Clearly although this technique is slow (requiring stops at each change point to allow the fibres to contract), it does permit control over the motions of the joints through regulation of the variable tendon compliances.

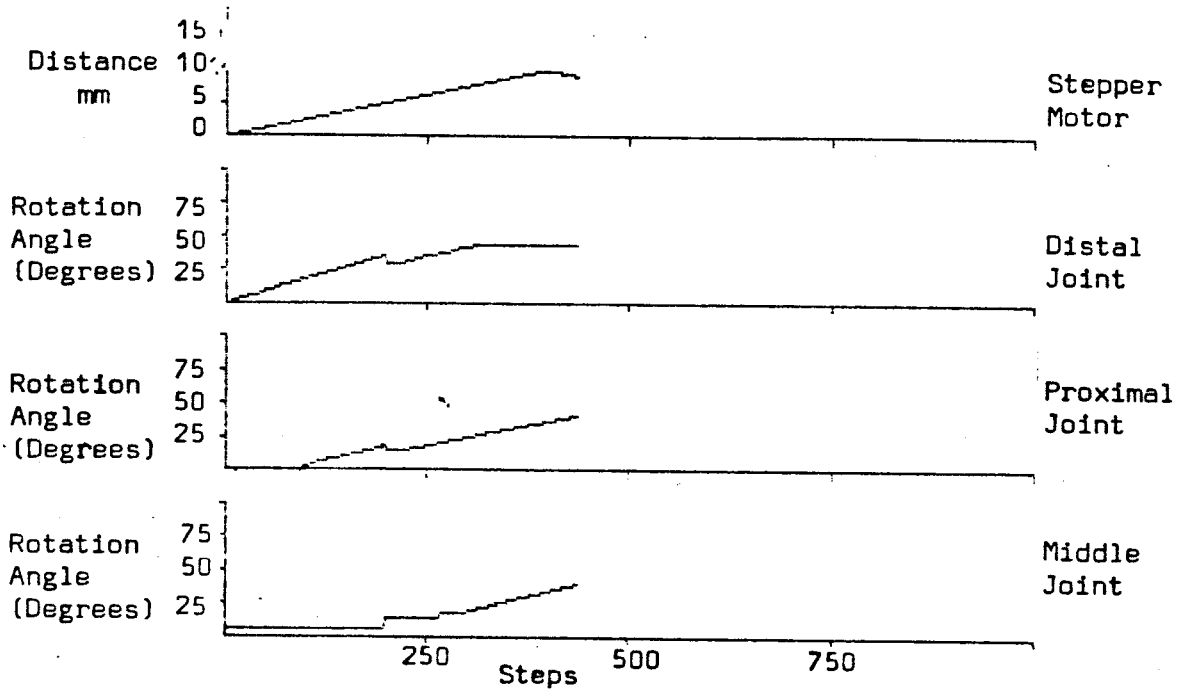

Figure 8.5a. Thermal Control of the Polymer Tendon.

The results also show some of the drawbacks associated with this technique. During the drying of the middle joint it will be noted that the position of the other joints changed. This was due to the disturbance caused by the rapid drying. By having some form of shielding this effect could be prevented but this will clearly add to the complexity of the design.

It is also possible that during the contraction the polymer tendon is acting as an actuator, and this could be contributing to the jump recorded in the middle joint position. This effect can probably only be corrected by reducing the tendon size or the contractile response, or by increasing the bearing friction. None of these solutions are ideal.

With the acetone stimulation tests the distal and proximal joints were in their unswollen state at the start of the test, the middle joint having been swollen to equilibrium in water. After 150 steps the middle joint was saturated in acetone which caused rapid contraction within the subsequent 10 sec.. At the end of this period the stepper motion was restarted and the plot continued, figure 8.5b.

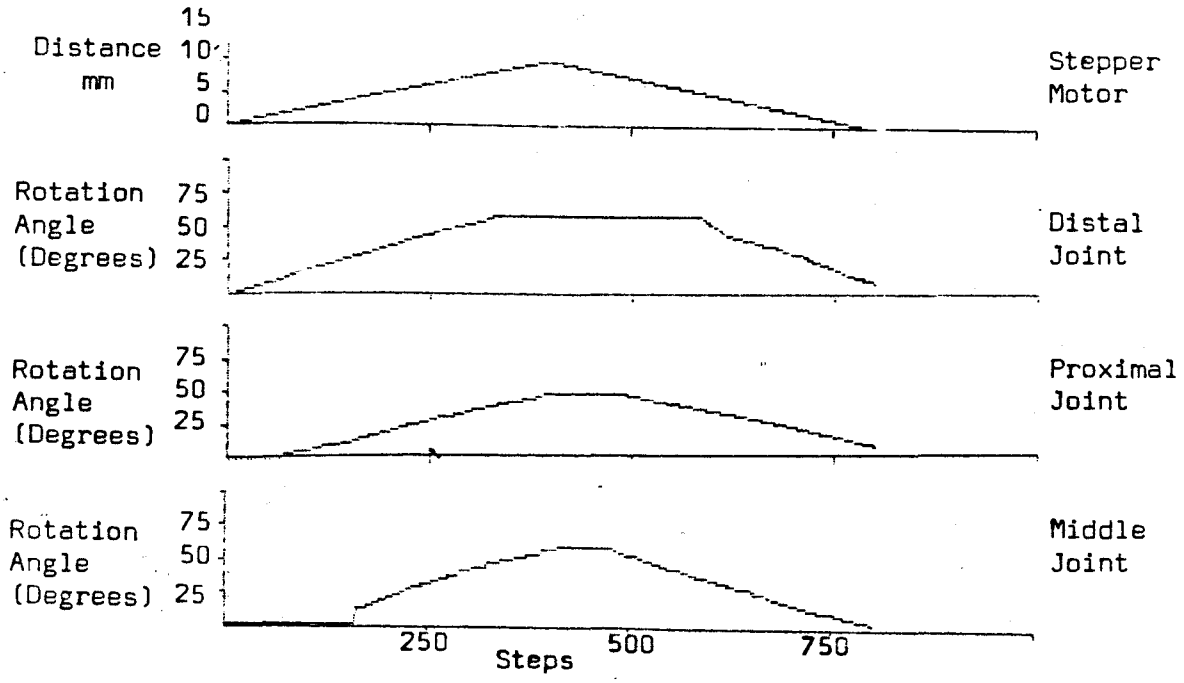

Figure 8.5b. Acetone Control of Joint Motion.

Using this chemical technique there is no motion in the middle joint prior to stimulation, but after stimulation motion is smooth and regular. Advantages with this system also include no disturbance of the other tendons and the reduced contractile motion which does not appear to cause any rotation of the joint.

8.6.2 Control by varying the Water Content of the Polymer

In the final mechanism for controlling the motion of the joints the tendons are each prestimulated to give a device with a preset modulus value and swelling fraction. These effects can be achieved using knowledge, obtained in previous chapters, of the modulus variation with swelling and the relationship between water/acetone concentration and swelling, chapter 4.8. Again either thermal or chemical stimulation can be used to set the swelling value. At this stage no attempt has been made to determine exactly how the swelling and modulus changes will effect the motion, since the primary object is to demonstrate that the swelling effect can be used to adjust the compliance and the final position of the joints. The results for the three joints with swelling fractions (set either themally or chemically) of 1.0, 1.15, and 1.3 are shown in figure 8.6a and b.

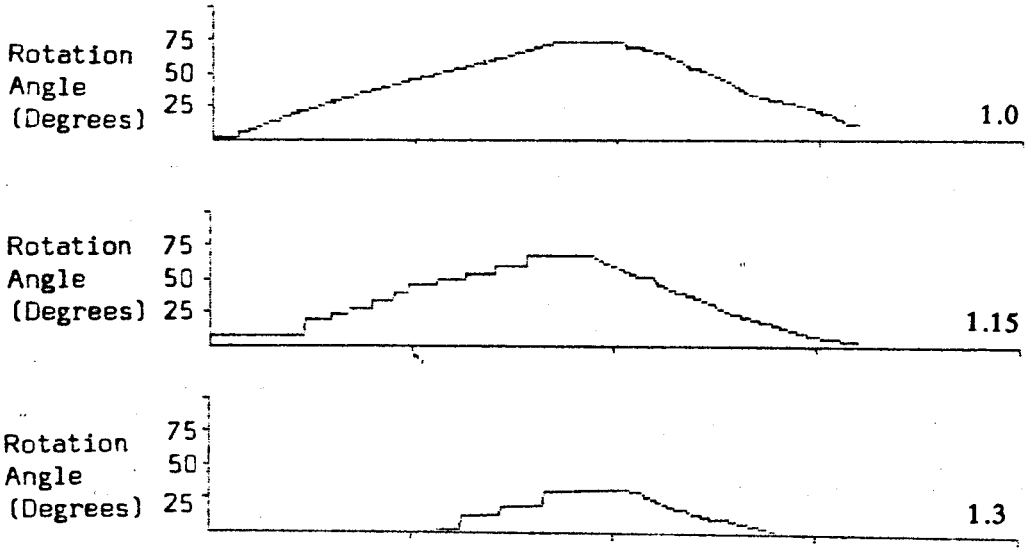

Figure 8.6a. Thermal Compliance Control of Power Transmission.

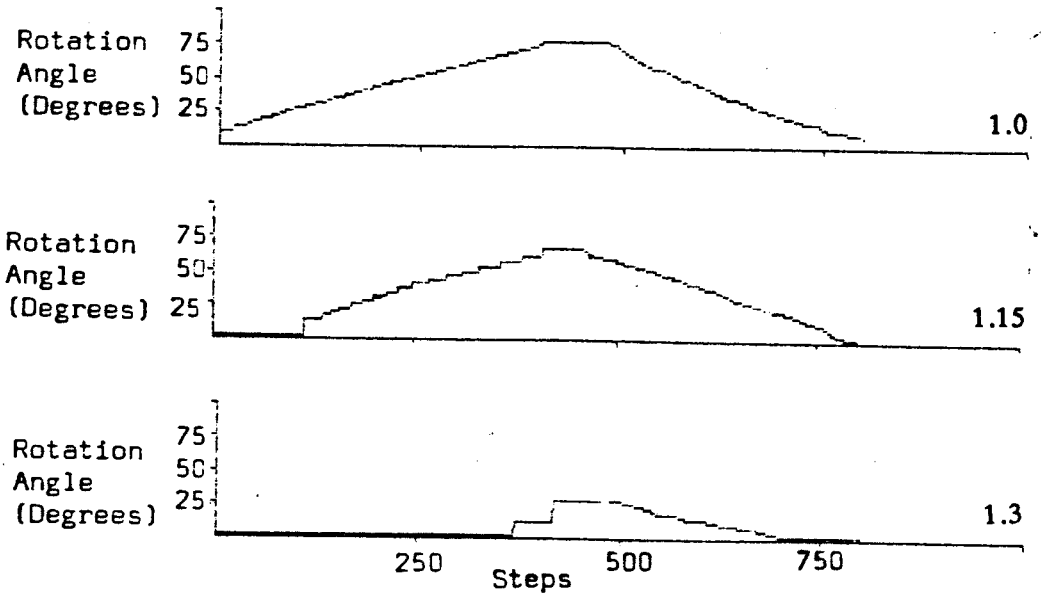

Figure 8.6b. Chemical Compliance Control of Power Transmission.

In these tests only the middle tendon response at the three set swelling fractions is recorded. At swelling fraction 1.0 the polymer is totally dry. Swelling fractions 1.15 and 1.3 in the thermal instance are set by expansion and subsequent evaporative contraction, while in the chemical tests these fractions are obtained by varying the acetone/water concentration of the stimulating fluid.

The results for both stimulation tests are in very good agreement as would be expected since the modulus condition of the tendon is the same in both experiments. The only observable difference is in fact in the period required to reach the set conditions. For the thermal samples this may require up to 45 mins. while with the chemical stimulation similar changes occur in under 20 sec..

There is also as expected a wide variation in the results across the swelling range. At zero swelling all the power is transmitted giving a smooth, linear joint rotation. At the intermediate swelling fraction (1.15), there is a slight initial delay until the swelling slack is taken up. As the stepper motor motion continues the gradient of the profile is not quite so steep nor totally linear, indicating stretching of the tendon.

With the most swollen samples, there is a further reduction in the gradient and an increase in the delay until slack is taken up. The most obvious effects of the reduced stiffness are, however, the jumps which occur. These are caused by stiction in the joints, which requires the development of an elastic tension before motion begins.

8.7 Conclusions

Experiments conducted in this chapter have shown that a second property of polyelectric gels, namely its variable compliance can be used to very good effect in controlling the motions of a dextrous hand.

Since each of the joints can be regulated independently using either thermal or chemical stimulation, power can be transmitted selectively to all or some of the joints. This ability means that any of the common grip and hand positions can be achieved using a single actuator power source. Using a semi-passive return mechanism; a spring, joint motions are possible in opposite directions at the same time, a manoevre which even humans can find difficult.

Two methods of inducing compliance control were tested, thermal and chemical. Both of these techniques succeeded in regulating the energy distribution, but the chemical method seems more suited to future exploitation as it gives the more rapid response, combined with a linear profile. Further the chemical system can achieve all this without disturbance to any other tendon.

Three control strategies have been tested, although in no instances were they meant to demonstrate more than the ability to obtain a rudimentary regulation of the motions of the joints. In all these controllers, regulation of the chemical stimulation seems to be the simplest and most promising method.

This technique although only having reached a very primitive stage appears to hold a considerable amount of promise for the future exploitation of actuation power in dextrous manipulators.

Chapter 9
Applications, Conclusions and Future Work

9.1 Introduction

With this final chapter the work in this thesis will be concluded, but this is by no means the end of the research which could be done to improve the potential of these pseudo-muscular systems. A variety of applications of this research are proposed in 9.2. Section 9.3 summmarises the conclusions which can be drawn from the work in the preceeding chapters, while in section 9.4 some ideas are suggested for future work detailing how these systems might actually be made viable, not only in the field of robotics but in the wider spectrum of general science.

9.2 Applications

This research with its aim of producing a new actuation system for use in a multi degree-of-freedom gripper has focused on two aspects of polymeric gel technology. There are, however, a great variety of other applications to which this materials could be applied, and these will now be considered.

Still operating as an actuator but using the thermal (drying) technique, the materials could be used to produce an turbine which is pollution-free and uses a reuseable fuel source, solar power. The gel could be expanded by sea water and then dried in the sun. Alternating the expansions and contractions would drive the turbine. Such a system would work best in a hot, dry region with easy access to water; the oceans. This is a particular set of conditions very

typically found in developing countries.

A second area where this technique might be used is in space. On space craft there is a very large difference in solar heating on the panels of the craft, with some areas at temperatures of 200°C or more, while an almost adjacent panel may be close to absolute zero. Using these temperature differences it may be possible to produce an alternative to solar cells as an energy generating source.

All the previous suggestions have dealt with the material when contracting, but it is also possible to produce useful effects using the swelling cycle. This is achieved by constraining the motions of the polymer while dilating. If this constraining mechanism has a mobile connection, the polymer can be used as a braking or jacking type device. The list of areas in which this could be applied is only limited by imagination.

There are also a number of ways in which the polymer could be used as a sensor. There are two aspects to this application;

1). Under compression and/or tension the material gives an electrical output. This could be used as a form of sensorized skin, with the added advantage that hysteris effects could be reduced by the active re-absordance of moisture by the sensing material. A self-balancing tactile sensor.

2). The material being very low cost, could also form a basis for a cheap throw away chemical sensor. In its present form the most obvious chemical to detect would be water, and it may be possible to combine humidity sensing with the actuation abilities, e.g. in a greenhouse, where automatic monitoring and adjustment of the shutters could be achieved. It may even be possible to use the equilibrium swelling extent to predict which chemical is present, while the use of materials other than PVA and PAA should make the detection of different components feasible. In fact using the solubilty parameters it should be possible to detect specific components since each solution will give a different specific swelling fraction.

Clearly these polymers have a wide range of applications both in robotics,

were this work has shown their potential as actuators and variable compliance devices, and in the more general areas of science.

9.3 Conclusions

The first conclusion which must be drawn when considering the development of a dextrous manipulator is, that there was and still is a considerable need for the development of superior actuation systems and power distribution technique.

While there are a number of ways of generating power only three are greatly used in presently available robots. These are hydraulic, pneumatic, and electrical systems, but each of these has its own particular problems. Concentrating on the method of power generation used by animals and plants this thesis has demonstrated the feasibility of using mechano-chemical energy cycles.

These mechano-chemical cycles can be produced in a number of gels (polyelectrolytes) but a PVA-PAA coploymer with a ratio (by weight) of 3:1 and crosslinked at 150°C for 60 mins appears to be the best material as yet available.

Although in this instance swelling/deswelling is equal in all direction the material can be made to produce one dimensional changes (which are more suitable for a muscle emmulator) by crosslinking under stress.

The response, when tested using a number of activation techniques, (pH, re-dox, ion exchange and drying) showed that the optimum results (most rapid, strong contractions) were produced when the fibres were stimulated by acetone (inducing contraction) and water (inducing dilation). Improvements to this fundamental response can be produced by raising the temperature, increasing the ionic content of the solvents and finally and most importantly by reducing the thickness, with an inverse square relationship being observed between the film thickness and the response rates.

Using theoretical analyses of the polymer and experimental results, mathematical models of the polymer response to chemical stimulation were developed. These models of the single fibres were used to explore the

performance of a number of control systems and there was found to be a good correlation between the model and the final full experimental muscle actuator system. This suggests that the model was a good representation.

A pseudo-muscular pair consisting of a flexor (to close the joint) and an extensor (to open the joint) was constructed using the PVA–PAA material described above. In this arrangement a new actuator design was demonstrated using chemical stimulation to power a robot joint.

The fibres (strips 0.1mm thick) contained within the muscle cells form bundles, which when stimulated contract and expand at rates of up to 11%/sec., simulating the macroscopic motion of natural muscle. These experimental muscle bundles produced contractile forces of up to .61N (30N/cm^2), a value comparable with the performance of natural muscle (20N/cm^2 – 40N/cm^2). Using these rate and force measurements, power/force and velocity/force profiles were obtained which are very similar to those of natural muscle. From these plots the maximum power weight output can subsequently be calculated. For these primitive systems a power output of up to 5.6mW/g was achieved, with an overall work potential of 0.4J/g (natural fibres have potential of 0.6J/g – 0.8/g). This is in good agreement with the simulation predictions.

Clearly the rate of contraction and the power/weight performance are presently much below the values of animal muscle (25%/sec – 2000%/sec and 40W–250W/Kg respectively). There is, however, no reason for dispondancy since both these values in the synthetic muscle can be increased very substantially by using thinner fibres (remember the inverse square relationship), and this will help to make the artificial muscle truely competitive.

Performance tests on the flexor/extensor actuator pair were then conducted using the force/position control algorithm developed using the system simulator. These experiments showed the actuator/gripper system to have an open/close cycle period of under 15. Additionally there is good repeatability and positional accuracy of better than 2°.

Using this mechanism a new linear direct drive actuator with excellent

power/weight ratios is a realistic long term possibility.

There are a number of other features which have as yet not been considered, and these will further help to enhance the abilities of the polymer actuator.

1). The muscle motion is linear. This is a very simple point but it also happens to be very useful and should not be overlooked.

2). The compliance of the actuator can be directly controlled, while the flexor/extensor arrangement gives a design were the joint flexibility can be modified by varying the inter-muscular opposition. This mimics animal muscle, but the direct chemical control is an advantage which even animal muscle doesn't possess in the compliance control struggle.

This variable complaince has been taken to a conclusion in chapter 8 where a series of variable compliance tendons are used to control the distribution of power to the joints in a dextrous gripper. Using this mechanism it is possible to have a multi degree-of-freedom device with independent control of each joint, which requires only a single conventional (or other) actuator. This provides a much more compact system because larger actuators can be used and they are generally more efficient. This will give a mechanism which has less joint loading than is presently encountered, but there is still the need for a much more powerful prime mover. This device will obviously also have the advantage of compliance control making in ideal for pick, place and insertion tasks as is true for the polymer actuator.

9.4 Future Work

While the conclusions drawn above show that new power distribution (variable compliance devices) and generating (pseudo-muscular actuators) systems are possible, the tests also reveal that a considerable amount of work would have to be done before this is possible. Areas most in need of development are;

i). Improvements in the construction of the materials, to improve the consistency, and reduce the film thickness. This would logically lead to the use of fibres in the form of long strands similar to natural muscle. 2D diffusion

would then be possible and this would further increase the response rate.

ii). Development of new mechano-chemical materials. It seems very unlikely that this PVA/PAA copolymer is the optimum design, and hence further chemical work will be required to produce new fibres with enhanced contractile response and force properties.

iii). New stimulation techniques. The present design is constrained not only by the thickness of films available, but also by the time required to deliver the chemicals. It is suggested that future work should be directed towards the discovery of new methods of stimulation. Electrical techniques would obviously be ideal, but this would require much more rapid changes in the response than are presently possible.

iv). New and improved control and monitoring techniques. This work could be done on the present system but would be of most use if directed towards the control of the new/improved stimulation techniques being sought.

With the potential for development outlined above, polymeric devices can clearly make a significantly contribution to future advances in robotic actuation techniques.

References

Alexander R.M., "Biomechanics",Chapman and Hall, London, (1975).

Automation, "Robot Survey", Automation, p.27-37, Vol.23 no.8, London, 1987.

Aviram A., "Mechanophotochemistry", Macromolecules, Vol.11, p.1275-80, 1978.

Bae Y.H., Okano T., Hsu R., and Kim S.W., "Thermo-sensitive Polymers as on- off Switches for Drug Release", Makromolecular Chemistry Rapid Commun., Vol.8, pp.481-85, 1987.

Banks D.D. and Banks D.S., "Industrial Hydraulic Systems, an Introduction", Prentice-Hall (UK), London, 1988.

Bannister B.R. and D.G.Whitehead D.G., "Transducers and Interfacing", Van Nostrand Reinhold Ltd., Wokingham, England, 1986.

Bawn C.E.H., "The Chemistry of High Polymers", Butterworths Ltd., London, 1948.

Belyakov R.V., "Artificial Muscles as Sensors for Automatic Control of Liquid Medium", Soviet Automatic Control, Vol.17., no.6. , pp34-40, 1985.

Brugel W, "An Introduction to Infra-red Spectroscopy", Metheun, New York, 1962.

Buckley D.J. and Berger M., "The Swelling of Polymer Systems in Solvents II Mathematics of Diffusion", J. Poly. Sci. Vol.56, p.175-188, 1962.

Caldwell D.G., "Novel Sensor and Gripper Design", Dept. Elec. Eng. Report No. 1611, 1986.

Caldwell D.G., "Polymer Gels as Robotic Actuators", Dept Elec.

Eng. Report No.45/88, Hull University, 1987.

Casey E.J., "Biophysics; Concepts and Mechanisms", Reinhold Corp, New York, 1962.

Crank J., "The Mathematics of Diffusion", Clarendon Press, Oxford, 1956.

Crossley F. and Umholtz F., "Design for a Three Fingered Hand", Mechanism and Machine Theory, Vol.12 p.85-93, 1977.

Cutkosky M.R. and Wright P.K., "Modeling Manufacturing Grips and Correlations with the Design of Robotic Hands", IEEE International Conf. on Robotics and Automation, p. 1533-39, San Francisco, USA, A pril, 1986.

Dario P., Beramasco M., Bernardi L., and Bicchi A., "A Shape Memory Alloy Actuating Module for Fine Manipulation", IEEE Micro-ro bots and Teleoperators Workshop, Hyannis, Mass. Nov.9-11, 1987.

De Rossi D.E., Parrini P., Chiarelli P., and Buzzigoli G., "Electrically Induced Contractile Phenomena in Charged Polymer Networks; Preliminary Study on the Feasibility of Muscle-like Structures", Trans. AM. Soc. Artif. Intern. Organs, Vol.31, pp.60-65, 1985.

De Rossi D.E., Chiarelli P., Buzzigoli G., Domenici C., Lazzeri L., "Contractile Behaviour Of Electrically Activated Mechanochemicl Polymer Actuators", Trans. Am. Soc. Artif. Organs, Vol.XXXII, 157, 1986.

De Rossi D.E., C.Domenici C. and P.Chiarelli P., "Analogs of Biological Tissues for Mechanoelectrical Transduction; Tactile Sensors and Muscle-like Actuators", in "Sensors and Sensory Systems for advanced robots", ed. P.Dario, Nato ASI series, Springer-Verlag , 1988.

De Rossi D.E., Private Communication, Oct. 1988.

Doll T.J. and Schneebeli H.J., "The Karlsruhe Hand", IFAC

Symposium on Robot Control, p.37.1, Karlsruhe, Oct.1988.

Drake S., "Using Compliance in Lieu of Sensory feedback for Automatic Assembly", Proc. 9th ISIR, 1979.

Electro-craft, "DC Motors, Speed Controls, Servo Systems", Electro -craft Corp.,Hopkins, Minnesota, 1980.

Elonka S.M. and Johnson O.H., "Standard Industrial Hydraulics Questions and Answers", McGraw-Hill, New York, 1967.

Esposito A., "Fluid Power with Application", Prentice-Hall, New Jersey, 1980.

Findaly Pub. Ltd. "Tiny Hydraulic Motors now challenge small Electric Drives", Eureka on Campus, Findlay Pub. Ltd., Horton Kirby , Kent, Autumn 1988.

Fitzgerald A.E., "Basic Electrical Engineering", McGraw-Hill, New York, 1945.

Flory P.J. and Rehner J., "Statistical Dynamics of Cross-linked Polymer Networks", J. Chem. Phys. Vol.11, p.512, 1943.

Flory P.J., "The Role of Crystallization in Polymers and Proteins" , Science, Vol.124, pp.153-60, 1956.

Flory P.J., "Principles of Polymer Chemistry", Cornell University Press, New York, 1957.

Fragala A., Enos J., LaConti A. and Boyack J., "Electrochemical Activation of a Synthetic Artificial Muscle Membrane", Electrochima Acta, Vol.17, pp.1507-22, 1972.

Freundlich H., "Colloid and Capillary Chemistry", Methuen & Co., London, 1926.

Gee G., "The Interaction between Rubber and Liquids III The Swelling of Vulcanized Rubber in Various Liquids", Trans. Faraday Soc., Vol.38, p.418-22, 1942.

Gerelle E.G.R., "Force Feedback Control", Proc. 8th ISIR, Stuttgart, June 1978.

Greenwood D.C., "Manual of Electromechanical Devices", McGraw-Hill Inc., New York, 1965.

Hamlen R.P., Kent C.E., and Shafer S.N., "Electrically Activated Contractile Polymer", Nature, Vol. 206, pp.1149-50, 1965.

Hanafusa H. and Osada H., "Stable Prehension by a Robot Hand with Elastic Fingers", 7th ISIR, p.361, Tokyo, Oct.1977.

Hill A.V., "The Heat of Shortening and the Dynamic Constants of Muscle", Proc. Roy. Soc. London. Ser., Vol. B.126, pp.136-195, 1938.

Hill A.V.,"First and Last Experiments in Muscle Mechanics", Cambridge University Press, Cambridge, U.K., 1970.

Hojo N., Shirai H. and Mori T., "Contractile Systems of Phosphorylated Polyvinyl Alcohol Films in Metal-Ion Aqueous-solution", Kogyo Kagaku Kaishi, Vol.74, p.269, 1971.

Huggins A.L., Ann. N.Y. Acad. Sci., Vol.44, p.431, 1943.

Ishihara K. and Shinohara I, "Photoinduced Permeation Control of Proteins Using Amphiphilic Azoaromatic Polymer Membrane", J. Polym. Sci., Polym. Lett. Ed. Vol.22, p.515-19, 1984.

Jacobsen S.C., Iversen E.K., Knutti D.F., Johnson R.T. and Biggers K.B., "Design of the Utah/MIT Dextrous Hand", Proc. IEEE Int. Conf. on Robotics and Automation, San Francisco, p.1520-32, April 1986.

Kaneko M., Imamura N., Yokoi K., and Tanie K., "Direct Compliance Control of Manipulator Arms", Sym. on Robot Control, Karlsruhe, W. Germany, Oct.1988.

Katchalsky A., "Rapid swelling and Deswelling of Reversible Gels of Polymeric Acids by Ionization", Experimentia, Vol.5, pp.319-320, 1949.

Katchalsky A. and Eisenberg H., "Polyvinylphosphate Contractile Systems", Nature, Vol.166, p.267., 1950.

Katchalsky A. and Zwick M., "Mechanochemistry and Ion Exchange", J . Polym. Sci., Vol.16, p.221-34, 1955.

Katchalsky A., Lifson S., Michaeli I., and Zwick M., "Elementary Mechano-Chemical Processes" In "Size and Shape Changes in Contractile Polymers", Ed. Wassermann A., Pergammon Press, London, 1960.

Katchalsky A. and Oplatka A., "Mechano-Chemical Conversion", Handbook of Sensory Physiology, Vol.1., Principles of Receptor Phys iology, pp.1-17, Springer-Verlag, Berlin, 1971.

Kruyt H.R., "Colloid Chemistry", Vol II, Elsevier Pub. Co. Inc., Amsterdam, 1949.

Kuhn W., "Reversible Dehnung und Kontraktion bei Anderung der Ionisation eines Netwerks polyvalenter Fadenmolekulionen", Experimentia, Vol.5, pp.318-319, 1949.

Kuhn W., Hargitay B., Katchalsky A. and Eisenberg H., "Reversible Dilation and Contraction by changing the state of ionization of High-polymer Acid Networks" Nature Vol.165, pp.515-517, 1950.

Kuhn W and Hargitay B., "Muskelahnliche Kontraktion und Dehung von Netzwerken Polyvalenter Fadenmolekulionen", Experimentia, Vol. 7., p.1-11, 1951.

Kuhn W., Ramel A. and Walters D.H., "Conversion of Chemical into Mechanical Energy by Homogeneous and Cross-straited Polymer Systems ", In "Size and Shape Changes of Contractile Polymers" ed. A. Wassermann), Pergamon Press, London, 1960.

LLyod W.G. and Alfrey T., "Network Polymers. II. Experimental Study of Swelling", J. Polymer Sci. Vol.62, p.301-16, 1962.

Mason M.T. and Salisbury J.K., "Robot Hands and the Mechanics of Manipulation", MIT Press, Mass., 1985.

Mason M.T. and Salisbury J.K., "Robot Hands and the Mechanics of Manipulation", MIT Press, 1986.

Maus R. and Allsup R., "Robotics: A manager's Guide", John Wiley & Sons Inc., New York, 1986.

Muller F., "Piezo-electric Positioners for Linear Motion", Feingeraetetechnik, Vol.35, no.11, p.487-90, 1986.

Okada T. and Tsuchiya S., "On a Versatile Finger System", 7th ISIR, p.345, Tokyo, Oct. 1977.

Okada T., "Computer Control of Multijointed Finger Systems", 6th Int. Conf. on AI, Tokyo, 1979.

Osada Y. and Hasebe M., "Electrically Activated Mechanochemical Devices using Polyelectrolyte Gels", Chemistry Letters, pp.1285-88, 1985.

Osada Y., Private Communication, Oct. 1988.

Palin G.R., "Electrochemistry for Technologists", Pergammon Press, Oxford, 1969.

Patrick D.R. and Fardo S.W., "Electricity and Electronics", Prentice-Hall, New Jersey, 1984.

Patton W.J., "Mechanical Power Transmission", Prentice-Hall Inc., New Jersey, 1980.

Paul R. and Shimano B., "Compliance and Control", Proc. Joint Automatic Control Conf., pp.262-67, Perdue University, July 1976.

Pedley T.J., "Scale Effects in Animal Locomotion", Academic Press, London, 1985.

Peppas N.A. and Korsmeyer R.W., "Transport Phenomena in Polymers; Diffusion and Anomalous Transport in Glassy Polymers", Polymer News, Vol. 9, pp.359-, 1984.

Radio-spares catalogue, Corby, U.K., Feb. 1989.

Raibert M.H. and Craig J.J., "Hybrid Position/Force Control of Manipulators", ASME J. of Dynamic Systems, Measurement and Control, Vol.103, pp.126-33, 1981.

Reynolds W.C. and Perkins H.C., "Engineering Thermodynamics",

McGraw-Hill Inc., New York, 1977.

Scott D., "Electro-Rheological (ER) Fluid near Commercial Stage", Automotive Engineering, Vol 93, pp75-9, Nov. 1985.

Simons G.L. "Is Man a Robot", John Wiley & Sons, Chichester, 1986.

Skinner F., "Designing a Multiple Prehension Manipulator", Mechanical Engineering, Sept. 1975.

Smets G., "New Develòpments in Photochromic Polymers", J. Polymer Sci., Polym. Chem. Ed., Vol.13, p.2223-31, 1975.

Steinberg I., Oplatka A., and Katchalsky A., "Mechanochemical Engines", Nature, Vol. 210, pp.568-71, 1966.

Sussman M.V. and Katchalsky A., "Mechanochemical Turbine: A New Power Cycle", Science, Vol.167., pp. 45-47, 1970.

Suzuki M., "Responsive Mechanochemical Actuator Materials by PVA Hydrogels", IUPAC CHEMRAWN VI, Tokyo Japan, 1987.

Takahashi S., "Piezo-electric Actuators and their Applications", J. Inst. Electron. Inf. Commun. Eng., Vol.70, no.3, p.295-7, 1987.

Tanaka T. and Fillmore D.J., "Kinetics of Swelling of Gels", J. Chem. Phys., Vol. 70, pp.1214-1218, 1979.

Tanaka T., Fillmore D., Sun S., Nishio I., Swislow G. and Shah A., "Phase Transition in Ionic Gels", Physical Review Letters, Vol.45, pp.1636 -39, 1980.

Tanaka T., Nishio I., Sun S., and Ueno-Nishio S., "Collapse of Gels in an Electric Field", Science, Vol.218, pp.467-69, 1982.

Tatara Y., "Mechanical Behaviour of Mechanochemical Materials: Part 1; Junction of Network and Equilibrium Swelling of a Mechanochemical Material",Bull. of J.S.M.E., Vol.15, pp.49-57, 1972a.

Tatara Y., "Mechanical Behaviour of Mechanochemical Materials: Part 2; Mechanical Outputs in an Equilibrium State", Bull. J.S.M.E., Vol.15, pp.58-72, 1972b.

Thomas N.L. and Windle A.H., "The Theory of Case-II Diffusion", Polymer, Vol. 23, p.529-42, 1982.

Tomovic R. and Boni G., "An Adaptive Artificial Hand", Trans. IRE, AC-7, p.3-10, 1962.

Treloar L.R.G., "The Physics of Rubber Elasticity", Clarendon Press, Oxford, 1975.

Whitney D.E., "Force Feedback Control of Manipulator Fine Motions", ASME J.of Dynamic Systems, Measurement and Control, June 1977.

Wilkie D.R., "Muscle", Edward Arnold, London, 1976.

Woledge R.C., Curtin N.A. and Homsher E., "Energetic Aspects of Muscle Contraction", Academic Press, London,1985.

Wolff H.S., "Biomedical Engineering", World University Library, London, 1970.

Appendix I

Infra-red Spectroscopy Test Results

The following plots were obtained from infra-red spectroscopy tests conducted to attempt to determine the chemical structure of the PVA-PAA copolymer under a variety of production conditions. The plots refer to the specifications shown in table 4.3.

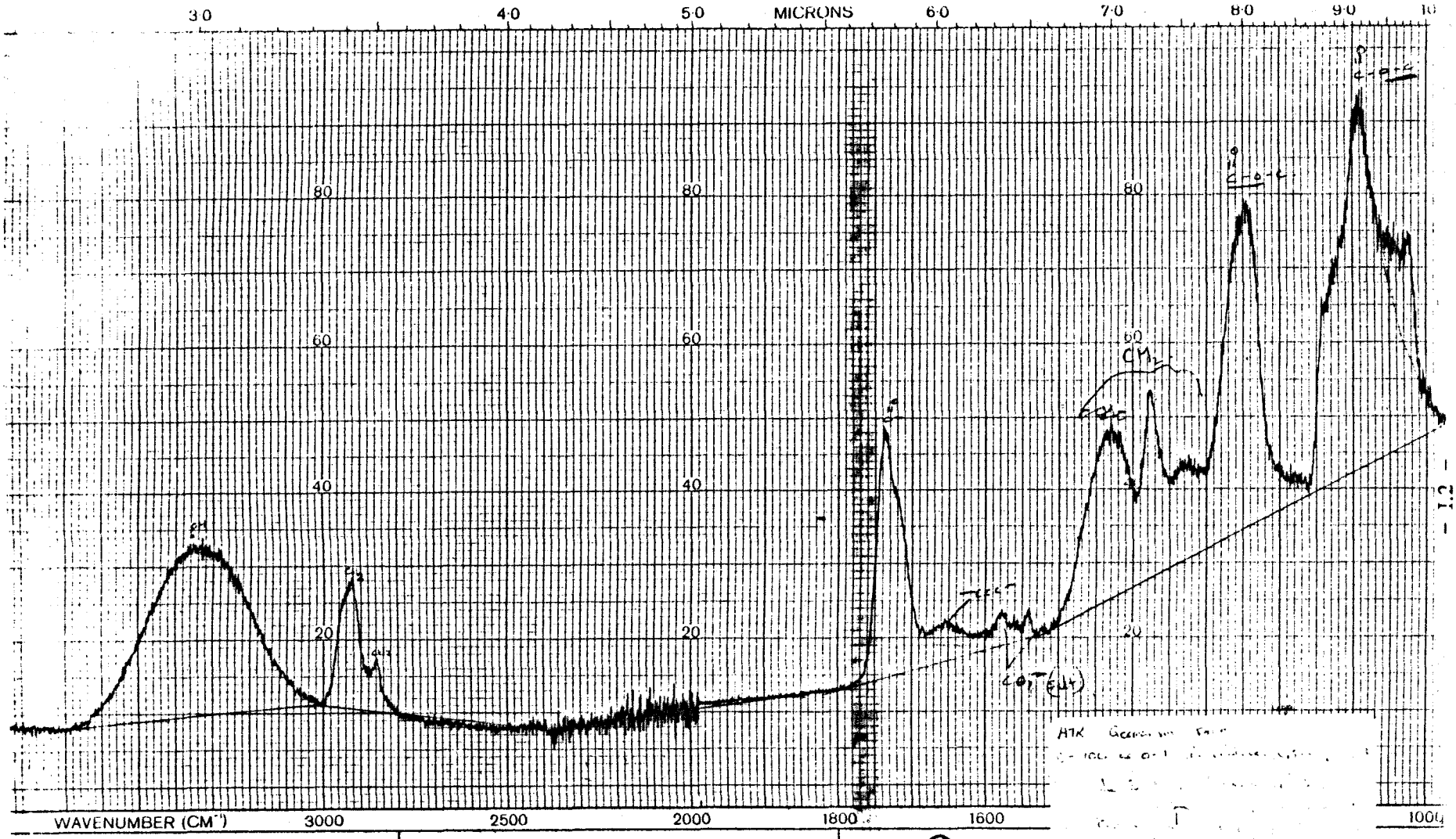
3·0
4·0
5·0
MICRONS
6·0
7·0
8·0
9·0
80
60
40
20
WAVENUMBER (CM⁻¹)
3000
2500
2000
1800
1600
1000
SOLVENT
CONCENTRATION
CELL PATH
REFERENCE
REMARKS

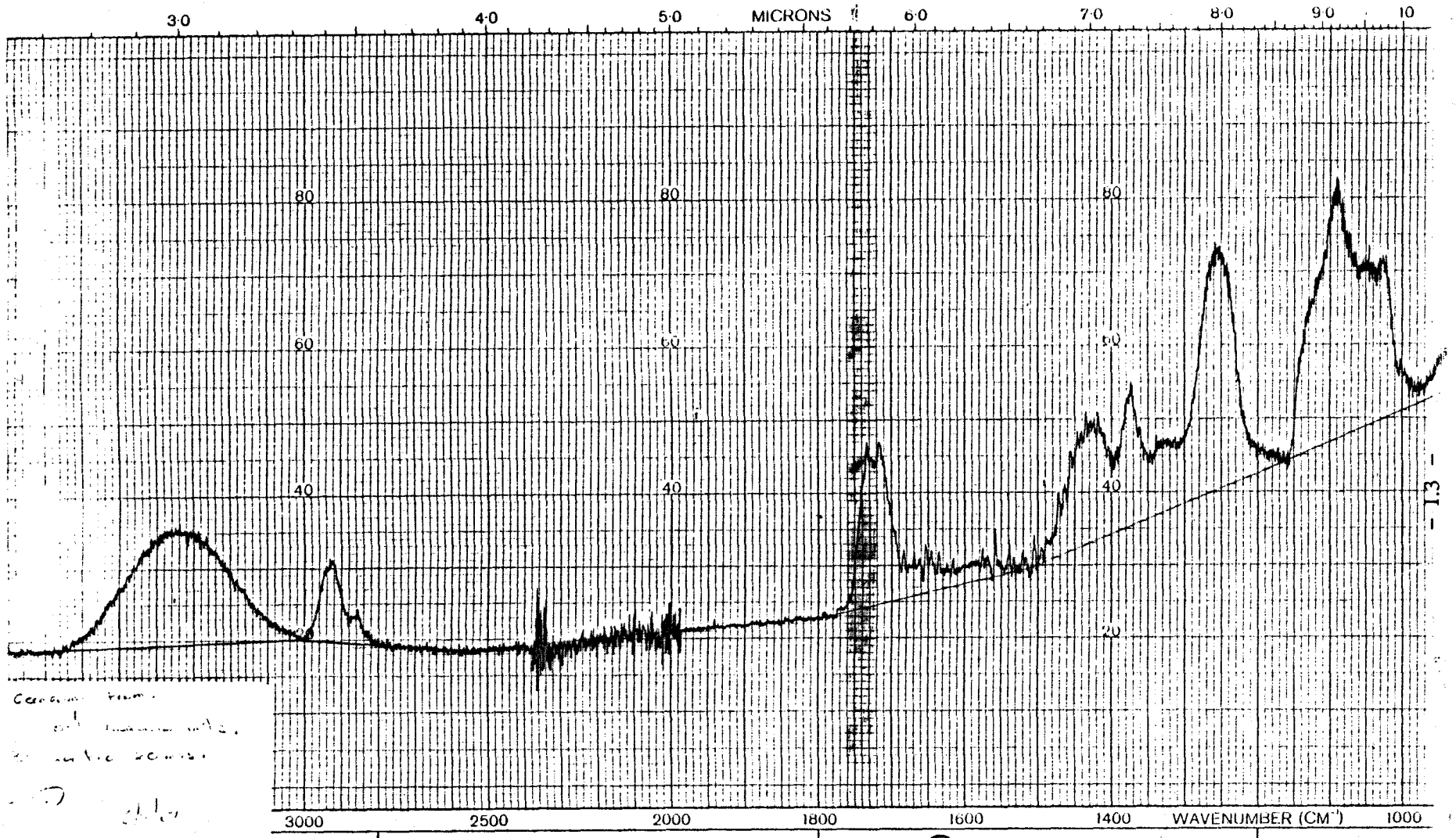

SOLVENT

CONCENTRATION

CELL PATH

REFERENCE

REMARKS (2)

INT. SCAN MODE

SCAN TIME

RESOLUTION

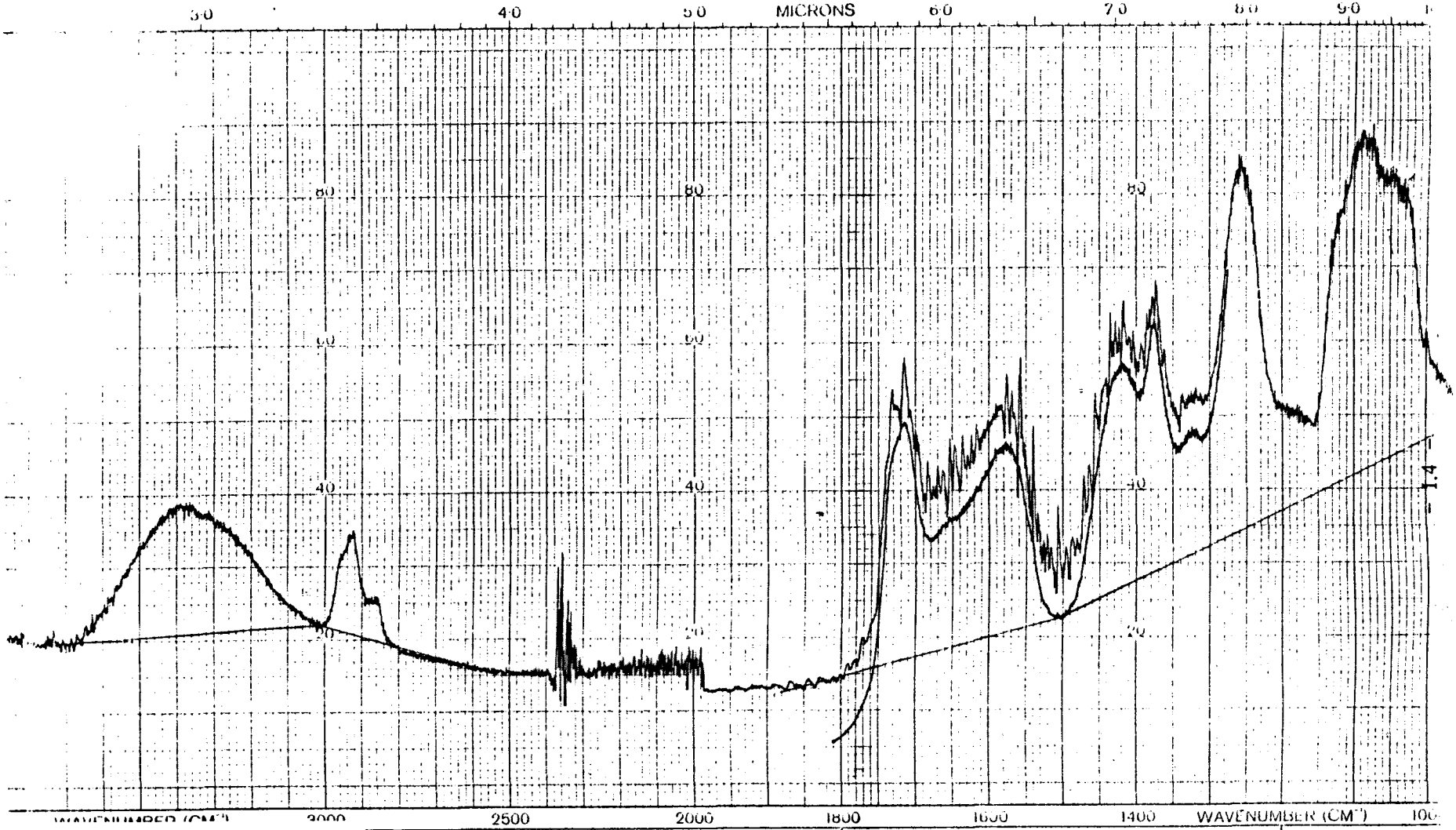
MICRONS
WAVENUMBER (CM⁻¹)
2500
2000
1800
1600
1400
WAVENUMBER (CM⁻¹)
SOLVENT
CONCENTRATION
CELL PATH
REFERENCE
REMARKS
3
INT. SCAN MODE
SCAN TIME
RESOLUTION

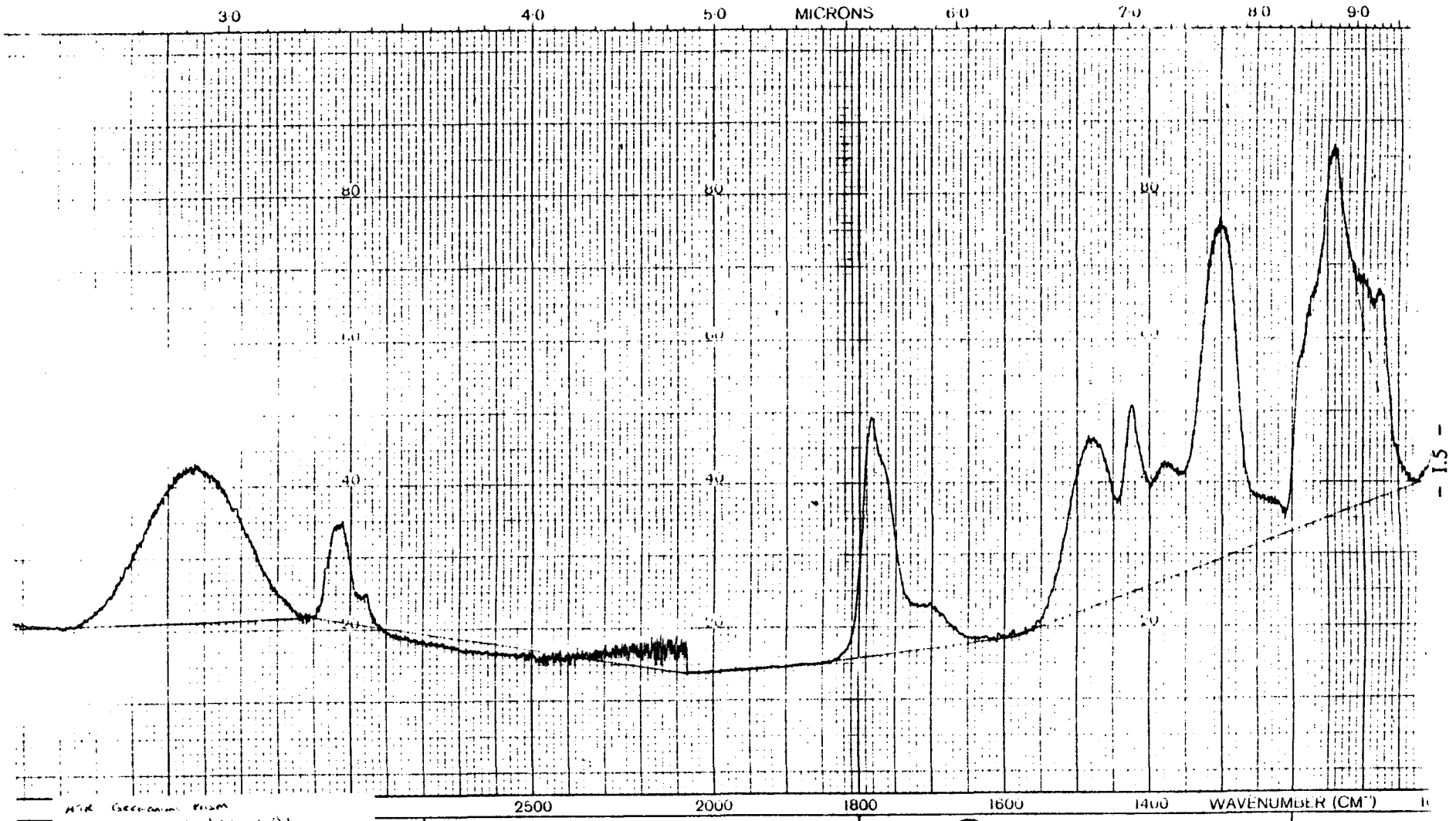

- 15 -

SOLVENT
CONCENTRATION
CELL PATH
REFERENCE

REMARKS (4)

INT. SCAN MODE
SCAN TIME
RESOLUTION

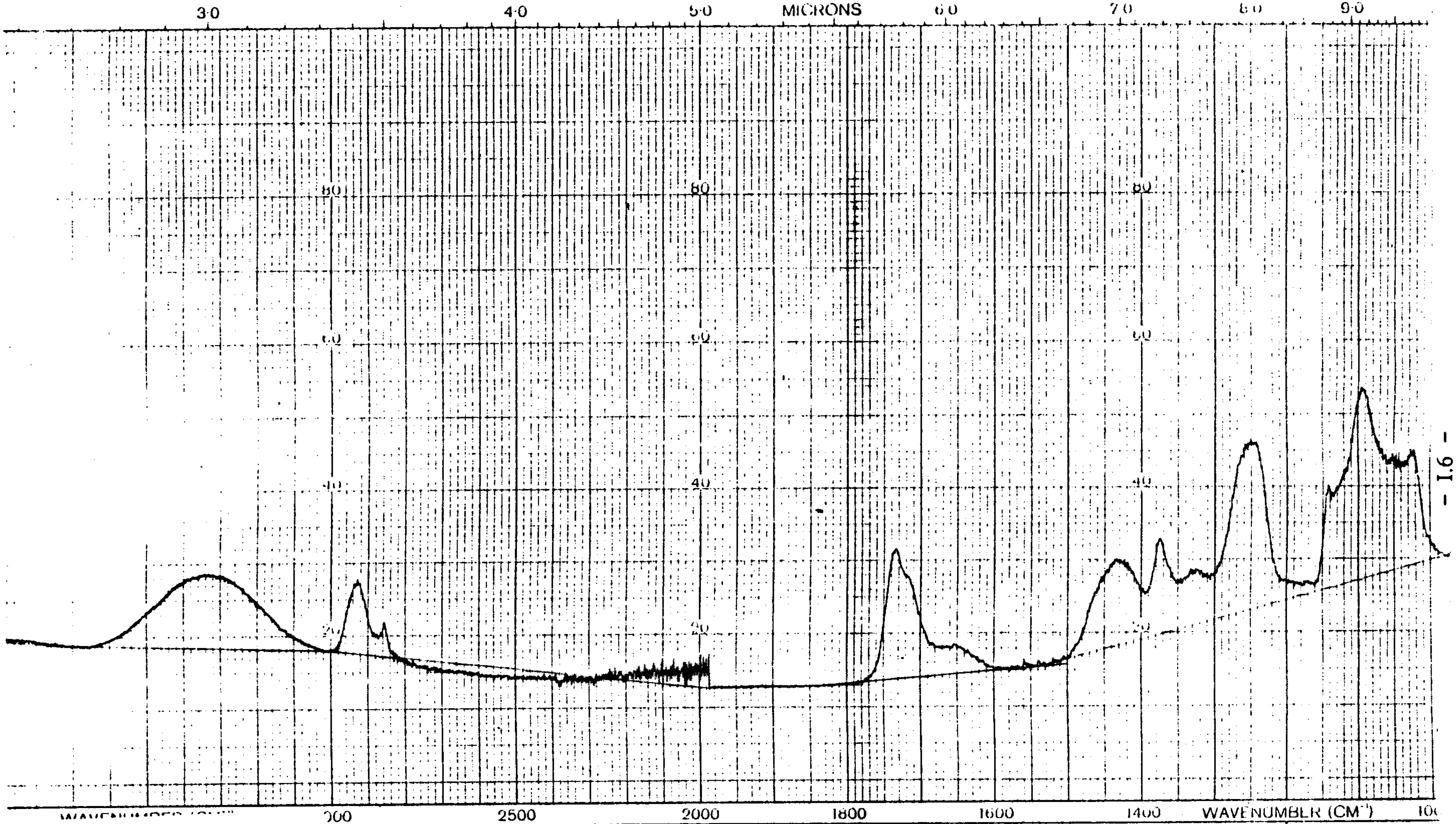

ATR - Germanium prism
... absorbance ...
... 20 min
(5) 8/7/67
AC

SOLVENT

CONCENTRATION

CELL PATH

REFERENCE

REMARKS (5)

INT. SCAN MODE

SCAN TIME

RESOLUTION

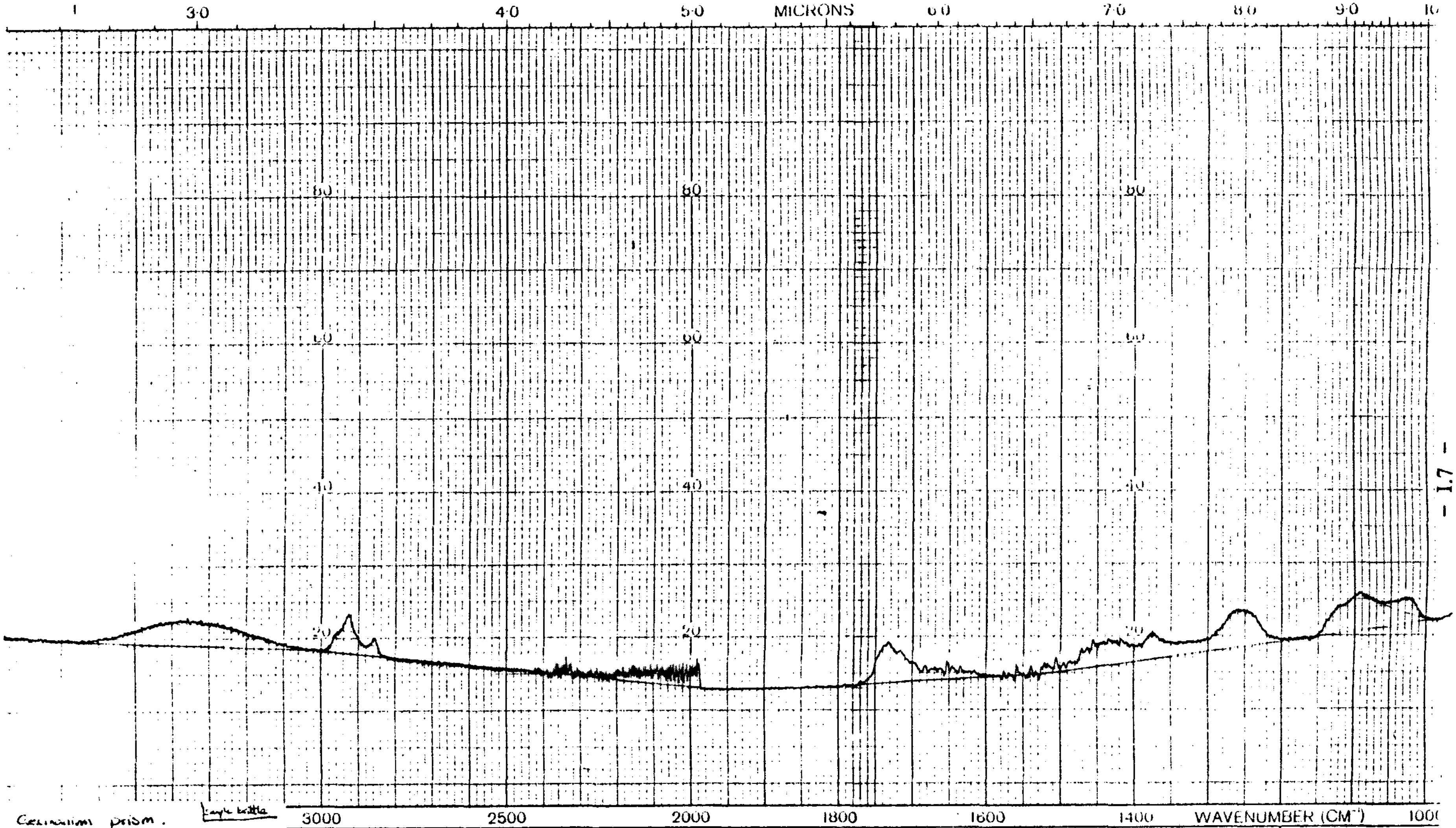

Germanium prism.

0 is 0-1 absorbance units

3 scans in 20mins

(1) 7/7/87

MC

SOLVENT

CONCENTRATION

CELL PATH

REFERENCE

REMARKS (6)

INT. SCAN MODE

SCAN TIME

RESOLUTION

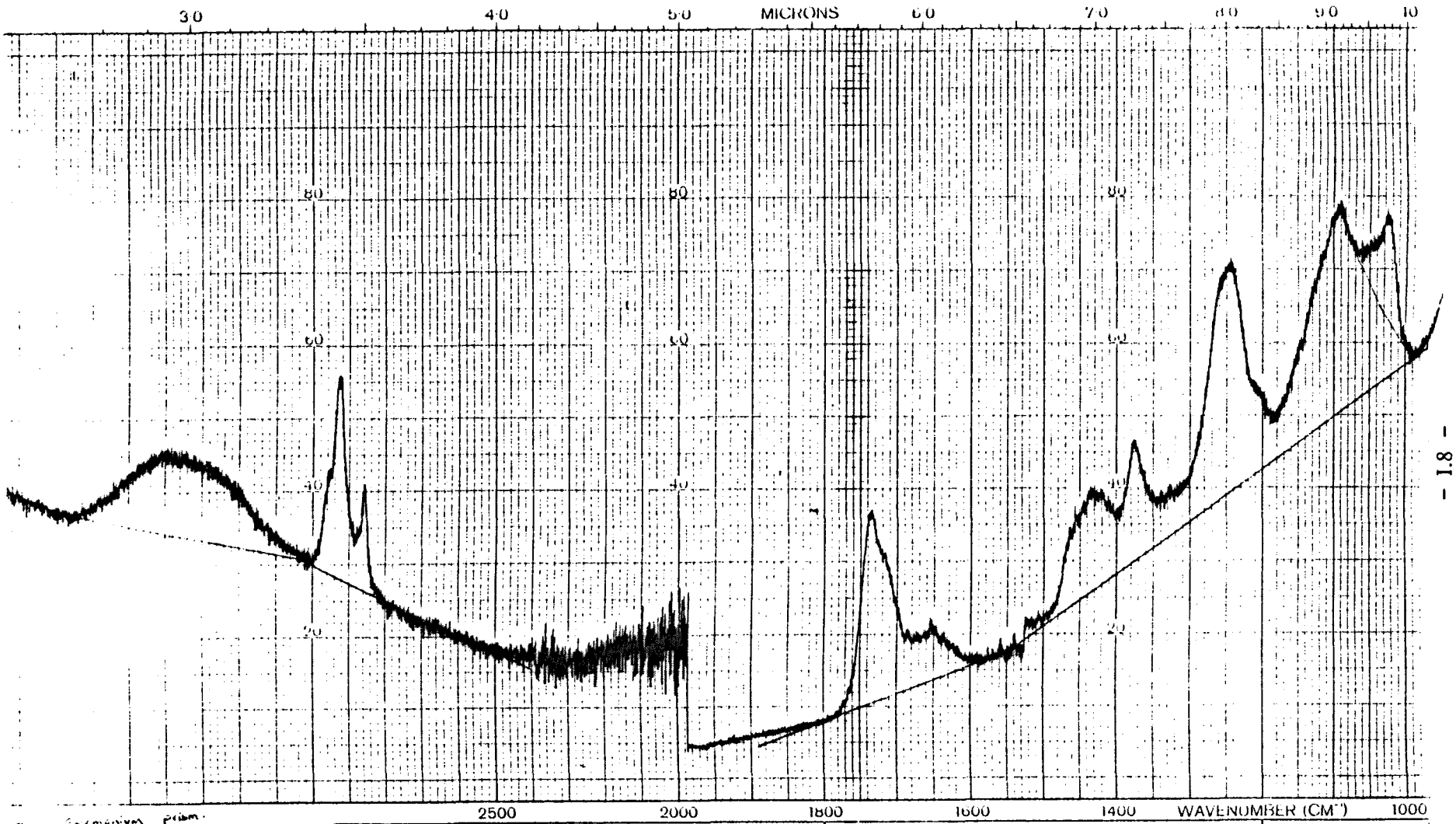

Germanium prism.

0 - 0·2 absorbance units

SOLVENT

CONCENTRATION

CELL PATH

REFERENCE

REMARKS (7)

INT. SCAN MODE

SCAN TIME

RESOLUTION

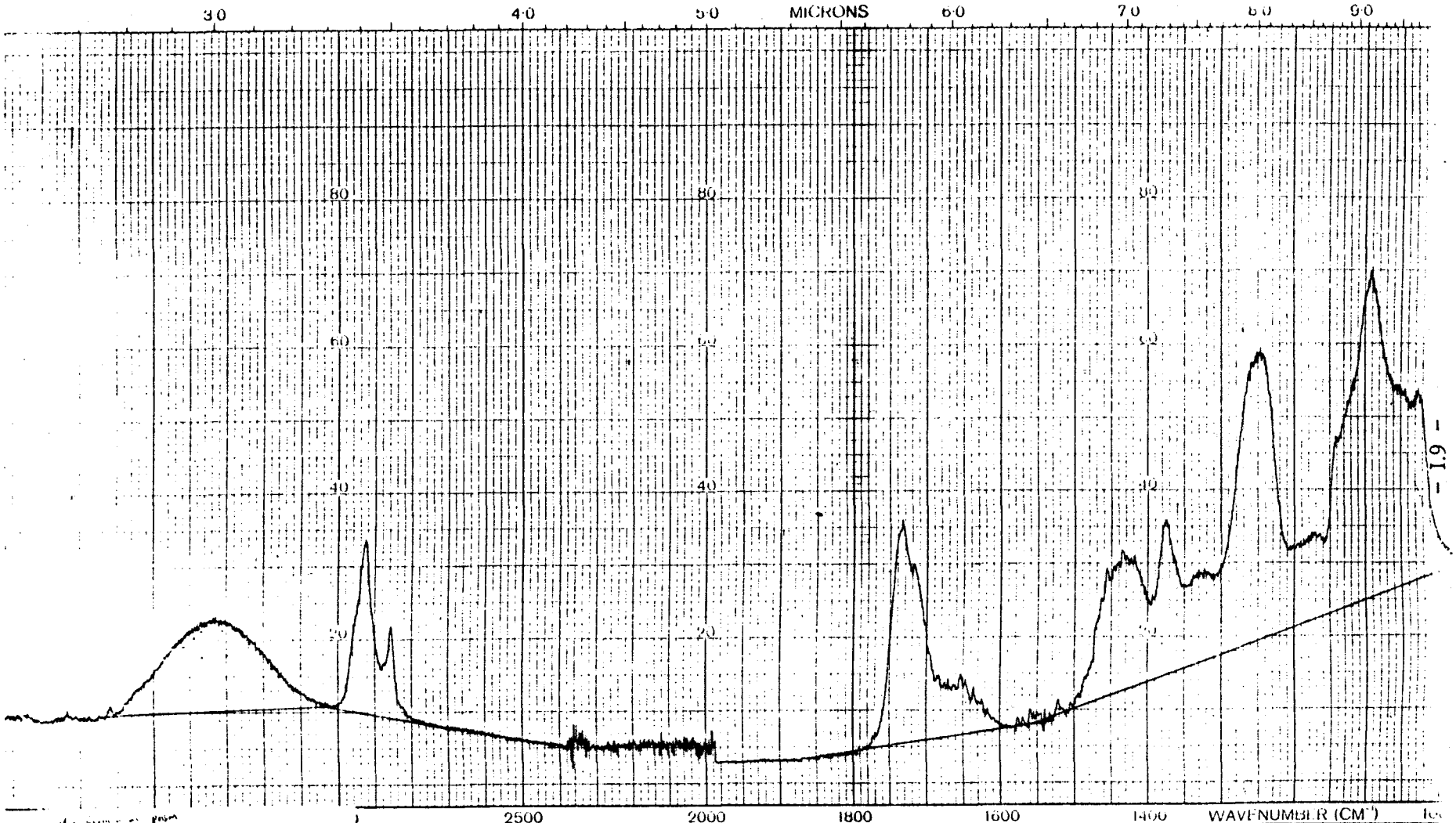

SOLVENT

CONCENTRATION

CELL PATH

REFERENCE

REMARKS

INT. SCAN MODE

SCAN TIME

RESOLUTION

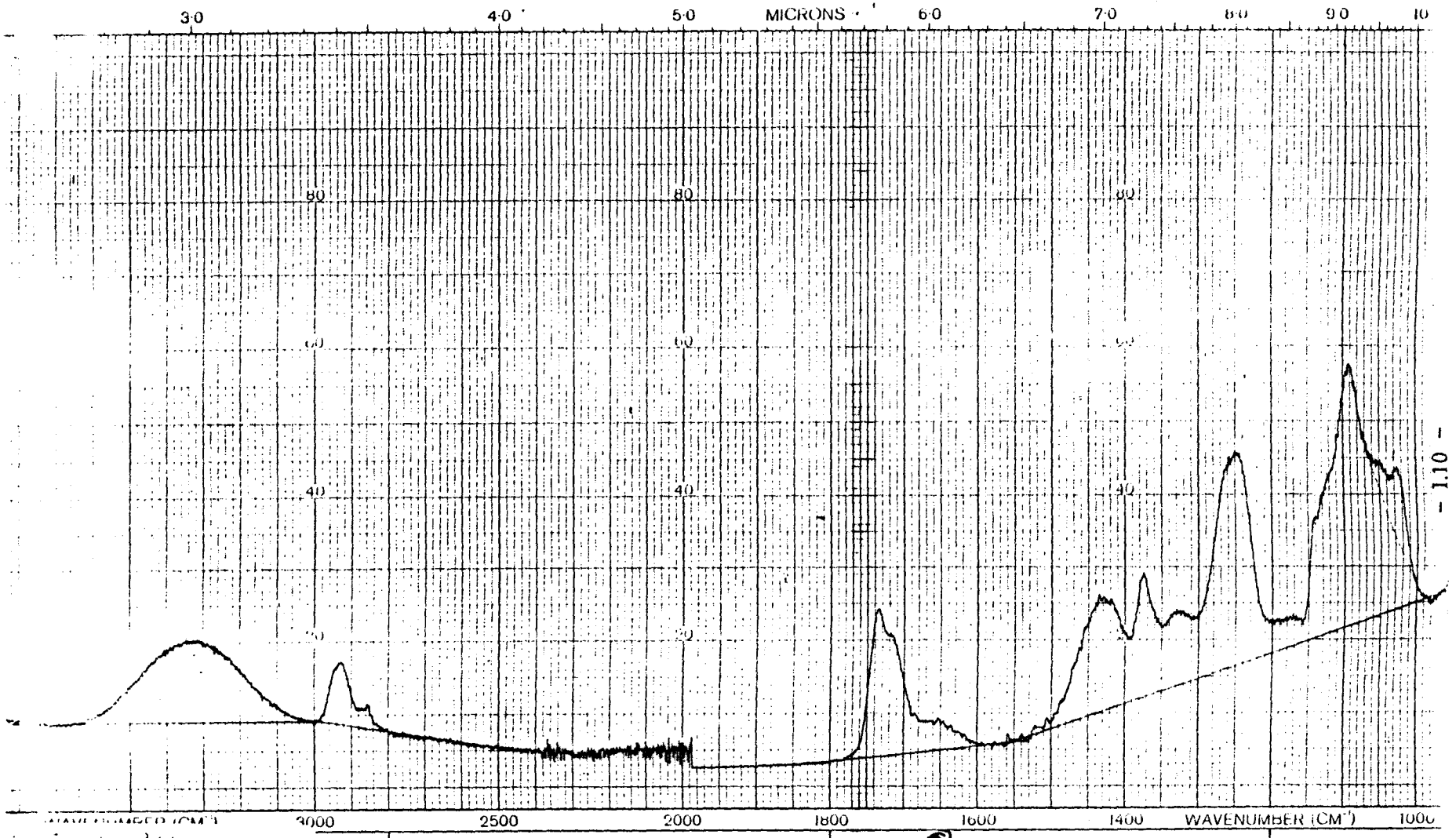

SOLVENT

CONCENTRATION

CELL PATH

REFERENCE

REMARKS (9)

INT. SCAN MODE

SCAN TIME

RESOLUTION

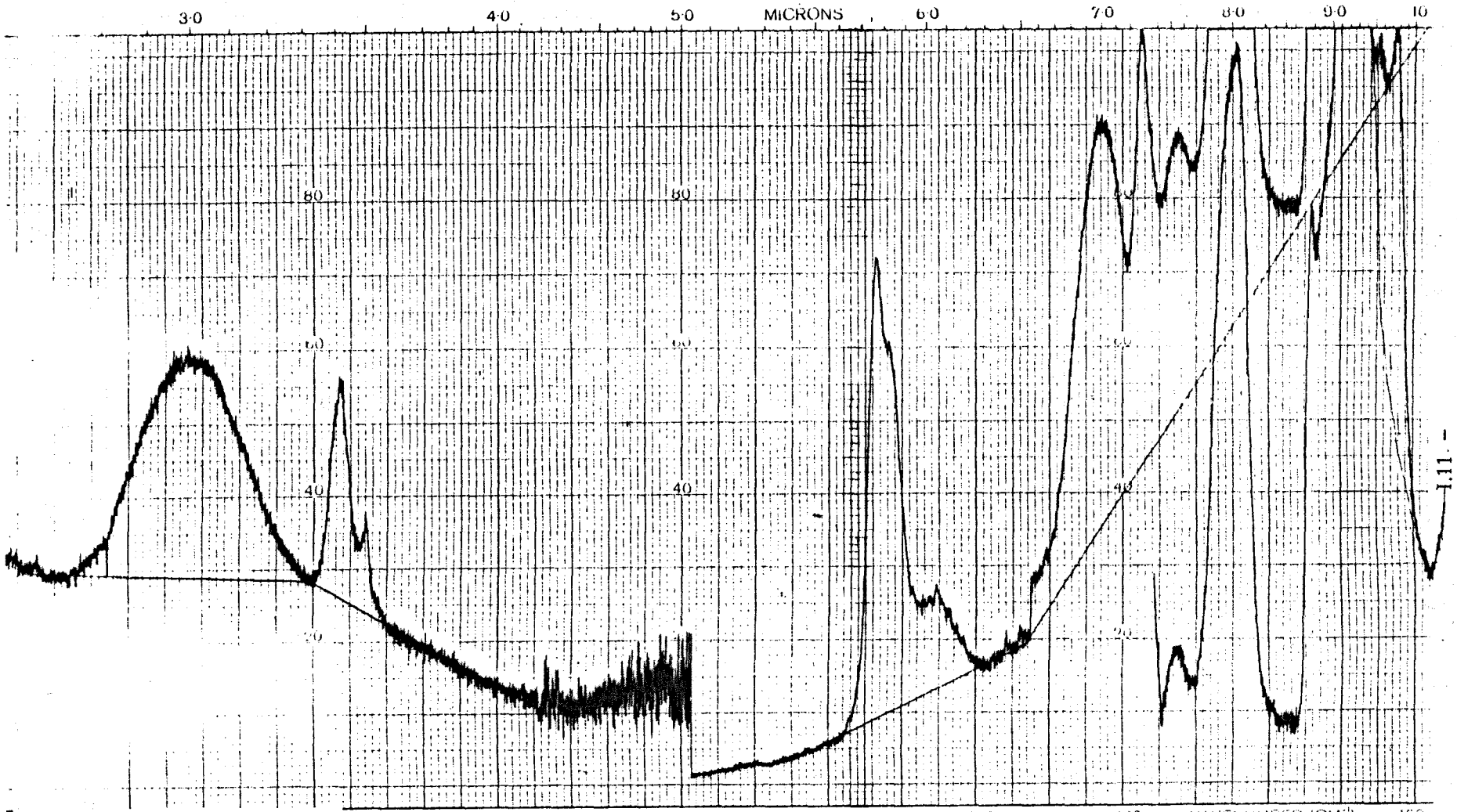

1.11 -

SOLVENT

CONCENTRATION

CELL PATH

REFERENCE

REMARKS (10)

INT. SCAN MODE

SCAN TIME

RESOLUTION

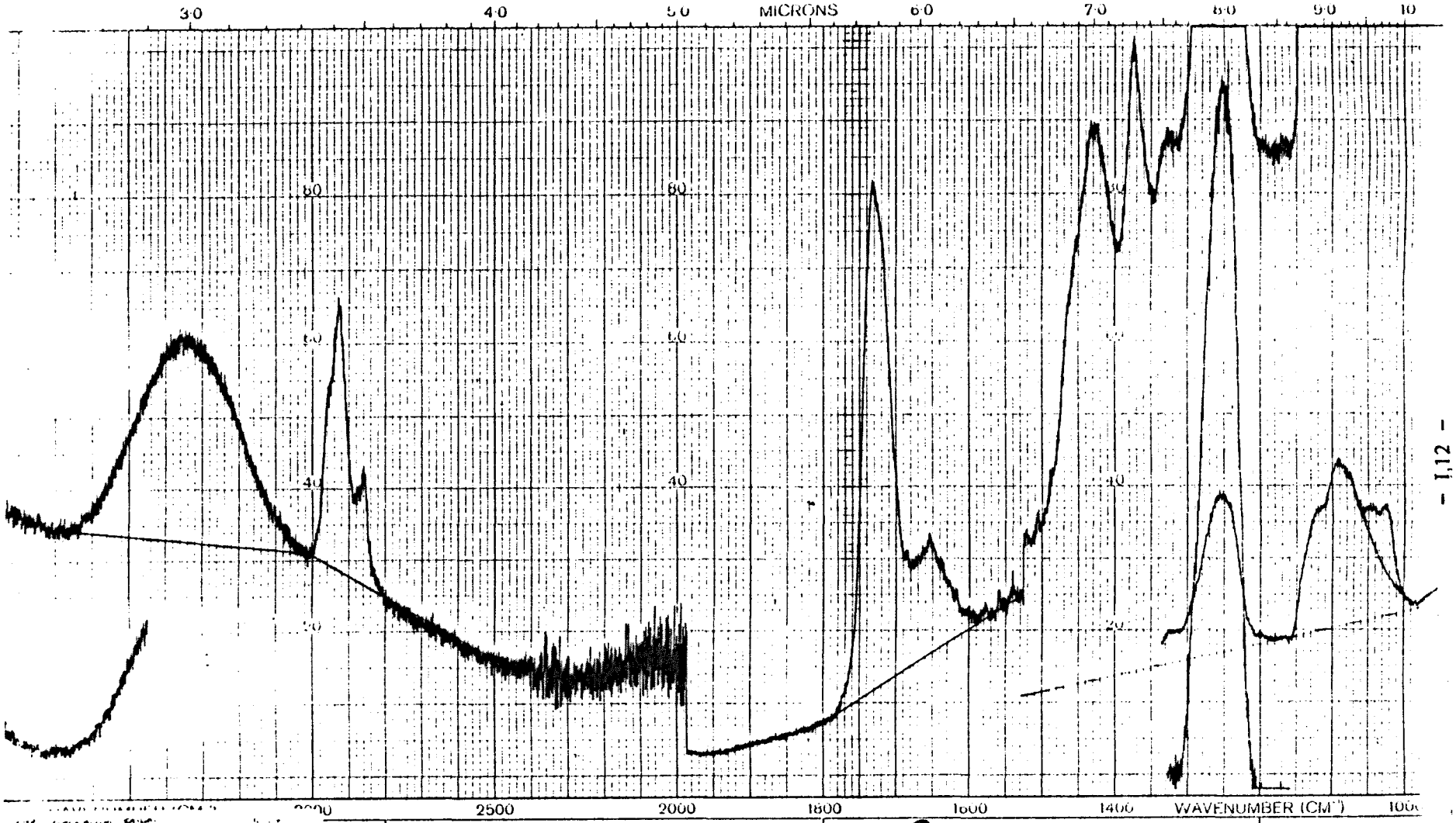

SOLVENT

CONCENTRATION

CELL PATH

REFERENCE

REMARKS (11)

INT. SCAN MODE

SCAN TIME

RESOLUTION

- 1,12 -

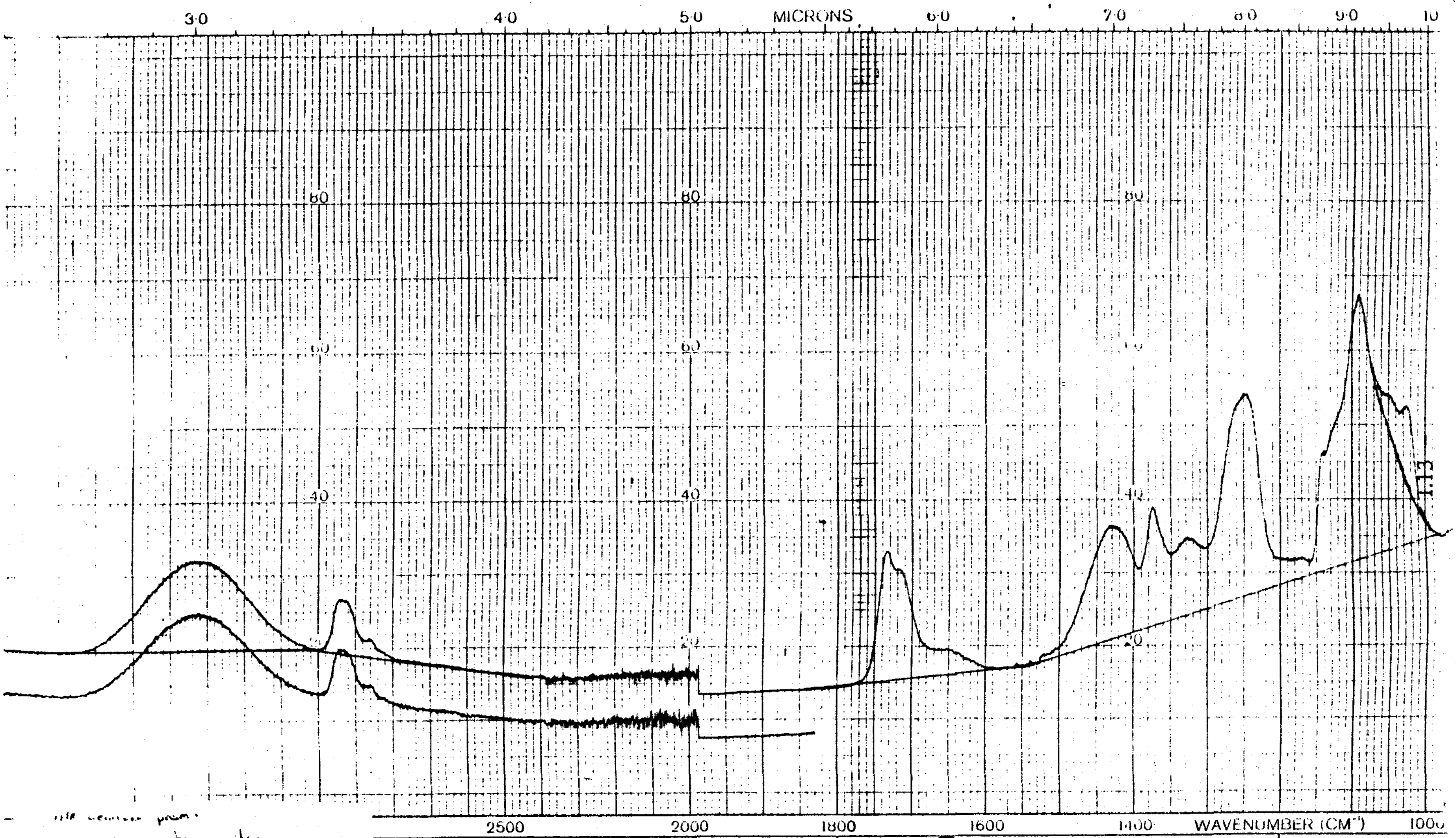

[illegible]
[illegible] absorbance units.
[illegible]
Sample (12) 8/7/87
AC

SOLVENT CONCENTRATION CELL PATH REFERENCE	REMARKS (12)	INT. SCAN MODE SCAN TIME RESOLUTION

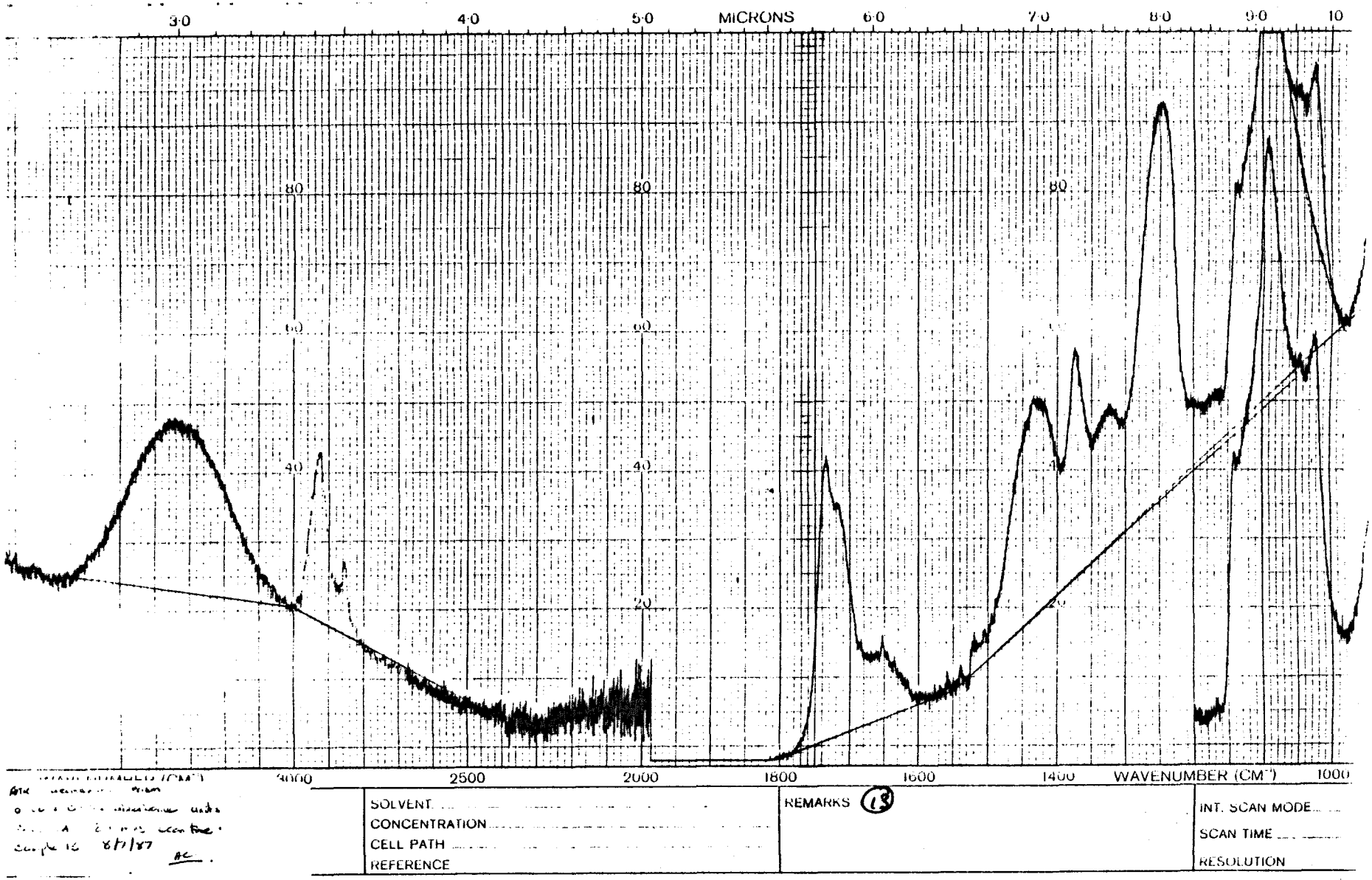

SOLVENT

CONCENTRATION

CELL PATH

REFERENCE

REMARKS (13)

INT. SCAN MODE

SCAN TIME

RESOLUTION

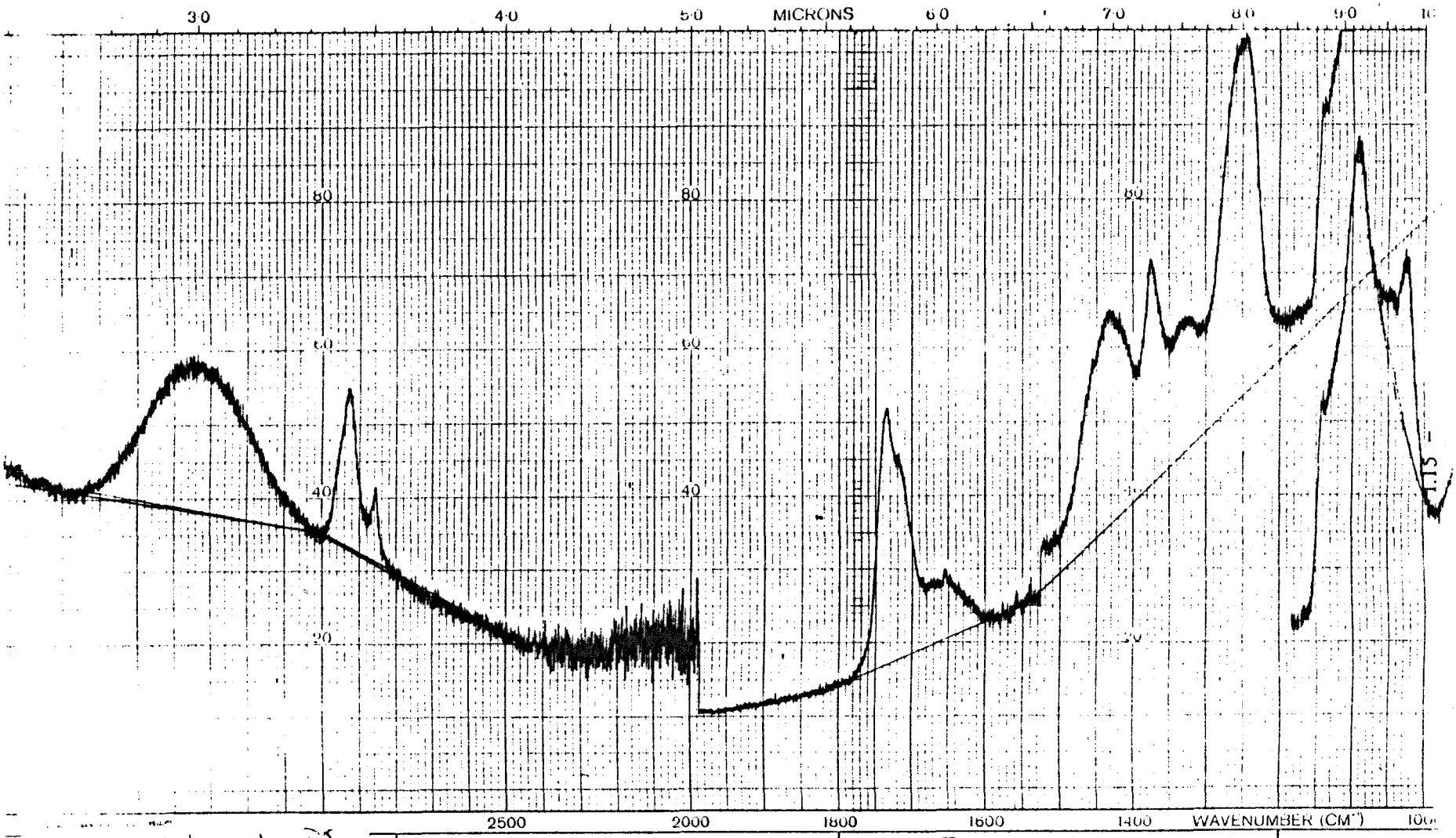

SOLVENT

CONCENTRATION

CELL PATH

REFERENCE

REMARKS (14)

INT. SCAN MODE

SCAN TIME

RESOLUTION

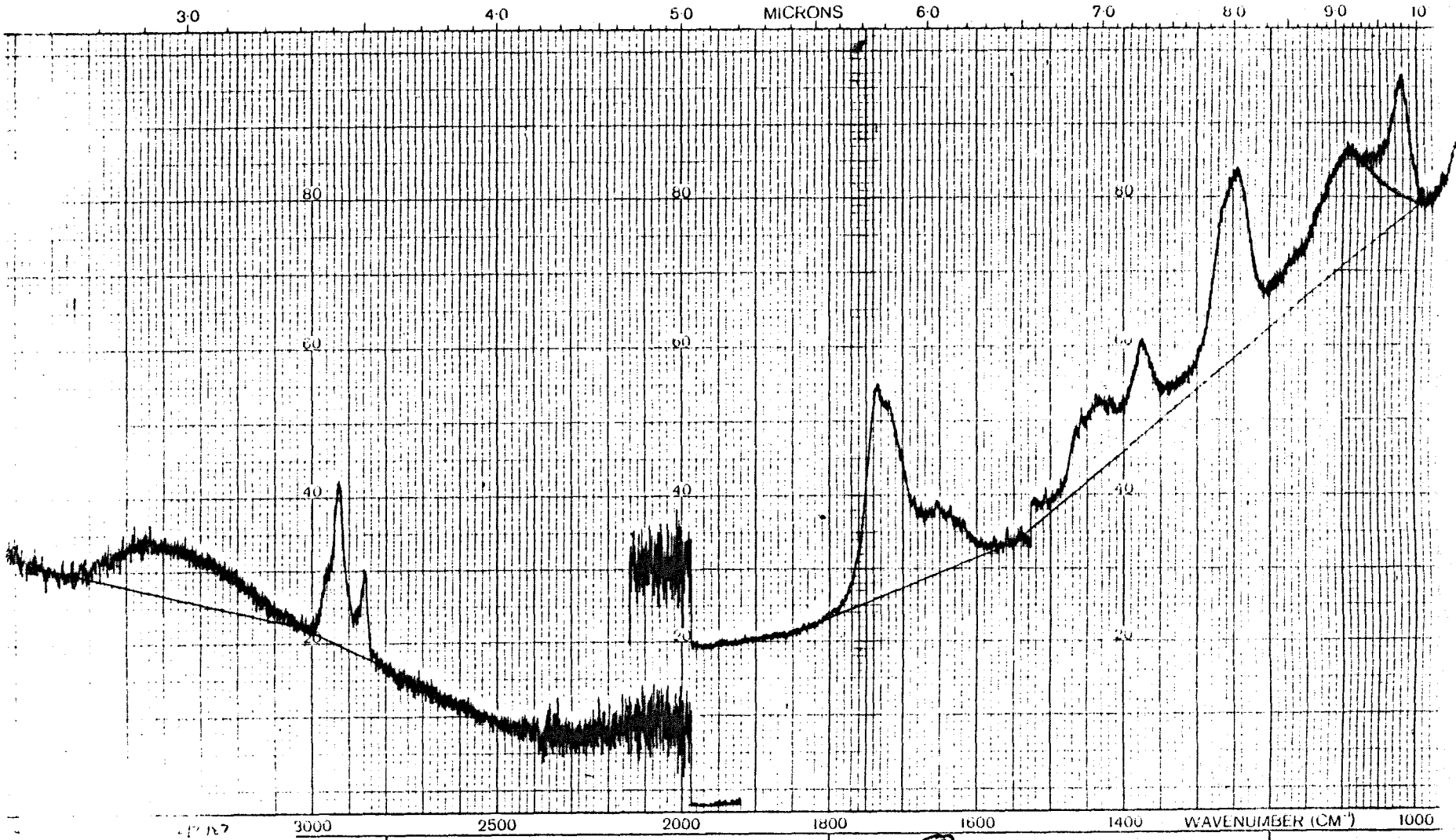
3·0
4·0
5·0
MICRONS
6·0
7·0
8·0
9·0
10
80
60
40
20
3000
2500
2000
1800
1600
1400
WAVENUMBER (CM⁻¹)
1000
SOLVENT
CONCENTRATION
CELL PATH
REFERENCE
REMARKS
(15)
INT. SCAN MODE
SCAN TIME
RESOLUTION

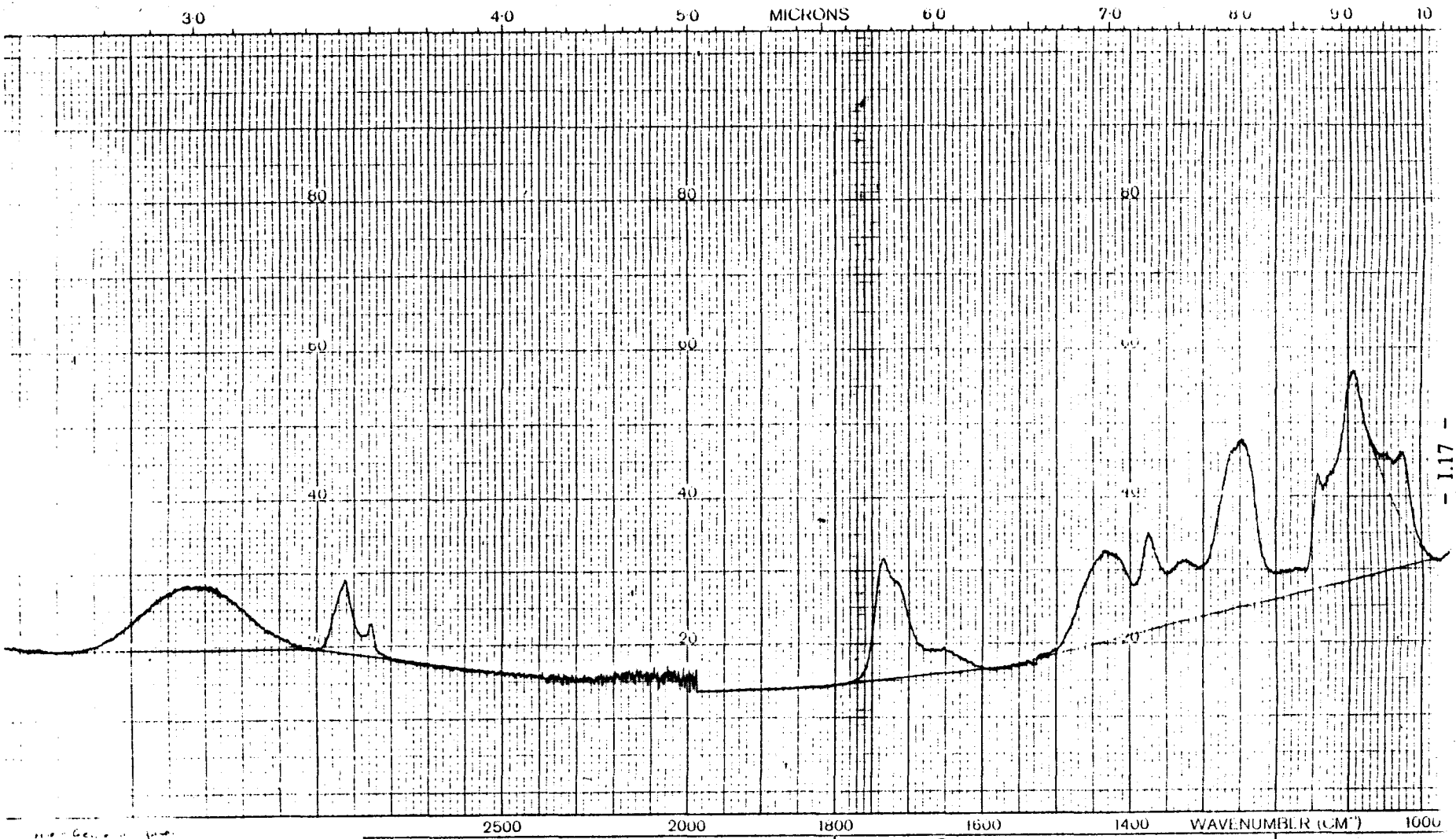

SOLVENT

CONCENTRATION

CELL PATH

REFERENCE

REMARKS (16)

INT. SCAN MODE

SCAN TIME

RESOLUTION

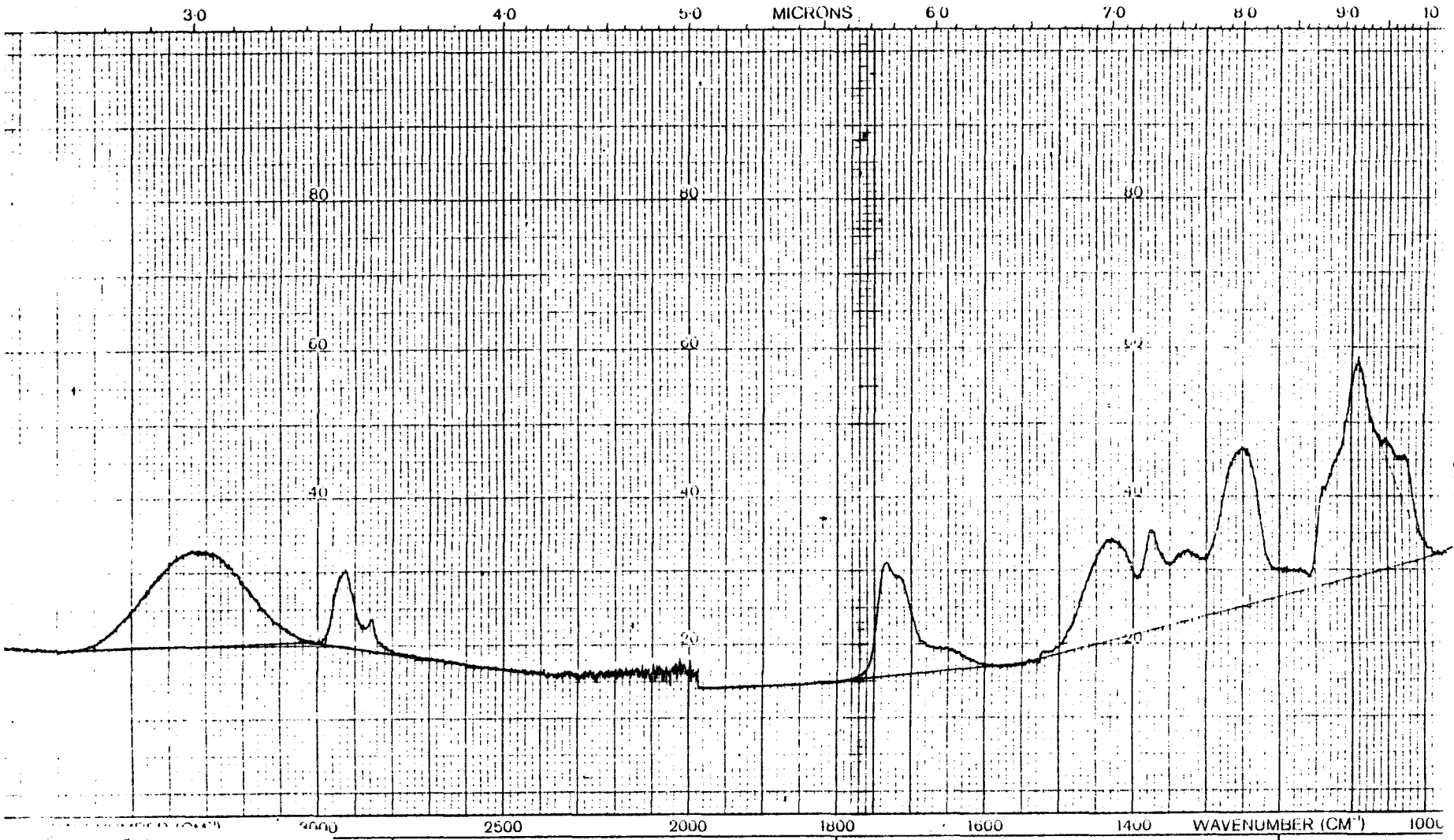

SOLVENT

CONCENTRATION

CELL PATH

REFERENCE

REMARKS (7)

INT. SCAN MODE

SCAN TIME

RESOLUTION

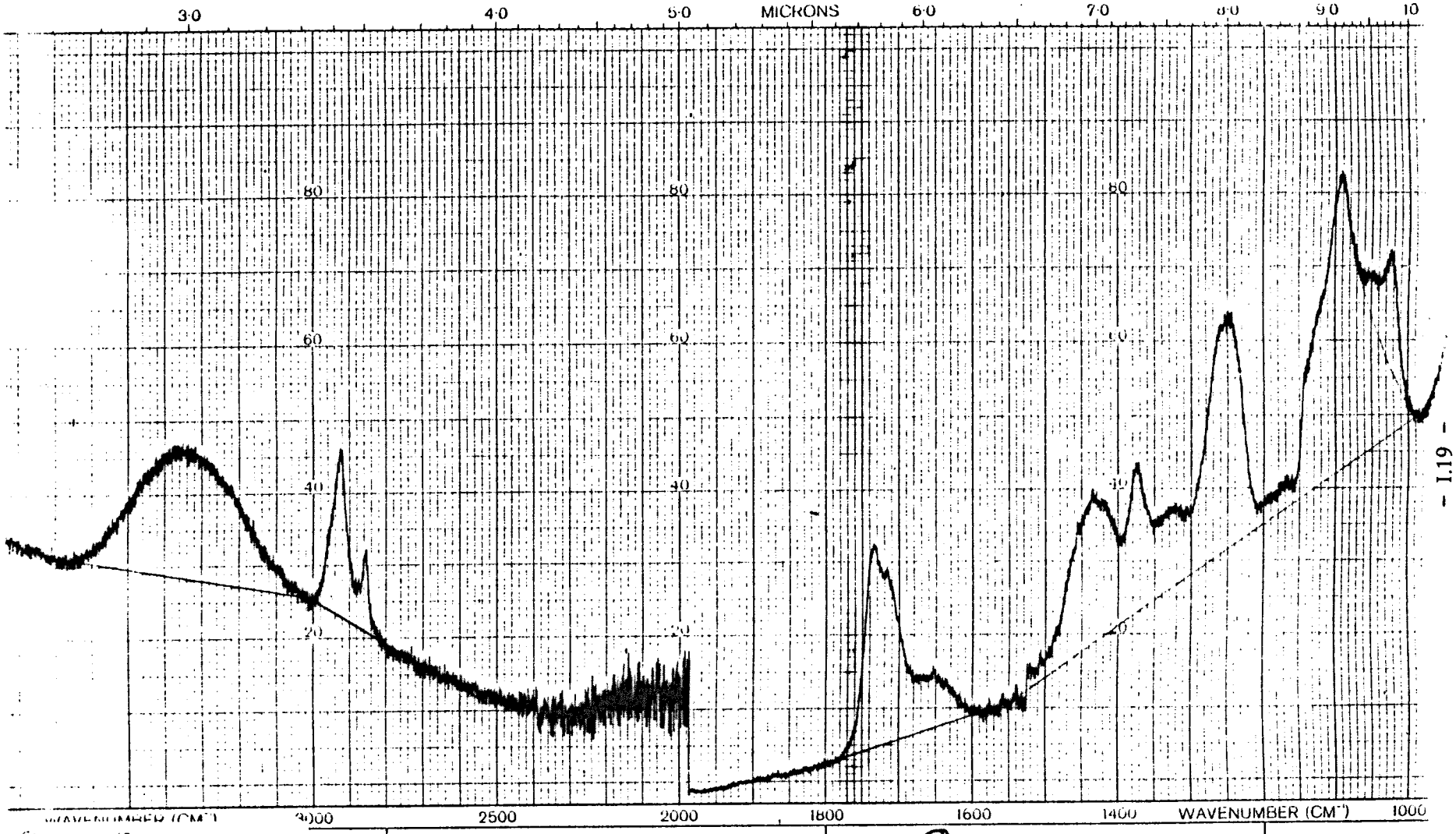
3·0
4·0
5·0
MICRONS
6·0
7·0
8·0
9·0
10
80
60
40
20
3000
2500
2000
1800
1600
1400
WAVENUMBER (CM⁻¹)
1000
SOLVENT
CONCENTRATION
CELL PATH
REFERENCE
REMARKS
(18)
INT. SCAN MODE
SCAN TIME
RESOLUTION

Appendix II

Acetone Sensor

It a great many of the experiments which were conducted during this work it was necessary to know the relative proportions of acetone and water present in any fluid sample. To permit this, an acetone sensor was developed based upon the techniques and circuitry described below.

The basic mode of operation of the sensor was as a conductance meter, the resistance within the solution changing as the water content was increased and decreased.

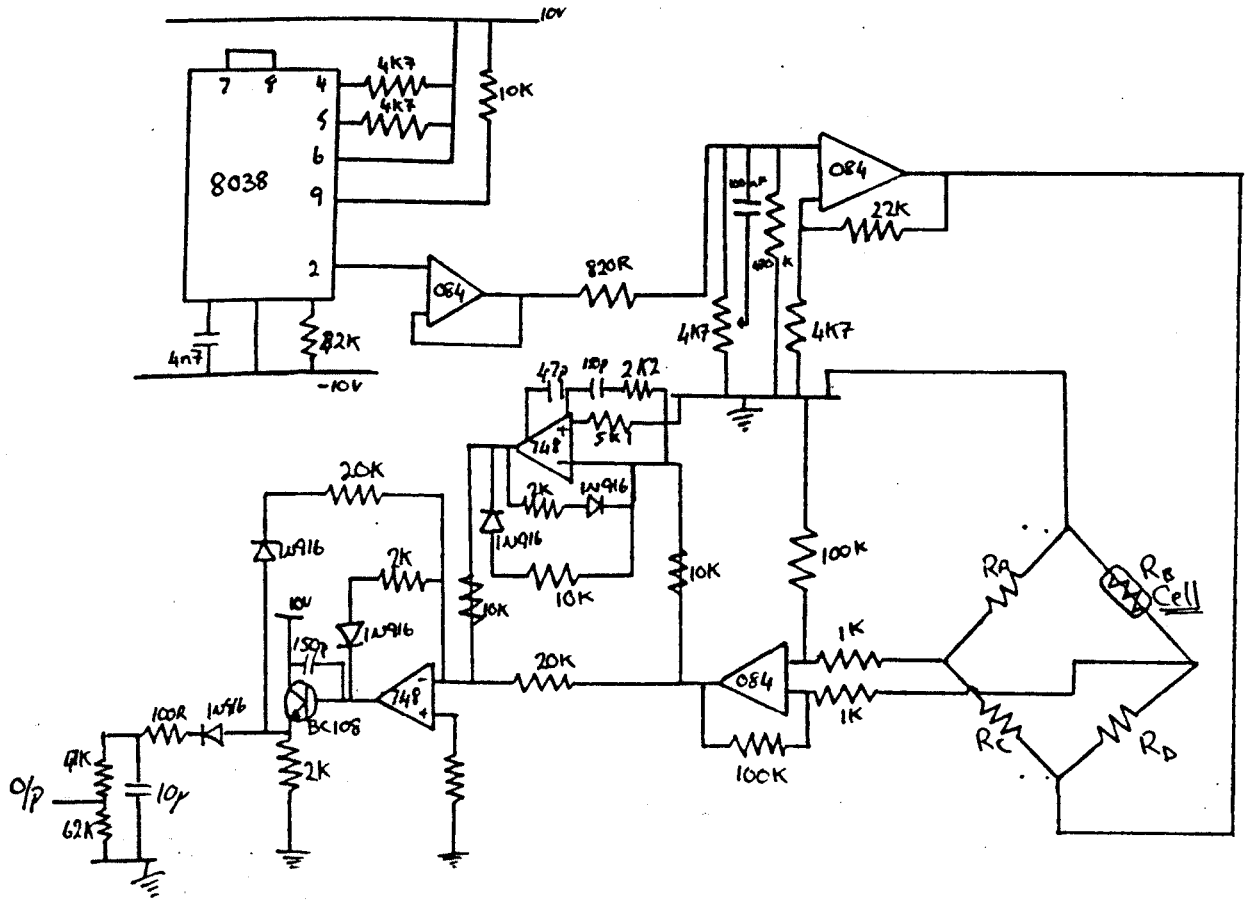

Figure II.1 Acetone Sensor Circuit

An A.C. signal of frequency 1000Hz (being generated using a 8038 waveform generator) was applied to the electrodes, figure II.1. This prevents polarization of the electrodes, which would cause degradation with use.

The signal detected at the electrodes was converted from A.C. to D.C. using an R.M.S. – D.C. converter, figure II.1. The D.C signal value obtained at this output then gave an indication of the relative acetone/water content. The calibration of this sensor has been shown in the main body of the thesis.

Appendix III

Load Cell Calibration

Calibration of the load cell was acieved by simlpy loading the cell with known masses and measuring the output at the A/D converter. The resultant linear calibration plot is shown in figure III.1.

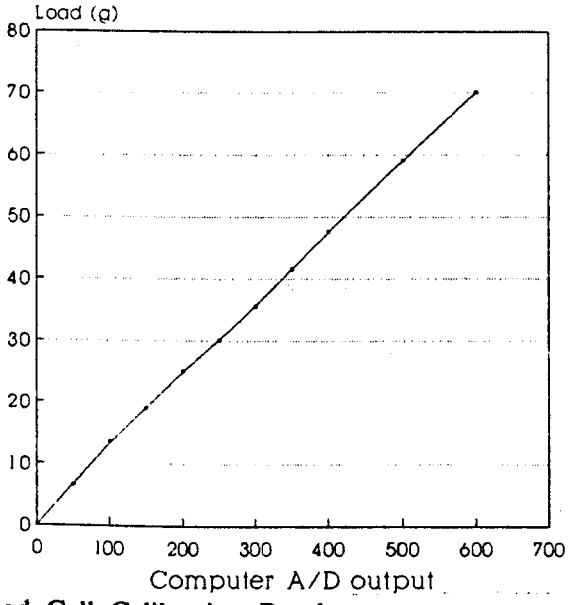

Figure III.1. Load Cell Calibration Results.

Appendix IV

The abbreviation used in the following analysis are:

F - Force (N) F_{norm} - Normalized Force

V - Contractile Velocity (%/s) V_{norm} - Normalized Velocity

l_f - Fibre Length (mm) F_0 - Maximum force (N)

m - Dry Mass of the Muscle (g)

The experimental relationship between velocity and force can be expressed by the rectangular hyperbola, as shown in figure 5.16.

$$(F + a)(V + b) = (F_0 + a)b \qquad \{IV.1\}$$

at F=0 the velocity is V_{max}, giving

$$a(V_{max}+b) = (F_0+a)b$$

$$aV_{max} = F_0b$$

$$V_{max}/b = F_0/a \qquad \{IV.2\}$$

the hyperbolic relationship {IV.1} may then be written in dimensionless form, as a relationship between F/F_0 and V/V_{max} which is given by;

$$(F/F_0+a/F_0)(V/V_{max}+b/V_{max}) = (1+a/F_0)b/V_{max} \qquad \{IV.3\}$$

Let $F' = F/F_0$; $V' = V/V_{max}$ and $E = F_0/a$

$$(F' + 1/E)(V' + 1/E) = (1 + 1/E)(1/E)$$

$$F'V' + F'/E + V'/E = 1/E$$

$$F'(V' + 1/E) = (1 - V')(1/E)$$

$$F' = (1 - V')/(1 + V'E) \qquad \text{(IV.4)}$$

$$V' = (1 - F')/(1 + F'E) \qquad \text{(IV.5)}$$

The maximum power output (force*velocity),found by equating {IV.4} and {IV.5}, occurs when F'=V'. Let G be the value of F' at which force equals V'. Then {IV.4} becomes;

$$G = (1 - G)/(1 + EG)$$

$$EG^2 + 2G - 1 = 0$$

Solving for G gives

$$G = [\sqrt{(1+E)} - 1]/E \qquad \text{(IV.6)}$$

Hence the normalized maximum power output (G^2) is

$$G^2 = (2 + E - 2\sqrt{(1+E)})/E^2 \qquad \text{(IV.7)}$$

The power output is in milliwatts with F_0 in newtons and V_{max} in mm/sec.. From {IV.6} and {IV.7} it is clear that the maximum power output and the force (and velocity) at which maximum power is produced both depend on the curvature ($E=F_0/a$) of the force/velocity curve.

Appendix V

Muscle Swelling Simulation

The following is a listing of the program used to simulate the swelling and deswelling of the polymer strips when chemically stimulated.

```
PROGRAM mussim;
(*************************************************************************
 *                                                                       *
 *         Pseudo-muscular Dilation/Contraction Simulation               *
 *                                                                       *
 *                  Written          March 1989                        *
 *                             By                                        *
 *                                                                       *
 *                           DARWIN                                      *
 *                                                                       *
 *************************************************************************)

  {$I typedef.sys}

  {$I graphix.sys}
                                        {Turbo Graphix Commands}
  {$I kernel.sys}

  {$I windows.sys}

  { $I dummy.inc}

Type
  counter = -100..100;                  {Define Variable Types}
  condition = (expand,contract);
  diff-coefficient = real;
  time-period = 0..1000;
  dimensions = real;
  nodal-array = ARRAY[1..10] OF real;
  nodal-conc = ARRAY[1..20,1..20] OF real;
  crank-nic-matrices = ARRAY[1..10,1..10] OF real;


Var                                     {list Variables Used}
  fx-liq-hgt:integer;
  water-conc,old-conc,alpha,swratio:real;
  diffus,flex-length,old-pos,mdpt,beta:real;
  fibre-thick,node-width,original-length,cross-area:dimensions;
```

```
   flexor:condition;
   d-0,cdiffus,ddiffus:diff-coefficient;      {Diffusion Coefficients}
   cycle-interval,fx-fill:time-period;        {Timing pointers       }
   flex-node:nodal-conc;
   matrixa,matrixb:crank-nic-matrices;
   node: nodal-array;                         { Number of nodes through the
polymer}
  p: ARRAY[1..20] OF real;                    { Crank-Nicolson p matrix }
   length: ARRAY[-5..20] OF dimensions;         {Length of swollen polymer
layer}
   fx-length: ARRAY[-5..20,-5..20] OF dimensions;{ Length of nodal sections
in flexor }


  {$I axis.pas}                               { Draw Display axis}



(*********************************************************************
 *     The procedures DATA and MASS read in information on the       *
 *     parameters of the muscle fibres, cell filling dynamics        *
 *     and loading.                                                  *
 *********************************************************************)

 PROCEDURE data;
 (*********************************************************************
  * This procedure reads in data necessary to set up the  initial    *
  * conditions in the muscle cells and the state of the fibres.      *
  *********************************************************************)
 Begin
   writeln ('                    MUSCLE INPUT INFORMATION');
   writeln('');
   writeln ('           What is the muscle thickness (microns)');
   readln (fibre-thick);
   fibre-thick:=fibre-thick/10000;
   writeln('');
   cross-area:=1;
   writeln ('           Cross-sectional area is ',cross-area);
   writeln('');
   cycle-interval:=1;
   writeln ('           Time interval between cycles is ',cycle-interval);
   writeln('');
   d-0:=9E-8;                                              { Gives a value fo
r
the diffusion coefficients}
   cdiffus:=d-0*9/25;ddiffus:=d-0;
   writeln ('What is the value of Beta for diffusion coefficient?');
   readln (beta);
   writeln('');
   writeln ('           What is the cell filling time ');
   readln (fx-fill);
   writeln('');
   original-length:=40;
   writeln ('           The initial polymer length is ',original-length);
   writeln('');
   swratio:=40/300;                                          { Set swellin
g
ratio parameter }
 End;
```

```
(*****************************************************************
 *       The procedures INITIAL, TRANSMAT, PSET, CONFIG, and GAUSS  *
 *       are used to solve for the water concentration at each node *
 *       using the Crank-Nicholson finite difference method. These  *
 *       relative conc. control the degree of swelling or deswelling*
 *****************************************************************)

 PROCEDURE initial;
 (*****************************************************************
  *                  This procedure is used to set up             *
  *                   the initial nodal concentrations.           *
  *****************************************************************)
Type
  counter = 0..10;
Var
  xdir:counter;
 BEGIN
   node[1]:=water-conc;                  { Set external node conc. equal }
   node[5]:=water-conc;                  { to the max. water intake level}
   node-width:=fibre-thick/4;            { Distance between nodes        }
   FOR xdir:=2 TO 4 DO
     BEGIN
       node[xdir]:=0;                    { Set internal node conc to zero }
     END;
 END;

PROCEDURE transmat;
(*****************************************************************
 *             This procedure is used to initialise              *
 *            the Crank-Nicolson tranformation matrices a and b.  *
 *****************************************************************)
Var
  count,count2:integer;
Begin
  FOR count:= 1 TO 5 DO
  BEGIN
    FOR count2:=1 TO 5 DO
    BEGIN
      matrixa[count,count2]:=0;
      matrixb[count,count2]:=0;
    END;
  END;
END;

PROCEDURE pset;
(*****************************************************************
 *               In this procedure the value of the              *
 *          Crank-Nicolson diffusion coefficient is set.         *
 *****************************************************************)
Var
tk:real;
  xdir:integer;
  thickx: ARRAY[1..20] OF dimensions;       { Distance between each swollen
node }

  (* Distance between nodes after uptake of solvent  (outer nodes) *)
BEGIN
```

```
  thickx[1]:=node-width+((node-width*((node[1]*100)/(1-node[1]))*swratio)/10
0);
  (* Diffusion rate set *)
  tk:=(thickx[1]-node-width)/thickx[1];
  diffus:=d-0*exp(beta*tk);
  p[1]:=(cycle-interval*diffus)/(thickx[1]*thickx[1]);
  thickx[5]:=thickx[1];
  p[5]:=p[1];

  (* Distance between nodes after uptake of solvent (internal nodes) *)
  FOR xdir:= 2 TO 4 DO
  BEGIN
    thickx[xdir]:=node-width+((node-width*((node[xdir]*100)/(1-node[xdir]))*
swratio)/100);
    (* Diffusion rate set *)
    tk:=(thickx[xdir]-node-width)/thickx[xdir];
    diffus:=d-0*exp(beta*tk);
    p[xdir]:=(cycle-interval*diffus)/(sqr(thickx[xdir-1]/2+thickx[xdir]/2));
  END;
END;

PROCEDURE config;
(*************************************************************************
 *          This routine is used to configure the matrices               *
 *           a and b depending on the values obtained for p.             *
 *************************************************************************)
VAR
  count,count2:integer;
BEGIN
  matrixa[1,1]:=1;
  matrixb[1,1]:=1;
  FOR count:= 2 TO 3 DO
   BEGIN
     matrixa[count,count-1]:=-0.5*p[count];
     matrixa[count,count+1]:=-0.5*p[count];
     matrixa[count,count]:=1+p[count];
     matrixb[count,count-1]:=0.5*p[count];
     matrixb[count,count+1]:=0.5*p[count];
     matrixb[count,count]:=1-p[count];
   END;
   FOR count:=0 TO 1 DO
   BEGIN
     FOR count2:=0 TO 4 DO
     BEGIN
       matrixa[5-count,count2+1]:=matrixa[count+1,5-count2];
     END;
   END;
END;

PROCEDURE gauss;
(*************************************************************************
 *              This routine uses gaussian elimination                   *
 *    to solve the difference equations set up in matrices a and b.      *
 *************************************************************************)
Var
 count,count2:integer;
 fact:real;
 rhs: ARRAY[1..20] OF real;

BEGIN
```

```
  For count:=2  TO 3 DO
  BEGIN
    rhs[count]:=0;
    FOR count2:=-1 TO 1 DO
    BEGIN
      rhs[count]:=matrixb[count,count+count2]*node[count+count2]+rhs[count];
    END;
  END;
  rhs[1]:=node[1];
  For count:=0 TO 1 DO
  BEGIN
    rhs[5-count]:=rhs[count+1];
  END;
  For count:= 2 TO 4 DO
  Begin
    fact:=matrixa[count-1,count-1]/matrixa[count,count-1];
    For count2:=-1 TO 1 DO
    Begin

matrixa[count,count-count2]:=matrixa[count-1,count-count2]-(fact*matrixa[cou
nt,count-count2]);
    END;
    rhs[count]:=rhs[count-1]-(rhs[count]*fact);
  END;
  count:=4;
  Repeat
   Begin
     node[count]:=(rhs[count]-matrixa[count,count+1]*node[count+1])/matrixa[
count,count];
   END;
  count:=count-1;
  Until count=0;
END;



PROCEDURE swell;
(*****************************************************************
 *                This procedure calculates the                  *
 *               degree of longitudinal swelling                 *
 *                for each nodal section                         *
 *****************************************************************)
TYPE
  counter = -100..100;
VAR
  count:counter;

BEGIN
  FOR count:=1 TO 5 DO
   BEGIN
     alpha:= (node[count]*100)/(1-node[count]);     {Parameter for the swell
ing degree}
     length[count]:=original-length+((original-length*alpha*swratio)/100);{
Swelling for each
internal node}
   END;
END;
```

```
PROCEDURE display;
(*********************************************************************
 *                  This procedure displays the water                *
 *                     concentration at the nodes.                   *
 *********************************************************************)
TYPE
  counter = -100..100;
VAR
  count:counter;

BEGIN
  FOR count:=1 to 5 DO
   BEGIN
     write(node[count]);
   END;
  writeln('');
END;


(*********************************************************************
 *     The procedure FLEX-INITIAL and FLEXOR-MUSCLE relate solely    *
 *     to the conditions and state of the flexor muscle during the   *
 *     the dilation/contraction cycles                               *
 *********************************************************************)

  PROCEDURE flex-initial;
  (*********************************************************************
   *                   Flexor Muscle  Initialization                   *
   *          Initialises the flexor muscle with nodal value           *
   *           set to give a fully contracted condition.               *
   *********************************************************************)
VAR
  zdir,xdir,loop:integer;

   BEGIN
     water-conc:=0.0;
     initial;                                    { call procedure initial }
     transmat;                                   { call procedure transmat
}
     loop:=0;
     REPEAT
      BEGIN
        pset;                                    { call procedure pset }
        config;                                  { call procedure config }
        gauss;                                   { call procedure gauss }
        swell;                                   { call procedure swell }
        loop:=loop+1;
        flex-length:=((length[3]+mdpt-original-length)*100)/original-length;
      END;
     FOR zdir:=1 TO fx-fill DO
      BEGIN
        FOR xdir:=1 TO 5 DO
         BEGIN                                   { Store water conc. values
 }
           flex-node[zdir,xdir]:=node[xdir];  { at each node in flexor.  }
         END;
      END;
     UNTIL loop>1;                               { Do until no chnag
```

```
e
}
   END;

PROCEDURE flexor-muscle;
   (********************Effect on the Flexor**************************
    *          Gives a value for the length of the flexor muscle     *
    *           by calculating the swelling of each nodal section    *
    ***************************************************************)
VAR
  zdir,xdir:integer;

 BEGIN
   flex-length:=0;
   IF fx-liq-hgt>fx-fill THEN
    BEGIN
      fx-liq-hgt:=fx-fill;     { Set max. cell filling level }
    END;
   FOR zdir:=1 TO fx-fill DO
    BEGIN
      FOR xdir:=1 TO 5 DO
       BEGIN
        If flexor=expand Then
         Begin
          If zdir<=fx-liq-hgt Then water-conc:=0.8 Else water-conc:=flex-nod
e[zdir,1];
          node[xdir]:=flex-node[zdir,xdir]; { transfers nodal conc. values }
         End
         Else
          Begin
           If zdir<=fx-liq-hgt Then water-conc:=0.5 Else water-conc:=flex-no
de[zdir,1];
           node[xdir]:=flex-node[zdir,xdir];
          End;
       END;                                                { to the NODE array.
}
        node[1]:=water-conc;node[5]:=water-conc;
        IF flexor=expand THEN
         BEGIN
          d-0:=ddiffus;
         END
        ELSE
         BEGIN
           d-0:=cdiffus;
         END;
        pset;
        config;                                           { Calculates the wate
r
conc for }
        gauss;                                            { each node cover by
solvent    }
        swell;
      FOR xdir:=1 TO 5 DO
       BEGIN
         fx-length[zdir,xdir]:=((length[xdir]-original-length)*100)/original
-length;
       END;
      IF fx-length[zdir,2]<fx-length[zdir,3] THEN    { Determines the sectio
n setting
swelling length }
```

```
      BEGIN
        flex-length:=(fx-length[zdir,3]/fx-fill)+flex-length;
      END
     ELSE                                                    {
Calculate the new length }
      BEGIN
        flex-length:=(fx-length[zdir,3]/fx-fill)+flex-length;
      END;
     FOR xdir:=1  TO 5 DO
      BEGIN
        flex-node[zdir,xdir]:=node[xdir];          { Store new nodal values }
      END;
   END;
END;



(*********************************************************************
 *                                                                   *
 *                  This is the main section of                      *
 *                   the controlling program                         *
 *                                                                   *
 *********************************************************************)

Var
  count,cycle,simtim:integer;
  ans:char;

Begin
  (*****************************************************************
   *          This section of program controls the                 *
   *           initial setup of the flexor and                     *
   *            extensor muscles.                                  *
   *****************************************************************)
  InitGraphic;
  DefineWorld(1,0,80,70,0);
  SelectWorld(1);
  SelectWindow(1);

  ClearScreen;
  data;                                          { call procedure data }
  fx-liq-hgt:=0;old-conc:=0;
  flex-initial;
  (*****************************************************************
   *          In this area of the program the cyclical             *
   *          expansions and contractions of the muscles           *
   *          are calculated and stored.                           *
   *****************************************************************)

  cycle:=0;simtim:=0;
  writeln ('What is the required simulation runtime (sec)?');
  readln (simtim);
  Repeat
  Begin
   flexor:=expand;
   writeln (' Input water or acetone (w or a)?');
   readln (ans);
   fx-liq-hgt:=0;
   If (ans='a') Or (ans='A') Then flexor:=_contract;
```

```
    cycle:=0;                          { Sets up the initial set of the  muscle
s}
    ClearScreen;
    graph(cycle,simtim);
    Repeat
    Begin
      fx-liq-hgt:=fx-liq-hgt+1;
      flexor-muscle;
      cycle:=cycle+1;
      graph (cycle,simtim);
    End;
    Until cycle>simtim;
    writeln(flex-length);
   End;
   writeln ('Do you wish to continue the simulation (y or Y)?');
   readln (ans);
  Until (ans='n') Or (ans='N');
 Leavegraphic;
End.
```

Appendix VI

Pseudo-Muscular Actuator Simulation

The following is a listing of the program used to simulate the control and regulation of the flexor/extensor muscle actuator pair.

```
PROGRAM mussim;
(*************************************************************************
 *                                                                       *
 *         Flexor / Extensor Pair Control Simulation                     *
 *                                                                       *
 *                  Written          March 1987                        *
 *                             By                                        *
 *                                                                       *
 *                           DARWIN                                      *
 *                                                                       *
 *************************************************************************)

   {$I typedef.sys}

   {$I graphix.sys}

   {$I kernel.sys}

   {$I windows.sys}

   { $I dummy.inc}

 Type
   counter = -100..100;
   condition = (expand,contract,fill,stop,empty);
   diff-coefficient = real;
   time-period = 0..1000;
   dimensions = real;
   nodal-array = ARRAY[1..10] OF real;
   nodal-conc = ARRAY[1..20,1..20] OF real;
   crank-nic-matrices = ARRAY[1..10,1..10] OF real;


 Var
   fx-liq-hgt,ex-liq-hgt:integer;
   water-conc,supp,max,min,old-conc,alpha,swratio:real;
   flex-length,old-pos,exten-length,beta:real;
   fibre-thick,node-width,original-length,cross-area:dimensions;
```

```
   flexor:condition;
   d-0,cdiffus,ddiffus:diff-coefficient;          {Diffusion Coefficients}
   cycle-interval,samp-freq,fx-fill:time-period;      {Timing pointers
   }
   flex-node,ex-node:nodal-conc;
   matrixa,matrixb:crank-nic-matrices;
   node: nodal-array;                          { Number of nodes through the
polymer}
   p: ARRAY[1..20] OF real;                              { Crank-Nicolson p ma
trix
}
   length: ARRAY[-5..20] OF dimensions;                  {Length of swollen p
olymer
layer}
   fx-length,ex-length: ARRAY[-5..20,-5..20] OF dimensions;      { Length of
 nodal
sections in flexor }


  {$I mpaxis.pas}



(*********************************************************************
 *     The procedures DATA and MASS read in information on the       *
 *     parameters of the muscle fibres, cell filling dynamics        *
 *     and loading.                                                  *
 *********************************************************************)

 PROCEDURE data;
 (*********************************************************************
  * This procedure reads in data necessary to set up the  initial    *
  * conditions in the muscle cells and the state of the fibres.      *
  *********************************************************************)
 Begin
   writeln ('                    MUSCLE INPUT INFORMATION');
   writeln('');
   writeln ('           What is the muscle thickness (mm*10-2)');
   readln (fibre-thick);
   fibre-thick:=fibre-thick/10000;
   writeln('');
   cross-area:=1;
   writeln ('           Cross-sectional area is ',cross-area);
   writeln('');
   cycle-interval:=1;
   writeln ('           Time interval between cycles is ',cycle-interval);
   writeln('');
   d-0:=70E-6;                                           { Gives a value f
or
the diffusion coefficients}
   cdiffus:=d-0*9/25;ddiffus:=d-0;
   writeln ('What is the value of Beta for diffusion coefficient?');
   readln (beta);
   writeln('');
   writeln ('           What is the cell filling time ');
   readln (fx-fill);
   writeln('');
   original-length:=40;
   writeln ('           The initial polymer length is ',original-length);
   writeln('');
```

```
   swratio:=40/300;                                          { Set swellin
g
ratio parameter }
   writeln ('          What is the sampling frequency');
   readln (samp-freq);
 End;


(*********************************************************************
 *       The procedures INITIAL, TRANSMAT, PSET, CONFIG, and GAUSS   *
 *       are used to solve for the water concentration at each node  *
 *       using the Crank-Nicholson finite difference method. These   *
 *       relative conc. control the degree of swelling or deswelling*
 *********************************************************************)

 PROCEDURE initial;
 (*********************************************************************
  *                  This procedure is used to set up                 *
  *                   the initial nodal concentrations.               *
  *********************************************************************)
Type
  counter = 0..10;
Var
  xdir:counter;
 BEGIN
   node[1]:=water-conc;                        { Set external node conc. equal
}
   node[5]:=water-conc;                        { to the max. water intake level
}
   node-width:=fibre-thick/4;                  { Distance between nodes
}
   FOR xdir:=2 TO 4 DO
     BEGIN
       node[xdir]:=0;                        { Set internal node conc to zero
}
     END;
 END;

PROCEDURE transmat;
(*********************************************************************
 *             This procedure is used to initialise                  *
 *            the Crank-Nicolson tranformation matrices a and b.     *
 *********************************************************************)
Var
  count,count2:integer;
Begin
  FOR count:= 1 TO 5 DO
  BEGIN
    FOR count2:=1 TO 5 DO
    BEGIN
      matrixa[count,count2]:=0;
      matrixb[count,count2]:=0;
    END;
  END;
END;

PROCEDURE pset;
(*********************************************************************
 *              In this procedure the value of the                   *
```

```
 *          Crank-Nicolson diffusion coefficient is set.          *
 ****************************************************************)
Var
  xdir:integer;
  diffus:real;
  thickx: ARRAY[1..20] OF dimensions;       { Distance between each swollen
node }

  (* Distance between nodes after uptake of solvent  (outer nodes) *)
BEGIN

  thickx[1]:=node_width+((node_width*((node[1]*100)/(1-node[1]))*swratio)/10
0);
  (* Diffusion rate set *)
  diffus:=d_0*exp(-beta*(1-node[1]));
  p[1]:=(cycle_interval*diffus)/(thickx[1]*thickx[1]);
  thickx[5]:=thickx[1];
  p[5]:=p[1];

  (* Distance between nodes after uptake of solvent (internal nodes) *)
  FOR xdir:= 2 TO 4 DO
  BEGIN
    thickx[xdir]:=node_width+((node_width*((node[xdir]*100)/(1-node[xdir]))*
swratio)/100);
    (* Diffusion rate set *)
    diffus:=d_0*exp(-beta*(1-node[xdir]));
    p[xdir]:=(cycle_interval*diffus)/(sqr(thickx[xdir-1]/2+thickx[xdir]/2));
  END;
END;

PROCEDURE config;
(****************************************************************
 *          This routine is used to configure the matrices      *
 *           a and b depending on the values obtained for p.    *
 ****************************************************************)
VAR
  count,count2:integer;
BEGIN
  matrixa[1,1]:=1;
  matrixb[1,1]:=1;
  FOR count:= 2 TO 3 DO
   BEGIN
     matrixa[count,count-1]:=-0.5*p[count];
     matrixa[count,count+1]:=-0.5*p[count];
     matrixa[count,count]:=1+p[count];
     matrixb[count,count-1]:=0.5*p[count];
     matrixb[count,count+1]:=0.5*p[count];
     matrixb[count,count]:=1-p[count];
   END;
   FOR count:=0 TO 1 DO
   BEGIN
     FOR count2:=0 TO 4 DO
     BEGIN
       matrixa[5-count,count2+1]:=matrixa[count+1,5-count2];
     END;
   END;
END;

PROCEDURE gauss;
(****************************************************************
```

```
 *              This routine uses gaussian elimination              *
 *    to solve the difference equations set up in matrices a and b. *
 ********************************************************************)
Var
 count,count2:integer;
 fact:real;
 rhs: ARRAY[1..20] OF real;

BEGIN
  For count:=-2  TO 3 DO
  BEGIN
    rhs[count]:=0;
    FOR count2:=-1 TO 1 DO
    BEGIN
      rhs[count]:=matrixb[count,count+count2]*node[count+count2]+rhs[count]
    END;
  END;
  rhs[1]:=node[1];
  For count:=0 TO 1 DO
  BEGIN
    rhs[5-count]:=rhs[count+1];
  END;
  For count:= 2 TO 4 DO
  Begin
    fact:=matrixa[count-1,count-1]/matrixa[count,count-1];
    For count2:=-1 TO 1 DO
    Begin

matrixa[count,count-count2]:=matrixa[count-1,count-count2]-(fact*matrixa[co
nt,count-count2]);
    END;
    rhs[count]:=rhs[count-1]-(rhs[count]*fact);
  END;
  count:=4;
  Repeat
   Begin
     node[count]:=(rhs[count]-matrixa[count,count+1]*node[count+1])/matrixa
count,count];
   END;
  count:=count-1;
  Until count=0;
END;


PROCEDURE swell;
(*******************************************************************
 *                This procedure calculates the                    *
 *               degree of longitudinal swelling                   *
 *                for each nodal section                           *
 *******************************************************************)
TYPE
  counter = -100..100;
VAR
  count:counter;

BEGIN
  FOR count:=1 TO 5 DO
   BEGIN
     alpha:= (node[count]*100)/(1-node[count]);     (Parameter for the sw
ing degree)
```

```
    length[count]:=original-length+((original-length*alpha*swratio)/100);{
Swelling for each
internal node)
   END;
END;



PROCEDURE display;
(************************************************************************
 *                This procedure displays the water                     *
 *                   concentration at the nodes.                        *
 ************************************************************************)
TYPE
  counter = -100..100;
VAR
  count:counter;

BEGIN
  FOR count:=1 to 3 DO
   BEGIN
     write(node[count]);
   END;
  writeln('');
END;


(************************************************************************
 *     The procedure FLEX-INITIAL and FLEXOR-MUSCLE relate solely       *
 *     to the conditions and state of the flexor muscle during the      *
 *     the dilation/contraction cycles                                  *
 ************************************************************************)

  PROCEDURE flex-initial;
  (************************************************************************
   *                   Flexor Muscle  Initialization                      *
   *         Initialises the flexor muscle with nodal value               *
   *          set to give a fully dilated condition.                      *
   ************************************************************************)
VAR
  zdir,xdir,loop:integer;

   BEGIN
     water-conc:=0.8;
     initial;                                  { call procedure initial }
     transmat;                                 { call procedure transmat
}
     loop:=0;
     For xdir:=1 To 5 Do
     Begin
       node[xdir]:=water-conc;
     End;
     REPEAT
      BEGIN
        pset;                                  { call procedure pset }
        config;                                { call procedure config }
        gauss;                                 { call procedure gauss }
        swell;                                 { call procedure swell }
        loop:=loop+1;
```

```
        flex-length:=((length[3]-original-length)*100)/original-length;
      END;
     FOR zdir:=1 TO fx-fill DO
      BEGIN
        FOR xdir:=1 TO 5 DO
         BEGIN                                              { Store water conc
.
values }
           flex-node[zdir,xdir]:=node[xdir];  { at each node in flexor.  }
           fx-length[zdir,xdir]:=flex-length;
         END;
      END;
     UNTIL loop>1;                                          { Do until no chnag
e
}
   END;

  PROCEDURE extens-initial;
  (*********************************************************************
   *                  Extensor Muscle  Initialization                  *
   *         Initialises the extensoror muscle with nodal value        *
   *          set to give a fully contracted condition.                 *
   *********************************************************************)
VAR
  zdir,xdir,loop:integer;

   BEGIN
     water-conc:=0.5;
     initial;                                          { call procedure initial }
     transmat;                                         { call procedure transmat
}
     loop:=0;
     For xdir:=1 To 5 Do
     Begin
       node[xdir]:=water-conc;
     End;
     REPEAT
      BEGIN
        pset;                                          { call procedure pset }
        config;                                        { call procedure config }
        gauss;                                         { call procedure gauss }
        swell;                                         { call procedure swell }
        loop:=loop+1;
        exten-length:=((length[3]-original-length)*100)/original-length;
      END;
     FOR zdir:=1 TO fx-fill DO
      BEGIN
        FOR xdir:=1 TO 5 DO
         BEGIN                                             { Store water conc
.
values }
           ex-node[zdir,xdir]:=node[xdir];  { at each node in flexor.  }
           ex-length[zdir,xdir]:=exten-length;
         END;
      END;
     UNTIL loop>1;                                         { Do until no chna
e
}
   END;
```

```
PROCEDURE flexor-muscle;
   (*******************Effect on the Flexor**************************
    *          Gives a value for the length of the flexor muscle    *
    *           by calculating the swelling of each nodal section   *
    ****************************************************************)
VAR
  zdir,xdir:integer;
  t-flex:real;

 BEGIN
   t-flex:=flex-length;
   flex-length:=0;
   IF fx-liq-hgt>fx-fill THEN
    BEGIN
      fx-liq-hgt:=fx-fill;     { Set max. cell filling level }
    END;
   IF fx-liq-hgt<0 THEN
    BEGIN
      fx-liq-hgt:=0;           { Set min. cell filling level }
    END;

If fx-liq-hgt>0 Then
 Begin
   FOR zdir:=1 TO fx-fill DO
    BEGIN
      FOR xdir:=1 TO 5 DO
       BEGIN
        If flexor=expand Then
         Begin
          If zdir<=fx-liq-hgt Then water-conc:=0.8 Else water-conc:=flex-nod
e[zdir,1];
          node[xdir]:=flex-node[zdir,xdir]; { transfers nodal conc. values }
         End
         Else
          Begin
           If zdir<=fx-liq-hgt Then water-conc:=0.5 Else water-conc:=flex-nc
de[zdir,1];
           node[xdir]:=flex-node[zdir,xdir];
          End;
       END;
        node[1]:=water-conc;node[5]:=water-conc;
        IF flexor=expand THEN
         BEGIN
          d-0:=ddiffus;
         END
        ELSE
         BEGIN
           d-0:=cdiffus;
         END;
if zdir<=fx-liq-hgt Then
 Begin
        pset;
        config;                          { Calculates the water conc for }
        gauss;                           { each node cover by solvent    }
        swell;
 End;
      FOR xdir:=1 TO 5 DO
       BEGIN
If zdir<=fx-liq-hgt Then
 Begin
```

```
        fx-length[zdir,xdir]:=((length[xdir]-original-length)*100)/original
-length;
 End;
      END;
       (* Calculates the length of the swollen polymer fibre    *)
       (* One section relates to dilation the other contraction *)
      IF fx-length[zdir,2]<fx-length[zdir,3] THEN
       BEGIN
         flex-length:=(fx-length[zdir,3]/fx-fill)+flex-length;
       END
      ELSE
       BEGIN
         flex-length:=(fx-length[zdir,3]/fx-fill)+flex-length;
       END;
      FOR xdir:=1  TO 5 DO
       BEGIN
         flex-node[zdir,xdir]:=node[xdir];    { Store new nodal values }
       END;
   END;
 End;
 If flex-length = 0 Then flex-length:=t-flex;
END;


PROCEDURE extens-muscle;
   (*********************************************************************
    *          Gives a value for the length of the extensor muscle  *
    *           by calculating the swelling of each nodal section   *
    *********************************************************************)
VAR
  zdir,xdir:integer;
  t-ext:real;

 BEGIN
   t-ext:=exten-length;
   exten-length:=0;
   IF ex-liq-hgt>fx-fill THEN
    BEGIN
      ex-liq-hgt:=fx-fill;              { Set max. cell filling level }
    END;
   IF ex-liq-hgt<=0 THEN
    BEGIN
      ex-liq-hgt:=0;                    { Set min. cell filling level }
    END;

If ex-liq-hgt>0 Then
 Begin
   FOR zdir:=1 TO fx-fill DO
    BEGIN
      FOR xdir:=1 TO 5 DO
       Begin
        If flexor=expand Then
         Begin
          If zdir<=ex-liq-hgt Then water-conc:=0.5 Else water-conc:=ex-noc
zdir,1];
         node[xdir]:=ex-node[zdir,xdir]; { transfers nodal conc. values }
         End
         Else
          Begin
           If zdir<=ex-liq-hgt Then water-conc:=0.8 Else water-conc:=ex-n
```

```
[zdir,1];
            node[xdir]:=ex-node[zdir,xdir];
           End;
        END;
         node[1]:=water-conc;node[5]:=water-conc;
         IF flexor-expand THEN
          BEGIN
           d-0:=cdiffus;
          END
         ELSE
          BEGIN
            d-0:=ddiffus;
          END;
If zdir<=ex-liq-hgt Then
Begin
         pset;
         config;                          { Calculates the water conc for }
         gauss;                           { each node covered by solvent  }
         swell;
End;
       For xdir:=1 TO 5 DO
        Begin
If zdir<=ex-liq-hgt Then
 Begin
            ex-length[zdir,xdir]:=((length[xdir]-original-length)*100)/origin
al-length;
 End;
        End;
        (* Calculates the length of the swollen polymer fibre     *)
        (* One section relates to dilation the other contraction *)
        If ex-length[zdir,2]<ex-length[zdir,3] Then
        BEGIN
          exten-length:=(ex-length[zdir,3]/fx-fill)+exten-length;
        END
       ELSE
        BEGIN
          exten-length:=(ex-length[zdir,3]/fx-fill)+exten-length;
        END;

       FOR xdir:=1  TO 5 DO
        BEGIN
          ex-node[zdir,xdir]:=node[xdir];          { Store new nodal values }
        END;
     END;
End;
 If exten-length = 0 Then exten-length:=t-ext;
END;



PROCEDURE PD-data (Var Kp,Kd:real);
(************ Inputs the values of the prop. and derivative gain ******)
Begin
  writeln('Input Kp');
  readln(Kp);
  writeln('Input Kd');
  readln(Kd);
End;
```

```
PROCEDURE controller (angle,end-pt,Kp,Kd,motion:real;
                      cycle:integer                    );
(************ Controls the flow of solvents into the cells *************)
Var
  error:real;

Begin
  If cycle=0 Then
   Begin
     error:=1;                          { Start error signal to          }
   End                                  { ensure filling of the cells.   }
   Else
   Begin
     If flexor=contract Then
      Begin
        error:=Kp*(angle-end-pt)-Kd*(motion);  { Calc. error signal     }
      End
      Else
      Begin
        error:=-Kp*(end-pt-angle)-Kd*(motion);
      End;
write(' e',error);
   End;

  If error>0 Then                       { If error set by the controller }
  Begin                                 { law is positive then continue  }
    If flexor=contract Then
     Begin
       fx-liq-hgt:=fx-liq-hgt+1;          { to fill the flexor.           }
       If supp>0  Then     { If there is tension in the     }
        Begin
          ex-liq-hgt:=ex-liq-hgt+1;       { fill the extensor cell.       }
        End
        Else
        Begin                             { Else empty the cell to slow    }
          ex-liq-hgt:=ex-liq-hgt-5;       { the relaxation rate and prevent}
        End;                              { 'flop'.                        }
     End
     Else
     Begin
       ex-liq-hgt:=ex-liq-hgt+1;          { to fill the extensor          }
       If supp>0  Then     { If there is tension in the     }
        Begin
          fx-liq-hgt:=fx-liq-hgt+1;       { fill the extensor cell.       }
        End
        Else
        Begin                             { Else empty the cell to slow    }
          fx-liq-hgt:=fx-liq-hgt-5;       { the relaxation rate and prevent}
        End;                              { 'flop'.                        }
     End
  End
  Else
  Begin                                 { Else empty the cell to slow    }
    fx-liq-hgt:=fx-liq-hgt-5;           { the rate of movement.          }
    ex-liq-hgt:=ex-liq-hgt-5;
  End;
{ If ABS(angle-end-pt)<2 Then
  Begin
    fx-liq-hgt:=fx-liq-hgt-5;
    ex-liq-hgt:=ex-liq-hgt-5;
```

```
  End;}
End;


PROCEDURE coupling;
(***************** Measure the intermuscle coupling extension
                   which can be used to calculate the true position *****)
Begin
  supp:=0;                                  { Supplementary position value  }
  If (max-flex-length)>(exten-length-min) Then
  Begin
    supp:=((max-flex-length)-(exten-length-min))/2;
  End;
End;


(*************************************************************************
 *                                                                       *
 *                    This is the main section of                        *
 *                     the controlling program                           *
 *                                                                       *
 *************************************************************************)

Var
  position,end-pt,Kp,Kd,old-position,motion,angle:real;
  count,cycle,simtim:integer;
  ans:char;

 Begin
   (*********************************************************************
    *           This section of program controls the                    *
    *            initial setup of the flexor and                        *
    *             extensor muscles.                                     *
    *********************************************************************)
   InitGraphic;
   DefineWorld(1,0,200,70,0);
   SelectWorld(1);
   SElectWindow(1);

   ClearScreen;
   data;                                    { call procedure data }
   fx-liq-hgt:=0;ex-liq-hgt:=0;             { Level of liquid in cells }
   old-conc:=0;
   flex-initial;                            { Call procedures to set up}
   extens-initial;                          { the extensor and flexor. }
   (*********************************************************************
    *           In this area of the program the cyclical                *
    *           expansions and contractions of the muscles              *
    *           are calculated and stored.                              *
    *********************************************************************)
   max:=flex-length;min:=exten-length;{Positions of max. and min motion}
writeln(flex-length,exten-length);
   writeln ('What is the required simulation runtime (sec)?');
   readln (simtim);
   PD-data (Kp,Kd);                         { Call routine to set control. values}

   (* Section of program controlling the motion of the muscle and the flow*)
   (* of the solvent into the cells.                                      *)
   cycle:=0;                                { Sets up the initial set of the  muscles
```

```
}
   ClearScreen;
   graph(cycle,simtim,angle);
   Repeat
   Begin
    If cycle>simtim Then
     Begin
       ClearScreen;
       cycle:=0;
       graph(cycle,simtim,angle);
     End;
    flexor:=expand;
    writeln (' Is the joint to open or close (O or C)?');
    readln (ans);
    writeln ('to what position');
    read(end-pt);
    position:=flex-length+supp;
    angle := (position-17.3)*5;
    If (ans='c') Or (ans='C') Then flexor := contract;
    coupling;
    Repeat
    Begin
      controller (angle,end-pt,Kp,Kd,motion,cycle);
      flexor-muscle;
      extens-muscle;
      cycle:=cycle+1;
      old-position:=position;
      coupling;
      position:=flex-length+supp;          { Position allowing for coupling}
      motion:=ABS((position-old-position)*5*samp-freq);{ Movement of beam d
ring
}
      angle := (position-17.3)*5;
      graph(cycle,simtim,angle);
    End;
writeln(fx-liq-hgt,ex-liq-hgt,flex-length,exten-length,angle);
read(ans);

    Until (cycle>simtim)
    OR ((flexor=contract) AND (angle<end-pt+2) AND (fx-liq-hgt=0))
    OR ((flexor=expand) AND (angle>end-pt-2) AND (fx-liq-hgt=0));
   End;
   writeln ('Do you wish to continue the simulation (y or Y)?');
   readln (ans);
  Until (ans='n') Or (ans='N');
 LeaveGraphic;
End.
```

Appendix VII

Valve Control Program

The following is a listing of the program used to control the valve sequencing and solvent distribution within the flexor–extensor actuator cells.

```
 10 REM ****************************
 20 REM
 30 REM    VALVE CONTROLLER
 40 REM       Written
 50 REM       JULY 1988
 60 REM         By
 70 REM       DARWIN
 80 REM
 90 REM ****************************
100 MODE 128: DIM A$(4)
110 PROCSETUP
120 PROCINFO
130 PROCPID_INFO
140 MODE 128
150 PROCAXIS
152 INPUT "OPEN OR CLOSE", A$
153 CNT=TIME
154 IF A$="C" THEN PROCCLOSE ELSE PROCOPEN
160 GOTO 152
170 END
180 REM ****************************
190 REM
200 REM ***************************
210 REM GRIPPER CLOSING CONTROLLER
220 DEFPROCCLOSE
260 PROCPOSITION       : REM CALCULATE PRESNT GRIPPER ANGLE
270 PROCDISPLAY        : REM DISPLAY PRESENT GRIPPER ANGLE
280 PROCPID_CLOSE      : REM CALCULATED THE PD SIGNAL ERROR
290 IF T_ERROR<0 THEN ?&FE60=96: GOTO 360 :REM -VE ERROR? EMPTY CELLS
310 IF ADVAL(3)>500 AND ADVAL(2)>500 THEN ?&FE60=0:GOTO 660: REM CELLS FULL?
315 PROCTENSION
320 IF TENSION>1 THEN ?&FE60=12 ELSE ?&FE60=8 : REM FILL FLEXOR & EXTENSOR?
350 ?&FE60=192          : REM REMOVE FLUID FROM BOTH CELLS, SLOW/STOP MOTION
360 IF ABS(ANGLE-MAX)<2 THEN ?&FE60=96;ENDPROC:REM FINAL POSITION? EMPTY CELLS

380 GOTO 260
390 ENDPROC
400 REM ****************************
500 REM ****************************
510 REM GRIPPER OPENING CONTROLLER
520 DEFPROCOPEN
560 PROCPOSITION    : REM CALCULATE PRESENT GRIPPER ANGLE
570 PROCDISPLAY     : REM DISPLAY PRESENT GRIPPER ANGLE
580 PROCPID_OPEN    : REM CALCULATED THE PD SIGNAL ERROR
590 IF T_ERROR<0 THEN ?&FE60=96: GOTO 660  :REM -VE ERROR? EMPTY CELLS
610 IF ADVAL(3)>500 AND ADVAL(2)>500 THEN ?&FE60=0:GOTO 660: REM CELLS FULL?
615 PROCTENSION
620 IF TENSION>1 THEN ?&FE60=18 ELSE ?&FE60=16 : REM FILL FLEXOR & EXTENSOR?
660 IF ABS(MIN-ANGLE)<2 THEN ?&FE60=96;ENDPROC:REM FINAL POSITION? EMPTY CELLS

680 GOTO 560
700 ENDPROC
710 REM ****************************
800 REM ****************************
810 REM SET-UP PROCEDURE
820 DEFPROCSETUP
830 ?&FE62=&FF    : REM SET COMPUTER PORTS TO O/P
840 ?&FE60=0      : REM TURN ALL VALVES OFF
850 PROCPOSITION : REM OBTAIN PRESENT GRIPPER POSITION
860 OLD_ANGLE=ANGLE
```

```
 870 DIM ANS$(4)
 880 INPUT "READY TO START?" ANS$
 890 IF ANS$<>"Y" THEN GOTO 880
 900 ENDPROC
 910 REM ******************************
1000 REM ******************************
1010 REM PRESENT GRIPPER POSITION
1020 DEFPROCINFO     : REM INFO ON DESIRED RANGE OF MOTION
1030 PRINT"PRESENT ANGLE IS ",ANGLE
1040 INPUT "WHAT IS THE MAXIMUM DESIRED DEFLECTION", MAX
1050 INPUT " WHAT IS THE MINIMUM DESIRED DEFLECTION", MIN
1060 IF MAX < ANGLE THEN GOTO 1030
1070 ENDPROC
1080 REM ******************************
1100 REM ******************************
1120 DEFPROCPID_INFO  : REM OBTAIN PROPORTIONAL & DRIVATIVE VALUES
1130 INPUT " WHAT IS THE PROPORTIONAL VALUE", PROP
1140 INPUT "WHAT IS THE DERIVATIVE VALUE", DERV
1150 ENDPROC
1160 REM ******************************
1200 REM ******************************
1210 DEFPROCTENSION
1220 TENSION=ADVAL(1)     :REM MEASURE TENDON TENSION
1230 ENDPROC
1240 REM ******************************
1300 REM ******************************
1310 DEFPROCPOSITION
1320 CALA=37000: CALB=90    : REM SET CALIBRATION VALUES
1330 ANGLE=((ADVAL(4)-CALA)*(130/65520))+CALB
1340 ENDPROC
1350 REM ******************************
1400 REM ******************************
1410 REM ERROR SIGNAL
1420 DEFPROCPID_CLOSE
1430 PROP_ERROR=(MAX-ANGLE)*PROP
1440 DERV_ERROR=(OLD_ANGLE-ANGLE)*DERV
1450 T_ERROR=PROP_ERROR+DERV_ERROR
1460 OLD_ANGLE=ANGLE
1470 ENDPROC
1480 REM ******************************
1500 REM ******************************
1510 REM ERROR SIGNAL (OPENING)
1515 DEFPROCPID_OPEN
1520 PROP_ERROR=(ANGLE-MIN)*PROP
1530 DERV_ERROR=(ANGLE-OLD_ANGLE)*DERV
1540 T_ERROR=PROP_ERROR+DERV_ERROR
1550 OLD_ANGLE=ANGLE
1560 ENDPROC
1570 REM ******************************
1600 REM ******************************
1610 REM DRAW THE AXES
1620 DEFPROCAXIS
1630 MOVE 10,10: DRAW 10,1090   : REM VERTICAL AXIS
1640 MOVE 10,10: FOR I=1 TO 9: MOVE 10,I*120+10: DRAW 20,I*120+10: NEXT I
1650 MOVE 10,10: DRAW 1210,10   : REM HORIZONTAL AXIS
1660 MOVE 10,10: FOR I=1 TO 6: MOVE I*200+10,10: DRAW I*200+10,20: NEXT I
1670 ENDPROC
1680 REM ******************************
1700 REM ******************************
1710 REM DISPLAY GRIPPER POSITION
1720 DEFPROCDISPLAY
1725 CTT=(TIME-CNT)/100
1730 IF CTT < .2 THEN PLACE=OLD_ANGLE  : REM INITIAL GRIPPER POINT
1740 MOVE CTT*20-10,PLACE*6: DRAW CTT*20+10,ANGLE*6 : REM PLOT POSITION
1750 PLACE=ANGLE
1800 ENDPROC
```

Appendix VIII

Compliant Tendon Controller

The circuit used in controlling the stepper motor used in the variable compliance tendon experiments is shown in figure VIII.1 below.

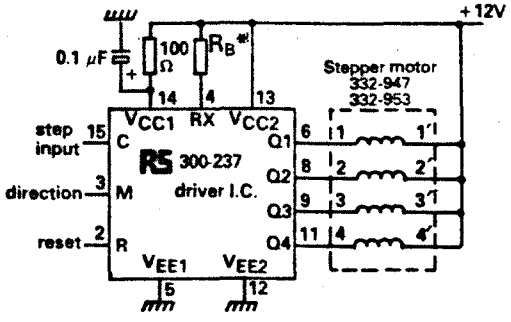

VIII.1. Stepper Motor Drive Circuit

The following is a listing of the program used to control this stepper and in the monitoring of the joint sensor outputs.

```
 10 REM ************************
 20 REM VARIABLE COMPLIANCE TENDONS
 30 REM JULY 1989
 40 REM ************************
 50 ?&FE62=&FF
100 MODE 0
105 P_M=800:P_ONE=550:P_TWO=300:P_THREE=50
107 I_ONE=ADVAL(3):I_TWO=ADVAL(2):I_THREE=ADVAL(4)
110 PROCAXIS
111 DAS=1
115 FOR CT=1 TO 800
120 PROCMOTOR
130 PROCJ_ONE
140 PROCJ_TWO
150 PROCJ_THREE
162 ?&FE60=0
166 ?&FE60=255
210NEXT CT
500 END
600 REM ************************
610 DEFPROCMOTOR
615 N_M=800+CT/4
617 IF CT>400 THEN N_M=1000-CT/4
620 MOVE (CT-1)+10,P_M: DRAW CT+10,N_M
630 P_M=N_M
650 ENDPROC
680 ENDPROC
690 REM ************************
700 REM ************************
710 DEFPROCJ_ONE
715 N_ONE=550+(ADVAL(3)-I_ONE)/300
720 MOVE (CT-1)+10,P_ONE: DRAW CT+10,N_ONE
730 P_ONE=N_ONE
750 ENDPROC
790 REM ************************
```

```
800 REM *************************
810 DEFPROCJ_TWO
815 N_TWO=300+(ADVAL(2)-I_TWO)/300
820 MOVE (CT-1)+10,P_TWO: DRAW CT+10,N_TWO
830 P_TWO=N_TWO
850 ENDPROC
890 REM *************************
900 REM *************************
910 DEFPROCJ_THREE
912 N_THREE=(60000-ADVAL(4))/300
915 N_THREE=50+N_THREE
920 MOVE (CT-1)+10,P_THREE: DRAW CT+10,N_THREE
930 P_THREE=N_THREE
950 ENDPROC
990 REM *************************
1000 REM *************************
1010 DEFPROCAXIS
1020 FOR I=1 TO 4
1030 PS=((I-1)*200)
1035 MOVE 10,PS+(I*50): DRAW 10,(I*200)+(I*50)
1040 MOVE 10,PS+(I*50): DRAW 1010,PS+(I*50)
1041 FOR J=1 TO 4
1042 MOVE 5,PS+(I*50)+J*50: DRAW 10,PS+(I*50)+J*50
1045 MOVE J*250+10,PS+(I*50)-10: DRAW J*250+10,PS+(I*50)
1047 NEXT J
1050 NEXT I
1190 ENDPROC
1200 REM *************************
```